

SYNTHESIS AND CHARACTERIZATION OF
ELECTRON DONOR/ACCEPTOR
SUBPHTHALOCYANINE DERIVATIVES AND
PORPHYRIN METAL COMPLEXES

By

LAKSHMI CHOCKALINGAM KASI VISWANATH

Bachelor of Science in Chemistry
MADRAS UNIVERSITY
Chennai, Tamilnadu
2004

Master of Science in Applied Chemistry
ANNA UNIVERSITY
Chennai, Tamilnadu
2006

Submitted to the Faculty of the
Graduate College of the
Oklahoma State University
in partial fulfillment of
the requirements for
the Degree of
DOCTOR OF PHILOSOPHY
July, 2013

SYNTHESIS AND CHARACTERIZATION OF
ELECTRON DONOR/ACCEPTOR
SUBPHTHALOCYANINE DERIVATIVES AND
PORPHYRIN METAL COMPLEXES

Dissertation Approved:

Dr. K. Darrell Berlin

Dissertation Adviser

Dr. Richard A. Bunce

Dr. Jeffery L. White

Dr. Toby L. Nelson

Dr. Estella A. Atekwana

ACKNOWLEDGEMENTS

First and foremost, I would like to thank my GOD and Savior, JESUS CHRIST for being with me all through this journey. It is an honor for me to express my deepest gratitude to my supervisor, Dr. K. D. Berlin, for giving me the opportunity to work under his guidance. I will always be indebted to him for giving me tremendous support for the successful completion of my dissertation. Without his constant support and motivation, it would have never been possible to complete this work within the time frame. As words are not sufficient to convey my gratitude and respect on him, I have to admit that I can never thank him enough for all he did. Next, I would like to thank my former advisor, Dr. Laura D. Shirtcliff for acknowledging my capability to perform this new field of research. I am always thankful for her wonderful guidance, support and providing good facilities at the correct time to perform this work without any hurdles.

I would also like to express my sincere thanks to my committee members Dr. Richard A. Bunce, Dr. Toby L. Nelson, Dr. Jeffery L. White and Dr. Estella Atekwana for their immense support throughout my research work by providing valuable inputs and enriching suggestions which considerably improved the overall presentation of my dissertation.

Acknowledgements reflect the views of the author and are not endorsed by committee members or Oklahoma State University.

I am very grateful to Dr. Sadagopan Krishnan, for his enthusiastic support, dedication, guidance in performing and understanding the principle behind the Cyclic Voltammetry, and UV-Vis experiments. I appreciate Dr. Steve Hartson who made available his help in MALDI-TOF experiments. I also want to thank Dr. Margaret Eastman and Dr. Dongtao Cui for their help in NMR spectroscopy.

My sincere and heartfelt thanks to Suaad, Nisha Nitin, Yohan, Aaron, Baskar, Sathish and Charmaine for being very kind and co-operative. I would really like to thank Krishnakumar Gnanasekaran for his memorable help and support not only as a colleague, but also as a friend.

My special thanks to Pas. Leroy, Bro. Antony, Bro. Varghese, for their support and encouragement provided in times of my need. It would be highly unfair if I don't acknowledge the people who have had an immense contribution in my upbringing. In this regard, I would like to express my deepest gratitude to my beloved and respected mother for her priceless love, care, dedication, sacrifice, encouragement, and efforts. My great appreciation goes to my Grandparents, Mr. K. Ramachandran and R. Lakshmi, uncles and aunts, Karthikeyan, Velu, Balu, Saravanan, Gomathy, Alamelu, Soundari and rest of the family for their love and care bestowed upon me.

Acknowledgements reflect the views of the author and are not endorsed by committee members or Oklahoma State University.

It is my privilege to convey my sincere thanks to all my brothers and sisters, Raju, Sundar, Kumar, Vicky, Deepak, Shiva, Venkat, Bhagavathy, Chandra, Sudha, Kavya, Subha and Nithya for being very caring, responsible, and supportive through thick and thin.

The research work reported in this thesis was carried out at the Department of Chemistry, Oklahoma State University starting from January 2009 to July 2013. The financial support from Oklahoma State University is gratefully acknowledged.

Acknowledgements reflect the views of the author and are not endorsed by committee members or Oklahoma State University.

DEDICATION

This dissertation is dedicated to God Almighty who has been my eternal rock and source of refuge, and for His word in Philippians 1:6 that kept me all through the journey of completing this work. I also dedicate this work to my Advisor, Dr. K. D. Berlin for being a pillar of support even through some painful situations.

Name: LAKSHMI CHOCKALINGAM KASI VISWANATH

Date of Degree: JULY, 2013

Title of Study: SYNTHESIS AND CHARACTERIZATION OF ELECTRON
DONOR/ACCEPTOR SUBPHTHALOCYANINE DERIVATIVES AND
PORPHYRIN METAL COMPLEXES

Major Field: CHEMISTRY

Abstract: Multicomponent electron–donor acceptor systems incorporating supramolecules such as porphyrins, phthalocyanines, subphthalocyanines, and perylenes have gained utmost importance in various fields of optoelectronics. Subphthalocyanines are unique, non-planar, aromatic supramolecules which have recently emerged as a platform for novel electron acceptors as they show great potential in photosynthetic systems. Subphthalocyanine is an excellent electron acceptor, when covalently linked to other electron donor species through the axial substitution and executes fast photoinduced electron transfer. The axial approach to a synthesis is advantageous in the sense that the electronic characteristics of the subphthalocyanine macrocycle are preserved. Subphthalocyanine derivatives prepared in this study are expected to have outstanding tunable properties for the development of artificial photosynthetic systems and various molecular electronic devices. This dissertation will center on the synthesis, characterization of various donor-acceptor conjugates of subphthalocyanine.

TABLE OF CONTENTS

Chapter	Page
BACKGROUND	
I. BORON SUBPHTHALOCYANINES	1
1.1 Introduction	1
1.2 Applications	2
1.3 Synthesis	3
1.4 Mechanism of Subphthalocyanine	7
1.5 Reactivity of Subphthalocyanine	9
1.6 Characterization	12
1.7 Subphthalocyanines as Building Blocks for Molecular Materials.....	16
1.8 References	19
II. EFFICIENCY OF HETEROJUNCTION ORGANIC CELLS	23
2.1 Introduction.....	23
2.2 From Photons to Photocurrent	24
2.3 Multicomponent Systems.....	25
2.4 Absorption Studies - Subphthalocyanines Vs Phthalocyanines.....	27
2.5 Covalently Linked Donor/Acceptor Conjugates of SubPcs.....	28
2.6 References	35
RESULTS AND DISCUSSION	
III. SYNTHESIS OF SYMMETRICAL AND UNSYMMETRICAL SUBPHTHALOCYANINE DIMERS CONTAINING A HYDROQUINONE BRIDGE	38
3.1 Introduction.....	38
3.2 Results and Discussion	39
3.3 NMR Spectroscopy.....	43
3.4 UV- Vis Spectroscopy	43
3.5 Experimental.....	45
3.6 Conclusions	52
3.7 References	52
3.8 Appendices	54

Chapter	Page
IV. SYNTHESSES, CHARACTERIZATION AND PROPERTIES OF NOVEL SUBPHTHALOCYANINE – PORPHYRIN CONJUGATES	58
4.1 Introduction.....	58
4.2 Substituted Porphyrins	59
4.3 Significance of the Different Entities in the Porphyrin-SubPc Systems.....	61
4.4 Results and Discussion	62
4.5 Experimental.....	75
4.6 References	88
4.7 Appendices	90
V. AXIAL REACTIVITY OF DODECAFLUOROSUBPHTHALOCYANINE ON THE HYDROQUINONE APPENDED PERYLENE DIIMIDES	100
5.1 Introduction.....	100
5.2 Perylene Diimides	101
5.3 Results and Discussion	105
5.4 Experimental.....	112
5.5 References.....	124
5.6 Appendices.....	127
VI. SYNTHESIS OF SUBPHTHALOCYANINE FUSED DIMERS.....	134
6.1 Introduction.....	134
6.2 Crown Ethers	136
6.3 Synthesis of Crown Ethers.....	136
6.4 Experimental.....	138
6.5 Synthesis of Phthalocyanine and Subphthalocyanine from Catechol.....	145
6.6 Synthesis of Subphthalocyanine Fused Dimers.....	152
6.7 References.....	155
6.8 Appendices.....	156
VII. SYNTHESIS OF STRAINED PORPHYRINOPHANES AS NOVEL SYSTEMS FOR REACTIVITY	160
7.1 Introduction.....	160
7.2 Specific Aims and Significance of the Research	161
7.3 Applications	163

Chapter	Page
7.4 Experimental	163
7.5 Synthesis of Model Porphyrins	164
7.6 Amine Substituted Porphyrins	167
7.7 Synthesis of Porphyrins with Terminal Alkyne Group from 4-Hydroxybenzaldehyde	173
7.8 Synthesis of Porphyrins with Terminal Alkyne Group from 4-Bromobenzaldehyde	176
7.9 Covalent Linkage of the Porphyrins	180
7.10 References	180
7.11 Appendices	182
CONCLUSIONS	185
VITA	186

LIST OF TABLES

Table	Page
1.1 Influence of Temperature	5
1.2 Influence of the Number of Equivalentents of BCl_3	5
1.3 Influence of the Cumene Co-Solvent.....	6
1.4 Reaction on the Peripheral Positions of SubPcs	10
1.5 SubPcs Exhibiting Liquid Crystalline Behavior	19
4.1 Reaction Conditions Followed for the Synthesis of ZnP-SubPc(OBu)_6	64
4.2 Reaction Conditions Followed for the Synthesis of 8a	65
4.3 Electrochemical Data of the Compounds	74
5.1 Electrochemical Data of the Compounds	11

LIST OF FIGURES

Figure	Page
1.1 Chemical Structure and CPK Model of a SubPc	1
1.2 Synthesis of SubPc.....	3
1.3 Peripheral Reactivity of SubPc	9
1.4 Axial Reactivity of SubPc.....	10
1.5 Ring Expansion Reaction of SubPc to Pc	11
1.6 Stick Model of SubPc Showing the Atom Bonds.....	12
1.7 UV-Vis Spectrum of SubPc and Nickel Pc.....	15
1.8 Types of Interaction Between SubPc Molecules in the Crystal.....	17
1.9 Types of Organization Within the SubPcs' Langmuir-Blodgett films	18
2.1 (a) Representation of Photovoltaic Cell	
(b) Energy Diagram of an Organic Solar Cell with a Donor-Acceptor.....	23
2.2 Potential Donor/Acceptor Candidates For Electron Energy Multicomponent Assemblies	26
2.3 (a) Molar Absorptivities of CuPc and SubPc Solutions	
(b) Absorption Coefficients of CuPc and SubPc in Thin Films.....	27
2.4 Chemical Structure of a SubPc- Pc Dyad	28
2.5 SubPc- C ₆₀ Dyad.....	29
2.6 SubPc Dimer- C ₆₀ Dyad.....	29
2.7 SubPc-Ferrocene Dyad	30
2.8 SubPc-Triphenylamine dyad.....	30
2.9 (a) SubPc – C ₆₀ Dyad (C-C bond) (b) SubPc – C ₆₀ Dyad (C-O bond)	31
2.10 SubPc- BODIPY Dyad (B-O bond).....	32
2.11 (a) SubPc- BODIPY Dyad (B-C bond) (b) SubPc-Os Complex Dyad	32
2.12 SubPc-Polymethine Conjugate	33
2.13 Structure of <i>hexa</i> -[B(SubPc)]	34
2.14 Ternary Complex of SubPc(CD)-TPPS- SiPc(CD) ₂	35
3.1 Tubular Representation of Various SubPc Dimers.....	39
3.2 NMR Spectra of the Dimers	44
3.3 ¹ H NMR Spectrum of 4a	55
3.4 ¹ H NMR Spectrum of 4b	55
3.5 ¹ H NMR Spectrum of 4c	56
3.6 UV-Vis Spectra of the Dimers.....	56

Figure	Page
3.7 Emission Spectra of the Dimers.....	57
4.1 Representation of Different <i>meso</i> -substituted Zinc Porphyrins (ZnP)	60
4.2 Significance of the Entities Involved in the Illustrated System.....	61
4.3 Representation of the Synthesized Compounds.....	67
4.4 Absorption Spectra of the Compounds in Toluene.....	68
4.5 Absorption Spectra of the Compounds in CH ₂ Cl ₂	69
4.6 Emission Spectrum of the Compounds in Toluene at 424 nm	70
4.7 Emission Spectrum of the compounds in CH ₂ Cl ₂ at 420/419 nm.....	70
4.8 Cyclic Voltammogram of Porphyrins MPP and DPP.....	72
4.9 Cyclic Voltammogram of SubPc, MPP and MPS	73
4.10 Cyclic Voltammogram of the Conjugates MPS, DPPS1 and DPPS2.....	73
4.11 Structure of DPPS1	75
4.12 ¹ H NMR Spectrum of 5b	91
4.13 ¹³ C NMR Spectrum of 5b	91
4.14 ¹ H NMR Spectrum of 8a	92
4.15 ¹³ C NMR Spectrum of 8a	92
4.16 ¹⁹ F NMR Spectrum of 8a	93
4.17 Mass Spectrum of 8a	93
4.18 ¹ H NMR Spectrum of 9a	94
4.19 ¹³ C NMR Spectrum of 9a	94
4.20 ¹⁹ F NMR Spectrum of 9a	95
4.21 Mass Spectrum of 9a	95
4.22 ¹ H NMR Spectrum of 9b	96
4.23 ¹³ C NMR Spectrum of 9b	96
4.24 ¹⁹ F NMR Spectrum of 9b	97
4.25 Mass Spectrum of 9b	97
4.26 ¹ H NMR Spectrum of 10a	98
4.27 ¹³ C NMR Spectrum of 10a	98
4.28 ¹⁹ F NMR Spectrum of 10a	99
4.29 Mass Spectrum of 10a	99
5.1 Covalently Linked SubPc-PDI Conjugate with B-N Bond.....	101
5.2 Chemical Structure of (a) Perylene (b) A Perylene Diimide	102
5.3 (a) Bond lengths in a PDI molecule (b) Preferred Conformation of the Phenoxy Substituents in Bay-Substituted PDI	104
5.4 Representation of the Synthesized Compounds.....	106
5.5 Absorption Spectra of Dihydroxybenzene Appended PDIs	107
5.6 Absorption Spectra of PDI-SubF Conjugates.....	108
5.7 Emission Spectra of Dihydroxybenzene Appended PDIs	109

Figure	Page
5.8 Emission Spectra of PDI-SubF Conjugates	109
5.9 Cyclic Voltammogram of Dihydroxybenzene Appended PDIs.....	110
5.10 Cyclic Voltammogram of PDI-SubF Conjugates	111
5.11 ¹ H NMR Spectrum of 7a	128
5.12 ¹³ C NMR Spectrum of 7a	128
5.13 ¹ H NMR Spectrum of 7b	129
5.14 ¹³ C NMR Spectrum of 7b	129
5.15 ¹ H NMR Spectrum of 7c	130
5.16 ¹³ C NMR Spectrum of 7c	130
5.17 ¹ H NMR Spectrum of 8a	131
5.18 ¹³ C NMR Spectrum of 8a	131
5.19 ¹ H NMR Spectrum of 8b	132
5.20 ¹³ C NMR Spectrum of 8b	132
5.21 ¹ H NMR Spectrum of 8c	133
6.1 Synthesis of a SubPc Fused Dimer	134
6.2 Syn and Anti Topoisomers of a SubPc Fused Dimer	135
6.3 Synthesis of Benzocrown Ethers	137
6.4 ¹ H NMR Spectrum of 10	157
6.5 ¹³ C NMR Spectrum of 10	157
6.6 Mass Spectrum of 10	158
6.7 ¹ H NMR Spectrum of 11	158
6.8 Mass Spectrum of 11	159
7.1 Representation of the Synthesis of the Deformed Porphyrinophanes	161
7.2 A Representative Sample of Deformation of the Base Porphyrinophanes	162
7.3 ¹ H NMR Spectrum of 6a	183
7.4 ¹ H NMR Spectrum of 7	183
7.5 ¹ H NMR Spectrum of 9a	184
7.6 ¹ H NMR Spectrum of 9b	184

LIST OF SCHEME

Scheme	Page
1.1 Formation of the Hydrolysis Product.....	8
1.2 Progressive Assembly of SubPc Macrocycle 6 through Intermediate 5	8
1.3 Ring Closure of the SubPc Precursor 6 into 7 and Reduction to SubPc.....	9
3.1 Synthesis of Subphthalocyanine Dimers	40
4.1 Synthesis of A ₃ B and <i>trans</i> meso-Substituted A ₂ B ₂ Porphyrins	63
4.2 Attempted Synthesis of Target ZnP-SubPc Conjugate.....	64
4.3 Synthesis of Porphyrin-SubPc-F ₁₂ Conjugate.....	66
5.1 Synthesis of SubPc-PDI.....	105
5.2 Synthesis of Terminal Alkyne Substituted PDI.....	122
6.1 Synthesis of 12-crown 4.....	139
6.2 Synthesis of 18-crown 6.....	139
6.3 Synthesis of SubPc and Pc.....	145
6.4 Synthesis of SubPc Fused Dimers	152
7.1 Synthesis of Model Porphyrins.....	165
7.2 Synthesis of Amine Substituted Porphyrins	168
7.3 Synthesis of Terminal Alkyne Substituted Porphyrin	172
7.4 Synthesis of Terminal Alkyne Substituted Porphyrins from 4-Bromo Benzaldehyde.....	177

CHAPTER I

BACKGROUND

BORON SUBPHTHALOCYANINES

1.1 Introduction

Subphthalocyanines (SubPcs) are the lowest homologues of phthalocyanines (Pcs) consisting of three diiminoisoindole rings which are N-fused around a boron core. The non-planar, cone-shaped structure and their 14π -electron aromatic core (Figure 1.1) make them very special, exhibiting unusual electrical and optical properties.¹ When Meller and Ossko¹ made an effort to synthesize the boron Pc by the cyclotetramerization of phthalonitrile, surprisingly they observed the formation of a purple compound which was later identified as boron SubPc by electron impact mass spectrometry, UV- visible spectrophotometry, and elemental analysis.²

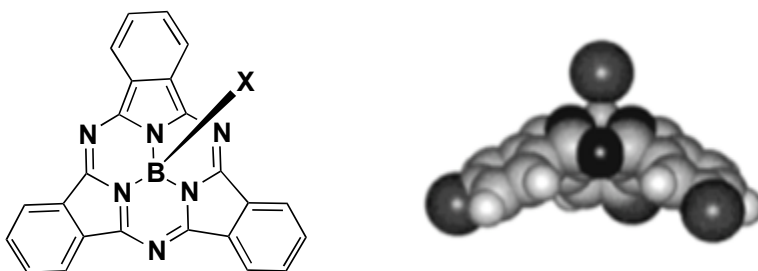


Figure 1.1 Chemical Structure and CPK Model of a SubPc.

SubPcs are among those very few known examples of non-planar aromatic compounds. The significance of SubPcs range from a purely synthetic point of view to the applied physical and optical properties. In general, SubPcs are obtained in good yields by the cyclotrimerization reaction of the phthalonitrile precursors in the presence of a boron derivative (typically BX_3).³

1.2 Applications

The applications of SubPcs are manifold.

1. The non-planar, constrained makeup of SubPcs allows them to be good precursors for the synthesis of unsymmetrically substituted phthalocyanines when reacted with suitable diiminoisoindoline derivatives.⁴ SubPcs are usually highly, reactive, relative to their phthalocyanine homologues. A halogen atom at the axial position can be easily displaced by nucleophiles such as oxygen, nitrogen and carbon to give substituted SubPc derivatives.⁵⁻⁷
2. While multifunctional molecular materials, as well as nonlinear optical properties are attractive fields of increasing research in the current scenario, SubPcs play a vibrant role in both fields as a consequence of their octupolar character. The high second-order nonlinear responses of SubPcs could be potentially employed as building blocks to create hybrid, inorganic-organic compounds which could exhibit combined physical properties of the inorganic and organic materials.⁸
3. SubPc chromophores can also participate in multistep electron-transfer processes when coupled with different chromophores.⁹
4. The purple color of the SubPcs is considered to be the basis of attractive dyes for electrolithography and/or for printing.¹⁰

5. The excited state properties of the SubPcs brand them as good photosensitizers which could be potentially applied in photodynamic therapy (PDT).¹¹
6. SubPcs could also act as recording media which could be utilized for rewriting at short wavelengths.¹²

1.3 Synthesis

1.3.1 Influence of the Boron reagent

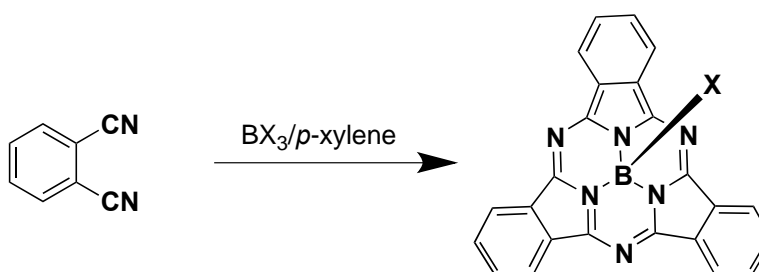
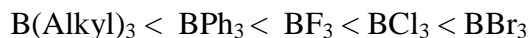


Figure 1.2 Synthesis of SubPc.

Thus far BX_3 and BX_2Y (X and Y may be butyl, phenyl, fluorine, chlorine, or bromine) are the general boron reagents that have been successfully employed (Figure 1.2) in the synthesis of SubPcs. The order of reactivity of these boron reagents¹³ toward the phthalonitrile derivative is closely related to their Lewis acidity and was experimentally observed to be:



The selection of the boron reagent is contingent on the purpose of the SubPc synthesis as well as on the chemical compatibility between the phthalonitrile derivative and the boron reagent.

(a) Boron tribromide

Although boron tribromide readily reacts with phthalonitrile to afford the corresponding bromosubphthalocyanine (BrSubPc), they are fairly unstable, relative to other axially substituted subphthalocyanines.¹⁴

(b) Boron trichloride

The most commonly reported boron reagent for SubPc synthesis is boron trichloride¹⁵ which is commercially available as a 1 *M* solution in *p*-xylene, dichloromethane, heptane or hexanes. The utilization of BCl₃ has allowed the synthesis of a wide range of chlorosubphthalocyanines (Cl-SubPcs) in a one step reaction. In the solid state, the Cl-SubPcs are stable on a month time-scale whereas decomposition in solution in the presence of light is observed. Both peripherally- and axially-substituted SubPcs are quite soluble (0.1 *M*) in a wide variety of organic solvents, such as toluene, benzene, acetone, ethyl acetate, dichloromethane, chloroform, diethyl ether, THF etc. The relative stability of the SubPcs depends solely on the nature of their peripheral substituents, with triiodo SubPc being the most stable of all the SubPcs reported.¹⁶

(c) Boron trifluoride and triphenylboron

The comparatively low reactivity and difficult handling of boron trifluoride has limited its use in the synthesis of SubPcs. Reactions conducted with triphenylboron are low yielding and demand high temperature as a consequence of their low reactivity.¹⁷

1.3.2 Influence of the temperature

Table 1.1 Influence of Temperature.

T (°C)	Yield (%)
0	0
45	19
100	57
138	82

The influence of temperature (Table 1.1) on the formation of a Cl-SubPc was studied by Claessens et al.¹⁸ Reaction of phthalonitrile with boron trichloride carried out in an ice bath resulted in no product. Although the reaction proceeded at 45 °C, it resulted only in a low yield (19%) of product after 2 h. However, the condensation of phthalonitrile was more efficient when the temperature of the reaction was increased from 100 °C to 138 °C, with yields ranging from 57% to 82%, respectively.

1.3.3 Influence of the Number of Equivalents of BCl₃

Table 1.2 Influence of the Number of Equivalents of BCl₃.

BCl ₃ equivalent (mol/mol SubPc)	Yield (%)
1	19
2	32
3	82
4	72

All of the synthetic procedures reported in the literature employ a large excess of BCl_3 . Higher reaction yields (82%) were obtained when three equivalents of BCl_3 per SubPc (one equivalent per starting phthalonitrile) were used (Table 1.2). Nevertheless, higher excesses of BCl_3 resulted in lower yields.

1.3.4 Influence of the Cumene Co-solvent

Table 1.3 Influence of the Cumene Co-Solvent.

Volume of cumene (mL)	Purification Method			
	(i)	(ii)	(iii)	(iv)
0	82	82	82	82
2	23	34	46	77
4	10	16	21	71

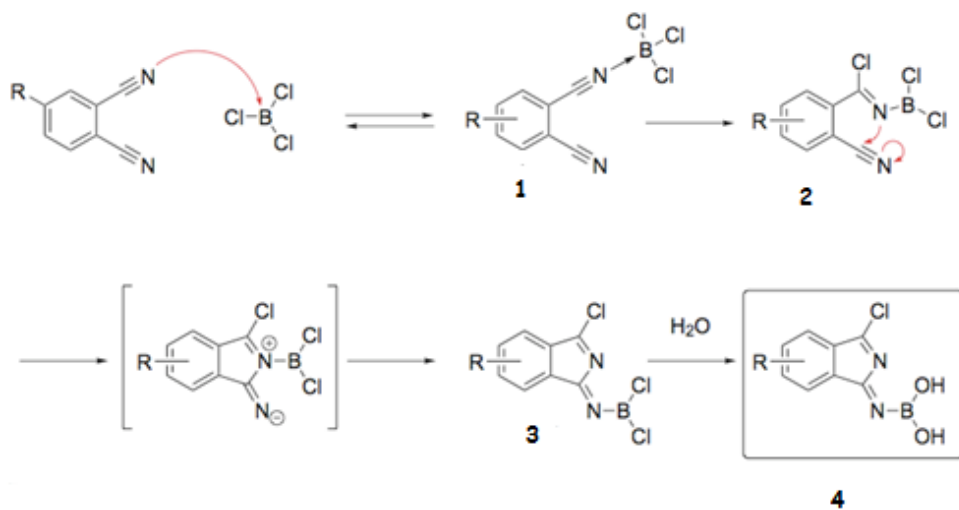
Solvents, such as 1-chloronaphthalene, 1-methylnaphthalene, naphthalene, 1,2,4-trichlorobenzene, and chlorobenzene, have been used for the synthesis of SubPcs.¹⁹ Both purity, as well as dryness of the solvents, are critical factors in determining the yields of the synthesized SubPcs. This became evident when a series of experiments were carried out engaging cumene as a co-solvent (Table 1.3) which was treated using four different methods prior to the reaction as shown below.

- i. cumene - without any treatment
- ii. cumene - dried through alumina column
- iii. cumene - purified by distillation
- iv. cumene – thoroughly purified and dried after washing with conc. sulfuric acid, followed by washing with water and 10% NaHCO_3 solution, drying (MgSO_4).

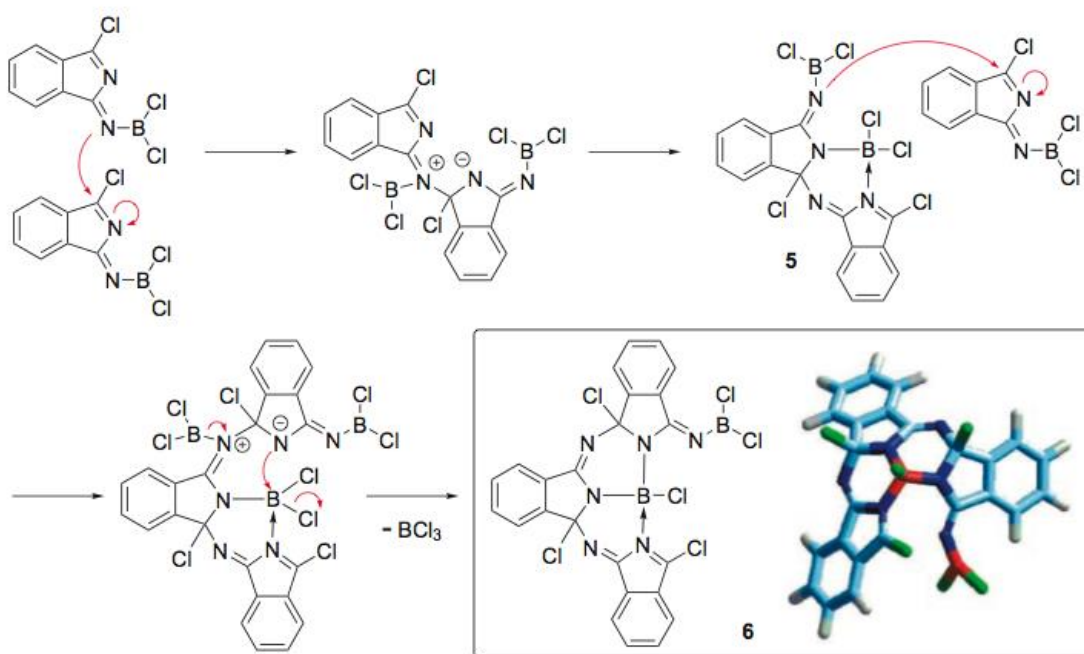
From Table 1.3 it is obvious that the yield of SubPcs increased with the use of cumene that was treated by method iv. In addition, higher dilution had a negative effect on the outcome of cyclotrimerization.¹⁹

1.4 Mechanism of SubPcs

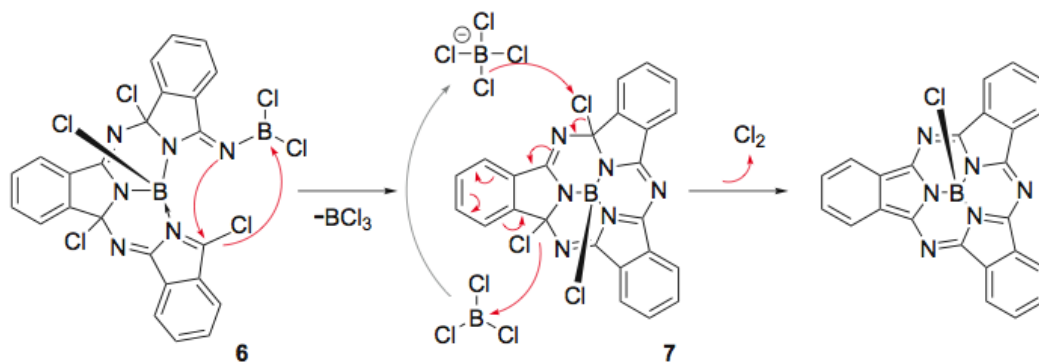
Until 2006, no convincing attempt was made on the determination of the mechanism of formation of a SubPc. However, in 2007 Claessens proposed a mechanism which was supported by computer thermochemical data. According to the proposed mechanism, the first stage in the oligomerization reaction in the phthalonitrile- BCl_3 systems of **1** and **2** results in the formation of the adduct **3** (Scheme 1.1). Rapid hydrolysis of compound **3** under adventitious moisture led to **4**. In Scheme 1.2 three molecules of **3** ($\text{R} = \text{H}$) lead to dimer **5** and then to **6**. It is of special significance for the three pyrrole nitrogen atoms to be coordinated to a central boron atom as this spatial arrangement assures the close proximity between the imine carbon and the *meso* nitrogen atom. The final ring closing step occurs by the linking of the imine carbon and the meso nitrogen atom. Moreover, it is significant that the boron atom acts as a template for the cyclization to proceed *via* **7**, precursor of the target (Scheme 1.3)



Scheme 1.1 Formation of the Hydrolysis Product.



Scheme 1.2 Progressive Assembly of SubPc Macrocycle **6** through Intermediate **5**.



Scheme 1.3 Ring Closure of the SubPc Precursor **6** into **7** and Reduction to a SubPc.

1.5 Reactivity of Subphthalocyanine

The reactivity of SubPc is divided into three different categories based on the reactive center:

- (i) peripheral reactivity,
- (ii) axial reactivity,
- (iii) ring expansion reaction.

While axial and peripheral reactions generate modified SubPcs, ring expansion results in the destruction of the subphthalocyanine skeleton and formation of a low symmetry phthalocyanine.⁴

1.5.1 Peripheral Reactivity

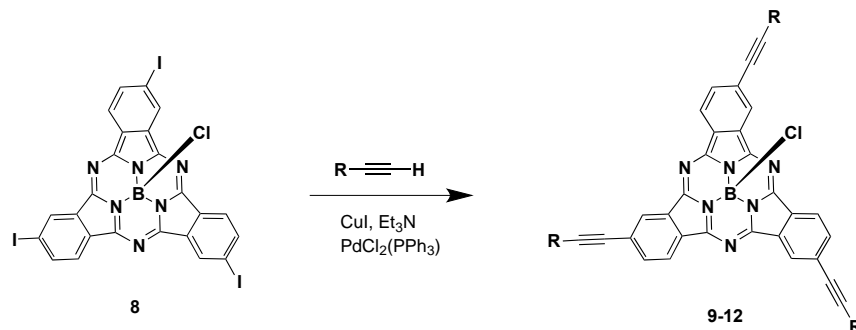


Figure 1.3 Peripheral Reactivity of SubPc.

In an effort to synthesize highly conjugated SubPcs, Torres performed a reaction involving alkynes and aryl iodides *via* a Sonogashira Pd-mediated cross coupling (Figure 1.3).²¹ The reaction yields were generally consistent (~30%) (Table 1.4), considering the fact that three C-C bonds had to be formed for each SubPc molecule.

Table 1.4 Reaction on the Peripheral Positions of SubPcs.

Product	R	Yield
9	TMS	60%
10	n-C ₃ H ₇	28%
11	CH ₂ OCH ₃	26%
12	(C ₆ H ₄)-4-NO ₂	29%

Recently, a series of Pc-SubPc dyads were prepared by coupling an alkynyl-substituted phthalocyanine to a series of unsymmetrically substituted I-SubPcs.²²

1.5.2 Axial Reactivity

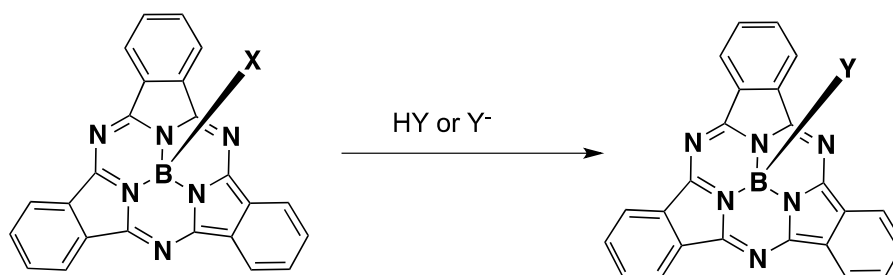


Figure 1.4 Axial Reactivity of SubPc.

An important aspect of the axial reactivity is that the electronic characteristics of the SubPcs are preserved (Figure 1.4). Different bromo- and chloroSubPcs were reacted with a wide variety of oxygen nucleophiles to afford axially substituted SubPcs. While

Br-SubPcs readily undergo nucleophilic substitution, it may require harsher conditions in the case of Cl-SubPcs.²³ The rates and yields of substitution increases with the presence of peripheral donor groups, perhaps by stabilization of an eventual positive charge on the boron atom.¹⁹ Hence, column chromatography over silica gel of some subphthalocyanines yielded substantial amounts of hydroxyl-substituted SubPcs. In most of the cases the hydrolyzed product, phthalimide, was also obtained.¹⁹

The substitution of the alkyl halide by a nucleophile is effected in many different ways. Hydroxyl-substituted SubPcs were synthesized by refluxing a suspension of the SubPc in water, pyridine/water, or acetonitrile/water.²⁴ Methods, such as ion-exchange resin and phase-transfer catalysis with 18-crown-6, also have been utilized for the axial exchange with OH groups.²⁵ Although hydroxyl groups were the most common nucleophiles, a few attempts were also made with carbon and nitrogen nucleophiles.³

1.5.3 Ring Expansion Reaction

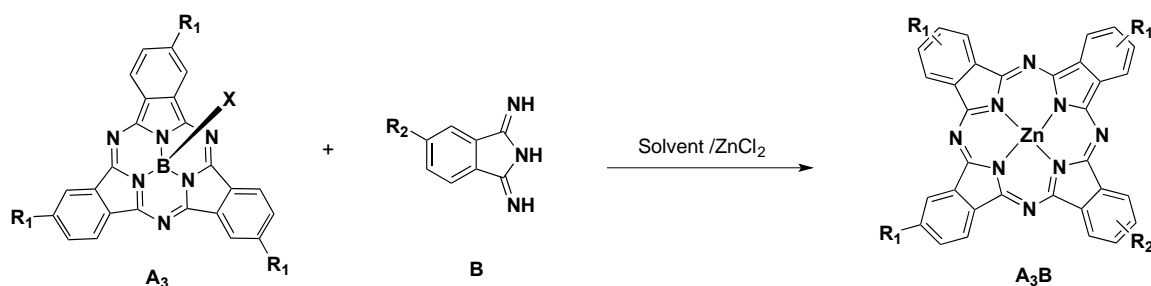


Figure 1.5 Ring Expansion Reaction of SubPc to Pc.

While a number of symmetrically substituted phthalocyanines (Pcs) are obtained by the cyclotetramerization of the phthalonitrile precursor, it is relatively difficult to synthesize the unsymmetrical phthalocyanine (A₃B). The most sophisticated route for the synthesis of unsymmetrically substituted phthalocyanines (A₃B) was devised by

Kobayashi *via* reacting a molecule of geometrically constrained SubPc (A_3) with 1,3-diiminoisoindoline derivatives (B) to form the A_3B phthalocyanines (Figure 1.5).⁴ The selectivity of this technique depends on several factors:

- i. nature of the peripheral substituents of the SubPc,
- ii. reactivity of the diiminoisoindoline derivative,
- iii. reaction temperature,
- iv. solvent.

Some advantages of this method over the statistical cyclotetramerization include (i) selectivity, (ii) high yields, and (iii) simple purification procedures as there are no by-products involved.

1.6 Characterization

1.6.1 X-ray Structure Analysis



Figure 1.6 Stick Model of SubPc Showing the Atom Bonds.

The remarkable feature of all X-ray crystal structures of SubPcs is their constrained cone shaped geometry (Figure 1.6). The SubPc macrocyclic core is exceptionally rigid in such a way that the N_i and $C_{\alpha,\beta,\gamma,\delta}$ atom positions are essentially independent of the axial or peripheral substitution. The main geometrical alterations occurring, due to the change of X ligand on the boron atom, remain limited to the $BX(N_i)_3$ tetrahedron. The angles

involving the boron atom are slightly deformed with respect to the ideal tetrahedron, N_i -B- N_i and Cl-B- N_i angles ranging from 103° to 105° and from 109° to 118° , respectively.¹⁹ Depending on the axial X ligand, the boron atom lies from 0.59 Å to 0.66 Å above the plane. With an increase in the electronegativity of the X ligand that is directly linked to the boron atom, the pyramidalicity of SubPc increases. The B-O bond is slightly tilted around 10° towards one of the pyrrole rings. The three B- N_i distances are identical and are significantly shorter than the standard B-N single bond (1.611 Å) holding an average value of 1.467 Å.²⁶ Since the boron atom is already tetra co-ordinated, further shortening of the B- N_i would be virtually impossible. In comparison to the phthalocyanine, the geometric parameters of SubPc vary only slightly with comparable bond lengths for most bonds with slightly shorter C_α - N_i and longer C_α - N_{br} bonds. The C_α - N_i - C_α bond angles are characteristically larger in the case of SubPcs, signifying that the coordination of a boron atom to the isoindole nitrogen N_i forces it away from the plane P. The N_i - C_α (1.366 Å) bond is longer than the N_{br} - C_α (1.345 Å)¹⁹ bond due to the partial loss of the single and double bond character, respectively. The N_i nitrogen atom is located above the plane, and the pyrrole rings are non planar.

1.6.2 ¹H NMR Spectroscopy

In contrast to the phthalocyanines, which form aggregates, the SubPcs yield well-defined ¹H NMR spectra. The chemical shifts of the SubPc protons do not depend on the concentration of the sample. The strong diamagnetic ring current of the SubPc macrocycle causes the protons attached to the C_γ and C_δ carbon atoms to shift to a low field (7.8 to 9.9 ppm). The protons of the axial ligand that are pointing towards the SubPc are shifted to high field (Figure 1.6).⁹

1.6.3 Mass Spectrometry

Meller and Ossko characterized their first SubPc molecule by electron impact mass spectroscopy.² The fragmentation pattern obtained was consistent and characteristic of a compound containing three diiminoisoindole units, a boron atom and a chlorine atom. MALDI, FAB and LSIMS spectrometry techniques are particular useful and, in most cases, the molecular ion is the major peak. The peak corresponding to the loss of the axial ligand is very commonly observed. Increases in intensities of such peaks are often observed for SubPc containing donor groups in the peripheral positions, which is attributed to the increased ionic character of the B-X bond.¹⁹

1.6.4 UV-Vis Spectroscopy

Both SubPcs and Pcs show a comparable UV-Vis spectra in the sense they exhibit a low energy Q band and a high energy Soret B band, analogous to those of the other aza aromatic macrocycles. The SubPcs exhibit a slight red shift for both Soret band (300 nm) and the Q band (560 nm) with respect to the Pcs as a result of the decrease of the π -conjugation system (Figure 1.7). Moving from Pcs to the Subpcs, the absorption coefficients of Q bands as well as B bands decreases. The non-planar nature of the SubPcs is responsible for the smaller Q-band intensity compared to the Pcs.²⁷ Although the peripheral donor and acceptor substituents tend to shift the Q-band toward longer wavelengths, no significant effect is caused by axial substitution.

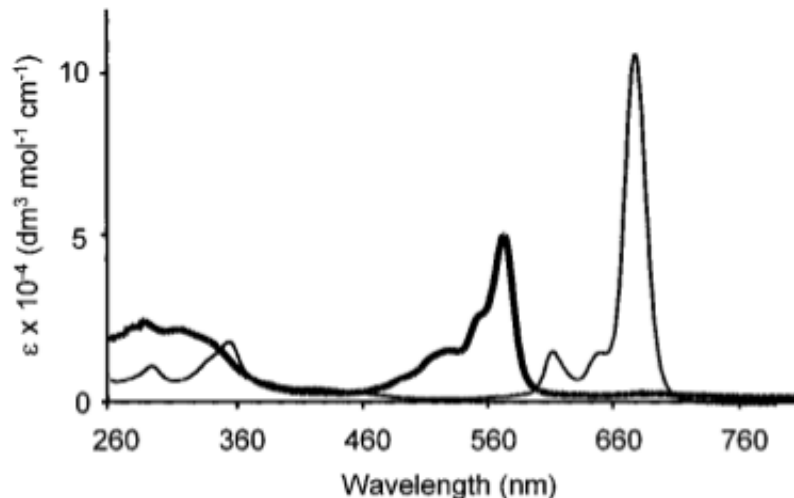


Figure 1.7 UV-Vis Spectrum of SubPc (thick line) and Nickel Pc (thin line).

1.6.5 Redox Properties

The first oxidative or reductive half-wave potentials of SubPcs involve one electron which is usually observed at around 1 V and -1 V, respectively. In general, the reduction appears to be reversible on the cyclic voltammetry scale while the oxidation is quasi-reversible and is also accompanied by some decomposition. The redox properties of SubPcs are altered intensely with the nature of the peripheral substituents on the macrocycle.²⁸ The fluoro and nitro derivatives are the easiest to reduce, relative to the unsubstituted SubPc.^{3,15}

1.6.6 Excited States of Subphthalocyanine

The bowl structure of SubPcs offers distinct photophysical properties that compare favorably to those shown by related planar phthalo- and naphthalocyanines. Extensive research is being done on the development of second-generation compounds for photodynamic therapy. The most commonly studied candidates are planar and lead to stacking in biological media, which results in effective loss of photosensitizing properties. On the other hand, SubPcs with their cone-shaped structures do not form aggregates,¹⁹

and, in turn, possess higher singlet and triplet oxygen quantum yields that makes them responsive to cytotoxicity for exploring their use in photodynamic therapy applications. Subphthalocyanines are fluorescent^{15a, 28} with quantum yields, ϕ_F , ca. 0.25, which is about one-half the value observed for related phthalocyanines, e.g., $\phi_F = 0.58$, for AlPcCl.¹⁹ Obviously, non radiative deactivation channels, i.e., internal conversion and intersystem crossing, are more efficient for SubPcs than Pcs. In addition, the lifetimes of the excited singlet state,¹⁹ τ_S , is about 3 ns for most compounds, about one-half the value for phthalocyanines. SubPcs also have larger triplet quantum yields than Pcs. The triplet state lifetime is of the order of 100 μ s which is long enough for efficient oxygen quenching. The singlet to triplet energy gap (30-40 kJ mol⁻¹)¹⁹ for SubPcs is smaller than the phthalocyanines. The SubPcs act as excellent photosensitizers and produce singlet oxygen in large quantities which occurs by the exothermic energy transfer from the highly populated, long-life triplet state. SubPcs are considered to be suitable and interesting candidates for use in photosensitization processes where absorption in the red part of the spectrum is not required.

1.7 Subphthalocyanines as Building Blocks for Molecular Materials

1.7.1 Organization in the Solid State

The type of intermolecular interactions that withstand the cohesion between identical molecules (Figure 1.8) can be derived from the packing in the solid state. In the case of subphthalocyanines, two types of interactions exist, depending on the axial substituent on the boron atom:

- i. SubPc **14** exhibits overlap between the concave faces of the SubPcs,²⁹
- ii. SubPc **15** exhibits a pronounced overlap between the isoindole units.⁵

The UV-Vis spectrophotometry performed in the solid state for **14** and **15** is consistent with the two different packings with noticeable broadening of spectra observed for SubPc **15**.¹⁹

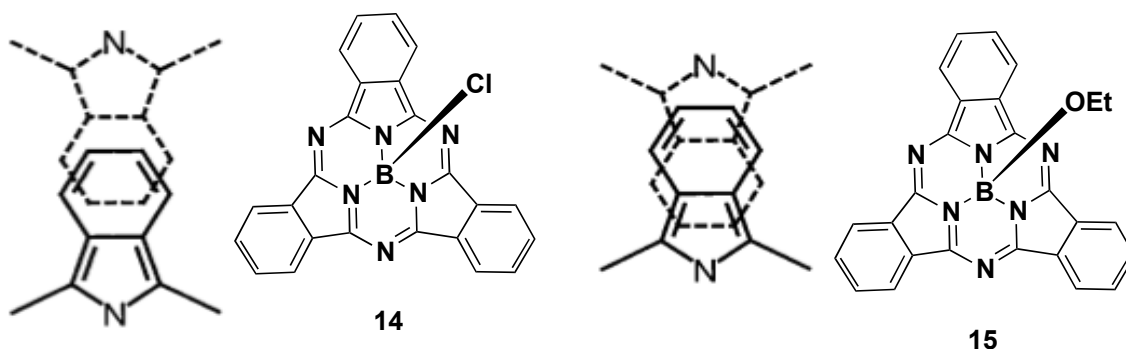


Figure 1.8 Types of Interaction Between SubPc Molecules in the Crystal.

1.7.2 Organization in Thin films

One of the best ways for obtaining well-defined multilayers of an organic compound on a solid support is the Langmuir-Blodgett films.³⁰ The organization of different SubPcs in Langmuir films revealed poor stability of the monolayer which is evident from the low collapse pressure of the films.⁷ The π - π interactions between the SubPc molecules were significantly prevented by the axial X ligand as observed in the case of phthalocyanines.³¹ A comparison of the calculated and experimental areas per molecules (Figure 1.9) suggested that SubPc **16** possesses an edge-on disposition whereas SubPc **17** lies flat on the surface at the water/gas interface (Figure 1.9). The results imply that by increasing the number of polar groups in the periphery, or by adding bulky groups in the axial position, the orientation of SubPcs in air/water interface can be chemically controlled.

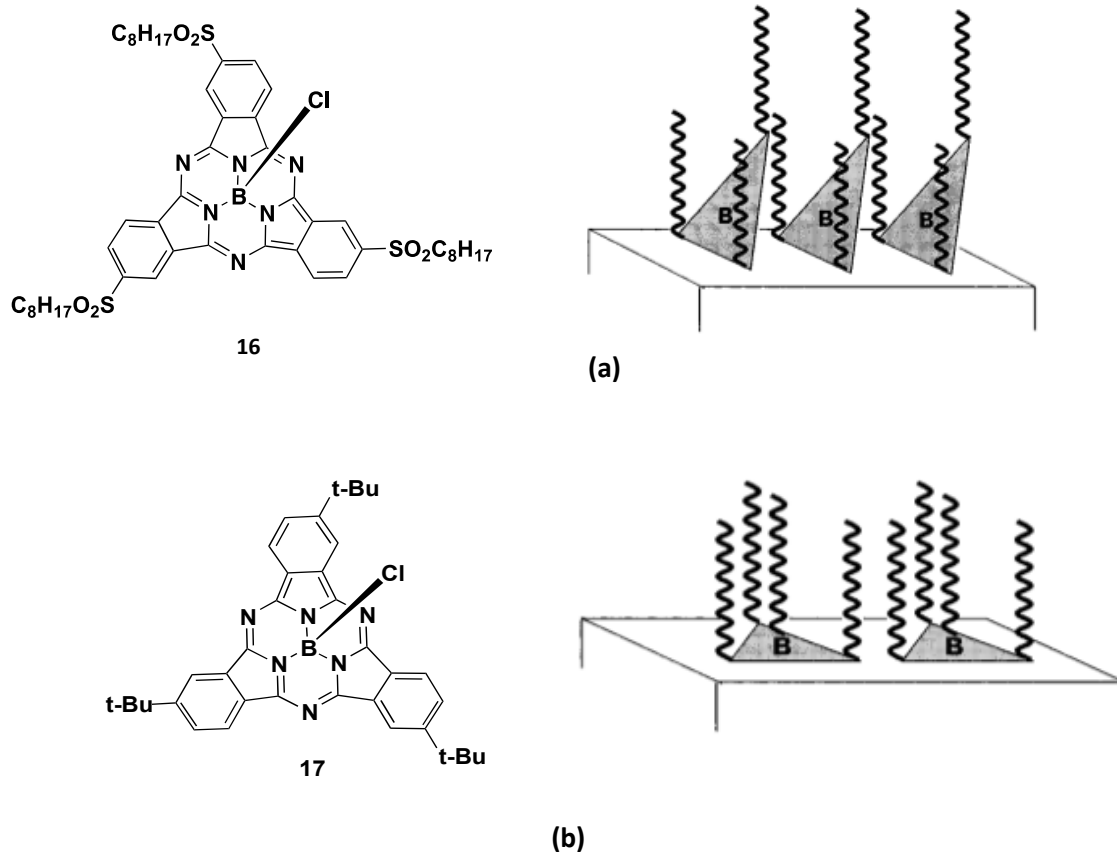


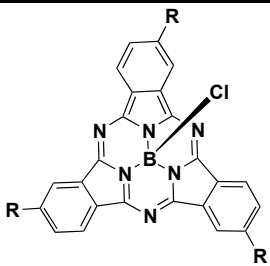
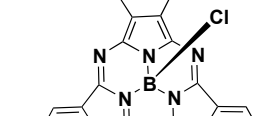
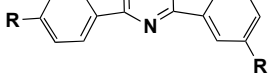
Figure 1.9 Types of Organization Within the SubPcs' Langmuir-Blodgett films.

1.7.3 Organization in Liquid Crystals

SubPcs have also been considered as potential columnar mesogens as a consequence of their cone shaped geometry. SubPcs **18-20** (Table 1.5) show enantiotropic liquid crystalline behavior revealed by differential scanning calorimetry (DSC), polarizing optical microscopy, and X-ray diffraction.⁸ SubPc **18** exhibited mesomorphic behavior at room temperature, and **19** showed transition from crystalline to mesophase close to the room temperature which finally transforms into an isotropic liquid at 75 °C.⁸ At room temperature, SubPc **20** is a solid while at 43 °C it melts to form a mesophase which turns into an isotropic liquid phase at 70 °C.⁸ Optical polarizing microscopy conducted on all

these compounds showed that they exhibit pseudo-focal conic textures, characteristic of columnar phases.⁸

Table 1.5 SubPcs Exhibiting Liquid Crystalline Behavior

Compound	R
	18 <i>S-n</i> -C ₁₀ H ₂₁
	19 <i>S-n</i> -C ₁₆ H ₃₃
	20 <i>S-n</i> -C ₁₈ H ₃₇

1.8 References

1. Kadish, K. M.; Smith, K. M.; Guillard, R. *The Porphyrin Handbook*, 2002, Vols. 13-16, Academic Press, San Diego.
2. Meller, A.; Ossko, A. *Monatsch. Chem.* **1972**, 103, 150-155.
3. Geyer, M.; Plenzig, F.; Rauschnabel, J.; Hanack, M.; del Rey, B.; Sastre, A.; Torres, T. *Synthesis*. **1996**, 1139-1151.
4. Kobayashi, N.; Kondo, R.; Nakajima, S.I.; Osa, T. *J. Am. Chem. Soc.* **1990**, 112, 9640-9641.
5. Kasuga, K.; Idehara, T.; Handa, M.; Ueda, Y.; Fujiwara, T.; Isa, K. *Bull. Chem. Soc. Jpn.* **1996**, 69, 2559-2563.
6. Potz, R.; Goldner, M.; Huckstadt, H.; Cornelissen, U.; Tutab A.; Homborg, H. Z. *Anorg.Allg. Chem.* **2000**, 626, 588-596.

7. Martinez-Diaz, M. V.; del Rey, B.; Torres, T.; Agricole, B.; Mingotaud, C.; Cuvillier, N.; Rojo, G.; Agullo-Lopez, F. *J. Mater. Chem.* **1999**, 9, 1521-1526.
8. Ho Kang, S.; Kang, Y. S.; Zin, W. C.; Olbrechts, G.; Wostyn, K.; Clays, K.; Persoons, A.; Kim, K. *Chem. Commun.* **1999**, 1661-1662.
9. Gonzalez-Rodriguez, D.; Torres, T.; Guldi, D.; Rivera, J.; Echegoyen, L. *Org. Lett.* **2002**, 4, 335-338.
10. Reynolds, S. J.; Gairns, R. S.; Simpson, P. A. (Zeneca Ltd.) PCT Int. Appl. WO 94,24,612, 1994; *Chem. Abstr.* **1995**, 122, 326420e.
11. Nonell, S.; Rubio, N.; del Rey, B.; Torres, T. *J. Chem. Soc. Perkin Trans.2* **2000**, 1091-1094.
12. Wang, Y.; Gu, D.; Gan, F. *Guangxue Xuebao.* **2001**, 21, 948- 951. (b) Wang, Y.; Gu, D.; Gan, F. *Phys. Status Solidi A* **2001**, 186, 71-77. (c) Wang, Y.; Gu, D.; Gan, F. *Opt. Commun.* **2000**, 183, 445-450. (d) Hunt, P. (Imperial Chemical Industries PLC, UK) Brit. UK Pat. Appl. GB 2,290,489, 1996; *Chem. Abstr.* **1996**, 124, 234870q.
13. Bailar, J. C.; Emeleus, H. J.; Nyholm, R.; Trotman-Dickenson, A. F. *Comprehensive Inorganic Chemistry*, 1973, Vol. 1, Pergamon, New York.
14. (a) Tu, H. Y.; Tian, H. *Yingyong Huaxue* **2000**, 17, 174-176. (b) Liang, Z. -J.; Tang, F. -L.; Gan, F. -X.; Xun, Z. -R.; Yang, X. -H.; Ding, L. -E.; Wang, Z. -G. *Wuli Xuebao.* **2000**, 49, 252-255.
15. (a) Kipp, R. A.; Simon, J. A.; Beggs, M.; Ensley, H. E.; Schmehl, R. H. *J.Phys.Chem.A* **1998**, 102, 5659-5664. (b) Lee, S.; Suh, H. *Bull. Korean Chem.*

- Soc.* **1999**, 20, 991-992. (c) Claessens, C. G.; Torres, T. *Chem. Eur. J.* **2000**, 6, 2168-2172.
16. Rojo, G.; Agullo-Lopez, F.; del Rey, B.; Torres, T. *J. Appl. Phys.* **1998**, 84, 6507-6512.
17. Wang, X.; Tang, D.; Zhen, Z.; Zhang, J.; Liu, X. *Ganguang Kexue Yu Guang Huaxue.* **1999**, 17, 168-171.
18. Claessens, C. G.; Gonzalez-Rodriguez, D.; del Rey, B.; Torres, T.; Mark, G.; Schuchmann, H. -P.; von Sonntag, C.; MacDonald, J. G.; Nohr, R. S. *Eur. J. Org. Chem.* **2003**, 2547-2551.
19. Claessens, C. G.; Gonzalez-Rodriguez, D.; Torres, T. *Chem. Rev.* **2002**, 102, 835-853.
20. Claessens, C. G.; Gonzalez-Rodriguez, D.; Mc Callum, C. M.; Nohr, R. S.; Schuchmann, H. -P.; Torres, T. *J. Porphyrins Phthalocyanines.* **2007**, 11, 181-188.
21. del Rey, B.; Torres, T. *Tetrahedron. Lett.* **1997**, 38, 5351-5354.
22. González-Rodríguez, D.; Claessens, C. G.; Torres, T.; Liu, S.; Echegoyen, L.; Vila, N.; Nonell, S.; *Chem. Eur. J.* **2005**, 11, 3881-3893.
23. Engel, M. K.; Yao, J.; Maki, H.; Takeuchi, H.; Yonehara, H. *Rep. Kawamura Inst. Chem. Res.* **1997**, 9, 53-65.
24. Kudrevich, S. V.; Gilbert, S.; van Lier, J. E. *J. Org. Chem.* **1996**, 61, 5706-5707.
25. Kobayashi, N.; Ishizaki, T.; Ishii, K.; Konami, H. *J. Am. Chem. Soc.* **1999**, 121, 9096-9110.
26. Burgi, H.-B., Dunitz, J. D. *Structure Correlation*, 1994, Vol. 2, VCH, Weinheim.

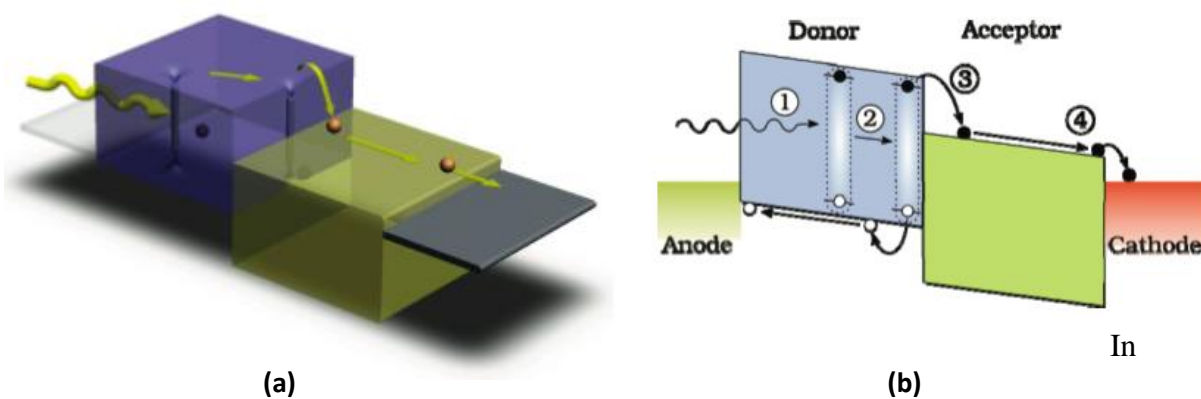
27. Kobayashi, N. *Chem. Commun.* **1991**, 1203-1205.
28. del Rey, B.; Keller, U.; Torres, T.; Rojo, G.; Agullo-Lopez, F.; Nonell, S.; Marti, C.; Brasselet, S.; Ledoux, I.; Zyss, J. *J. Am. Chem. Soc.* **1998**, 120, 12808-12817.
29. Kietaihl, H. *Monatsh.Chem.* **1974**, 105, 405-418.
30. Roberts, G. *Langmuir-Blodgett Films*, 1990, Plenum, New York.
31. Pfeiffer, S.; Mingotaud, C.; Garrigou-Lagrange, C.; Delhaes, P.; Sastre, A.; Torres, T. *Langmuir.* **1995**, 11, 2705-2712. (b) Albouy, P. -A. *J. Phys. Chem.* **1994**, 98, 8543-8549. (c) Bourgoïn, J. -P.; Doublet, F.; Palacin, S.; Vandevyver, M. *Langmuir.* **1996**, 12, 6473-6479.

CHAPTER II

BACKGROUND

EFFICIENCY OF HETEROJUNCTION ORGANIC CELLS

2.1 Introduction



In
the last

decade, the efficiency of organic cells has steadily increased reaching up to 6% presently.^{1,2} The excellence of the photovoltaic cells is based on their power conversion efficiency and the ratio of electrical power that can be generated vs the power of incident solar radiation (Figure 2.1). Considering and defying the various loss mechanisms that ensue between optical excitation to charge collection should generate photovoltaic cells with efficiencies on the order of 10% in the near future.³

Figure 2.1 (a) Representation of Photovoltaic Cell (b) Energy Diagram of an Organic Solar Cell with a Donor-Acceptor Interface

An organic cell with power efficiency (η_p) equal to 1%, which is 1-2 orders of magnitude larger than that of other organic-based devices at that time, was demonstrated by Tang in 1986.^{1,2} The novelty was the insertion of an interface between two organic semiconductors, the so called donor and acceptor concept. The excited organic molecules possess large binding energies of the order of 0.2-1 eV.³ This donor-acceptor interface is the basic criterion for the effectual dissociation of the excitons into free electrons and holes which are then transported on the donor and acceptor material, respectively, generating a photocurrent. This induced advancement in the organic solar cell research constructing cells with $\eta_p \sim 5\text{-}6\%$ ^{1,2} and as high as 6.7%.⁴

2.2 From Photons to Photocurrent

The conversion of incident solar illumination to photocurrent proceeds in four sequential steps (Figure 1):

- i. generation of excitons by photon absorption,
- ii. diffusion of excitons to the heterojunction,
- iii. dissociation of the excitons into free charge carriers,
- iv. transport of the carriers to the contacts.

Compared to the acceptor, the donor material has a smaller HOMO and LUMO. The donor is the hole transporting material and makes ohmic contact with the anode, while the acceptor material transports electrons and contacts the cathode. The first step is the absorption, the result of which is an exciton, that is able to diffuse within the layer where it was created. The absorption efficiency (η_A) is governed by the absorption spectra of the organic molecular layers, especially their thickness, and also by the device's architecture.

The second stage is the exciton diffusion and the efficiency (η_{ED}) of this process is determined by the exciton diffusion length (L_D), as well as the morphology of the DA interface. The exciton dissociation into free charges is represented by an efficiency (η_{CT}) which is noteworthy if energetically favorable. The final process, termed as charge collection efficiency (η_{CC}), is the percentage of dissociated excitons that are collected at the electrodes. This process is dependent primarily on the morphology and mobility of the active layers. The overall efficiency for the conversion of the incident photons to current, called the external quantum efficiency (η_{EQE}), is calculated by the equation below,³ where, λ is the wavelength of incident light, and V is the voltage across the cell.

$$\eta_{EQE}(\lambda, V) = \eta_A(\lambda) \eta_{ED} \eta_{CT}(V) \eta_{CC}(V)$$

2.3 Multicomponent systems

Substantial efforts have been made on the construction of photovoltaic cells involving charge separated states exhibiting long life times and high energy content. The most common approach is the design of complex, multicomponent systems which can separate the photogenerated charges over long distances either by dissociation of the charged components in supramolecular ensembles⁵ or by a cascade of sequential charge migration steps.⁶ However, in simple donor-acceptor models several optimizable parameters play decisive roles in the kinetics of charge separation and recombination. In order to minimize the energy loss, a proper compromise between the redox gradients and the electronic couplings between the different active units must be reached. The degree of electronic communication existing between different molecules in the multicomponent systems is regulated by (i) their relative distances of co-ordination, (ii) their orientation, and (iii) the nature of the linkages between them. Materials of different classes, such as

fullerenes, porphyrins, perylene diimides, subphthalocyanines, subnaphthalocyanines, phthalocyanines, etc., can be used as either donors or acceptors (Figure 2.2).

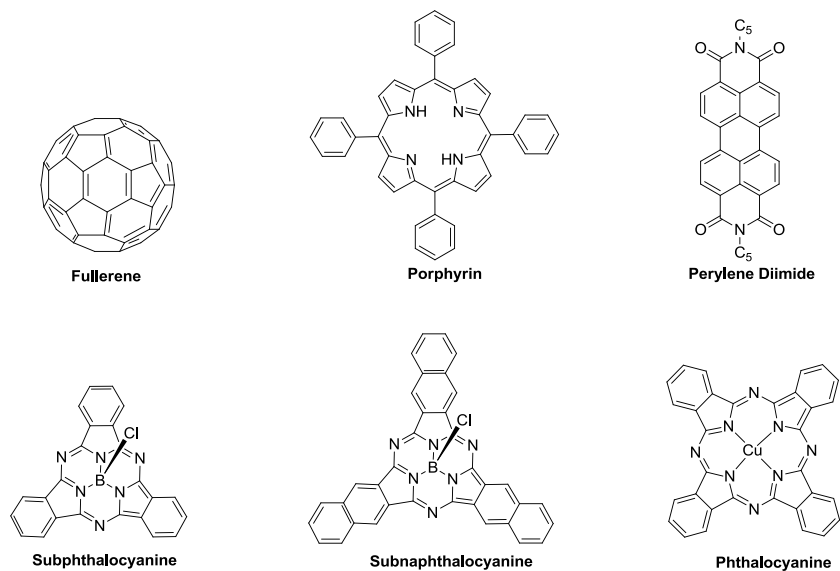


Figure 2.2 Potential Donor/Acceptor Candidates for Electron Energy Multicomponent Assemblies.

Among the different chromophores, Subphthalocyanines (SubPcs) are of particular interest as they possess promising properties to be exploited in artificial photosynthetic systems.⁷ Some striking features of SubPcs are:

- i. excellent antenna units that absorb in the 550-650 nm region with excitation energy above 2.0 V,⁸
- ii. low reorganizational energies,⁹
- iii. tunable redox properties by varying the different substituents,¹⁰
- iv. SubPcs do not form aggregates as do other planar supramolecules due to their non planar nature.^{5a}

2.4 Absorption studies - Subphthalocyanines Vs. Phthalocyanines

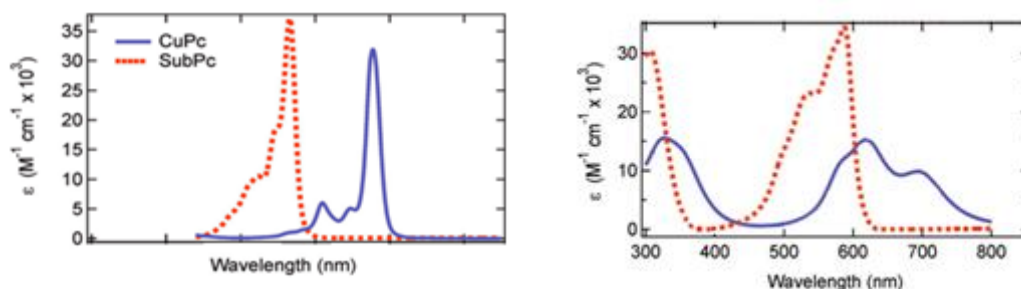


Figure 2.3 (a) Molar Absorptivities of CuPc and SubPc Solutions.

(b) Absorption Coefficients of CuPc and SubPc in thin films.

Absorption studies performed on the CuPc and SubPc revealed that unlike Pcs, the SubPcs do not form aggregates.¹¹⁻¹³ The molar absorptivity spectra of the Q-bands of CuPc and SubPc in solution show characteristically similar features, which are related to the different vibronic transitions of the first exciton absorption (Figure 2.2). Furthermore, the absorption strengths have similar amplitudes, with peaks up to $\epsilon = 3 \times 10^4 M^{-1} cm^{-1}$.³ These spectra which are recorded for very dilute solutions can be accounted on the basis of monomeric absorption of these species. However, the absorption spectra of these molecules in the solid state are quite different. In poor solvents, as well as in thin films, planar phthalocyanines, including CuPc, form cofacial aggregates^{5a,14} and finally crystallize which is evidenced from the changes in the broadening of the Q-band absorption. On the other hand, the spectra of SubPc in solution, as well as in thin films, closely resemble each other. Each of the peaks in the Q band is restored, although there is a red shift of approximately 20 nm³ and changes in the relative intensities of each transition. The similarity of the two spectra implies that there is only weak intermolecular interactions between nonplanar SubPc molecules in the film.

2.5 Covalently linked Donor/Acceptor Conjugates of SubPcs

Owing to the versatile chemistry of subphthalocyanine derivatives, their assemblies as multicomponent photoactive systems are constructed *via* different routes involving both peripheral and axial approaches. The advantage of the axial substitution is to preserve the electronic characteristics of the SubPc macrocycles. SubPcs can act as both electron donor and acceptor depending on the peripheral substituents. Photophysical studies of a Pc-SubPc dyad¹⁵ (Figure 2.4) ensured by a rigid and π -conjugated alkynyl spacer demonstrated that, when the charge transfer state lies at a high energy ($R^1 = R^2 = \text{SC}_8\text{H}_{17}$), a quantitative singlet-singlet energy-transfer mechanism occurs from the excited subphthalocyanine to the phthalocyanine. On the other hand, by lowering the redox gap between electron donor and acceptor ($R^1 = \text{H}$ and $R^2 = \text{NO}_2$), stabilization of the radical pair occurs. This resulted in a highly efficient photo-induced electron-transfer process, even in less polar solvents such as toluene.

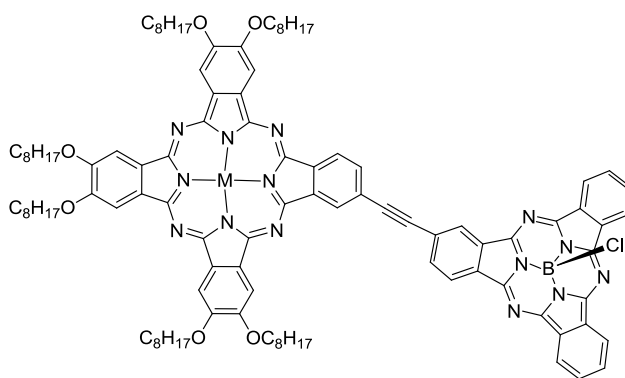


Figure 2.4 Chemical Structure of a SubPc- Pc Dyad.

SubPcs linked with C_{60} fullerene (Figure 2.5) in the axial position¹⁶ have shown to be excellent electron-donor units. The energy level of the charge transfer state may be tuned

by peripheral functionalization of the SubPc macrocycle with different electron withdrawing and electron donating substituents. The lifetime of the formed radical pair may span from 0.65 ns to 72 ns in benzonitrile solution.¹⁶

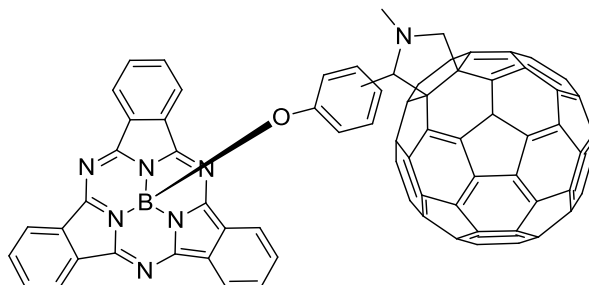


Figure 2.5 SubPc- C₆₀ Dyad.

A SubPc fused dimer bearing two axial positions,¹⁷ (Figure 2.6) doubly linked to C₆₀ was prepared by Iglesias.¹⁷ Photophysical studies revealed that the dyad undergoes a series of energy transfer events similar to those of the SubPc-C₆₀ analogues. Photoexcitation of the dimer (donor), follows a singlet-singlet energy transfer to the C₆₀ fullerene (acceptor), which decays by intersystem crossing to the triplet state of C₆₀ ending with the energy back transfer to the triplet state of the dimer.

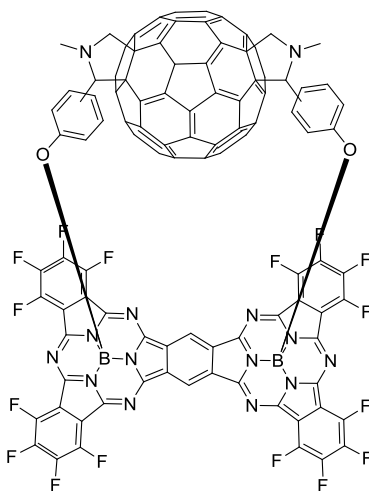


Figure 2.6 SubPc Dimer- C₆₀ Dyad.

SubPcs, when covalently linked to a very strong donating molecules, such as ferrocene⁸ (Figure 2.7), may act as the acceptor counter part. Photoinduced charge separation takes place from the singlet excited state to a stabilized radical ion pair. The longest recombination lifetime (ca. 100 μ s) was recorded for this dyad. The increase in length and ionic character of the axial polar bond upon reduction is likely responsible for this stabilization.

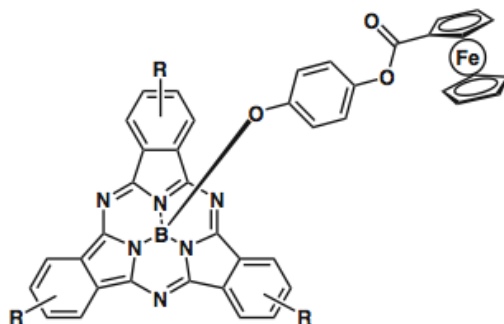


Figure 2.7 SubPc-Ferrocene Dyad.

A related SubPc- triphenylamine dyad¹⁸ (Figure 2.8) with a rigid phenyl ring as the spacer and triphenylamine acting as the donor moiety exhibited extremely rapid charge separation (3 ps) process associated with a similarly fast charge recombination (10 ps).

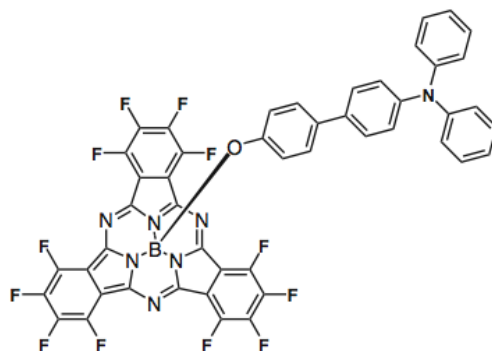


Figure 2.8 SubPc-Triphenylamine Dyad.

Dyads (Figure 2.9) incorporating C₆₀, ferrocene, and SubPc with varying linkage¹⁹ (C-C bond and C-O-C bond) to the SubPc macrocycle have been prepared. The concave side

of the SubPc ideally covers a large surface of C_{60} which potentially affords a high degree of orbital overlap between the two π -conjugated molecules. The distance between the two components, C_{60} and SubPc, varied by the semi rigid spacer, influences not only the regioselectivity of the Bingel trisaddition reaction but also the distance and degree of interaction between the two π - surfaces in the dyads and triads. When C_{60} and SubPc units are held at close distance, a sequential electron transfer is triggered, leading to the long-lived (0.1 ms), spatially separated $C_{60}^{\cdot-}$ -SubPc-Fc $^{\cdot+}$ radical pair.¹⁹

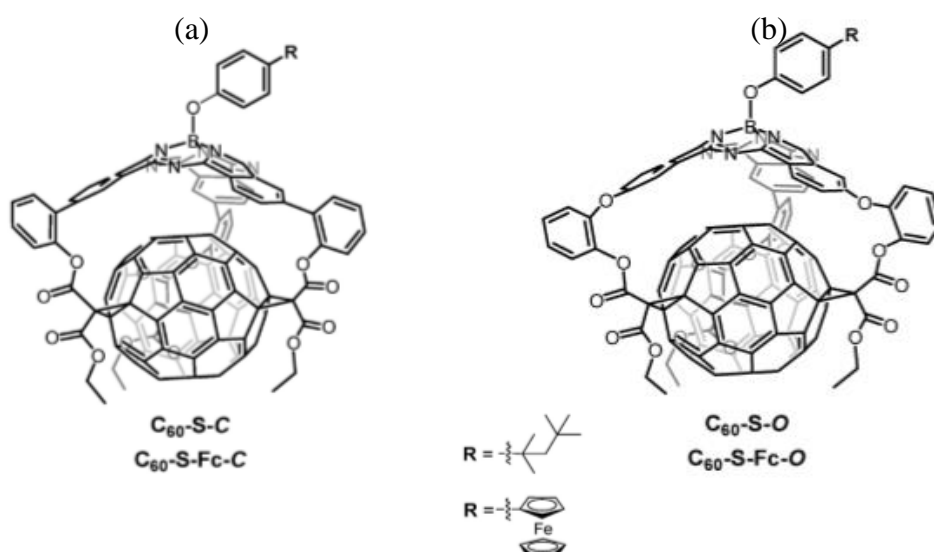


Figure 2.9 (a) SubPc – C_{60} Dyad (C-C bond) (b) SubPc – C_{60} Dyad (C-O bond).

SubPc-distyryl BODIPY²⁰ (Figure 2.10) is an excellent donor-acceptor pair showing the overlap between the fluorescence spectrum of SubPc and the absorption spectrum of distyryl BODIPY. Energy transfer studies indicated the presence of an efficient singlet-singlet energy transfer process in the dyads, from the excited BODIPY part to the SubPc unit which was also confirmed by the excitation spectrum monitored at 570 nm.²

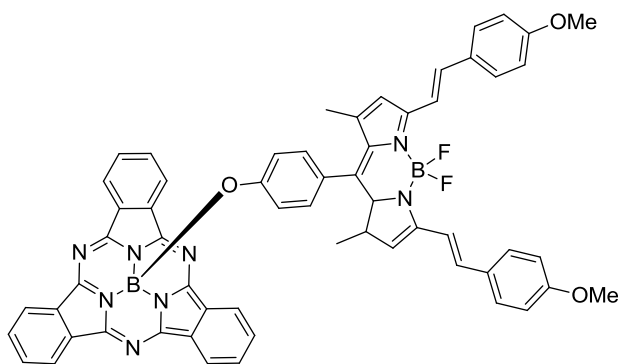


Figure 2.10 SubPc- BODIPY Dyad (B-O bond).

Two highly soluble molecular dyads, SubPc-BODIPY²¹ and SubPc-Os-complex²¹ linked by ethynyl bridge (Figure 2.11), provides improved stereochemical rigidity and better electronic properties than the B-O connections. In both cases, efficacious intramolecular energy transfer takes place, involving singlet-singlet, singlet-triplet, and triplet-triplet processes.

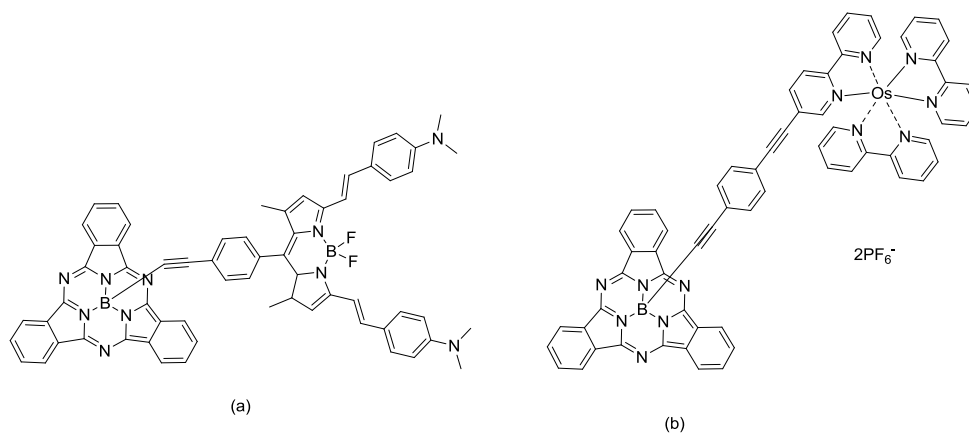


Figure 2.11 (a) SubPc- BODIPY Dyad (b) SubPc-Os Complex Dyad.

SubPc-polymethine conjugate (Figure 2.12) showed a panchromatic absorption over the entire range between 350 nm and 1000 nm.²² Two stronger absorption maxima (571 nm and 903 nm) evolved corresponding to the SubPc and the polymethine constituent,

respectively. Although no appreciable interactions occur in the ground state, electronic communication between the different constituents in the excited state was evidenced by photophysical studies. The different singlet excited state energies of 2.2 eV for the SubPc and 1.35 eV for the cyanine relative to the charge separated state energy 1.1 eV evoke very different charge separation dynamics -5.7 ± 0.5 ps, while no effect on charge recombination was observed.²²

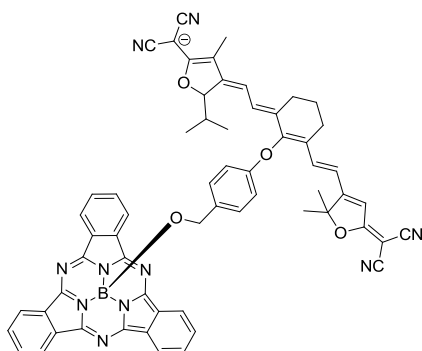


Figure 2.12 SubPc-Polymethine Conjugate

The *hexa*-[B(SubPc)]²³ (Figure 2.13) synthesized from hexakis(4-hydroxyphenyl)benzene executes fast energy migration between the SubPc units as explained by the stationary fluorescence anisotropy experiments using polyethylene glycol as a viscous medium. Energy migration was also suggested by time-resolved fluorescence measurements which showed no dependence on excitation power when using a 200 fs laser pulse (50-180 μ W, excitation at 488 nm). The conjugate exhibited single component decay profiles with fluorescence lifetimes of 1.9 ns in the non-polar solvent toluene. Under ambient conditions, the internal motion of *hexa*-[B(SubPc)] was restricted by the solvent polarity as observed through photoinduced symmetry-breaking charge.

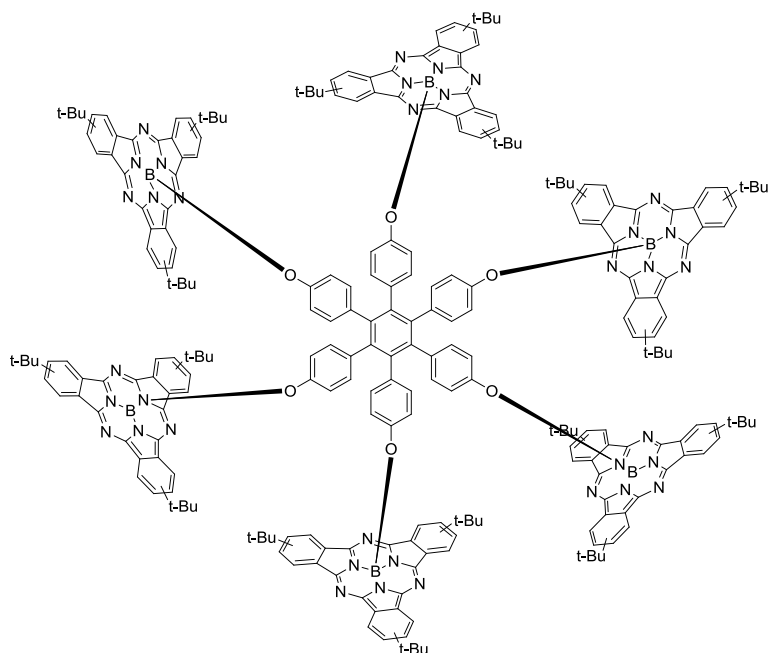


Figure 2.13 Structure of *hexa*-[B(SubPc)].

A ternary supramolecule²⁴ (Figure 2.14), consisting of three components, tetrasulfonated porphyrin (TPPS), β -cyclodextrin conjugated phthalocyanine (SiPc(CD)₂), and β -cyclodextrin conjugated subphthalocyanine, [SubPc(CD)] was reported by Menting.²⁴ The association constants K were calculated to be $1.5 \times 10^6 \text{ M}^{-1}$ and $1.8 \times 10^5 \text{ M}^{-1}$ for SubPc(CD)-TPPS and TPPS-SiPc(CD)₂, respectively and this suggested that both SubPc(CD) and SiPc(CD)₂ undergoes complexation with TPPS spontaneously. The complexation constant for TPPS-SiPc(CD)₂ was found to be $7.3 \times 10^5 \text{ M}^{-1}$ which showed high probability for the formation of a ternary complex. Upon photoexcitation of the SubPc part of this complex, the excitation energy was delivered to the Pc part, and TPPS acted as an energy transfer media enabling the transfer process.²⁴

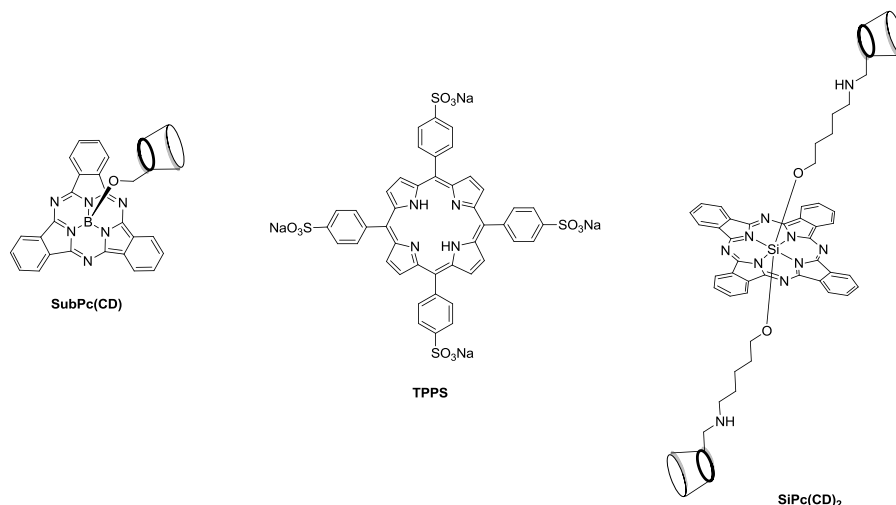


Figure 2.14 Ternary Complex of SubPc(CD)-TPPS- SiPc(CD)₂.

2.6 References

- 1 Li, G.; Shrotriya, V.; Huang, J. S.; Yao, Y.; Moriarty, T.; Emery, K.; Yang, Y. *Nat. Mater.* **2005**, 4, 864-868.
- 2 Park, S. H.; Roy, A.; Beaupre, S.; Cho, S.; Coates, N.; Moon, J. S.; Moses, D.; Leclerc, M.; Lee, K.; Heeger, A. J. *Nat. Photonics.* **2009**, 3, 297-302.
- 3 Heremans, P.; Cheyns, D.; Rand, B. P. *Acc. Chem. Res.* **2009**, 42, 1740-1747.
- 4 Kim, J. Y.; Lee, K.; Coates, N. E.; Moses, D.; Nguyen, T.; Dante, M.; Heeger, A. J. *Science.* **2007**, 317, 222-225.
- 5 (a) Claessens C. G.; Gonzalez-Rodriguez, D.; Torres, T. *Chem Rev.* **2002**, 102, 835-853. (b) Torres, T. *Angew. Chem.* **2006**, 45, 2834-2837.
- 6 Gust, D.; Moore, T. A.; Moore, A. L. *Acc. Chem. Res.* **2001**, 34, 40-48.
- 7 (a) del Rey, B.; Keller, U.; Torres, T.; Rojo, G.; Agullo-Lopez, F.; Nonell, S.; Marti, C.; Brasselet, S.; Ledoux, I.; Zyss, J. *J. Am. Chem. Soc.* **1998**, 120, 12808-

12817. (b) Iglesias, R. S.; Claessens, C. G.; Torres, T.; Rahman, G. M. A.; Guldi, D. M. *Chem. Commun.* **2005**, 2113-2115.
- 8 Gonzalez-Rodriguez, D.; Torres, T.; Olmstead, M. M.; Rivera J, Herranz, M.A.; Echegoyen, L.; Castellanos, C.A.; Guldi, D. M. *J. Am. Chem. Soc.* **2006**, 128, 10680-10681.
- 9 Kipp, R. A.; Simon, J. A.; Beggs, M.; Ensley, H. E.; Schmehl, R. H. *J. Phys. Chem. A* **1998**, 102, 5659-5664.
- 10 (a) Gonzalez-Rodriguez, D.; Torres, T.; Herranz, M. A.; Rivera, J.; Echegoyen, L.; Guldi, D. M. *J. Am. Chem. Soc.* **2004**, 126, 6301-6313.
- 11 Mutolo, K. L.; Mayo, E. I.; Rand, B. P.; Forrest, S. R.; Thompson, M. E. *J. Am. Chem. Soc.* **2006**, 128, 8108–8109.
- 12 Gommans, H.; Cheyns, D.; Aernouts, T.; Giroto, C.; Poortmans, J.; Heremans, P. *Adv. Funct. Mater.* **2007**, 17, 2653–2658.
- 13 Peumans, P.; Yakimov, A.; Forrest, S. R. *J. Appl. Phys.* **2003**, 93, 3693–3723.
- 14 George, R. D.; Snow, A. W.; Shirk, J. S.; Barger, W. R. *J. Porphyrins Phthalocyanines.* **1998**, 2, 1–7.
- 15 González-Rodríguez D.; Claessens C. G.; Torres T.; Liu S.; Echegoyen L.; Vila N.; Nonell S. *Chem. Eur. J.* **2005**, 11, 3881.
- 16 González-Rodríguez, D.; Torres, T.; Herranz, M. A.; Echegoyen, L.; Carbonell, E.; Guldi, D. M. *Chem.Eur. J.* **2008**, 14, 7670.
- 17 Claessens, C. G.; Gonzalez-Rodriguez, D.; Iglesias, R. S.; Torres, T. *C. R. Chimie.* **2009**, 9, 1094-1099.
- 18 Medina, A.; Claessens, C. G.; Torres, T. *Chem. Commun.* **2008**, 1759-1761.

- 19 Gonzalez-Rodriguez, D.; Carbonell, E.; de Miguel Rojas, G.; Castellanos, C. A.; Torres, T. *J. Am. Chem. Soc.* **2010**, 132, 16488-16500.
- 20 Liu, J. -Y.; Yeung, H. -S.; Xu, W.; Li, X.; Dennis, K. P. Ng. *Org Lett.* **2008**, 10, 5421-5424.
- 21 Ziesel, R.; Ulrich, G.; Elliott, K. J.; Harriman, A. *Chem. Eur. J.* **2009**, 15, 4980-4984.
- 22 Nieto, C. R.; Guilleme, J.; Villegas, C.; Delgado, J. L.; Gonzalez-Rodriguez, D.; Martin, N.; Torres, T.; Guldi, D. M. *J. Mater. Chem.* **2011**, 21, 15914-15918.
- 23 Morisue, M.; Suzuki, W.; Kuroda, Y. *Dalton. Trans.* **2011**, 40, 10047-10054.
- 24 Menting, Roel.; Lau, J. T. F.; Xu, H.; Dennis, K. P. Ng.; Roder, B.; Ermilov, E. A. *Chem. Commun.* **2012**, 48, 4597-4599.

CHAPTER III

RESULTS AND DISCUSSION

SYNTHESIS OF SYMMETRICAL AND UNSYMMETRICAL SUBPHTHALOCYANINE DIMERS CONTAINING A HYDROQUINONE BRIDGE

3.1 Introduction

To date, a few subphthalocyanine derivatives have been reported through different synthetic pathways involving the peripheral and axial approaches.¹ The axial substitution of the SubPcs is advantageous in many respects, especially since the electronic structure of the SubPc is preserved. Although the chloro-subphthalocyanines (Cl-SubPcs) were substituted with different groups, the phenol derivatives were found to be beneficial regarding: (i) a variety of phenol derivatives are available, (ii) facile introduction of new functional groups can be achieved in the axial position of SubPcs, and (iii) the geometry of the adducts formed with SubPcs can be controlled by modulating the substitution pattern.² A few subphthalocyanine dimers³ in which the two macrocycles are in close proximity have been synthesized (Figure 3.1). We report for the first time the synthesis (Scheme 3.1) and spectroscopic characterization of three different symmetrical and unsymmetrical dimers that are linked by a hydroquinone moiety.

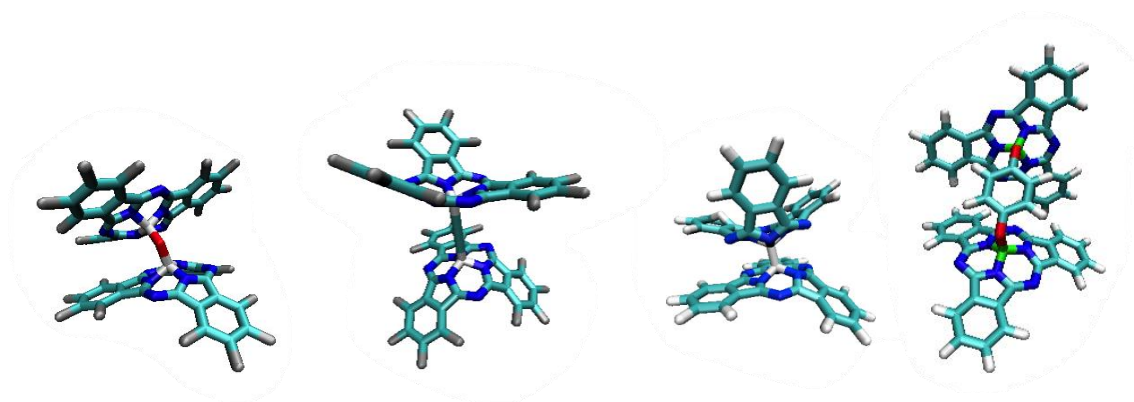


Figure 3.1 Tubular Representation of Various SubPc Dimers.

3.2 Results and Discussion

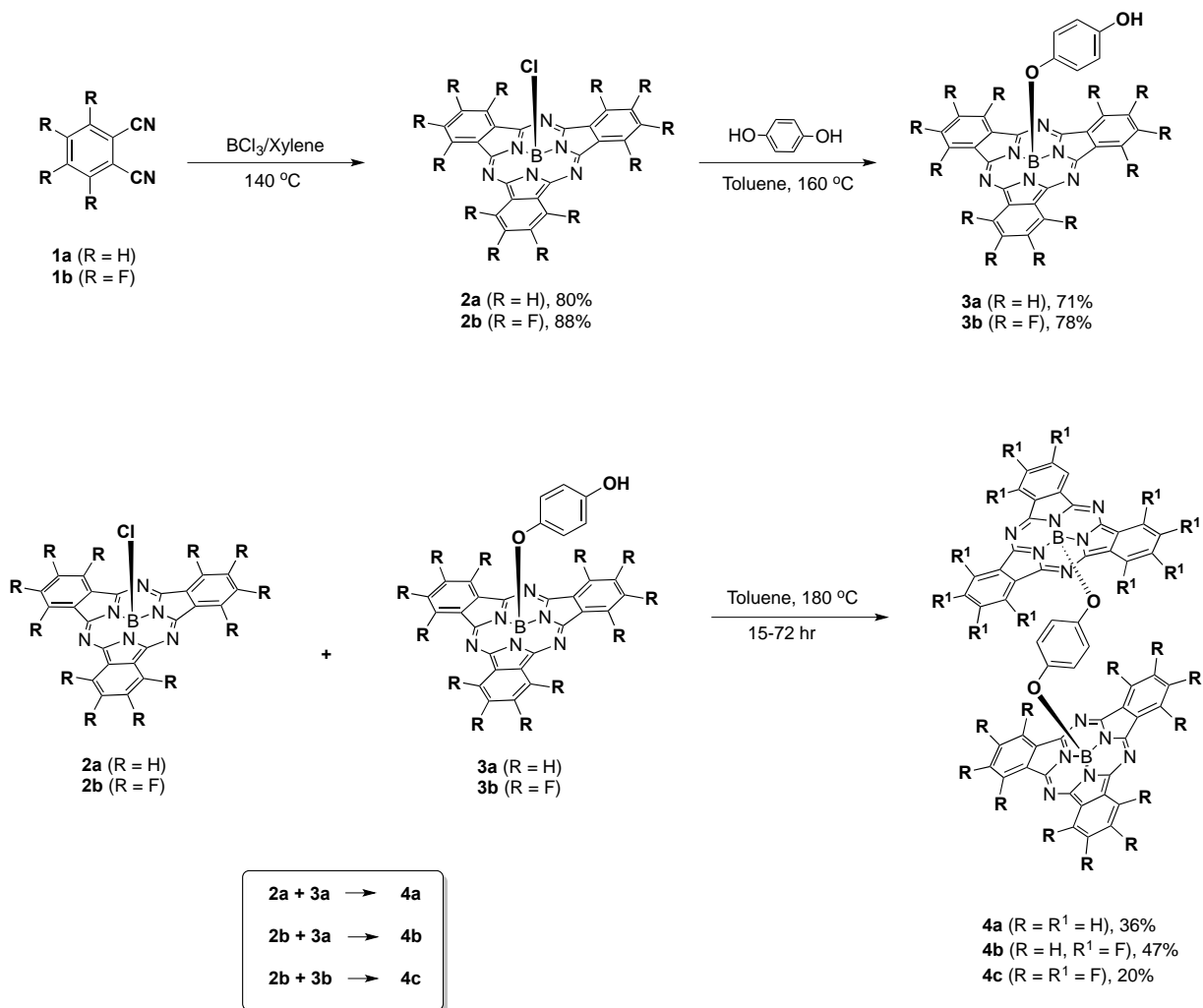
3.2.1 Synthesis

The synthetic pathway to the dimers is shown in Scheme 3.1. The synthesis involved the cyclotrimerization of the phthalonitriles **1a(1b)** with BCl_3 (1 M solution in *p*-xylene) to give the parent Cl-SubPcs, **2a** and **2b**. This was then followed by the axial replacement of the chlorine atom in **2a** and **2b** by hydroquinone to generate the electron rich, hydroquinone-substituted Hq-SubPcs, **3a** and **3b**, respectively. The final step is the nucleophilic attack of Hq-SubPcs **3a** and **3b** at the electropositive boron atom of **2a** and **2b** to give symmetrical and unsymmetrical dimers, **4a**, **4b**, and **4c**.

3.2.2 Synthesis of Cl-SubPcs, **2a** and **2b**

Both Cl-SubPcs, **2a** and **2b** were synthesized from the corresponding phthalonitriles **1a(1b)** by modifying a general reported procedure.⁴ Condensation of the starting phthalonitriles with a commercial 1 M solution of BCl_3 in *p*-xylene under argon at reflux conditions for 20-30 min afforded **2a** and **2b**. Easy handling and the sufficiently high boiling point of *p*-xylene made it an excellent solvent for reactions involving the

initial phthalonitriles.⁵ Extraction of the crude material with toluene, followed by drying, filtration and evaporation of the solvent, yielded Cl-SubPcs **2a** and **2b** that were sufficiently pure to be taken to the next step.



Scheme 3.1 Synthesis of Subphthalocyanine Dimers.

3.2.3 Synthesis of Hq-SubPcs, **3a** and **3b**

Thus far only a few phenoxy substituents have been used to replace the axial chlorine atom.⁶ Solvent, reaction temperature, the nature of the phenolic substituent, and the electronic characteristics of the Cl-SubPcs together play leading roles in determining the yields obtained and the time required for each reaction. In general, with the use of a polar solvent, such as acetonitrile, the reaction appears to proceed faster but only with an average yield, presumably resulting from decomposition of the SubPcs in the polar media.⁷ In an effort to increase the efficiency for the conversion of **2a** and **2b** to the key starting materials **3a** and **3b**, respectively, we attempted to employ a 1:1 ratio of **2a** with hydroquinone in dry toluene in a pressure vessel. A prior method utilized a 1:5 ratio of such reagents.⁸ In our hands, the reaction in the pressure vessel in boiling toluene gave only moderate yields. However, heating the mixture to 160 °C for 10 hours gave a comparable yield (~71%) of **3a** to that reported.⁸ Purification of our crude product *via* chromatography was straightforward for **3a** and for **3b**, the latter being obtained in a similar fashion but with only 1 hour of reaction time. It is conceivable that the presence of the electronegative fluorine atoms in **2b** increased the electron deficiency of the boron atom which facilitated the nucleophilic attack.

3.2.4 Synthesis of SubPc-Hq-SubPc Dimers, 4a-c

Regarding the synthesis of the SubPc-hydroquinone dimers, various alterations were made on the reaction conditions. Since a few of the SubPcs previously reported were found to decompose with the addition of bases, such as NaH and DBU,⁴ the parameters that can be altered were solvent and the temperature. Reacting a 1:1 mixture of **2a** and **3a** in the high boiling solvent, *o*-dichlorobenzene under reflux conditions had no effect on the reaction.

Next, we attempted the reaction of **2a** and **3a** in toluene at 180 °C using a pressure vessel. In which case, it was possible to isolate dimer **4a** in a yield of 36% after 3 days. No improvement in yield was observed with longer reaction times, but rather decomposition occurred. Dilution of the reaction mixture reduced the rate of the reaction. The reaction mixture did not require work up, but the crude product was directly chromatographed over silica gel using ethyl acetate:hexane (1:5) to give **4a** (36%).

With the intent to synthesize the unsymmetrical dimer, it was assumed that **3a** would be a better nucleophile for **2b** due to the electropositive boron atom present in the latter. As expected, the reaction of **3a** and **2b** proceeded smoothly to give **4b** in a yield of 47% after purification by column chromatography using CH₂Cl₂:hexane (1:4). The symmetrical SubPc dimer **4c** was synthesized from reaction of **2b** with **3b** under similar conditions, but the yield was modest (20%), presumably because **3b** was a poor nucleophile. Mostly starting material was recovered.

3.3 NMR Spectroscopy

All intermediates and target dimers were characterized by ^1H NMR and ^{13}C NMR spectroscopy. As a result of the diamagnetic ring currents from the two SubPc units in the dimer, the ^1H NMR resonances of the linking hydroquinone moiety showed considerable upfield shifts. For the symmetrical dimers **4a** and **4c** all the hydroquinone protons experienced the same environment with a sharp singlet at 4.79 ppm, corresponding to protons of the hydroquinone moiety. In contrast, for the unsymmetrical dimer **4b**, as expected, two different proton signals appeared as two doublets centered at 4.74-4.82 ppm (Figure 3.2). These dimers are the first examples of subphthalocyanine dimers where the spacer hydroquinone moiety bridged the two systems. These upfield shifts of the hydroquinone protons are in contrast to the corresponding proton signals (6.21 and 5.20 ppm) for a previously reported, single phenolic linker system.⁸

3.4 UV- Vis Spectroscopy

The UV-Vis experiments showed three distinct absorption curves for the SubPc dimers with $\lambda_{\text{max}} = 562, 566$ and 572 nm for **4a**, **4b** and **4c**, respectively. The fluorinated dimer **4c**, showed a considerable red shift of about 10 nm from the unsubstituted dimer, **4a**. As expected, the λ_{max} for the unsymmetrically substituted SubPc dimer **4b** was found between the 562-572 nm range, which suggested that the absorption maximum of the dimers can be accordingly tailored by incorporating SubPcs containing different peripheral groups.

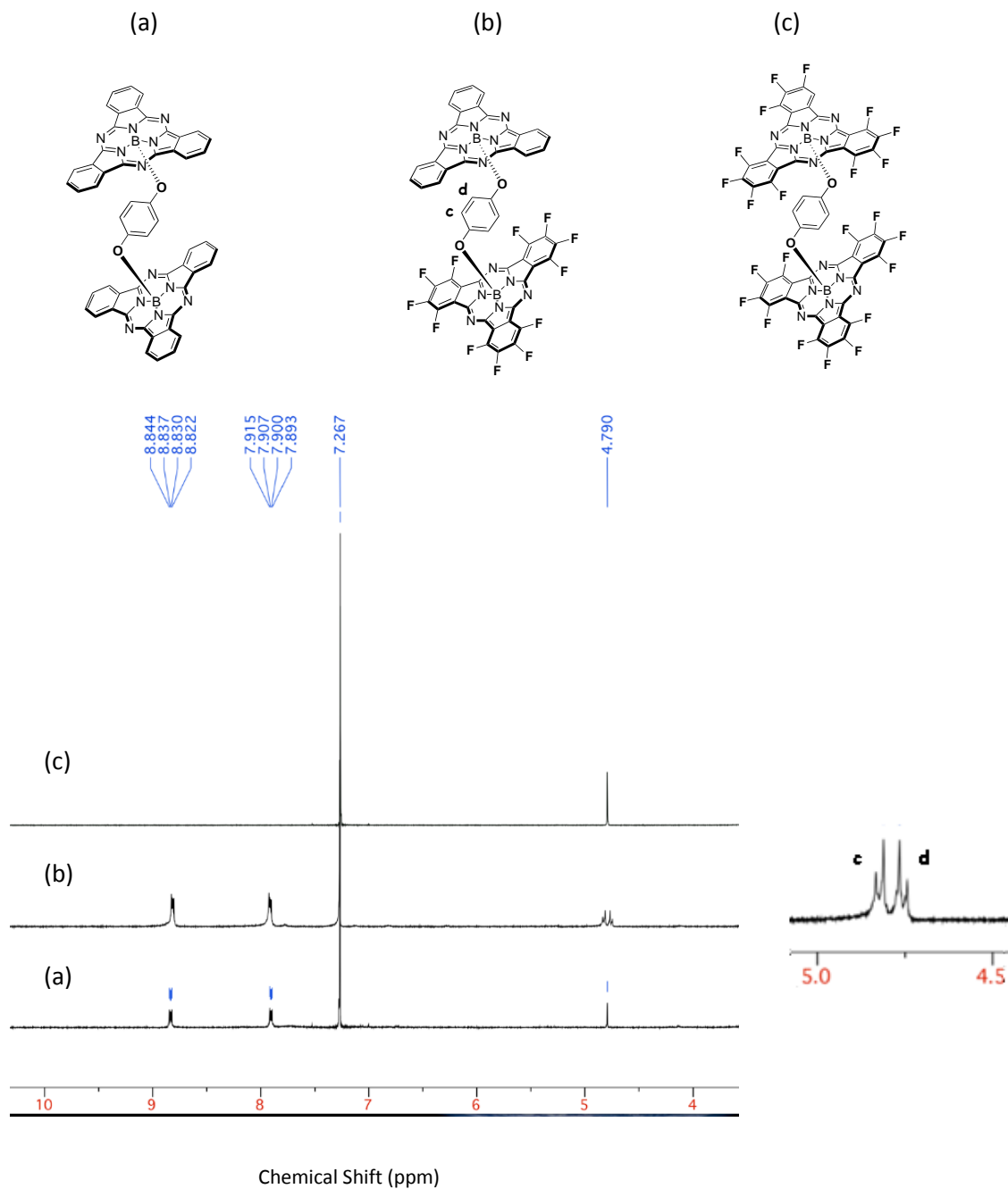


Figure 3.2 NMR Spectra of the Dimers (a) SubPc_(H)-Hq-SubPc_(H), (b) SubPc_(H)-Hq-SubPc_(F), (c) SubPc_(F)-Hq-SubPc_(F), and (d) Partially expanded ¹H NMR Spectrum of SubPc_(H)-Hq-SubPc_(F).

3.5 Experimental

3.5.1 General

Melting points (mp) were determined using a Stuart SMP10 instrument. Both ^1H and ^{13}C NMR spectra were acquired in CDCl_3 using a Varian Inova 400 MHz spectrometer. Chemical shifts (δ) are expressed in ppm relative to residual chloroform (^1H : 7.26 ppm, ^{13}C : 77.0 ppm) or to TMS. Fourier Transform Infrared (IR) measurements were performed on a Varian 800 FT-IR spectrometer. UV-Vis spectra were recorded on Cary 5000 UV-VIS-NIR spectrophotometer. Fluorescence spectra were recorded on a Cary Eclipse fluorescence spectrophotometer. All UV-Vis and fluorescence spectra were recorded at a concentration of $1.0 \times 10^{-7} \text{ M}$ at $23 \text{ }^\circ\text{C}$. The sealed tube reaction was conducted in a unit from Chem Glas, Model 1880. Column chromatography was carried out on silica gel (Sorbent Technologies, 230-400 mesh), and TLC was done with polyester sheets precoated with silica gel (Sorbent Technologies). Phthalonitrile (Alfa Aeser), tetrafluorophthalonitrile, BCl_3 (Sigma Aldrich) and hydroquinone (Fischer) were purchased from commercial suppliers and used as received unless otherwise indicated.

3.5.2 Standard Procedure A for the Synthesis of SubPcs (2a-b)

To a 100-mL, two-necked, round-bottomed flask fitted with a condenser, magnetic stirrer and septum, was added the corresponding dry phthalonitrile (2 mmol), under argon, followed by dropwise addition of BCl_3 (2 mL, 1 M solution in *p*-xylene) at room temperature. The mixture was refluxed for 30 min to yield a purple solution. The system was flushed with argon for 15 min. The solvent was evaporated, and the solid obtained was extracted with toluene (1 x 20 mL), washed with brine (1 x 20 mL), dried (Na_2SO_4) and evaporated to yield pure SubPcs.

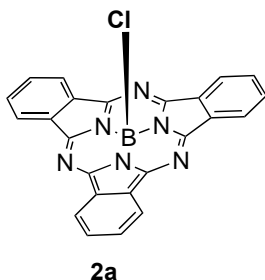
3.5.3 Standard Procedure B for the Axial Substitution of SubPcs with Hydroquinone (Hq-SubPc) (3a-b)

A mixture of Cl-SubPc (1.0 equiv) and hydroquinone (1-5 equiv) was refluxed in dry toluene in a 100-mL, single-necked, round-bottomed flask fitted with a condenser for 1-10 hr. The reaction mixture was allowed to cool to room temperature, the solvent was evaporated and the crude material was purified by column chromatography over silica gel using ethyl acetate:hexane in various ratios (1:3 to 1:5).

3.5.4 Standard Procedure C for the Synthesis of SubPc Dimers (4a-c)

The starting Cl-SubPc (1.0 equiv), SubPc hydroquinone derivative, Hq-SubPc (1.0 equiv), and dry toluene were placed in a pressure vessel and heated at 180 °C for 15-72 hr. The solvent was evaporated, and the crude material was subject to column chromatography on silica gel using ethyl acetate:hexane or CH₂Cl₂:hexane in varying ratios to afford the dimers.

3.5.5 Synthesis of Cl-SubPc 2a

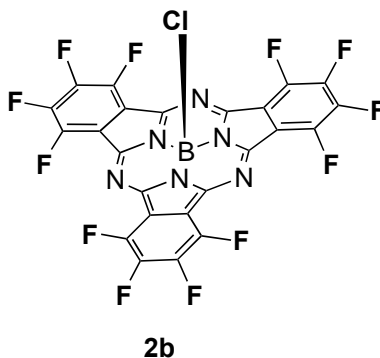


Phthalonitrile (**1a**, 0.5 g, 3.9 mmol) and BCl₃ (4 mL, 1 M solution in *p*-xylene) were allowed to react according to procedure A. The solvent was evaporated, the solid was dissolved in toluene (1 x 20 mL), and the organic layer was washed with brine (1 x 20 mL), dried (Na₂SO₄) and evaporated to afford **2a** as a pink solid.

Yield: 1.34 g (80%).

Mp: > 300 °C (lit,⁴ **Mp:** > 250 °C).

3.5.6 Synthesis of Cl-SubPc 2b

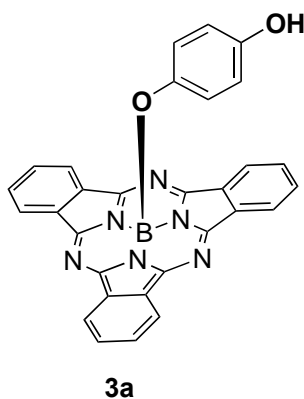


Tetrafluorophthalonitrile (**1b**, 0.5 g, 2.5 mmol) and BCl_3 (4 mL, 1 M solution in *p*-xylene) were allowed to react according to procedure A. The solvent was evaporated, the solid was dissolved in toluene (1x 20 mL), and the organic layer was washed with brine (1 x 20 mL), dried (Na_2SO_4) and evaporated to afford **2b** as a pink solid.

Yield: 1.41 g (88%).

Mp: > 300 °C (lit,⁴ **Mp:** > 250 °C).

3.5.7 Synthesis of Hq-SubPc 3a



The starting Cl-SubPc (**2a**, 0.4 g, 0.9 mmol) and hydroquinone (0.1 g, 0.9 mmol) were heated to 160 °C in dry toluene (5 mL) for 10 hr according to procedure B. After cooling to RT,

the reaction mixture was evaporated to dryness and chromatographed over silica gel using ethyl acetate:hexane (1:3) to afford **3a** as pink solid.

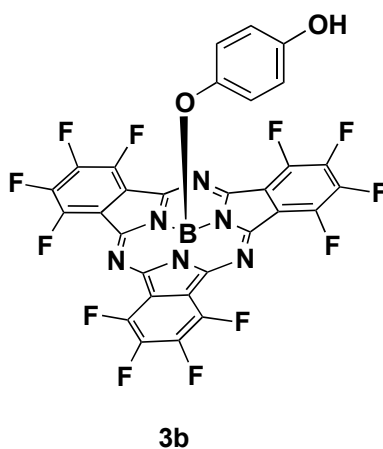
Yield: 0.33 g (71%) .

Mp: > 300 °C (lit,⁸ **Mp:** > 250°C).

UV-Vis (toluene): $\lambda_{\text{max}} = 562$ nm (Q band).

Fluorescence: ($\lambda_{\text{exc}} = 562$ nm) $\lambda_{\text{em}} = 573$ nm.

3.5.8 Synthesis of Hq-SubPc **3b**



The starting Cl-SubPc (**2b**, 0.2 g, 0.31 mmol) and hydroquinone (0.17 g, 1.5 mmol) were refluxed in dry toluene (3 mL) for 1 hr according to procedure B. The reaction mixture was evaporated to dryness, and the residue was chromatographed over silica gel using ethyl acetate:hexane (1:5) to afford **3b** as a pink solid.

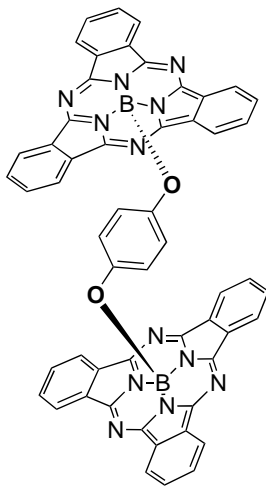
Yield: 0.17 g (78 %).

Mp: > 300 °C (lit,⁸ **Mp:** > 250 °C).

UV-Vis (toluene): $\lambda_{\text{max}} = 572$ nm (Q band).

Fluorescence ($\lambda_{\text{exc}} = 572$ nm): $\lambda_{\text{em}} = 586$ nm.

3.5.9 SubPc_(H)-Hq-SubPc_(H) Dimer 4a



4a

A mixture of Cl-SubPc_(H) (**2a**, 50 mg, 0.1 mmol) and Hq-SubPc_(H) (**3a**, 55.4 mg, 0.1 mmol) in dry toluene (2 mL) were treated according to procedure C for 3 days. Purification by column chromatography on silica gel using ethyl acetate:hexane (1:5) afforded **4a** as a pink solid.

Yield: 37.5 mg (36%).

Mp: > 300 °C.

IR (CH₂Cl₂) cm⁻¹: 3023, 2922, 2855, 1697, 1651, 1497, 1457, 1376, 1288, 1217, 1132, 1054 (B-O bond), 738, 698.

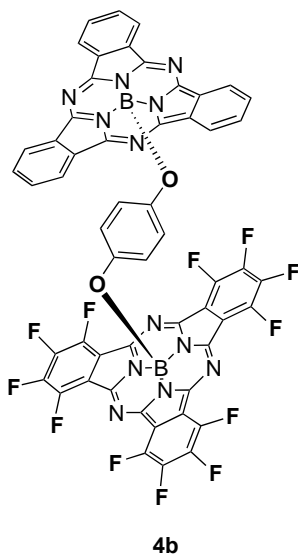
¹H NMR (400 MHz, CDCl₃): δ 8.84-8.82 (AA'BB', 12H, SubPc), 7.91-7.89 (AA'BB', 12H, SubPc), 4.79 (s, 2H, Hq).

¹³C NMR (100 MHz, CDCl₃): δ 151.0, 145.2, 130.8, 129.7, 122.3, 119.5.

UV-Vis (toluene): λ_{max} = 562 nm (Q band). Fluorescence (λ_{exc} = 562 nm): λ_{em} = 573 nm.

MS-MALDI-TOF: *m/z* for C₅₄H₂₈B₂N₁₂O₂: Calcd: 899.2644, Found: 899.2713 [M]⁺.

3.5.10 SubPc_(H)-Hq-SubPc_(F) Dimer 4b



A mixture of Cl-SubPc_(F) (**2b**, 25 mg, 0.038 mmol), and Hq-SubPc_(H) (**3a**, 19.53 mg, 0.038 mmol) in dry toluene (1 mL) were treated according to procedure C for 15 hr. The crude product was subjected to column chromatography on silica gel using CH₂Cl₂:hexane (1:4) to yield **4c** as a pink solid.

Yield: 20 mg (47%).

Mp: > 300 °C.

IR (CH₂Cl₂) cm⁻¹: 3054, 2989, 1422, 1264, 1054 (B-O bond), 896, 778, 739, 699.

¹H NMR (400 MHz, CDCl₃): δ 8.84-8.82 (AA'BB', 6H, SubPc), 7.91-7.89 (AA'BB', 6H, SubPc), 4.80 (d, J=4 Hz, 2H), 4.75 (d, J=4 Hz, 2H).

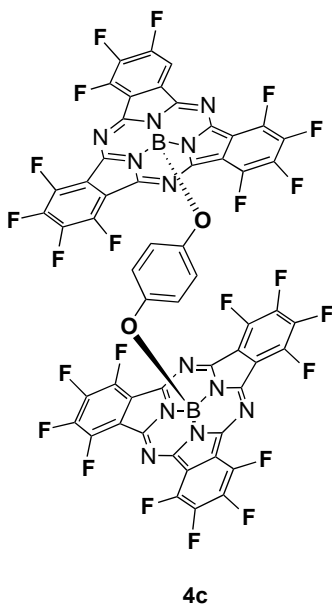
¹³C NMR (100 MHz, CDCl₃): δ 148.2, 145.9, 144.0(m), 141.3(m), 119.1, 114.7(m).

UV-vis (toluene): λ_{max}= 566 nm (Q band).

Fluorescence: (λ_{exc}= 566 nm) λ_{em}= 585 nm.

MS-MALDI-TOF: *m/z* for C₅₄H₁₆B₂F₁₂N₁₂O₂ Calcd: 1115.1514, Found: 1115.1532 [M]⁺.

3.5.11 SubPc(F)-Hq-SubPc(F) Dimer 4c



A mixture of Cl-SubPc(*F*) (**2b**, 50 mg, 0.07 mmol), and Hq-SubPc(*F*) (**3b**, 55.8 mg, 0.07 mmol) in dry toluene (2 mL) were treated according to procedure C. Purification by column chromatography on silica gel using ethyl acetate:hexane (1:7) afforded **4b** as a pink solid.

Yield: 20 mg (20 %).

Mp: > 300 °C.

IR (CH₂Cl₂) cm⁻¹: 3058, 2930, 1780, 1743, 1486, 1265, 1055 (B-O bond), 116, 967, 779, 739, 698.

¹H NMR (400 MHz, CDCl₃): δ 4.79 (s, 4H).

¹³C NMR (100 MHz, CDCl₃): δ 148.3, 146.0, 144.1, 141.4, 119.3, 114.8.

UV-Vis (toluene): λ_{max} = 572 nm (Q band).

Fluorescence (λ_{exc} = 572 nm): λ_{em} = 584 nm.

MS-MALDI-TOF: *m/z* for C₅₄H₄B₂F₂₄N₁₂O₂, Calcd. 1331.0383, Found: 1331.0416 [M]⁺.

3.6 Conclusions

In summary we have synthesized three new hydroquinone-based, subphthalocyanine dimers, **4a**, **4b**, and **4c**, by using a 1:1 ratio of the ligand vs SubPc in a pressure vessel at 180 °C. All structures were characterized using ¹H NMR and ¹³C NMR spectroscopy. The hydroquinone bridge in the dimers showed characteristic upfield shifted aromatic protons because of the diamagnetic ring current of the two axial, covalently-linked SubPcs. In comparison to the symmetrical dimers **4a** and **4c**, the synthesis of the unsymmetrical dimer **4b** obtained by reacting **3a** with **2b** proceeded at higher yield (47%) and less reaction time (15 h). This is attributed to the increased axial reactivity of **2b**. The nucleophilicity of **3a** towards another SubPc molecule suggested the potential usefulness of such compounds as building blocks for the construction of higher order molecular assemblies. Furthermore, the new dimers possess improved solubility, compared to the systems with one hydroxyl phenolic linker⁸ and may be useful in several thin film applications in optoelectronic devices.

3.7 References

1. Yu Tolbin, A.; Tomilova, L. G. *Russ. Chem. Rev.* **2011**, 80, 531-551.
2. Gonzalez-Rodríguez, D.; Torres, T.; Guldi, D. M.; Rivera, J.; Echegoyen, L. *Org. Lett.* **2002**, 4, 335-338.
3. (a) Eckert, A. K.; Salomé Rodríguez-Morgade, M.; Torres, T. *Chem. Commun.* **2007**, 4104-4106. (b) Jacquot de Rouville, H. P.; Garbage, R.; Ample, F.; Nickel, A.; Meyer, J.; Moresco, F.; Joachim, C.; Rapenne, G. *Chem. Eur. J.* **2012**, 18, 8925-8928.

4. Claessens, C. G.; Gonzalez-Rodriguez, D.; del Rey, B.; Torres, T.; Mark, G.; Schuchmann, H. -P.; von Sonntag, C.; MacDonald, J. G.; Nohr, R. S. *Eur J. Org. Chem.* **2003**, 2547-2551.
5. (a) Martin, G.; Rojo, G.; Agulló-López, F.; Torres, T.; Ferro, V. R.; Garcia de la Vega, J. M. *J. Phys. Chem. B.* **2002**, 106, 13139-13145. (b) Dabak, S.; Gul, A.; Bekaroglu, O. *Chem. Ber.* **1994**, 127, 2009-2012.
6. Gonzalez-Rodriguez, D.; Torres, T. *J. Organomet. Chem.* **2009**, 694, 1617-1622.
7. Potz, R.; Goldner, M.; Huckstadt, H.; Cornelissen, U.; Tutab, A.; Homborg, H. *Anorg. Allg. Chem.* **2000**, 626, 588-596.
8. Gonzalez-Rodriguez, D.; Victoria Martinez-Diaz, M.; Abel, J.; Perl, A.; Huskens, J.; Echegoyen, L.; Torres, T. *Org. Lett.* **2010**, 2970-2973.

3.8 Appendices

Figure 3.3 ^1H NMR Spectrum of **4a**

Figure 3.4 ^1H NMR Spectrum of **4b**

Figure 3.5 ^1H NMR Spectrum of **4c**

Figure 3.6 UV-Vis Spectra of the dimers

Figure 3.7 Emission Spectra of the Dimers

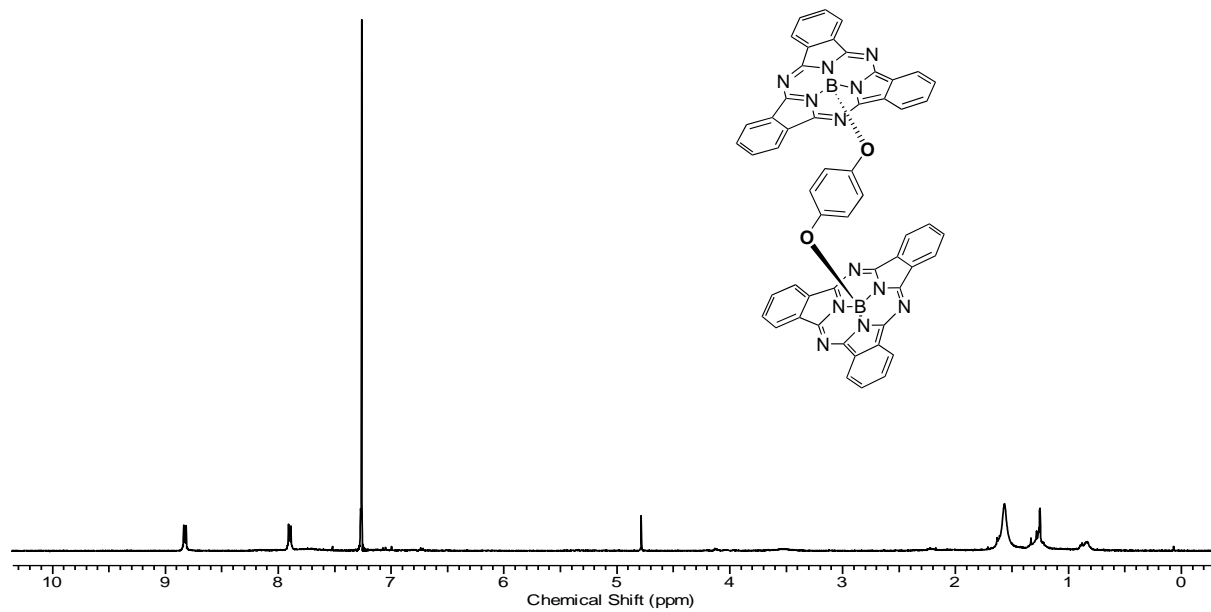


Figure 3.3 ^1H NMR Spectrum of **4a**

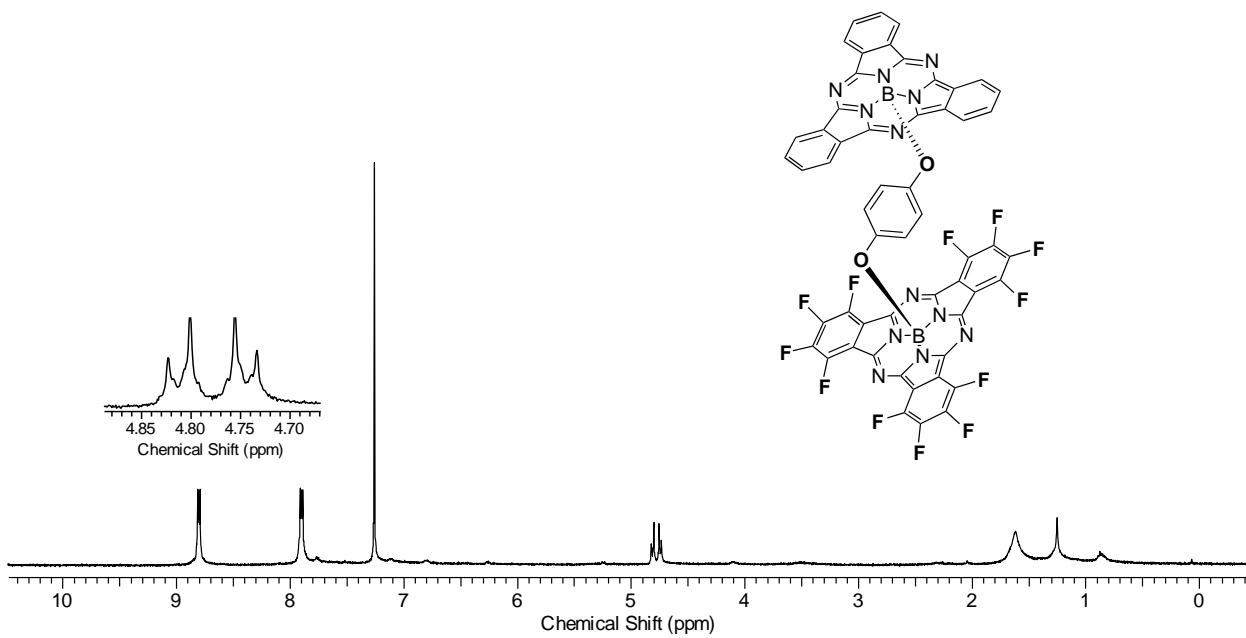


Figure 3.4 ^1H NMR Spectrum of **4b**

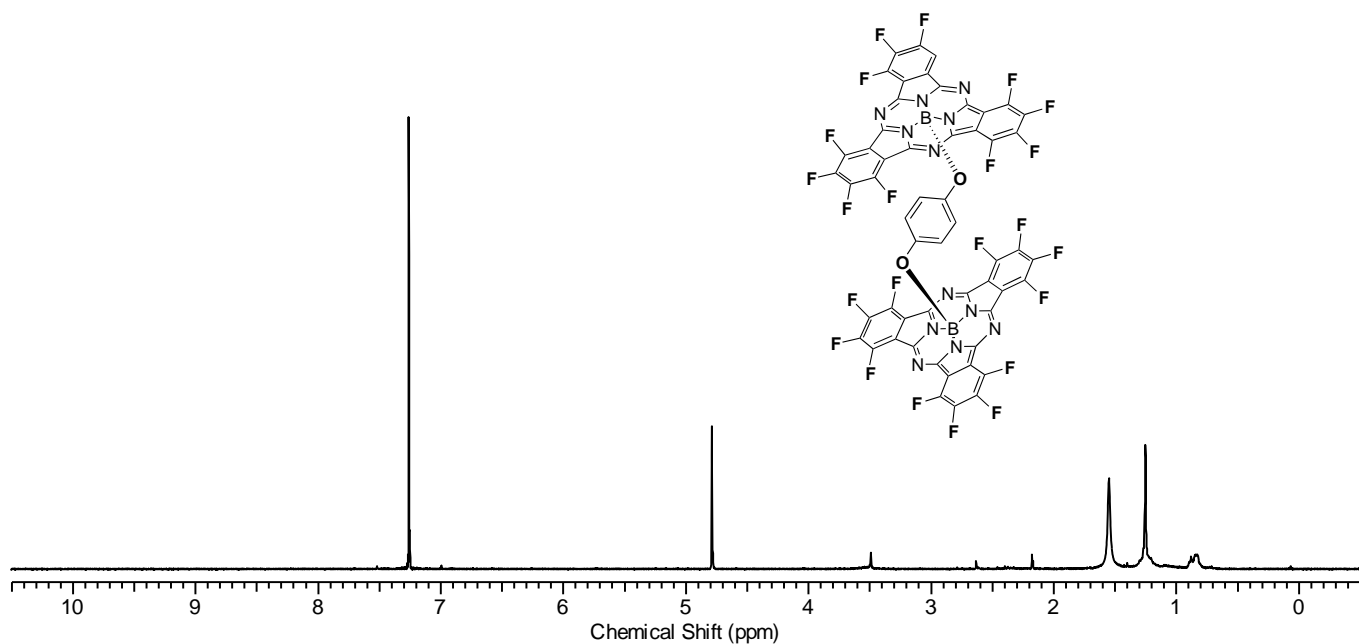


Figure 3.5 ^1H NMR Spectrum of **4c**

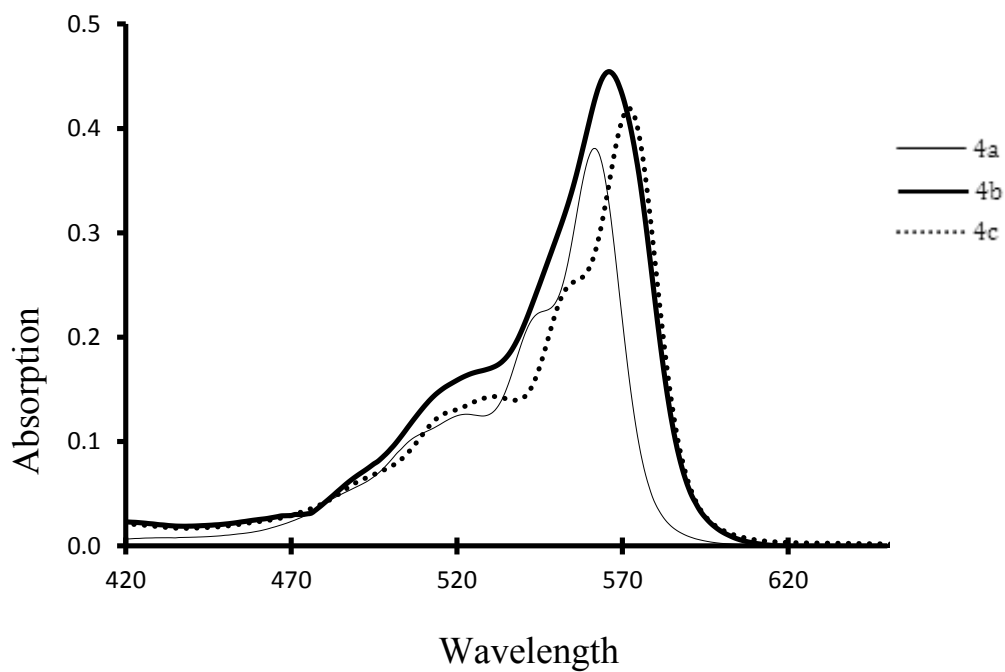


Figure 3.6 UV-Vis Spectra of the dimers

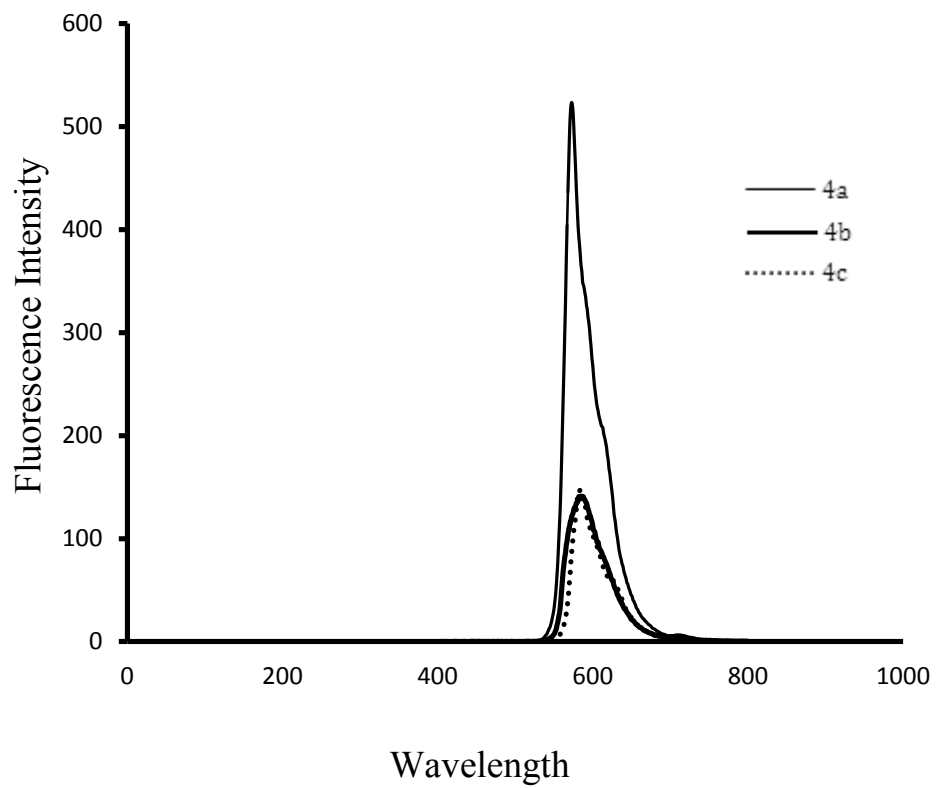


Figure 3.7 Emission Spectra of the Dimers

CHAPTER IV

RESULTS AND DISCUSSION

SYNTHESES, CHARACTERIZATION AND PROPERTIES OF NOVEL SUBPHTHALOCYANINE-PORPHYRIN CONJUGATES

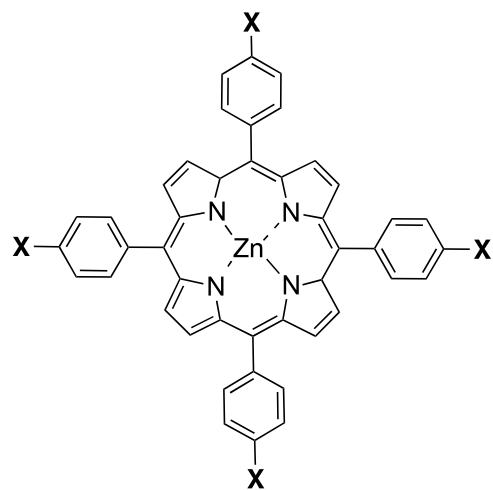
4.1 Introduction

In the recent years, the field of organic solar cells have fascinated scientists. A great deal of research work has been invested towards improving the efficiency of solar cells by not only collecting the solar energy throughout the entire solar spectrum but also in the effectual conversion of solar energy into resourceful chemical energy.¹ This conversion involves three sequential steps: light absorption, (ii) excitation energy transduction, and (iii) photoinduced electron transfer.²⁻⁴ Notwithstanding that fullerene derivatives are considered to be one among the most employed n-type material for photovoltaic applications.^{5,6} with exceptional electron accepting properties, they display only weak absorption cross sections in the visible part of the solar spectrum. This alters the sunlight capture thereby impeding the output of photon-to-electron conversion.⁷ In the quest to find promising alternatives to fullerenes, subphthalocyanines (SubPcs)^{8,9} are identified as suitable candidates which possess strong absorption in the visible region with high extinction coefficients. Additionally subphthalocyanines can play a dual role acting as both electron acceptor and donor,¹⁰⁻¹³ depending on the nature of the counterpart. Due to the synthetic versatility and the tunable properties of the

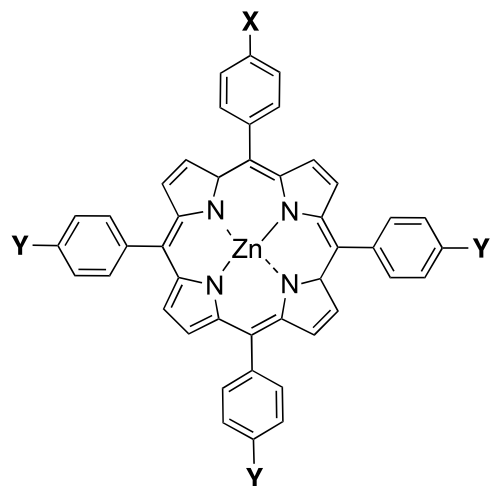
subphthalocyanines, several peripheral substituted derivatives of subphthalocyanines have been prepared. However, there are only a few axially coordinated subphthalocyanine derivatives where the electronic characteristics of the macrocycle are preserved.¹⁴⁻¹⁷ Donor acceptor conjugates of subphthalocyanines are particularly interesting because their excited states can be potentially applied in various molecular electronic devices and artificial photosynthetic systems.¹²⁻¹³ Furthermore, the incorporated subphthalocyanines impart additional solubility to the conjugates. Thus, in order to achieve highly soluble donor-acceptor conjugates covering a broad range of the solar spectrum, with increased efficiency of solar energy conversion, the construction of dyads and triads comprised of porphyrin and subphthalocyanine units has been established. A covalently linked B-O bond in the axial position acts as the electron donor and acceptor pair.

4.2 Substituted Porphyrins

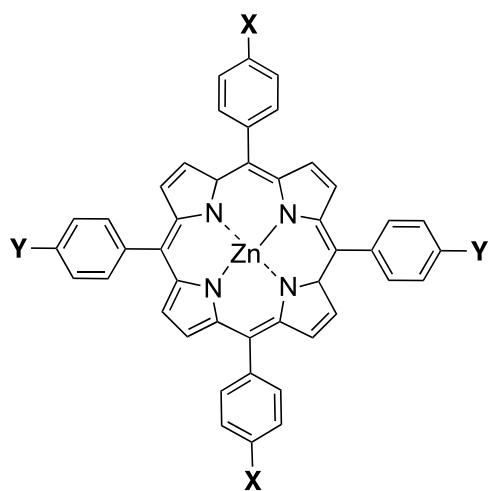
Tetraarylporphyrins (A_4) have been employed as building blocks for various assemblies that are of interest to materials scientists and bioinorganic chemists. These assemblies include multiporphyrin arrays¹⁸ and also porphyrins with appended axial ligands. Although many of the *meso*-substituted porphyrins used for such purposes have four identical aryl substituents, less symmetric porphyrins (A_3B , A_2B_2) are expected to make more varied structures possible. Particularly, the *trans-meso*- A_2B_2 porphyrins may be utilized to form assemblies that are difficult to make from the conventional *meso*- A_4 porphyrins. (Figure 4.1).



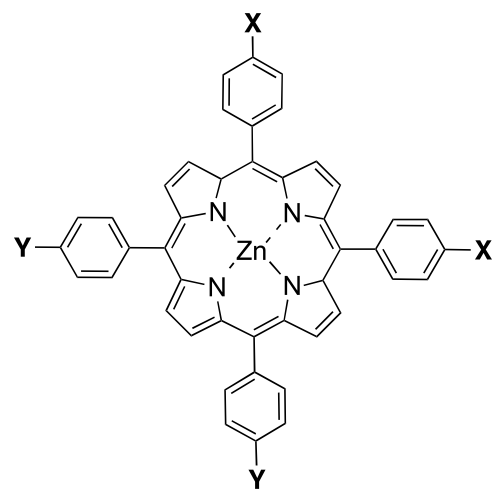
A₄ - ZnP



A₃B - ZnP



***trans*-A₂B₂ - ZnP**



***cis*-A₂B₂ - ZnP**

Figure 4.1 Representation of Different *meso*-substituted Zinc Porphyrins (ZnP).

4.3 Significance of the different entities in the porphyrin-SubPc systems

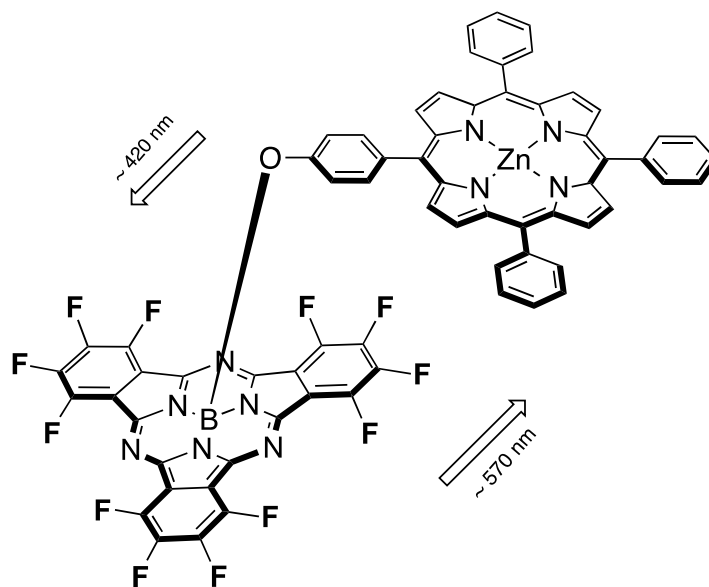


Figure 4.2 Significance of the Entities Involved in the Illustrated System.

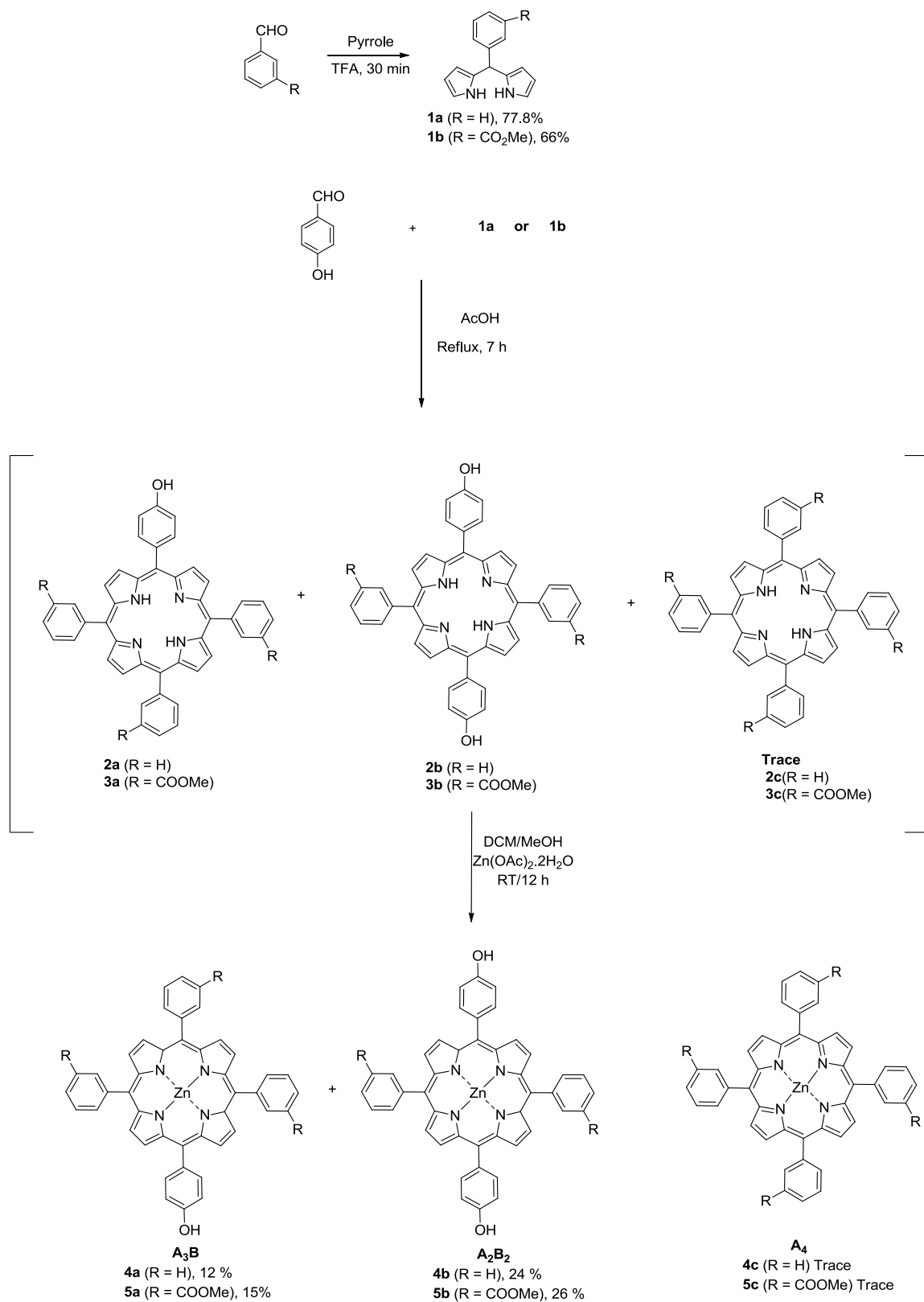
The rationale for choosing the different entities is as follows: (Figure 4.2):

1. The *meso*-substituted zinc porphyrin (A₃B/A₂B₂-ZnP) unit with its low oxidation potential and relatively high-lying triplet state could be superior photoinducible electron donor.
2. The phenoxy group substituted in the *meso*- position of the porphyrin promotes delocalization of electrons around the aromatic core.
3. The introduction of the 12 electron-withdrawing fluorine atoms on the peripheral position of the subphthalocyanine induces the electron accepting capability of the macrocycle thereby playing the role of the antenna unit.

4.4 Results and Discussion

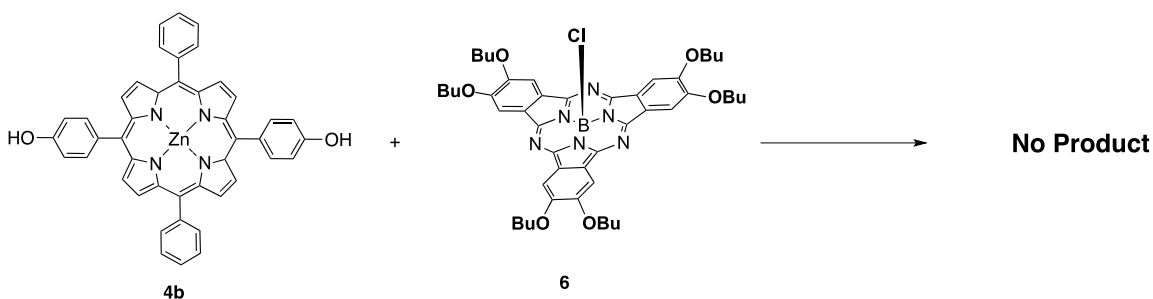
4.4.1 Synthesis

The synthesis of A_3B and *trans meso*-substituted A_2B_2 porphyrins proceeded with the synthesis of dipyrromethane (Scheme 4.1). Two different dipyrromethanes **1a** and **1b** were synthesized from the corresponding aldehydes (benzaldehyde or methyl 3-formyl benzoate) *via* a condensation with freshly distilled pyrrole in the presence of TFA. Reaction of the synthesized dipyrromethane precursors with *p*-hydroxybenzaldehyde in acetic acid under reflux conditions with air as the oxidant afforded a mixture of A_3B -(**2a**, **3a**) and A_2B_2 -(**2b**, **3b**), plus a trace of A_4 -(**2c**, **3c**) porphyrins (Scheme 4.1). Since the base porphyrin intermediates were difficult to handle, they were converted to zinc complexes by reacting with $Zn(OAc)_2$. Initially with a 1:1 ratio of dipyrromethane **1a** and *p*-hydroxybenzaldehyde, a mixture of monohydroxy triphenyl porphyrin, A_3B (**4a**-28%), dihydroxydiphenylporphyrin A_2B_2 (**4b**-13%), and tetraphenylporphyrin, A_4 (**4c**-3%), was isolated. However, with 1:1.5 ratio of the starting materials, the yield of **4b** was increased to 24% and **4a** was decreased to 12% although a trace amount of tetraphenylporphyrin A_4 was also isolated. Adopting similar conditions (ratio 1:1.5), the synthesis of the mono (**5a**, 15%), dihydroxy-substituted (**5b**, 26%) plus a trace of **5c** derivatives was achieved.



Scheme 4.1 Synthesis of A₃B and *trans meso*-substituted A₂B₂ porphyrins.

To initiate the formation of a covalent linkage of the SubPc with the porphyrin **5b** (Scheme 4.2) a first attempt was made with a peripheral butoxy-substituted subphthalocyanine in toluene. However, no product was isolated under a variety of conditions (Table 4.1), presumably because of the electron donating properties of the peripheral butoxy groups in the subphthalocyanine which made the boron atom less positive.



Scheme 4.2 Attempted Synthesis of Target ZnP-SubPc Conjugate.

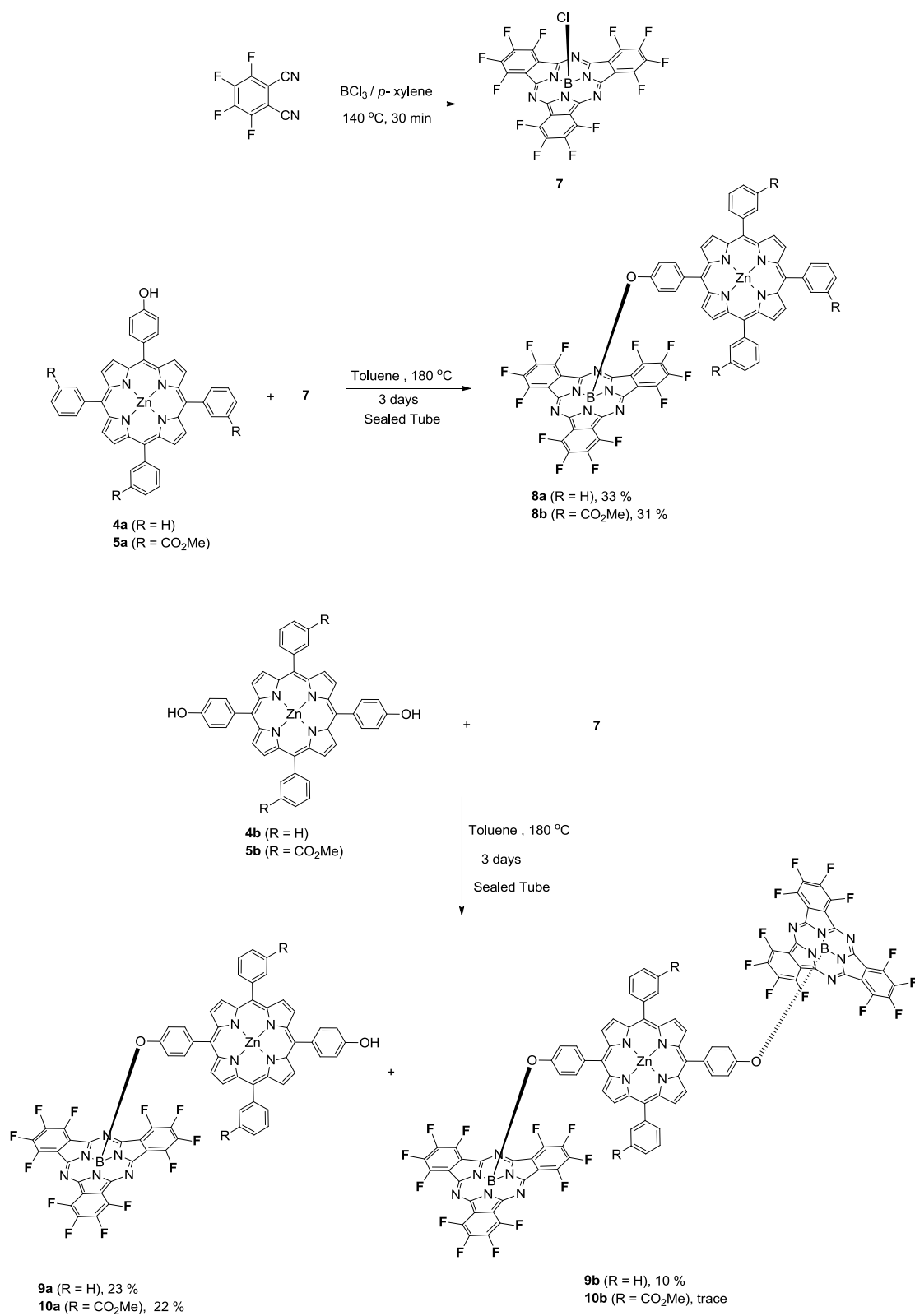
Table 4.1 Reaction Conditions Followed for the Synthesis of ZnP-SubPc(OBu)₆.

Base	Solvent	T (°C)	Product
None	Toluene	120 °C	No product
DMAP	Toluene	120 °C	No product
DBU	Toluene	120 °C	No product
Pyridine	Toluene	120 °C	No product
NaH	THF	70 °C	Decomposition
K ₂ CO ₃ /18 crown	THF:Toluene (1:1)	100 °C	Decomposition

A good electron acceptor, dodecafluorophthalocyanine **7** was synthesized by the cyclotrimerization of tetrafluorophthalonitrile with BCl₃ (1.0 M solution in *p*-xylene) using the standard reaction conditions (Scheme 4.3). A conventional nucleophilic substitution required 1:5 molar ratio of the SubPc:nucleophile concentration and reflux temperature. The nucleophilic substitution of the chlorine atom by the phenoxy group was first attempted with the monohydroxy substituted ZnP **4a**. Reaction of **7** and **4a** in 1:5 ratio in dry toluene (Table 4.2) at reflux conditions afforded the product **8a** in less yield (12%) after 4 days. However in order to reduce the concentration of nucleophile to 1:1 molar ratio, the temperature was increased to 180 °C using a sealed tube to perform the reaction. The reaction of an equimolar mixture of **7**:**4a** conducted in a sealed tube at 180 °C afforded the SubPc-Porphyrin conjugate **8a** in 33% yield (Table 4.2, Scheme 4.3). Adopting similar conditions, the reaction of *trans*- A₂B₂ porphyrin **4b** with the SubPc-F₁₂ **7** gave two products **9a** and **9b** which were isolated by column chromatography. The ester substituted compounds **8b**, **10a**, and **10b** were also prepared adopting similar conditions. Structures of all synthesized compounds are illustrated in Figure 4.3.

Table 4.2 Reaction Conditions Followed for the Synthesis of **8a**.

Ratio (7:4a)	Equipment	Solvent	T (°C)	Time	Product Yield
1:5	Round bottomed Flask	Toluene	120 °C	4 days	12%
1:1	Sealed Tube	Toluene	180 °C	3 days	33%



Scheme 4.3 Synthesis of Porphyrin-SubPc-F₁₂ Conjugate.

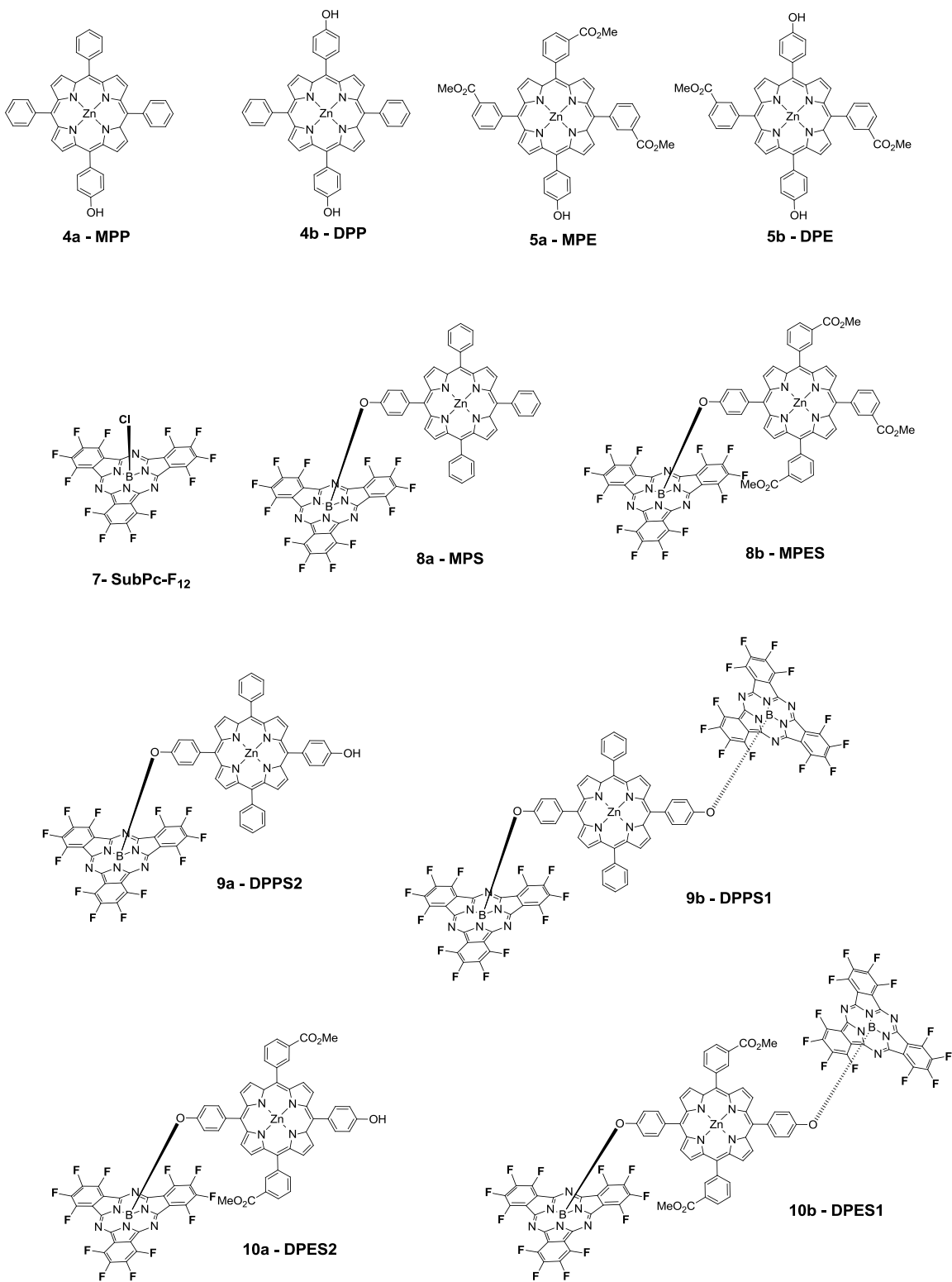


Figure 4.3 Representation of the Synthesized Compounds.

4.4.2 Absorption Studies

The electronic interaction between the SubPc and A₃B/A₂B₂-ZnP were investigated *via* absorption and emission studies. The steady-state absorption spectra of the parent compounds and the conjugates in toluene and CH₂Cl₂ are shown in Figure 4.4 and Figure 4.5, respectively. The absorption spectra of MPP and DPP consists of a Q band arising from a π - π^* transition associated with 14 π electron systems. The absorption spectra of the conjugates (MPS, DPPS1, DPPS2 – Figures 4.3 and 4.5) exhibited common features of the SubPc and ZnP, and the spectra were red shifted about 3-4 nm in toluene.

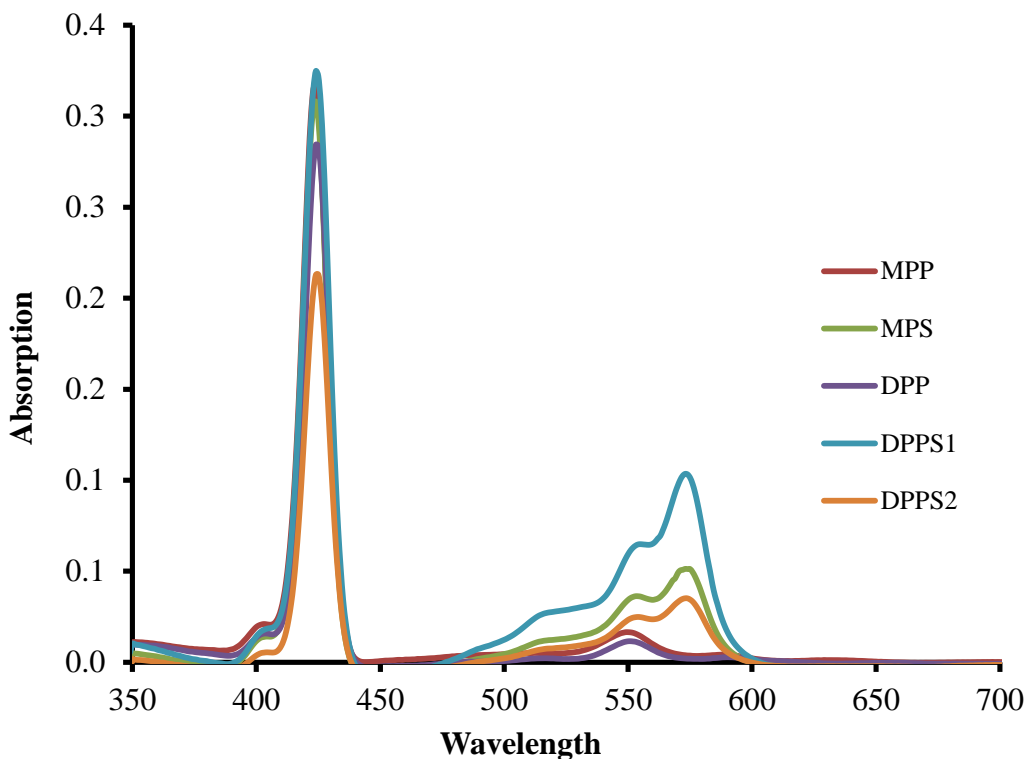


Figure 4.4 Absorption Spectra of the Compounds in Toluene.

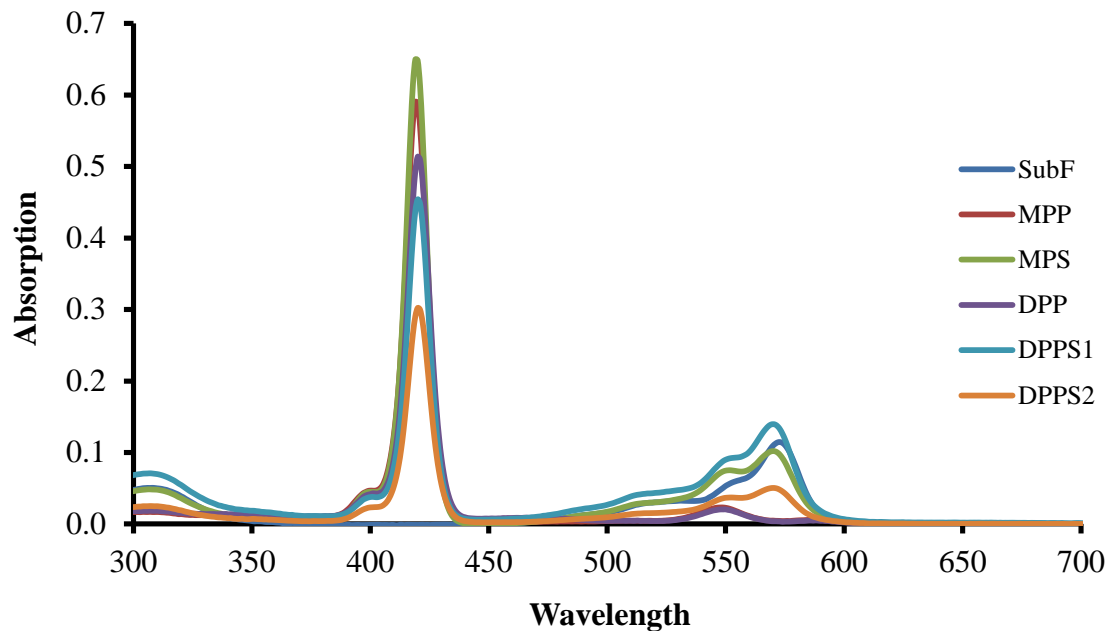


Figure 4.5 Absorption Spectra of the Compounds in CH_2Cl_2 .

4.4.3 Emission Studies

The emission spectra of the compounds recorded in toluene and CH_2Cl_2 are shown in Figure 4.6 and Figure 4.7, respectively. Excitation of the porphyrins DPP and MPP at 420 nm in CH_2Cl_2 revealed two emission bands centered at 597 nm and 644 nm. Whereas excitation of the conjugates displayed no such emission bands, which suggested that charge transfer might have occurred between the ZnP and SubPc species.

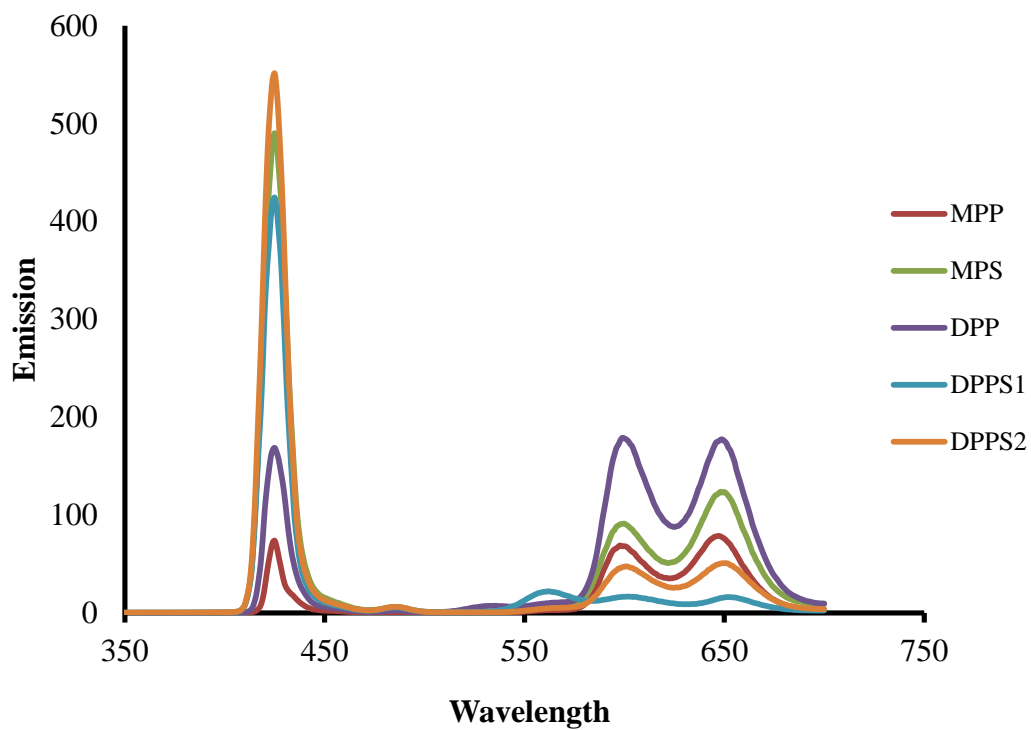


Figure 4.6 Emission Spectra of the Compounds in Toluene at 424 nm.

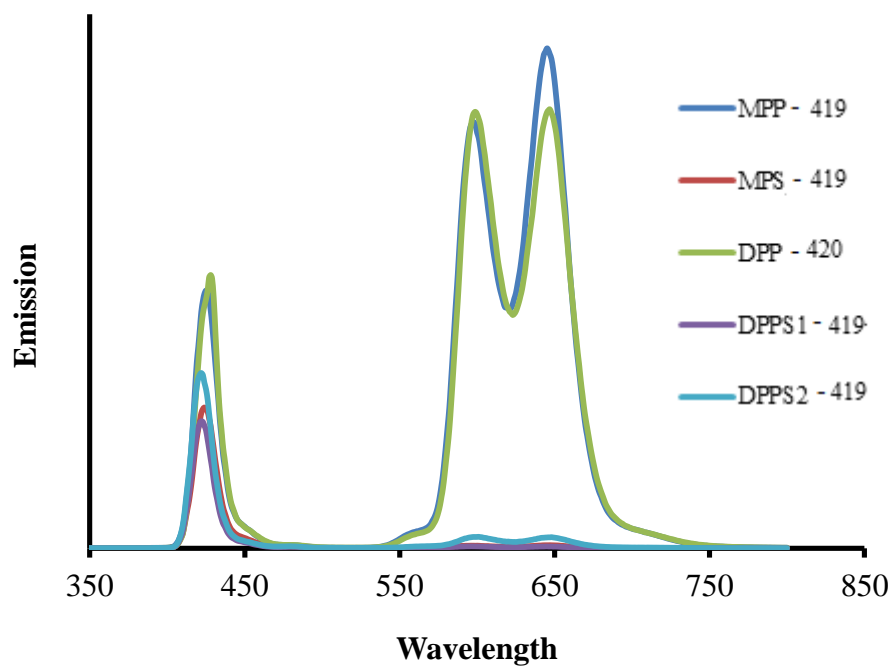


Figure 4.7 Emission Spectra of the Compounds in CH_2Cl_2 at 419/420 nm.

4.4.4 Electrochemical Studies

The redox behavior of the dyads and triads was investigated by cyclic voltammetry experiments. The results were compared with those of the reference compounds SubPc-F₁₂, MPP and DPP (Figure 4.3). All experiments were performed at room temperature in deaerated acetonitrile solution by bubbling nitrogen gas containing *tetra-n*-butylammonium hexafluorophosphate (TBAPF₆, 0.1 M) as the supporting electrolyte, with a glassy carbon as the working electrode, platinum as the counter electrode, and Ag/AgNO₃ as the reference electrode.

The representative cyclic voltammograms (CVs) of porphyrins, SubPc-F₁₂ and SubPc-porphyrin conjugates (MPS, DPPS1 and DPPS2) are shown in Figures 4.8, 4.9, and 4.10, respectively. The CVs of the SubPc-Porphyrin conjugates share common features with respect to those of parent porphyrins and SubPc-F₁₂. SubPc-F₁₂ presents several characteristic reduction waves of SubPcs with a reversible one electron reduction process occurring at -0.986 V versus Ag/AgNO₃.

In the cathodic direction (between 1 and -2.5 V), MPS show successive three reduction processes, which are electrochemically reversible, two waves corresponding to the porphyrin (0.481 V and -1.878 V) and one wave corresponding to the SubPc-F₁₂ located at -0.948 V versus Ag/AgNO₃. In comparison to the unsubstituted SubPc-F, the conjugate MPS exhibited a more positive reduction peak ~40 mV vs Ag/AgNO₃ which supports the strong coupling between the subphthalocyanine and the porphyrin units. Moreover, an irreversible oxidation processes was exhibited by the conjugate MPS which occurred at -1.43 V (Table 4.3). This supports the concept that, in general, the fluorosubphthalocyanines are difficult to oxidize. The dyad DPPS2 and the triad DPPS1

retains the common features of MPS. A close inspection of the redox features of these compounds reveals that though the reduction waves based on both porphyrin and SubPc-F₁₂ do not change significantly, both the oxidative and reductive voltammograms of MPS, DPPS1 and DPPS2 are not exactly the sum of those of the parent SubPc-F₁₂ and porphyrins. These are good indications that electronic communications between the chromophores are present in the conjugate which forms Por⁺-SubPc-F⁻ species. Thus the electrochemical investigation confirmed the formation of different porphyrin-SubPc conjugates and additionally provided further insights into the electronic properties of the synthesized complexes.

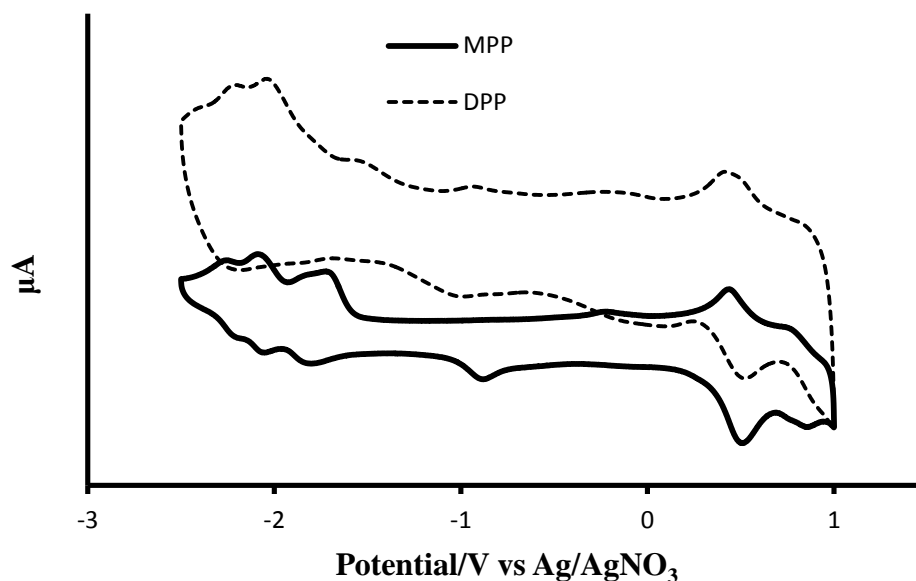


Figure 4.8 Cyclic Voltammogram of Porphyrins MPP and DPP.

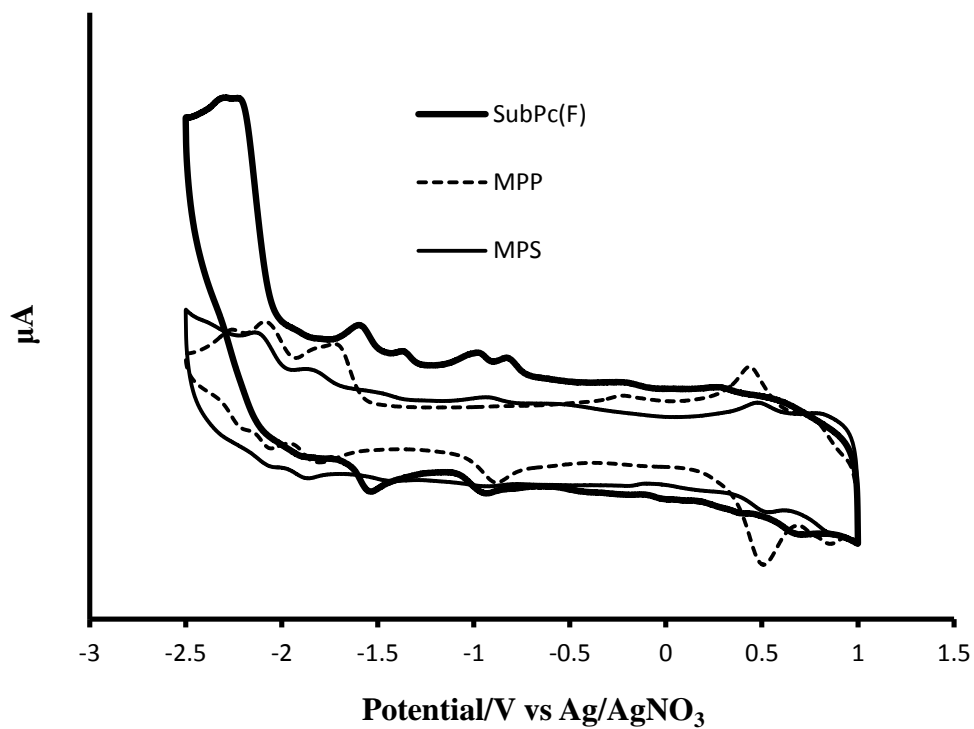


Figure 4.9 Cyclic Voltammogram of SubPc, MPP and MPS.

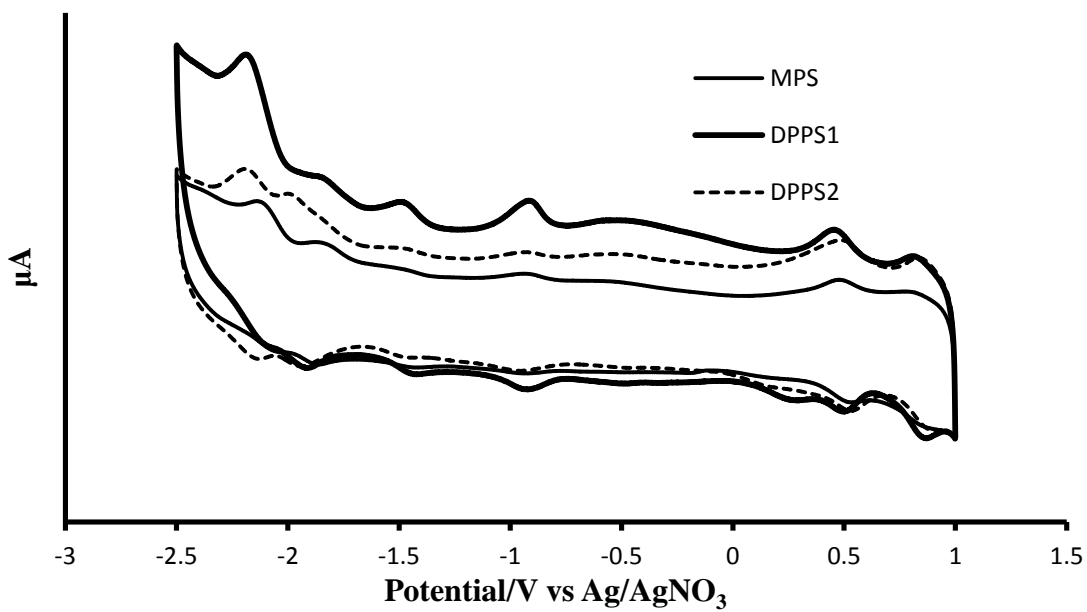


Figure 4.10 Cyclic Voltammogram of the Conjugates MPS, DPPS1 and DPPS2.

Table 4.3 Electrochemical Data of the Compounds.

Compound	E ¹ (red)	E ² (red)	E ³ (red)	E ¹ (ox)	E ² (ox)	E ³ (ox)	E ⁴ (ox)
SubPc-F	0.2659	-0.986	-1.593	-1.541	-	-0.937	0.706
MPP	0.430	-	-1.725	-1.811	-	-0.885	-
DPP	0.421	-0.931	-1.531	-	-	-1.026	0.510
MPS	0.481	-0.948	-1.878	-1.861	-1.431	-0.942	0.538
DPSS1	0.447	-0.919	-1.844	-1.919	-1.424	-0.925	0.493
DPSS2	0.4815	-0.925	-1.96	-1.93	-1.450	-0.953	0.510

4.4.5 Structure of DPSS1

The assumed structure of DPSS1 is shown in the Figure 4.11. The relatively linear orientation of the two phenol units places the ZnP plane perpendicular to the convex center of the two subphthalocyanine units. As a consequence of the incorporated non-planar subphthalocyanine units, the planarity of the POR-SUBF conjugate is reduced.

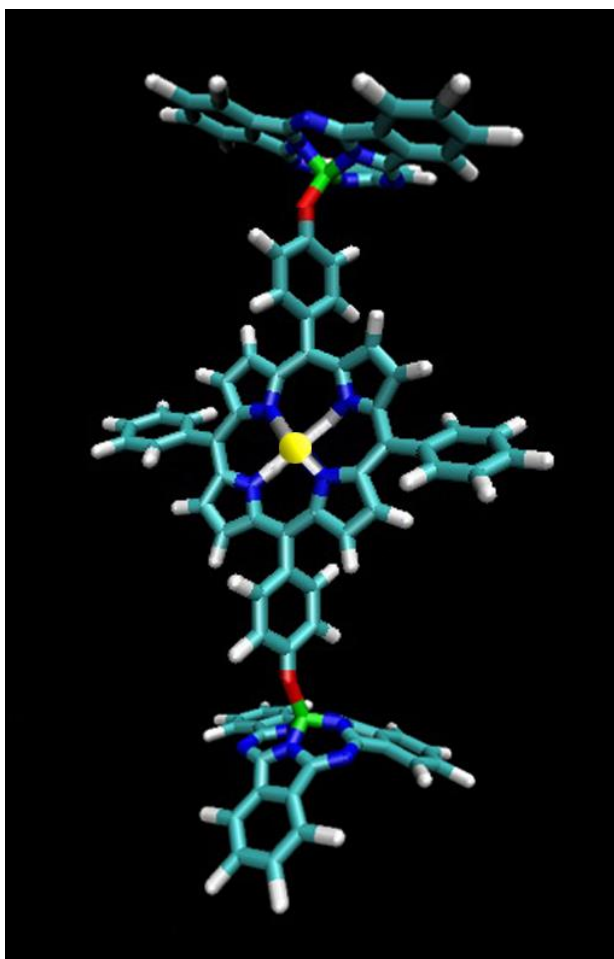


Figure 4.11 Structure of DPPS1

4.5 Experimental

4.5.1 General

Melting points were determined using a Stuart SMP10 instrument. NMR spectra (^1H , ^{13}C , and ^{19}F) were acquired in CDCl_3 , CD_2Cl_2 , or DMSO using a Varian Inova 400 MHz spectrometer. Chemical shifts (δ) are expressed in ppm relative to residual chloroform (^1H : 7.26 ppm, ^{13}C : 77.0 ppm), DMSO (^1H : 2.5 ppm, ^{13}C : 39.5 ppm), and dichloromethane (^1H : 5.32 ppm, ^{13}C : 54.0 ppm, ^{19}F : -76.5 ppm, CF_3COOH). Fourier

Transform Infrared measurements were performed on a Varian 800 FT-IR spectrometer. UV-Vis spectra were recorded on Cary 5000 UV-VIS-NIR spectrophotometer. Fluorescence spectra were recorded on a Cary Eclipse fluorescence spectrophotometer. All UV-Vis and fluorescence spectra were recorded at a concentration of $1.0 \times 10^{-7} M$ at 23 °C. The sealed tube reaction was conducted in a unit from Chem Glas, Model 1880. Column chromatography was carried out with silica gel (Sorbent Technologies, 230-400 mesh), and TLC was performed with polyester sheets precoated with silica gel (Sorbent Technologies). Compounds pyrrole, phthalonitrile, *p*-hydroxybenzaldehyde, (Alfa Aesar), tetrafluorophthalonitrile (TCI), benzaldehyde, TFA, 1.0 M BCl_3 solution in *p*-xylene (Sigma Aldrich) and 3-methylformyl benzoate (Acros Organics) were purchased from commercial suppliers and used as received unless otherwise indicated.

4.5.2 General Method for the Synthesis of Porphyrin (A)

A mixture of the dipyrromethane (1.0 equiv) and *p*-hydroxybenzaldehyde (1.5 equiv) was taken in a 250-mL, single-necked, round-bottomed flask fitted with a condenser and a magnetic stir bar. Acetic acid (20 volumes w.r.t dipyrromethane) was added to the reaction mixture, and the resulting pale yellow solution was refluxed with continuous stirring for 7 hr. After allowing the thick, black mixture to cool to room temperature, the solvent was removed under vacuum to give a black solid. The solid was then filtered over a pad of silica which was washed with THF. The filtrate and washings were combined, and the solvent was evaporated to afford the crude base porphyrin. Without further purification, the crude base porphyrin intermediate was taken to the next step of complexation with zinc.

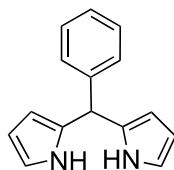
4.5.3 General Method for the Synthesis of Zn-Porphyrin (B)

Metallation of the base porphyrin was achieved by treating the crude black solid and an excess of $\text{Zn}(\text{OAc})_2 \cdot 2\text{H}_2\text{O}$ with a 1:1 mixture of CH_2Cl_2 :MeOH (10 volumes w.r.t crude) in a 100-mL, single-necked round-bottomed flask fitted with a magnetic stirrer at room temperature for 12 h. The progress of the reaction was monitored by TLC. The solvent from the reaction mixture was evaporated, and the residue obtained was extracted with ethyl acetate (10 volumes) and washed with brine, dried (Na_2SO_4), and concentrated to provide a dark purple solid containing a mixture of A_3B and A_2B_2 porphyrins. Flash chromatography of the mixture using ethyl acetate:hexane (1:3) afforded pure mono and di-substituted porphyrins.

4.5.4 General Method for the Synthesis of Porphyrin– SubPc-F₁₂ Conjugates

A mixture of porphyrin (1.0 equiv) and dodecafluorosubphthalocyanine (1.0-2.0 equiv) dissolved in dry toluene (10 volumes w.r.t porphyrin) was taken in a sealed tube and heated to 180 °C for 3 days. The progress of the reaction was monitored by TLC. The solvent from the reaction mixture was removed under vacuum and the residue was purified by column chromatography over silica gel using ethyl acetate:hexane in varying ratios.

4.5.5 Synthesis of 5-Phenyldipyrromethane



1a

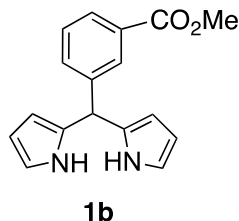
A solution of benzaldehyde (0.5 g, 0.0047 mol) and freshly distilled pyrrole (13 mL, 0.188 mol) were placed in a 250-mL, two-necked, round-bottomed flask fitted with a magnetic stirrer and a gas inlet. The solution was degassed by bubbling argon through the solution for 15 min at room temperature. Then TFA (35 μ L, 0.47 mmol) was added, and the resulting mixture was stirred for 20 min at which point no starting material was seen *via* TLC analysis. The crude material was diluted with CH_2Cl_2 (30 mL) and washed with 0.1 M NaOH (25 mL), followed by a brine wash and drying (Na_2SO_4). The solvent and the unreacted pyrrole were removed under vacuum. The crude material was flash chromatographed using ethyl acetate:hexane (1:9) over silica gel to give the pure dipyrromethane **1a**.

Yield: 0.81 g (77.8 %).

Mp: 100-102 $^\circ\text{C}$ (lit,¹⁹ 101 $^\circ\text{C}$).

^1H NMR (400 MHz, CDCl_3): δ 5.47 (s, 1H); 5.91 (s, 2H); 6.15-6.18 (m, 2H); 7.21-7.32 (m, 5H); 7.91 (br s, 2H).

4.5.6 Synthesis of 5-(3-Methoxycarbonylphenyl)dipyrromethane



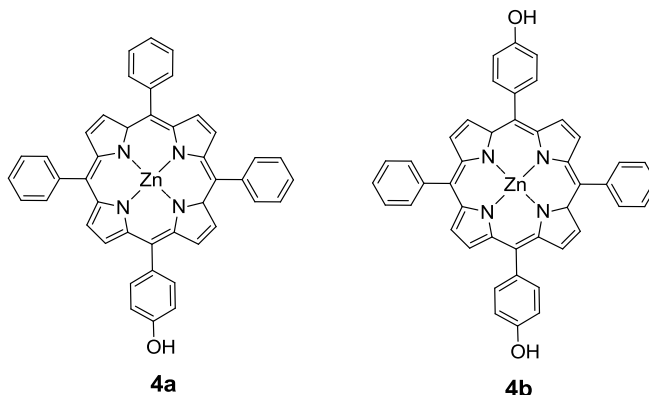
A solution of methyl 3-formylbenzoate (0.5 g, 0.003 mol) and freshly distilled pyrrole (8.4 mL, 0.12 mol) was placed in a 100-mL, two-necked, round-bottomed flask fitted with a magnetic stirrer and a gas inlet. The solution was degassed by bubbling argon through the solution for 15 min at room temperature. Then TFA (23 μ L, 0.0003 mol) was added, and the resulting mixture was stirred for 20 min at which point no starting material was seen on TLC analysis. The crude material was diluted with CH_2Cl_2 (30 mL) and washed with 0.1 M NaOH (25 mL), followed by a brine wash and drying (Na_2SO_4). The solvent and the unreacted pyrrole were removed under vacuum. The crude material was flash chromatographed using ethyl acetate:hexane (1:5) over silica gel to give the pure dipyrromethane **1b**.

Yield: 0.56 g (66%).

Mp: 125-127 $^\circ\text{C}$ (lit,²⁰ 124-127 $^\circ\text{C}$).

$^1\text{H NMR}$ (300 MHz, $\text{DMSO}-d_6$): δ 3.81 (s, 3H); 5.53 (s, 1H); 5.67 (s, 2H); 5.91 (m, 2H); 6.64 (s, 2H); 7.42 (m, 2H); 7.80 (m, 2H), 10.61 (br s, 2H).

4.5.7 Synthesis of 4a and 4b



A mixture of dipyrromethane **1a**, (1 g, 0.004 mol), *p*-hydroxybenzaldehyde (0.822 g, 0.006 mol) and acetic acid (20 mL) was reacted according to the general procedure A. This was then followed by the metallation with Zn(OAc)₂·2H₂O (1.93 g, 0.008 mol) in CH₂Cl₂:MeOH solution (50 mL, 1:1) according to the standard procedure B to afford a mixture of A₃B and *trans*-A₂B₂ porphyrins corresponding to the mono hydroxyl (**4a**) and di-hydroxy porphyrins (**4b**), respectively. Purification of the mixture by column chromatography with ethyl acetate:hexane (1:3) afforded a pure **4a** and **4b**.

4a

Yield: 0.37 g (12%).

Mp: >250 °C (lit,²¹ >250°C).

¹H NMR (400 MHz, DMSO-*d*₆): δ 8.99 (d, 4.8 Hz, 2H), 8.95-8.94 (m, 6H); 8.23-8.21 (d, J = 6.8 Hz, 6H); 8.07 (d, J = 8 Hz, 2H); 7.73-7.76 (m, 9H); 7.20 (d, J = 5.6 Hz, 2H).

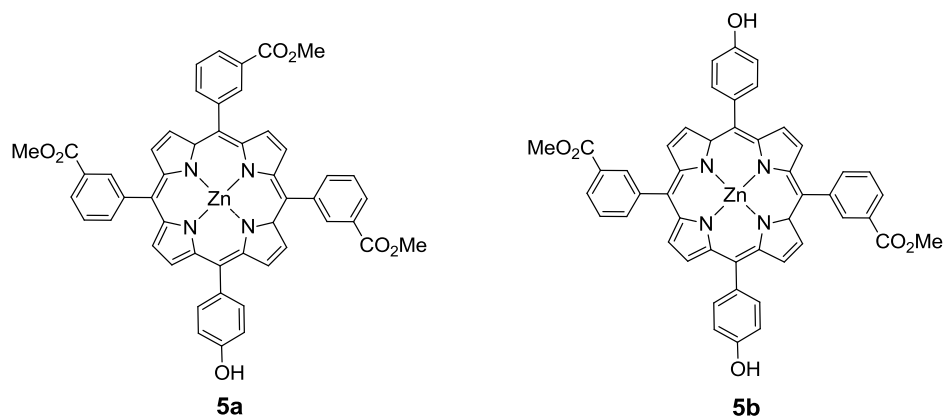
4b

Yield: 0.76 g (24%).

Mp: >250 °C.

¹H NMR (400 MHz, DMSO-*d*₆): δ 9.80 (s, 2H); 8.82 (d, J = 4.4 Hz, 4H); 8.73 (d, J = 4.4 Hz, 4H); 8.17 (m, 4H); 7.94 (d, J = 8 Hz, 4H); 7.79-7.78 (m, 6H); 7.15 (d, J = 8 Hz, 4H).

4.5.8 Synthesis of 5a and 5b



A mixture of dipyrromethane **1b**, (1 g, 0.0035 mol), *p*-hydroxybenzaldehyde (0.653 g, 0.0053 mol) and acetic acid (200 mL) were reacted according to general procedure A. This was then followed by the metallation with Zn(OAc)₂·2H₂O (0.76 g, 0.0035 mol) in CH₂Cl₂:MeOH solution (50 mL, 1:1) according to the standard procedure B to afford a mixture of A₃B and *trans* A₂B₂ porphyrins corresponding to the mono hydroxyl **5a** and di-hydroxy porphyrins **5b**, respectively. Purification of the mixture by column chromatography using ethyl acetate:hexane (1:3) afforded pure **5a** and **5b**.

5a

Yield: 0.46 g (15%). **Mp:** >250 °C.

IR (CH₂Cl₂) cm⁻¹: 3052, 2989, 1719, 1484, 1422, 1264, 1170, 1109, 735, 709.

¹H NMR (400 MHz, CDCl₃): δ 8.95 (d, J = 4.8, 2H), 8.86 (s, 6H), 8.67 (s, 3H), 8.41 (m, 6H), 8.01 (d, J = 8 Hz, 2H), 7.82 (m, 3H), 7.12 (d, J = 8.8 Hz, 2H).

¹³C NMR (100 MHz, CDCl₃): δ 167.2, 157.3, 150.6, 149.3, 143.5, 138.9, 135.3, 134.7, 133.4, 132.4, 131.3, 128.4, 128.3, 127.9, 121.9, 121.3, 119.1, 114.0, 52.8.

MS (MALDI-TOF) *m/z* for C₅₀H₃₄N₄O₇Zn: Calcd: 868.2132; Found: 868.2654.

ELEMENTAL ANAL.: Calcd: C₅₀H₃₄N₄O₇Zn·0.5 H₂O: C, 68.46; H, 4.02; N, 6.39.

Found: C, 68.27; H, 4.07; N, 6.43.

5b

Yield: 0.76 g (26%). **Mp:** >250 °C.

¹H NMR (400 MHz, DMSO-*d*₆): δ 9.97 (s, H), 8.84 (d, J = 4.8, 4H), 8.69 (d, J = 4.8 Hz, 4H), 8.67 (s, 2H), 8.43 (d, J = 8 Hz, 2H), 8.38 (d, J = 8 Hz, 2H), 7.93-7.96 (m, 6H), 7.15 (d, J = 8.8 Hz, 4H).

IR (CH₂Cl₂) cm⁻¹: 3055, 2985, 1721, 1422, 1264, 1169, 895.53, 734, 707, 619.

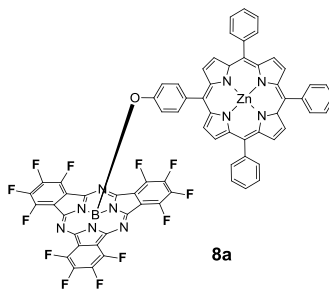
¹³C NMR (100 MHz, DMSO-*d*₆): δ 167.1, 157.4, 150.5, 149.4, 143.7, 138.8, 135.9, 134.5, 133.6, 132.6, 131.6, 128.8, 128.5, 127.8, 121.8, 121.4, 119.2, 114.1, 52.9.

MS (MALDI-TOF) *m/z* for C₄₈H₃₂N₄O₆Zn: Calcd: 826.1716; Found: 826.1532

ELEMENTAL ANAL.: Calcd: C₄₈H₃₂N₄O₆Zn·1.3 H₂O: C, 67.86; H, 4.10; N, 6.59.

Found: C, 67.47; H, 4.16; N, 6.43.

4.5.9 Synthesis of 8a



A mixture of **7** (0.025 g, 0.03 mmol) and **4a** (0.026 g, 0.03 mol) was reacted in dry toluene (2 mL) using a sealed tube according to the general procedure C. Repeated washing of the product with pentane and drying under vacuum did remove the solvent impurities and water.

Yield: 16.3 mg (33%). **Mp:** >250 °C.

IR (CH₂Cl₂) cm⁻¹: 3058, 2924, 2853, 1531, 1480, 1264, 1107, 1002, 965, 798, 741.

¹H NMR (400 MHz, CD₂Cl₂): δ 8.94 (s, 4H), 8.92 (d, J = 4.8, 2H), 8.70 (d, J = 4.4 Hz, 2H), 8.20 (d, J = 6.8 Hz, 6H), 7.75-7.78 (m, 9H), 7.64 (d, J = 8 Hz, 2H), 5.73 (d, J = 8 Hz, 2H).

¹³C NMR (100 MHz, CD₂Cl₂): δ 151.5, 150.5, 148.8, 144.2, 143.0, 142.2, 137.4, 135.4, 132.2, 131.9, 127.8, 126.9, 121.4, 120.4, 117.4, 115.5.

¹⁹F NMR (376 MHz, CD₂Cl₂): δ -137, -149 (δ -76.5, CF₃COOH)

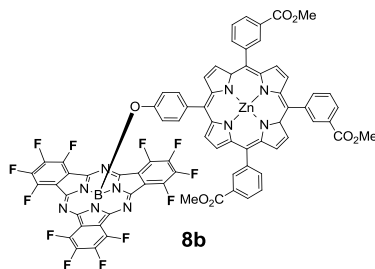
MS (MALDI-TOF) *m/z* for C₆₈H₂₇BF₁₂N₁₀OZn: Calcd: 1304.1719; Found: 1304.1516

ELEMENTAL ANAL.: C₆₈H₂₇BF₁₂N₁₀OZn·6H₂O:

Calcd: C, 57.83; H, 2.78; N, 9.92

Found: C, 57.64; H, 2.63; N, 10.06.

4.5.10 Synthesis of 8b



A mixture of **7** (0.025 g, 0.056 mol) and **5a** (0.026 g, 0.03 mmol) were reacted in dry toluene (2 mL) using a sealed tube according to the general procedure C. Repeated washing of the product with pentane and drying under vacuum did remove the solvent impurities and water.

Yield: 13 mg (31%). **Mp:** >250 °C.

IR (CH₂Cl₂) cm⁻¹: 3058, 2924, 2853, 1531, 1483, 1392, 1265, 1223, 1169, 1114, 995, 965, 796, 741, 718.

¹H NMR (400 MHz, CD₂Cl₂): δ 8.86 (m, 8H), 8.69 (s, 2H), 8.39-8.46 (m, 6H), 7.85 (d, J = 8 Hz, 3H), 7.65 (d, J = 7.2 Hz, 2H), 5.72 (d, J = 8.8 Hz, 2H), 3.97 (s, 9H).

¹³C NMR (100 MHz, CD₂Cl₂): δ 155.7, 151.3, 150.6, 148.5, 144.5, 143.5, 137.5, 136.4, 134.5, 133.5, 132.6, 131.4, 130.5, 129.6, 128.3, 127.8, 120.7, 115.5, 113.6, 57.3

¹⁹F NMR (376 MHz, CD₂Cl₂): δ -136, -148 (δ -76.5, CF₃COOH)

MS (MALDI-TOF) *m/z* for C₇₄H₃₃BF₁₂N₁₀O₇Zn: Calcd: 1478.1883; Found: 1478.1674.

ELEMENTAL ANAL.: C₇₄H₃₃BF₁₂N₁₀O₇Zn·0.5 H₂O·1.25 C₆H₁₄:

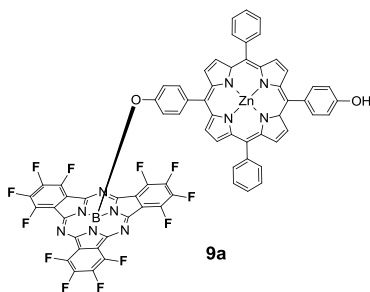
Calcd: C, 61.37; H, 3.25; N, 8.78.

Found: C, 61.22; H, 3.15; N, 8.73.

4.5.11 Synthesis of 9a and 9b

A mixture of **7** (0.1 g, 0.154 mmol) and **4b** (0.055 g, 0.07 mmol) were reacted in dry toluene (2 mL) using a sealed tube according to the general procedure C. Repeated washing of the products with pentane and drying under vacuum did remove the solvent impurities and water.

9a



Yield: 23 mg (23%). **Mp:** >250 °C.

IR (CH₂Cl₂) cm⁻¹: 3053, 2924, 2854, 1531, 1481, 1264, 1224, 1094, 1000, 965, 799, 740.

¹H NMR (400 MHz, CDCl₃): δ 8.97 (d, J = 4.8 Hz, 2H), 8.92 (d, J = 4.8, 2H), 8.90 (d, J = 5.2 Hz, 2H), 8.69 (d, J = 4.8 Hz, 2H), 8.18 (d, J = 7.2 Hz, 4H), 8.04 (d, J = 8.4 Hz, 2H), 7.75-7.80 (m, 6H), 7.64 (d, J = 8.4 Hz, 2H), 7.20 (t, J = 6.4 Hz, 2H), 5.77 (d, J = 8.4 Hz, 2H).

¹³C NMR (100 MHz, CD₂Cl₂): δ 155.6, 151.2, 150.7, 150.3, 150.2, 148.6, 144.3, 143.9, 142.9, 141.6, 141.1, 137.3, 135.7, 135.2, 134.6, 132.1, 131.7, 127.6, 126.7, 121.2, 120.1, 117.3, 115.3, 113.6.

¹⁹F NMR (376 MHz, CD₂Cl₂): δ -137, -148 (δ -76.5, CF₃COOH).

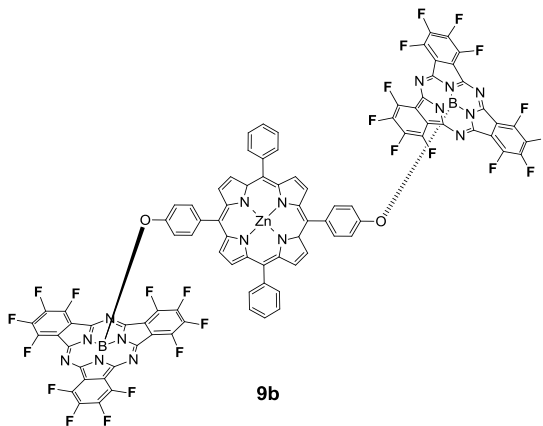
MS (MALDI-TOF) *m/z* for C₆₈H₂₇BF₁₂N₁₀O₂Zn: Calcd: 1320.1668; Found: 1320.1418

ELEMENTAL ANAL.: C₆₈H₂₇BF₁₂N₁₀O₂Zn · 0.7 H₂O · 0.5 C₆H₁₄:

Calcd: C, 61.98; H, 2.59; N, 10.18.

Found: C, 61.85; H, 2.53; N, 10.09.

9b



Yield: 14 mg (10%). **Mp:** >250 °C.

IR (CH₂Cl₂) cm⁻¹: 3052, 2925, 2854, 1531, 1480, 1265, 1095, 1003, 964, 799, 740.

¹H NMR (400 MHz, CD₂Cl₂): δ 8.90 (d, J = 4.4 Hz, 4H), 8.67 (d, J = 4.8, 2H), 8.18 (d, J = 6.4 Hz, 4H), 7.76-7.81 (m, 6H), 7.63 (d, J = 6.8 Hz, 4H), 5.73 (t, J = 8.8 Hz, 4H)

¹³C NMR (100 MHz, CD₂Cl₂): δ 151.5, 150.4, 148.8, 144.5, 144.2, 142.9, 141.1, 141.4, 137.4, 135.4, 134.7, 1322.2, 131.9, 132.2, 131.9, 127.9, 126.9, 121.4, 120.4, 117.4, 115.5.

¹⁹F NMR (376 MHz, CD₂Cl₂): δ -137, -148 (δ -76.5, CF₃COOH)

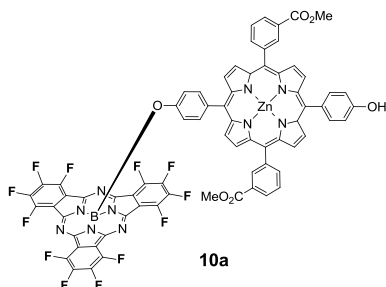
MS (MALDI-TOF) *m/z* for C₉₂H₂₆B₂F₂₄N₁₆O₂Zn: Calcd: 1930.17; Found: 1930.16

ELEMENTAL ANALYSIS: C₉₂H₂₆B₂F₂₄N₁₆O₂Zn · 0.1 H₂O · 3.5 C₆H₁₄:

Calcd: C, 60.76; H, 3.39; N, 10.03.

Found: C, 60.71; H, 3.22; N, 10.01.

4.5.12 Synthesis of 10a



A mixture of **7** (0.1 g, 0.154 mmol) and **5b** (0.064 g, 0.077 mmol) were reacted in dry toluene (2 mL) in a sealed tube according to the general procedure C. Repeated washing of the product with pentane and drying under vacuum did remove the solvent impurities and water.

Yield: 24 mg (22%). **Mp:** >250 °C.

IR (CH₂Cl₂) cm⁻¹: 3058, 2924, 2854, 1532, 1483, 1392, 1265, 1223, 1169, 1114, 995, 966, 797, 741, 718.

¹H NMR (400 MHz, CD₂Cl₂): δ 8.95 (d, J = 4.4 Hz, 2H), 8.84 (m, 4H), 8.80 (s, 2H), 8.68 (d, J = 4.8 Hz, 2H), 8.40 (m, 4H), 8.01 (d, J = 8.4 Hz, 2H), 7.84 (t, J = 5.2 Hz 2H), 7.63 (d, J = 7.6 Hz, 2H), 7.15 (d, J = 8.4 Hz, 2H), 5.72 (d, J = 8.4 Hz, 2H). 3.91 (s, 6H).

¹³C NMR (100 MHz, CDCl₃): δ 167.5, 155.9, 151.0, 150.3, 144.1, 143.1, 138.1, 135.1, 132.6, 132.1, 131.9, 129.1, 127.1, 120.1, 117.4, 115.4, 113.5, 52.5.

¹⁹F NMR (376 MHz, CD₂Cl₂): δ -137, -148 (δ -76.5, CF₃COOH)

MS (MALDI-TOF) *m/z* for C₇₂H₃₁BF₁₂N₁₀O₆Zn: Calcd: 1436.18; Found: 1436.13

ELEMENTAL ANAL.: C₇₂H₃₁BF₁₂N₁₀O₆Zn·0.7 H₂O·2.5 C₆H₁₄:

Calcd: C, 62.78; H, 4.08; N, 8.42.

Found: C, 62.78; H, 4.03, N, 8.37.

4.6 References

1. Hagfeldt, A.; Graetzel, M. *Acc. Chem. Res.* **2000**, *33*, 269-277.
2. Bach, U.; Lupo, D.; Comte, P.; Moser, J. E.; Weissortel, F.; Salbeck, J.; Spreiter, H.; Gratzel, M. *Nature.* **1998**, *395*, 583-585.
3. Bonhote, P.; Moser, J. -E.; Humphry-Baker, R.; Vlachopoulos, N.; Zakeeruddin, S. M.; Walder, L.; Graetzel, M. *J. Am. Chem. Soc.* **1999**, *121*, 1324-1336.
4. Granstrom, M.; Petritsch, K.; Arias, A. C.; Lux, A.; Andersson, M. R.; Friend, R. H. *Nature.* **1998**, *395*, 257-260.
5. Ohkubo, K.; Kotani, H.; Shao, J.; Ou, Z.; Kadish, K. M.; Li, G.; Pandey, R. K.; Fujitsuka, M.; Ito, O.; Imahori, H.; Fukuzumi, S. *Angew. Chem.* **2004**, *43*, 853-856.
6. Roncali. *J. Chem. Soc. Rev.* **2005**, *34*, 483-495.
7. Romero-Nieto, C.; Medina, A.; Molina-Ontoria, A.; Claessens, C. G.; Echegoyen, L.; Martin, N.; Torres, T.; Guldi, D. M. *Chem.. Commun.* **2012**, *48*, 4953-4955.
8. Claessens, C. G.; Gonzalez-Rodriguez, D.; Torres, T. *Chem. Rev.* **2002**, *102*, 835-853.
9. de, I. T. G.; Claessens, C. G.; Torres, T. *Chem. Commun.* **2007**, 2000-2015.
10. El-Khouly, M. E.; Shim, S. H.; Araki, Y.; Ito, O.; Kay, K.-Y. *J. Phys. Chem. B.* **2008**, *112*, 3910-3917.
11. Gonzalez-Rodriguez, D.; Carbonell, E.; Rojas, G. d. M.; Castellanos, C. A.; Guldi, D. M.; Torres, T. *J. Am. Chem. Soc.* **2010**, *132*, 16488-16500.

12. Gonzalez-Rodriguez, D.; Torres, T.; Olmstead, M. M.; Rivera, J.; Angeles, H. M.; Echegoyen, L.; Atienza, C. C.; Guldi, D. M. *J. Am. Chem. Soc.* **2006**, 128, 10680-10681.
13. Medina, A.; Claessens, C. G.; Rahman, G. M. A.; Lamsabhi, A. M.; Mo, O.; Yanez, M.; Guldi, D. M.; Torres, T. *Chem. Commun.* **2008**, 1759-1761.
14. Claessens, C. G.; Torres, T. *J. Am. Chem. Soc.* **2002**, 124, 14522-14523.
15. del, R. B.; Torres, T. *Tetrahedron Lett.* **1997**, 38, 5351-5354.
16. Gonzalez-Rodriguez, D.; Torres, T.; Guldi, D. M.; Rivera, J.; Echegoyen, L. *Org. Lett.* **2002**, 4, 335-338.
17. Kim, J.-H.; El-Khouly, M. E.; Araki, Y.; Ito, O.; Kay, K.-Y. *Chem. Lett.* **2008**, 37, 544-545.
18. Wojaczynski, J.; Latos-Grazynski, L. *Coord. Chem. Rev.* **2000**, 204, 113-171.
19. Littler, B. J.; Miller, M. A.; Hung, C. H.; Wagner, R. W.; O'Shea, D. F.; Boyle, P. D.; Lindsey, S. *J. Org. Chem.* **1999**, 64, 1391-1396.
20. Bruckner, C.; Zhang, Y.; Rettig, S.J.; Dolphin, D. *Inorganica Chimica Acta.* **1997**, 279-286.
21. Ogi, T.; Ohkita, Hideo.; Ito, S.; Yamamoto, M. *Thin Solid Films.* **2002**, 415, 228-235.

4.7 Appendices

Figure 4.12 ^1H NMR Spectrum of **5b**

Figure 4.13 ^{13}C NMR Spectrum of **5b**

Figure 4.14 ^1H NMR Spectrum of **8a**

Figure 4.15 ^{13}C NMR Spectrum of **8a**

Figure 4.16 ^{19}F NMR Spectrum of **8a**

Figure 4.17 Mass Spectrum of **8a**

Figure 4.18 ^1H NMR Spectrum of **9a**

Figure 4.19 ^{13}C NMR Spectrum of **9a**

Figure 4.20 ^{19}F NMR Spectrum of **9a**

Figure 4.21 Mass Spectrum of **9a**

Figure 4.22 ^1H NMR Spectrum of **9b**

Figure 4.23 ^{13}C NMR Spectrum of **9b**

Figure 4.24 ^{19}F NMR Spectrum of **9b**

Figure 4.25 Mass Spectrum of **9b**

Figure 4.26 ^1H NMR Spectrum of **10a**

Figure 4.27 ^{13}C NMR Spectrum of **10a**

Figure 4.28 ^{19}F NMR Spectrum of **10a**

Figure 4.29 Mass Spectrum of **10a**

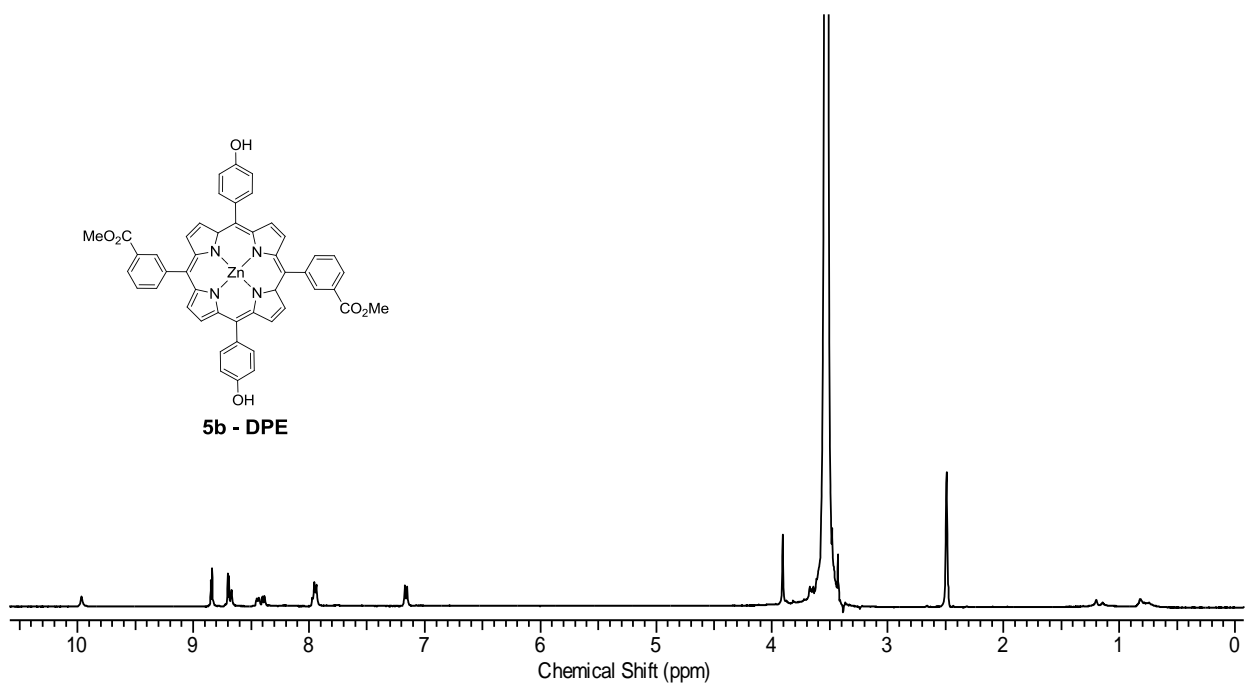


Figure 4. 12 ^1H NMR Spectrum of **5b**

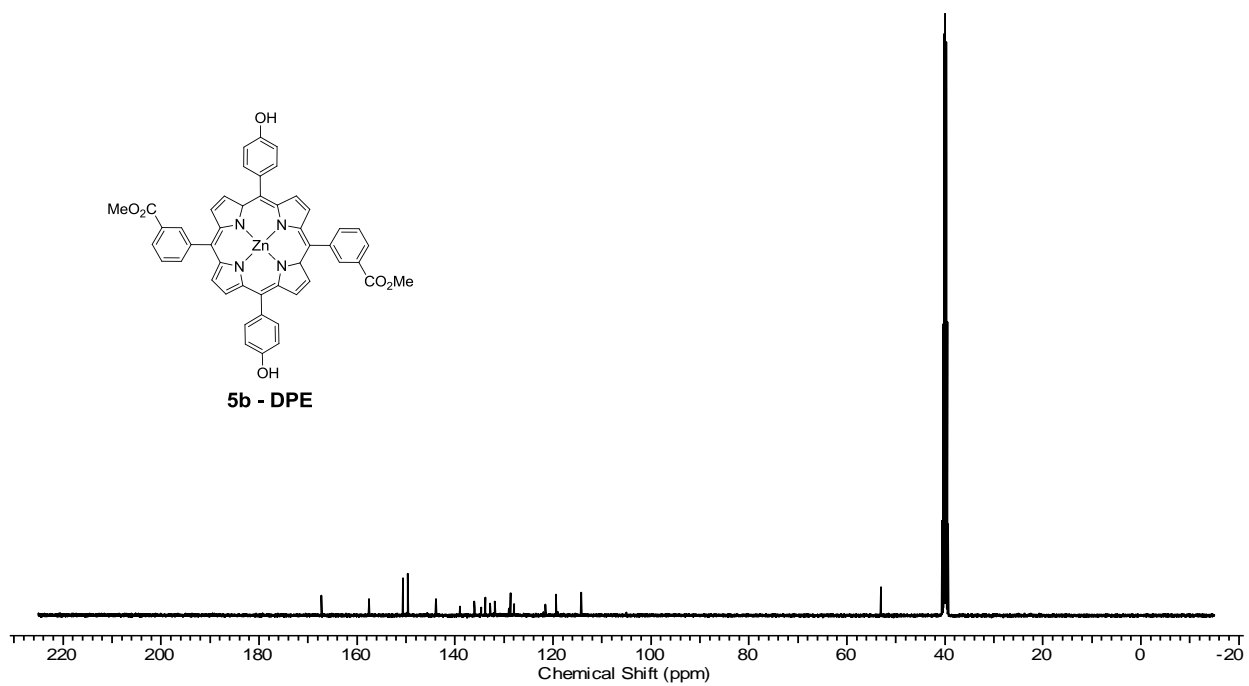


Figure 4. 13 ^{13}C NMR Spectrum of **5b**

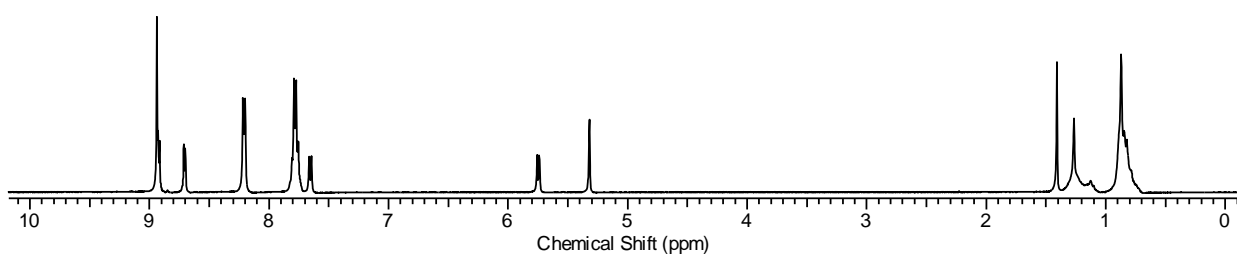
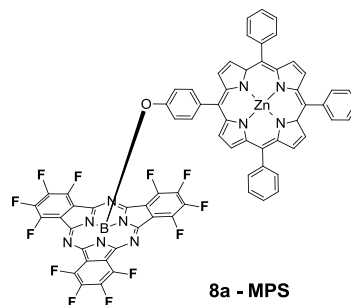


Figure 4.14 ^1H NMR Spectrum of **8a**

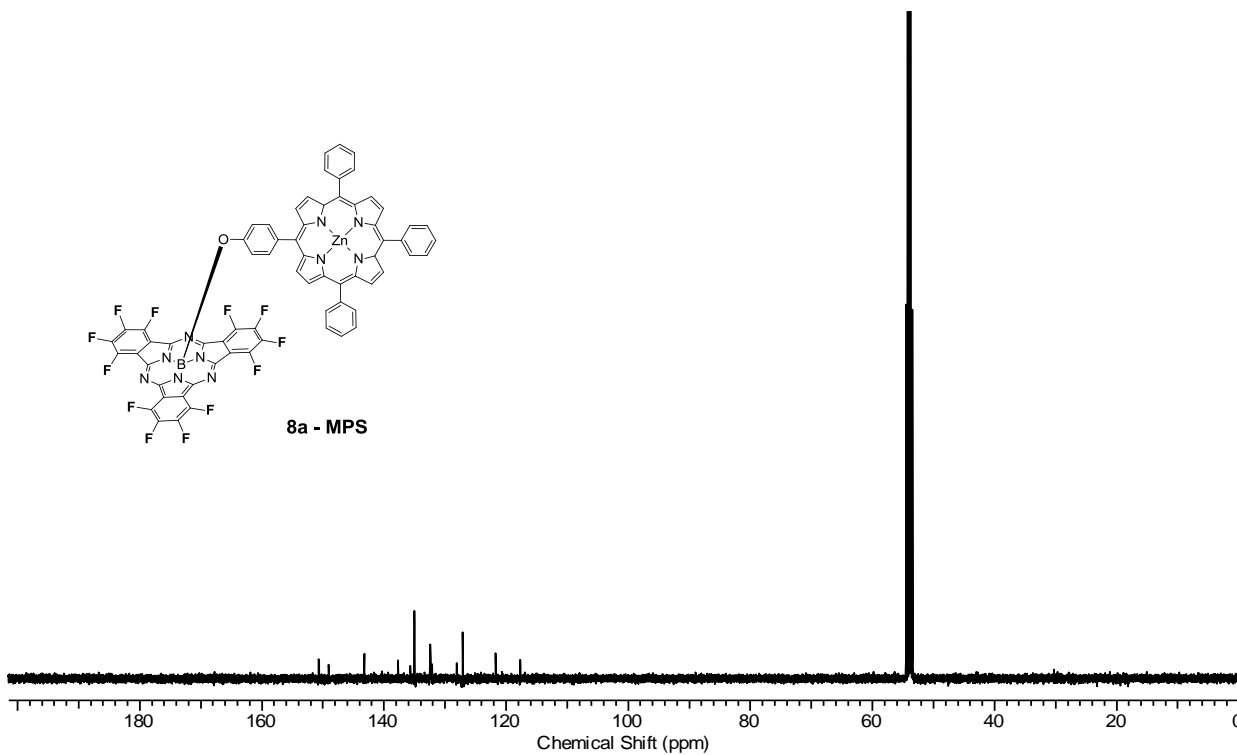
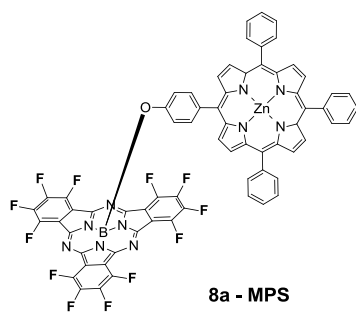


Figure 4.15 ^{13}C NMR Spectrum of **8a**

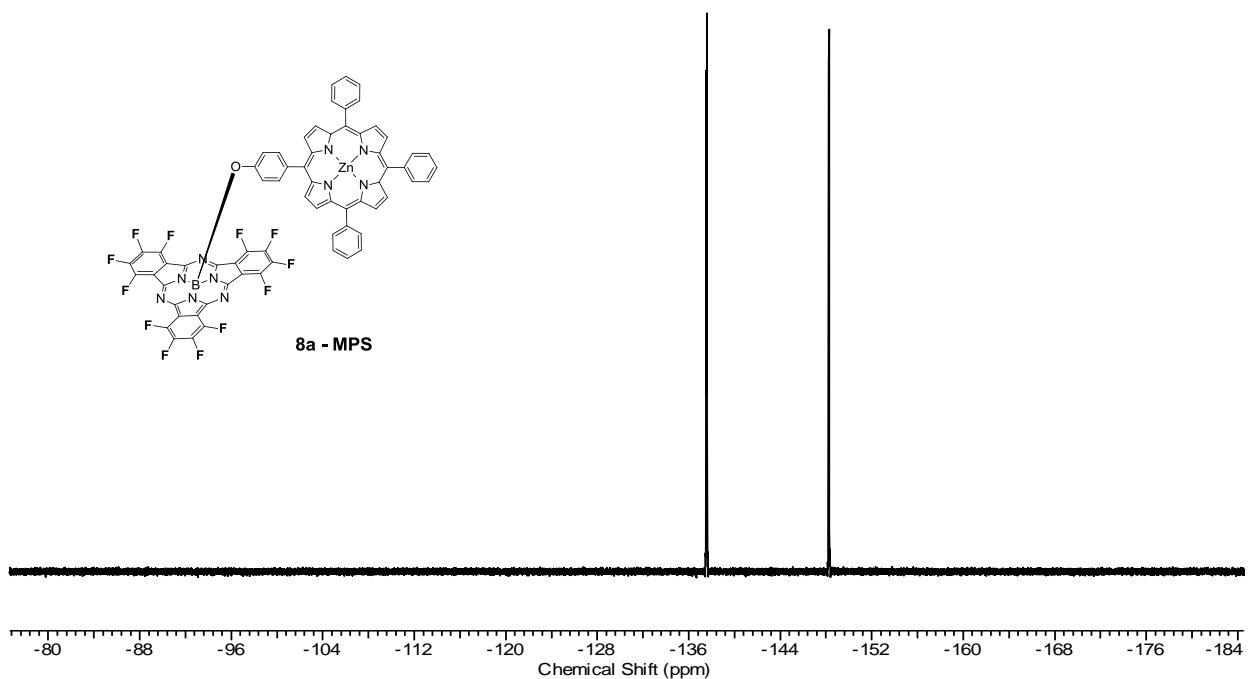


Figure 4. 16 ^{19}F NMR Spectrum of **8a**

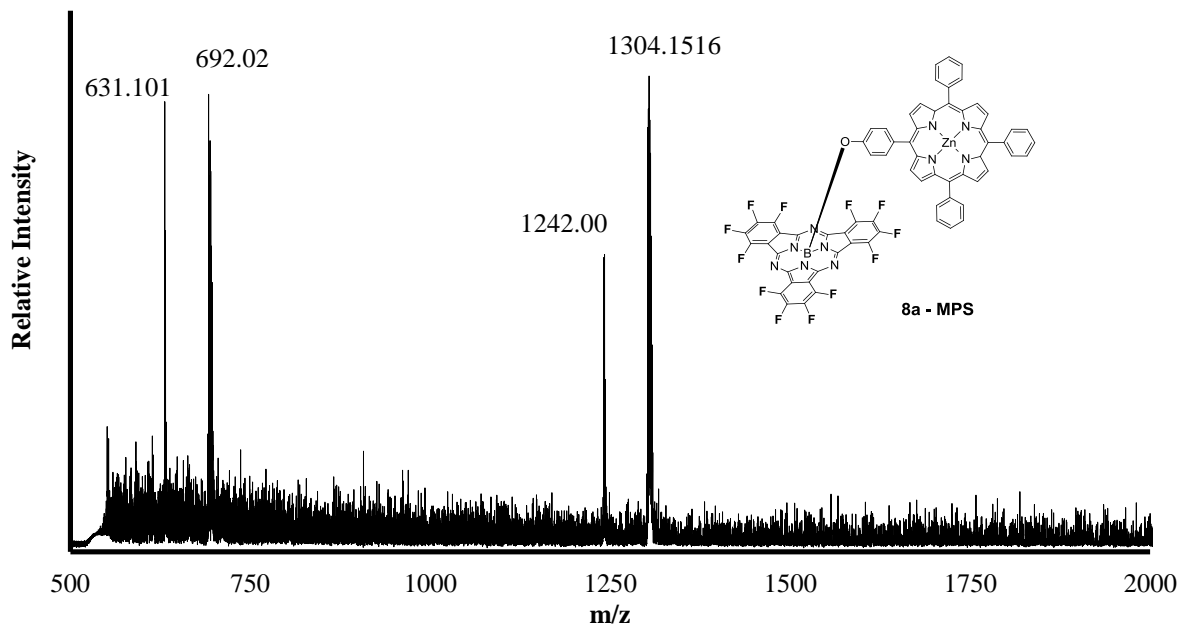


Figure 4. 17 Mass Spectrum of **8a**

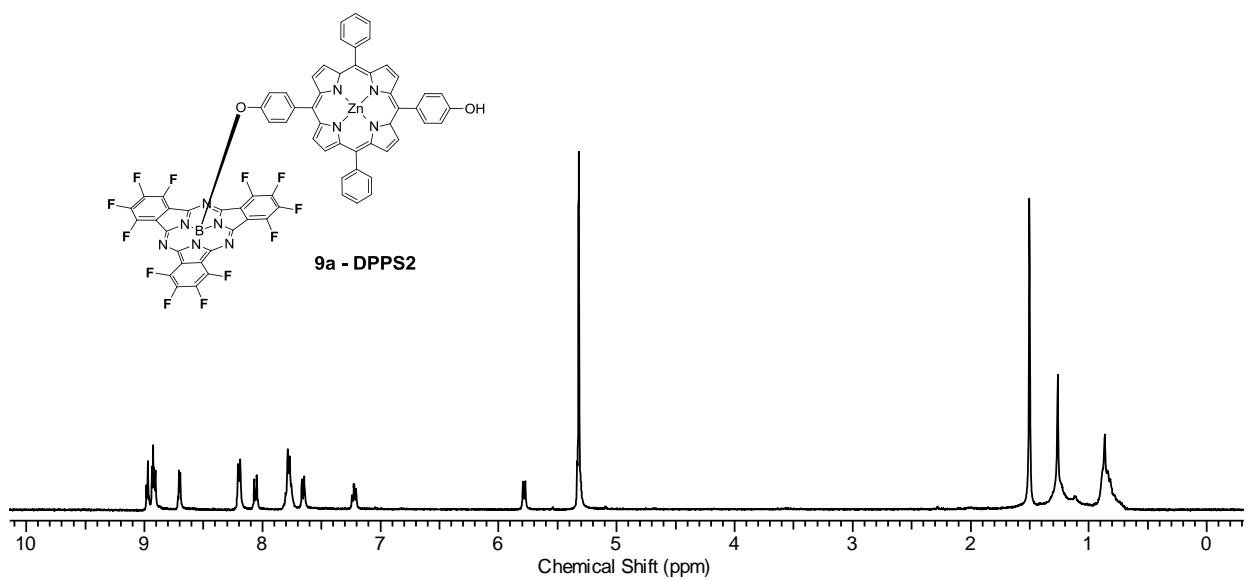


Figure 4. 18 ^1H NMR Spectrum of **9a**

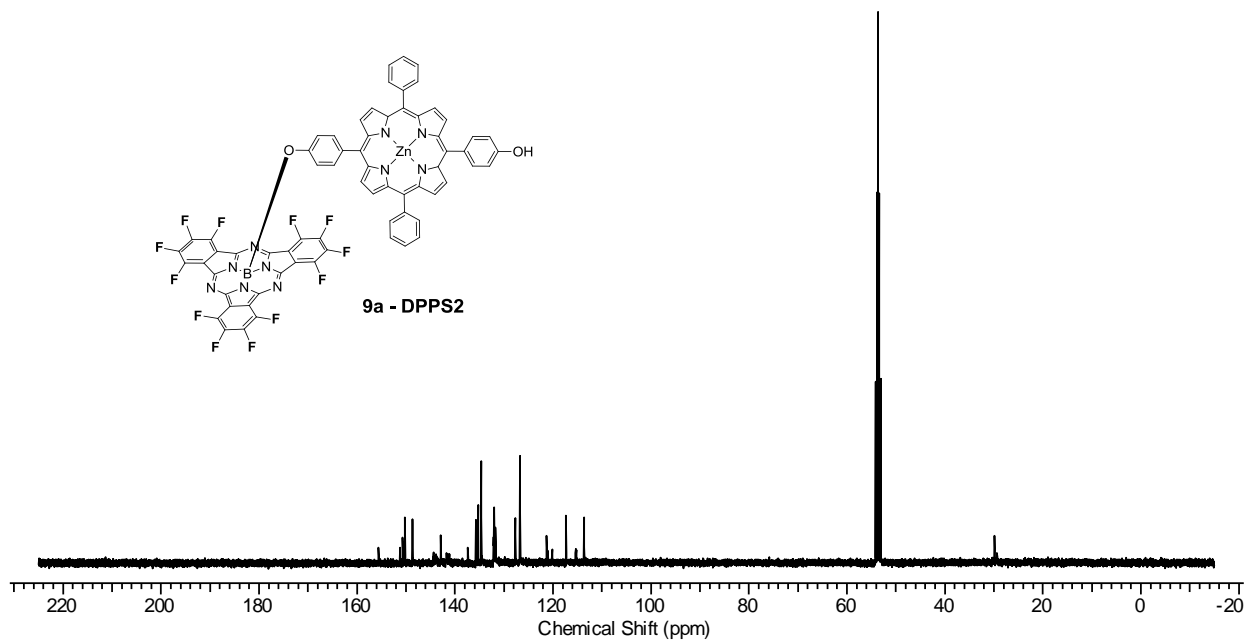


Figure 4. 19 ^{13}C NMR Spectrum of **9a**

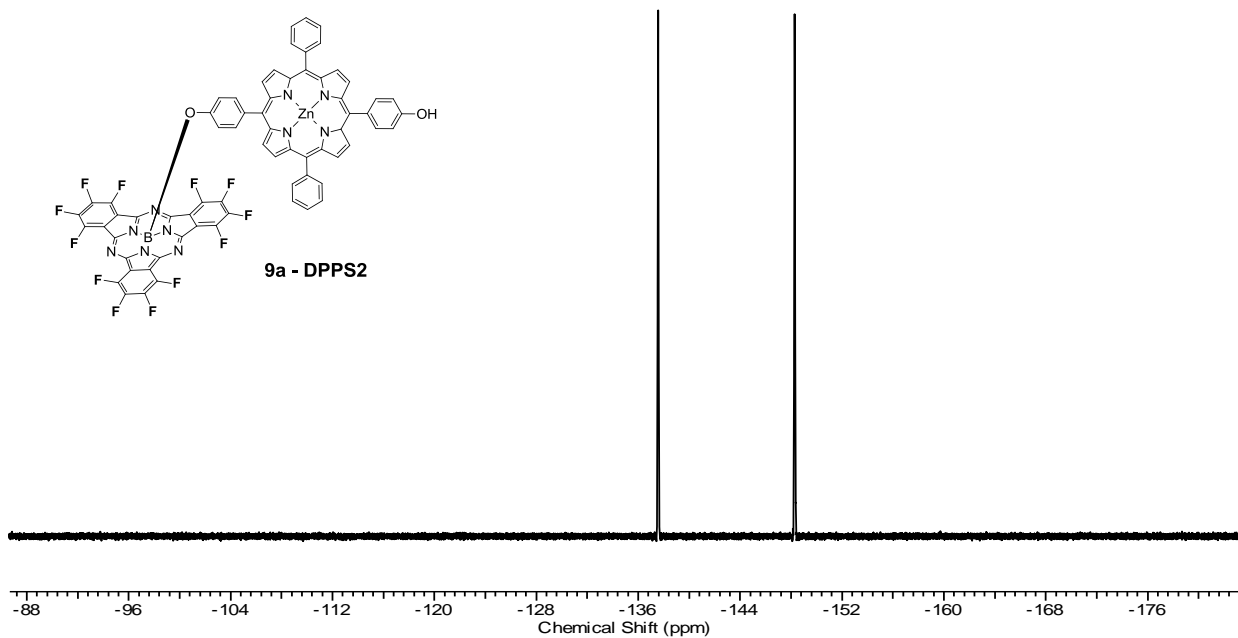


Figure 4. 20 ^{19}F NMR Spectrum of 9a

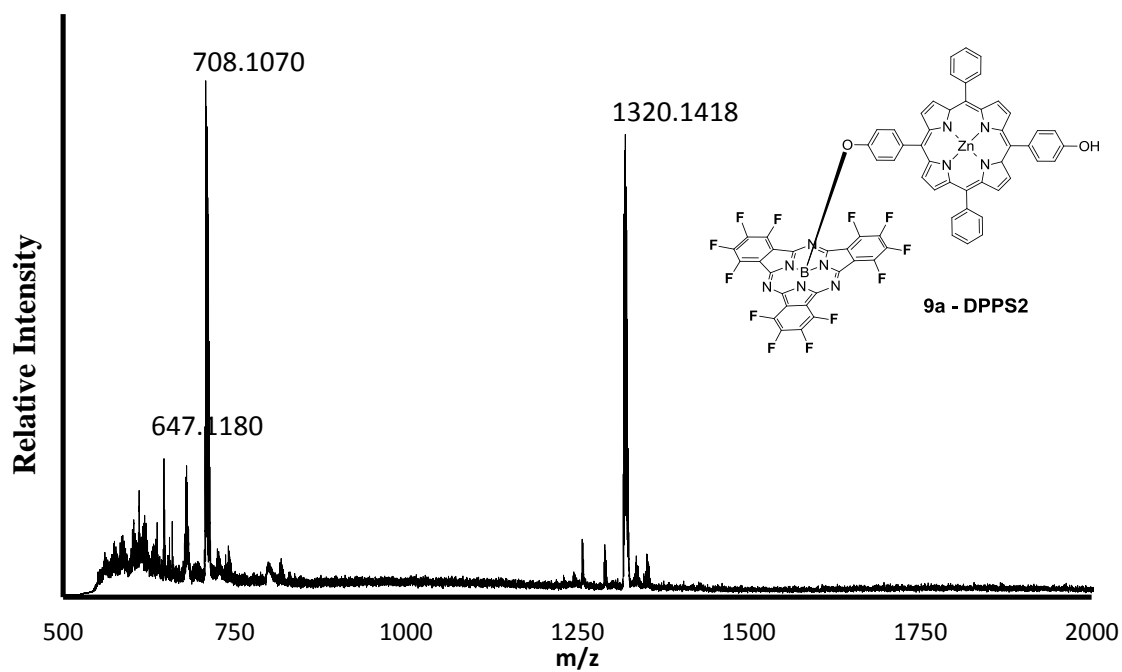


Figure 4. 21 Mass Spectrum of 9a

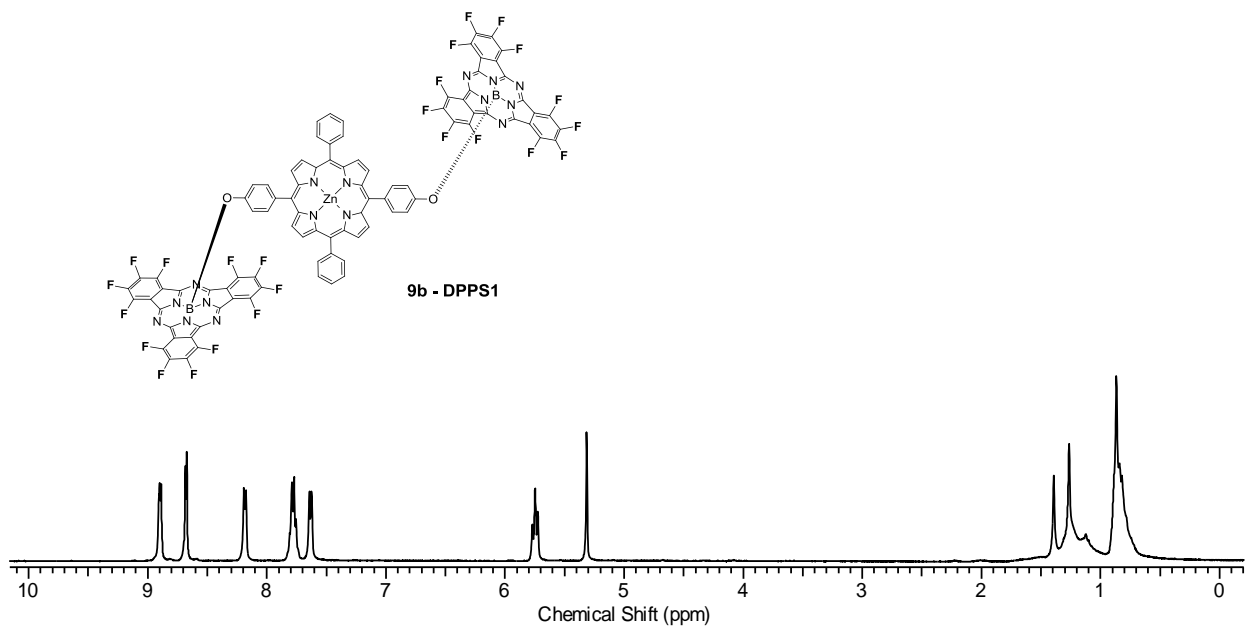


Figure 4. 22 ^1H NMR Spectrum of **9b**

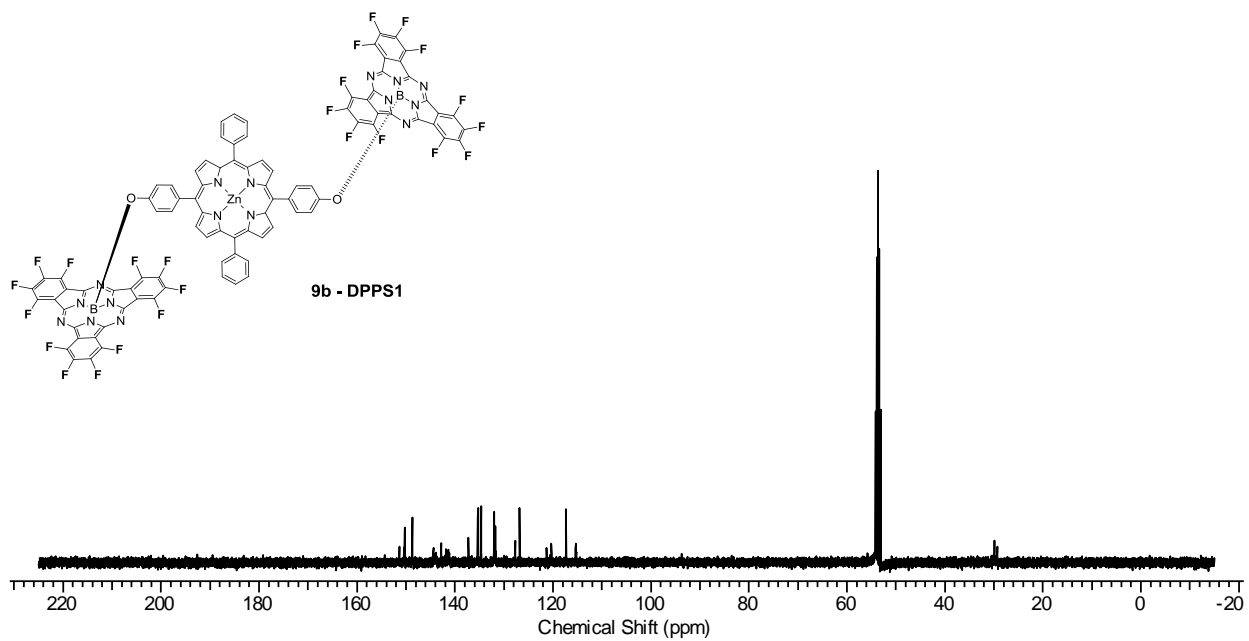


Figure 4. 23 ^{13}C NMR Spectrum of **9b**

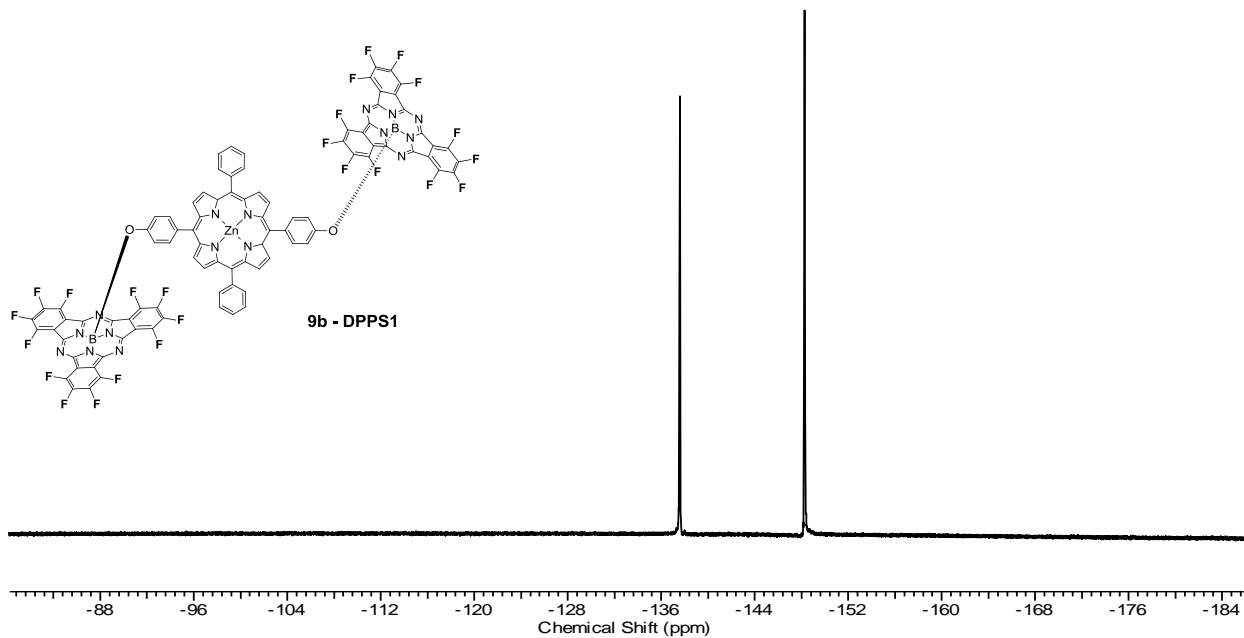


Figure 4. 24 ^{19}F NMR Spectrum of **9b**

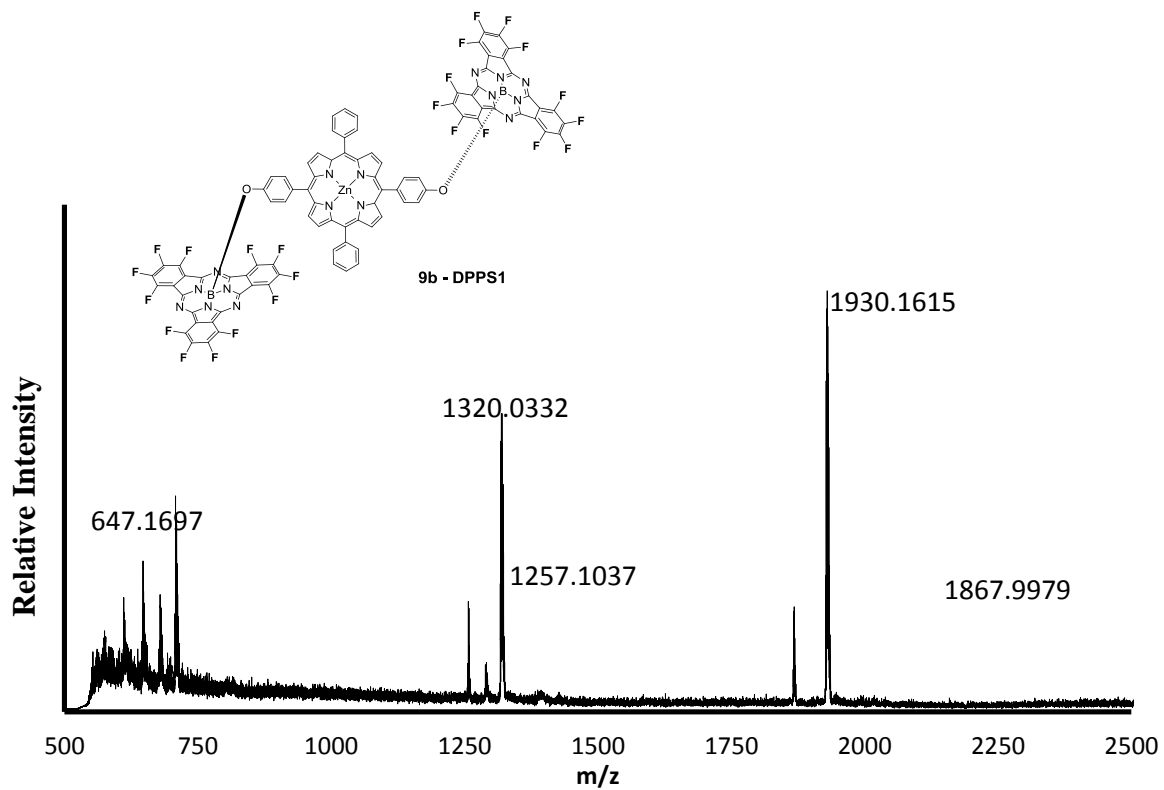


Figure 4. 25 Mass Spectrum of **9b**

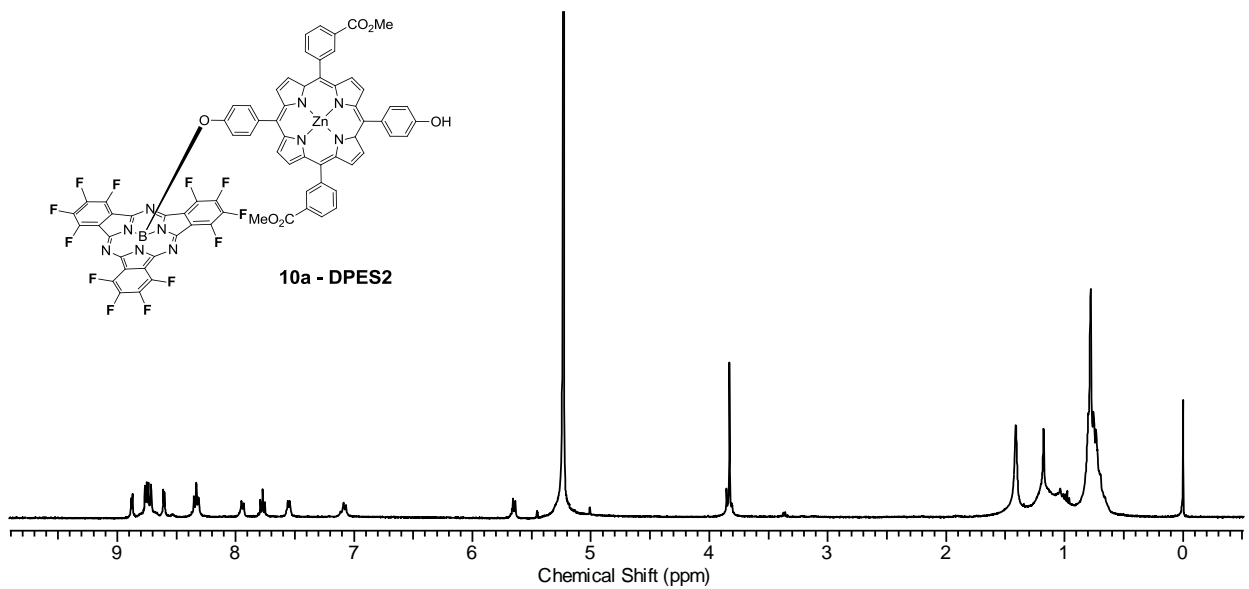


Figure 4. 26 ^1H NMR Spectrum of **10a**

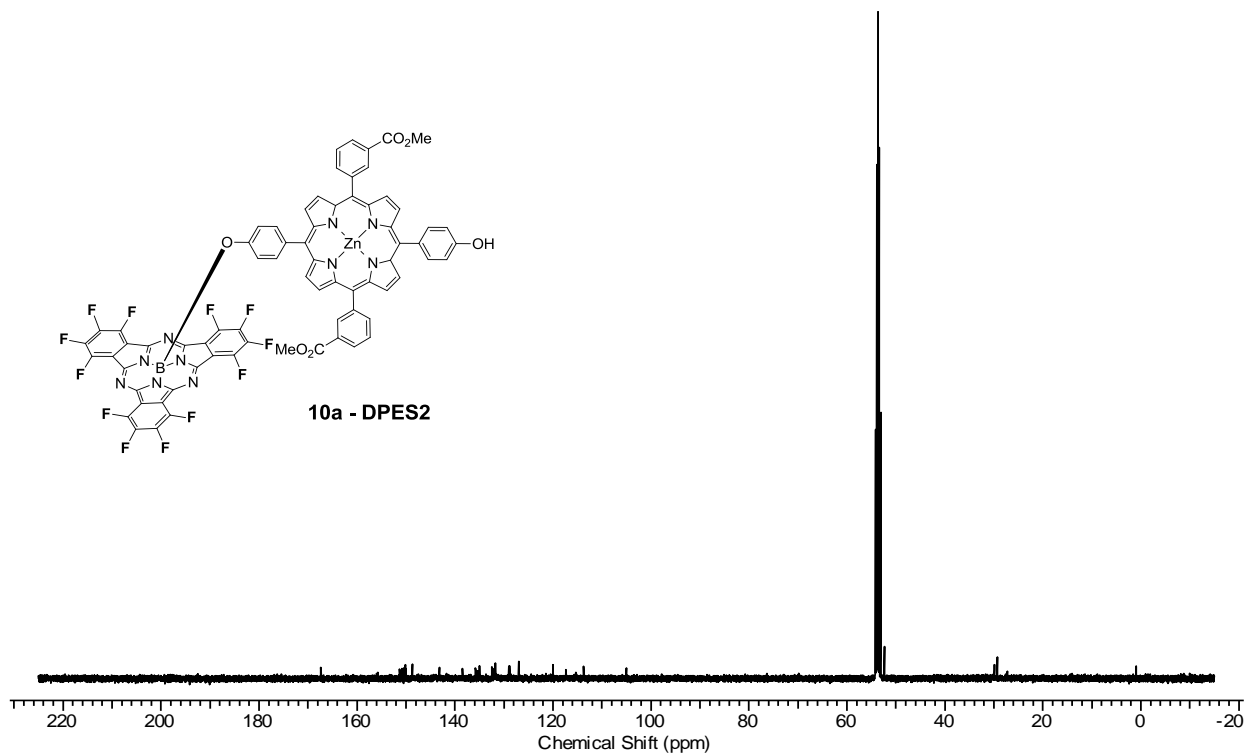


Figure 4. 27 ^{13}C NMR Spectrum of **10a**

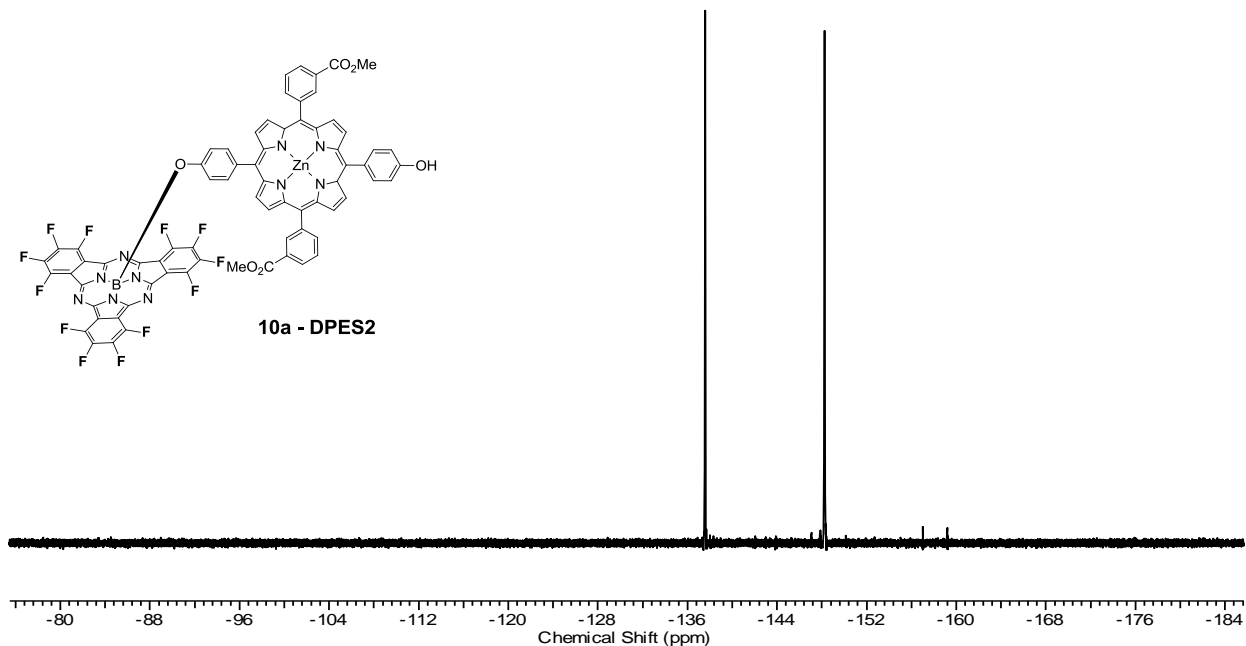


Figure 4. 28 ^{19}F NMR Spectrum of **10a**

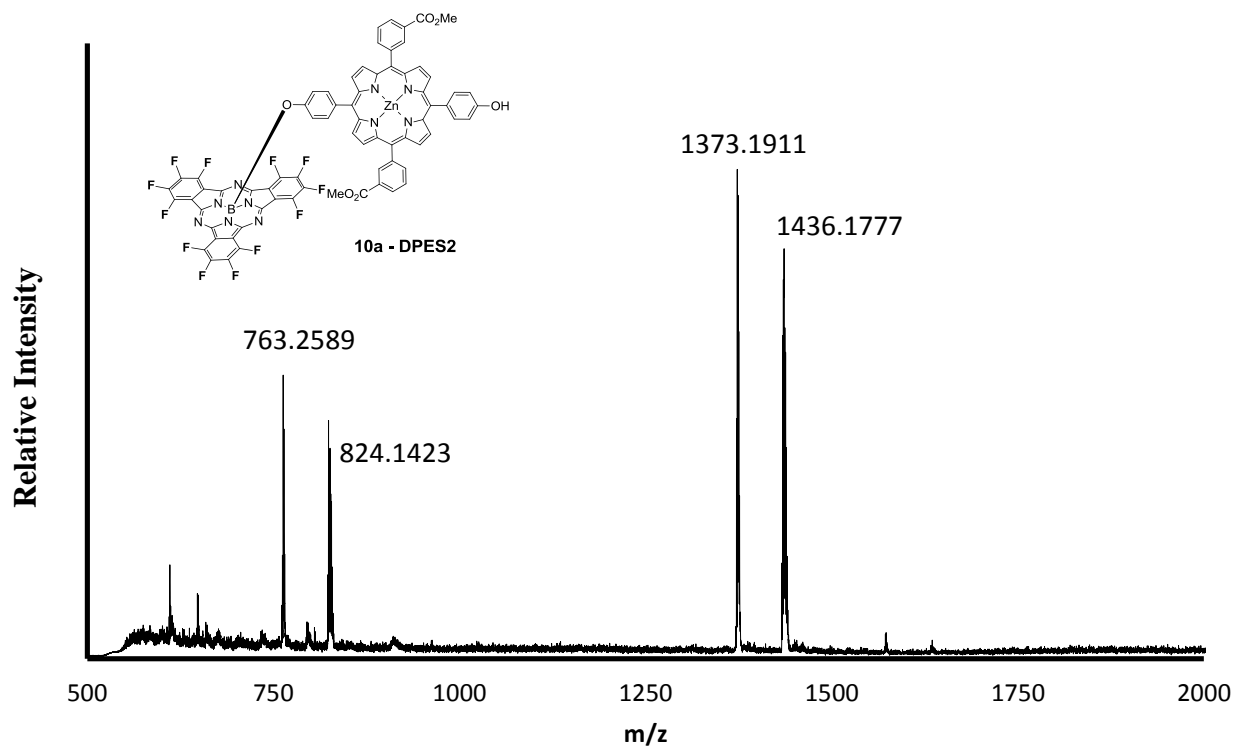


Figure 4. 29 Mass Spectrum of **10a**

CHAPTER V

RESULTS AND DISCUSSION

AXIAL REACTIVITY OF DODECAFLUOROSUBPHTHALOCYANINE ON SUBSTITUTED DIHYDROXY BENZENE APPENDED PERYLENE DIIMIDES

5.1 Introduction

Substantial efforts have been contributed towards the broadening of research in multicomponent molecular assemblies.^{1,2} The utilization of such systems in various molecular photoelectronic devices and also as artificial light energy harvesting systems demands efficacious electron transfer *via* photoexcitation with light of specific wavelength.³⁻⁵ The competence of electronic communication in a multicomponent assembly relies on the orientation, relative distance, types of linkages and the electronic characteristics of the macrocycles involved.⁶⁻⁹ Perylene diimides (PDIs) have recently emerged as a good platform for the synthesis of such multicomponent systems.^{10,11} Although a variety of donor acceptor conjugates involving PDIs¹²⁻¹⁷ with covalent linkages have appeared in the literature, the poor solubility of such multicomponent systems remains a major issue for their potential use in molecular devices. As a means to overcome this problem, subphthalocyanines (SubPcs) have been chosen as suitable candidates as their counterparts. SubPcs possess high solubility in the resulting conjugates due to their convex shaped geometry. To the best of our knowledge, there is only one example of Perylene-SubPc dyad¹⁸ reported in the literature. Nonetheless, the SubPc in this dyad is covalently linked in the imide region of the perylene diimide by

forming a B-N bond (Figure 5.1). Our expectation is that the fusion of a SubPc with a PDI in the bay region can execute fast electron transfer and thereby can be utilized in various optoelectronic devices.

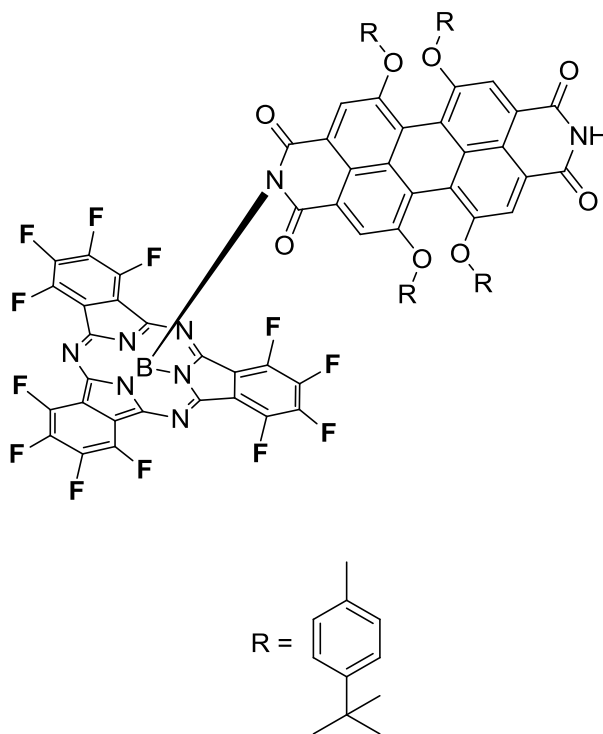


Figure 5.1 Covalently Linked SubPc-PDI Conjugate with B-N Bond.

5.2 Perylene Diimides

Perylene diimides (PDIs), also called perylene tetracarboxylic acid bisimides (Figure 5.2), have received significant attention due to their excellent photophysical properties. They were discovered in 1913 by Kardos.⁶ The PDIs are known for their strong absorption with high molar absorption coefficients ($\sim 58,000 \text{ M}^{-1}$ at 490 nm in CHCl_3), long fluorescence lifetimes, near unity fluorescence quantum yields and high photostability.¹⁰⁻¹¹

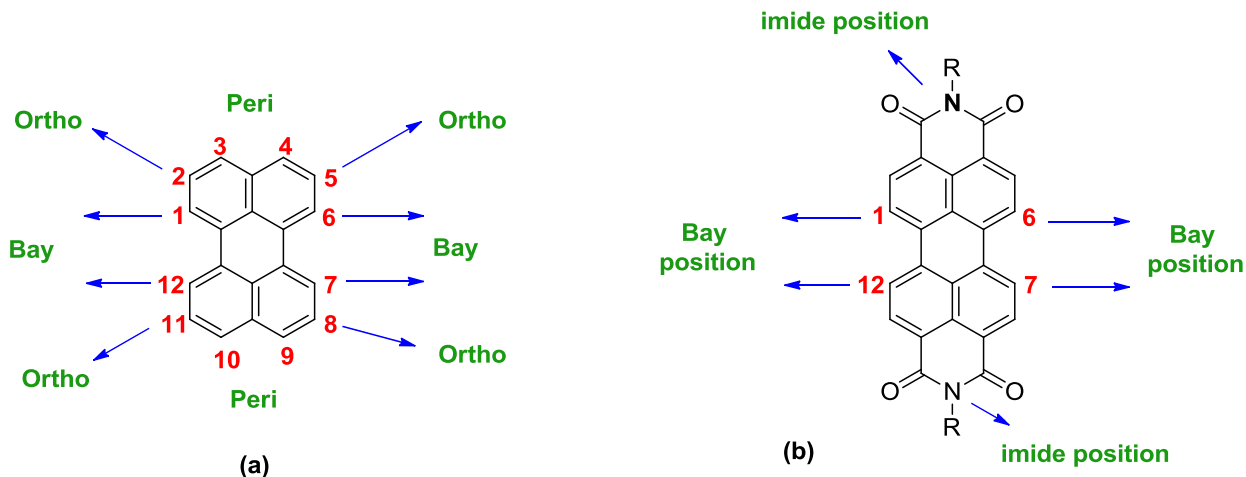


Figure 5.2 Chemical Structure of (a) Perylene (b) A Perylene Diimide.

5.2.1 Applications

Perylene diimides were initially used as red vat dyes in industries.¹⁹ Due to the favorable combination of insolubility and migrational stability, thermal stability and chemical inertness of perylene diimides, scientists began using such compounds for high grade industrial applications. PDIs are the best n-type semiconductors currently available.²⁰ The combined optical, redox, and stability properties of perylene diimides have been investigated for their utilization in electrophotography (xerographic photoreceptors).²¹ PDI derivatives have also been widely scrutinized as active compounds in different areas, such as in biochemical applications for living cell staining sensors, in fingerprint detection and in electronic sensors, and light emitting diodes.^{22,23} The research on PDIs accelerated in 1959 when their potential as fluorescent dyes with high fluorescence quantum yield and photostability was discovered.²⁴ Although PDI material with large melting points find enormous use in the pigment industry, there is a high demand for PDIs which are reasonably soluble in common solvents for organic electronics, photoinduced processes, and supramolecular organization.

5.2.2 Chemical modifications of PDIs

5.2.2a Imide Substitution

Modification on the PDI structure can be readily established by introducing alkyl or aryl substituents at the N-positions and/or at the bay region. Imide substituents have very little effect on the molecular-level electronic and optical properties but such groups affect aggregation, solubility, etc. Symmetrical N,N'-substituted PDIs are in general obtained by the condensation of perylene tetracarboxylic acid dianhydride (PTCDA) with a corresponding primary amine at 160 °C in molten imidazole or quinoline with zinc acetate as the catalyst.²⁵ The syntheses of unsymmetrical PDIs are usually performed by complex multistep methods which involve partial hydrolysis of symmetrical PDIs to the corresponding perylene monoimide monoanhydride, followed by hydrolysis with a second amine.²⁵

5.2.2b Bay Substitution

While good solubility of the PDI derivatives can be achieved by incorporating long alkyl chains in the imide region, substitution in the bay positions (1,6,7,12) induces both structural and electronic effect (Figure 5.2) on the PDI chromophore.²⁶ The steric hindrance imparted by the substituents in the bay region lead to twisting of the two naphthalene half units and disturbs the planarity of the core system. Consequently, there is a decrease in π - π stacking aggregation tendencies with considerable effect on the optical properties. For applications of PDIs as fluorescent standards in fluorescent light collectors, it is advantageous that the imide substituent has a negligible influence on the absorption and emission properties of perylene bisimides because of the nodes of the HOMO and LUMO orbitals at the imide nitrogens. Hence, PDIs can be considered as a

closed chromophoric system with an S_0 - S_1 transition with unaltered intensity and position by the respective imide substituents.²⁷

5.2.3 Redox Properties

The electrochemical properties of PDIs investigated by Wasielewski²⁸ and Würthner and co-workers²⁹ suggested that they are fairly electron deficient dyes that are more easy to reduce than to oxidize. Most compounds exhibited two reversible reduction waves and one reversible oxidation waves in cyclic voltammetry. Significant effects were observed for bay substituted PDIs. The electron-deficient nature of the PDIs are responsible for their photochemical stability. The behavior of these molecules as strong reductants in their photoexcited state has been extensively applied to demonstrate long-lived, charge separated states in photoinduced electron transfer cascades.¹⁴

5.2.4 Structural Properties

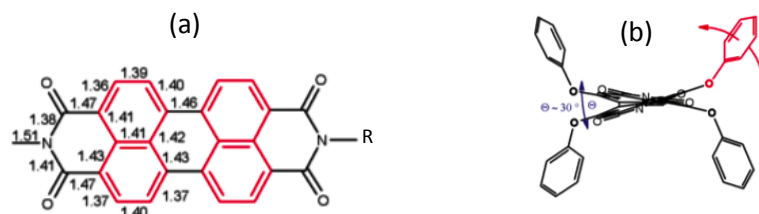
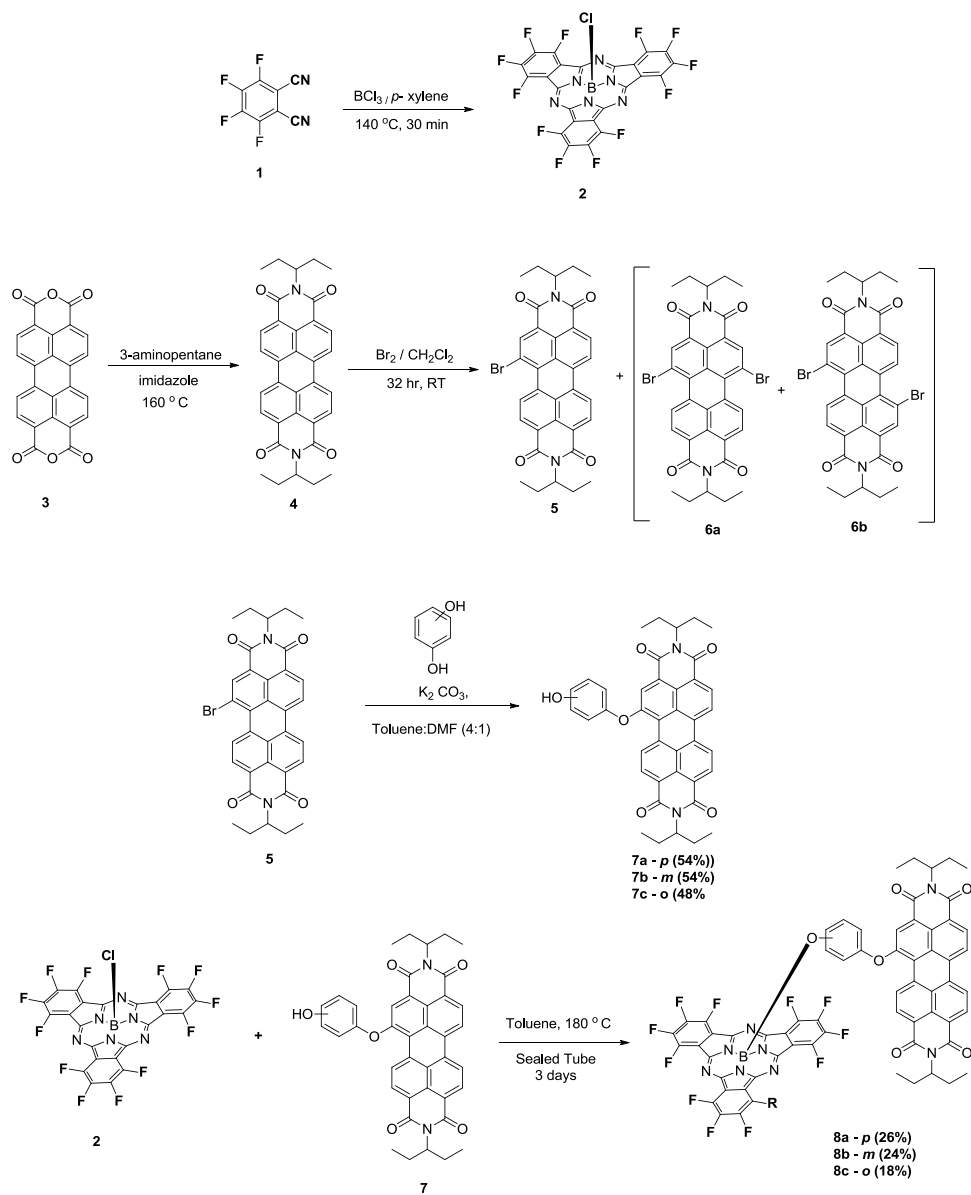


Figure 5.3 (a) Bond Lengths in a PDI Molecule (b) Preferred Conformation of the Phenoxy Substituents in a Bay-Substituted PDI.

The X-ray diffraction studies of several single crystals of the parent PDIs revealed flat pi-systems.³⁰ In accordance with the calculated bond lengths (Figure 5.3) in the crystals, PDIs can be considered to have two naphthalene half units each of which are linked to an imide unit. The two naphthalene units are connected together by two sp^2 - sp^2 carbon single bonds which impart sterical strain in the bay-region, leading to a propeller-like twisting of the two naphthalene halves.

5.3 Results and Discussion

The synthesis of SubPc-PDI conjugates is depicted in Scheme 5.1.



Scheme 5.1 Synthesis of SubPc-PDI **8a**, **8b**, and **8c**.

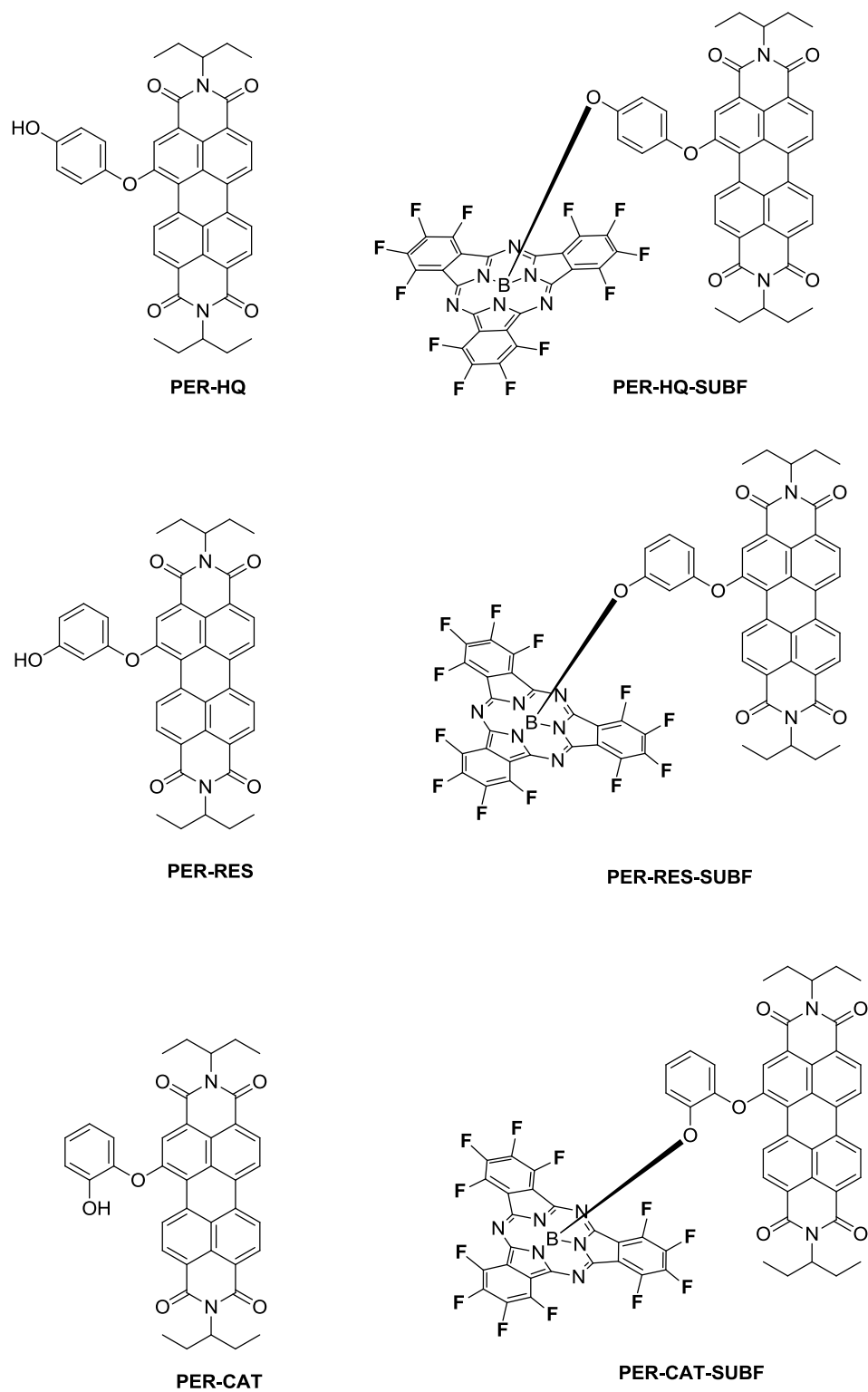


Figure 5.4 Representation of the Synthesized Compounds.

5.3.1 Absorption Studies

The electronic interaction between the SubPc and PDI was investigated *via* absorption and emission studies. The steady-state absorption spectra of the parent compounds and the conjugates in CH₂Cl₂ are shown in Figure 5.5 and Figure 5.6, respectively. The absorption spectra of the dihydroxybenzene appended PDIs (PDI-HQ, PDI-RES, PDI-CAT) consists of a Q band arising from a π - π^* transition associated with 14 π electron systems. The absorption spectra of the PDI-SUBF conjugates (PDI-HQ-SUBF, PDI-RES-SUBF, PDI-CAT-SUBF) exhibited common features of the SubPc-F₁₂ and the dihydroxybenzene appended PDIs.

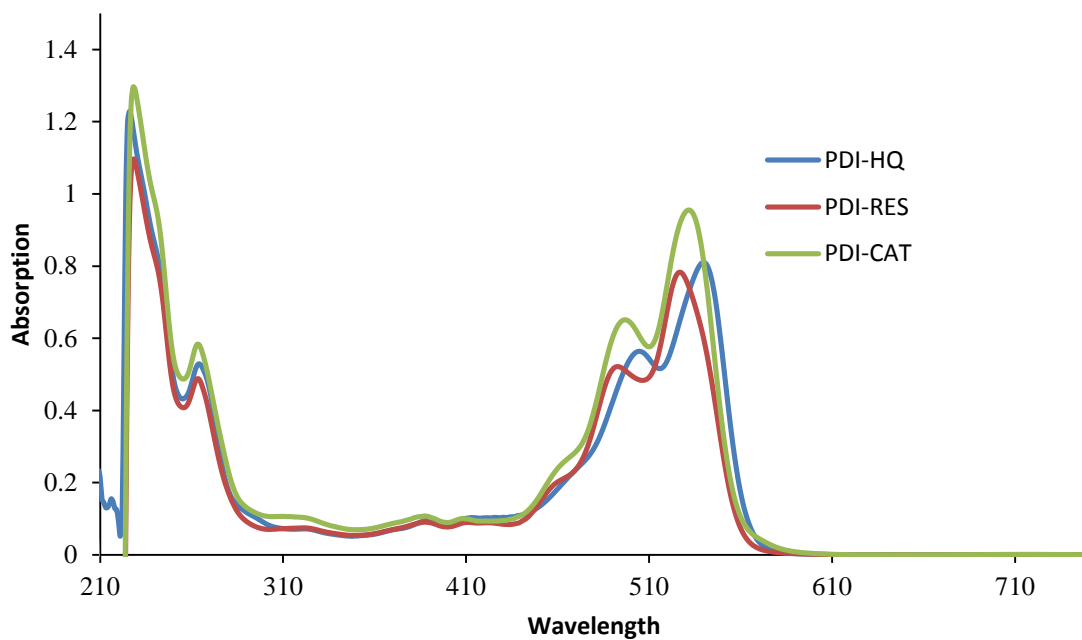


Figure 5.5 Absorption Spectra of Dihydroxybenzene Appended PDIs.

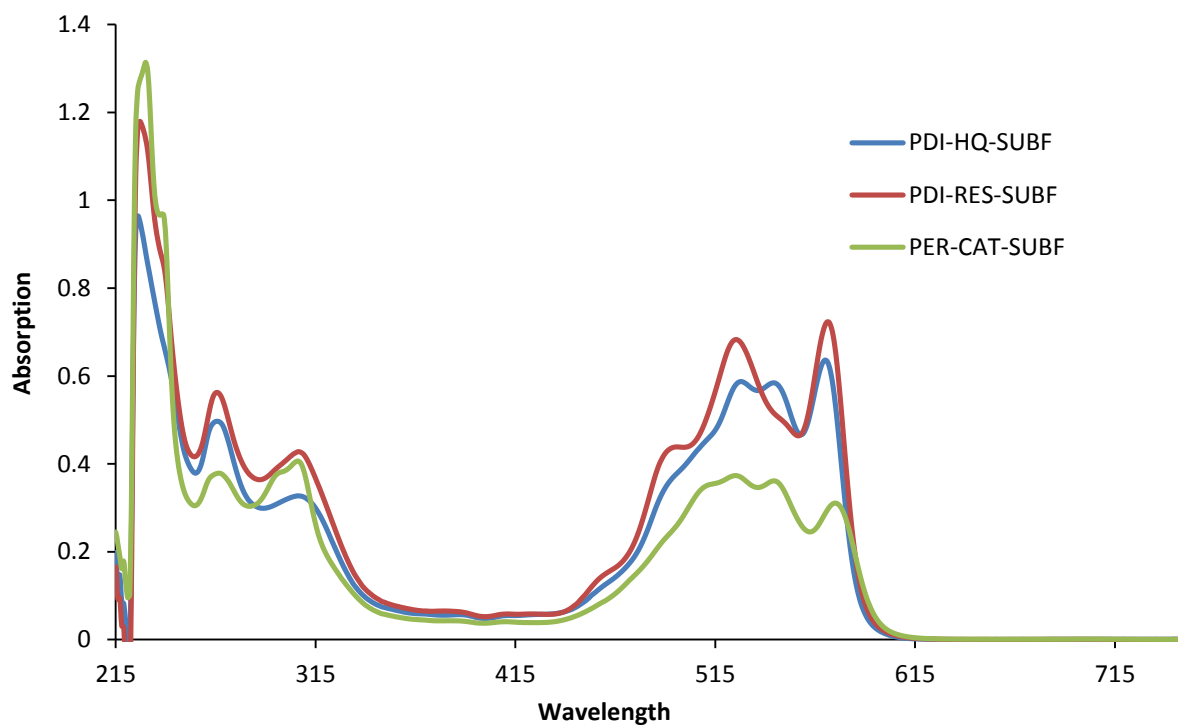


Figure 5.6 Absorption Spectra of PDI-SubF Conjugates.

5.3.2 Emission Studies

The emission spectra of the compounds recorded in CH_2Cl_2 are shown in Figure 5.6 and Figure 5.7. Excitation of the dihydroxybenzene appended PDIs at the corresponding λ_{max} exhibited emission bands at around 553 nm. Considerable shifts were observed for the conjugates which exhibited two emission bands for PDI-HQ-SUBF and PDI-CAT-SUBF and one emission band at 582 nm for PDI-RES-SUBF. This strongly suggests the existence of electronic communication between the PDI and SUBF moieties.

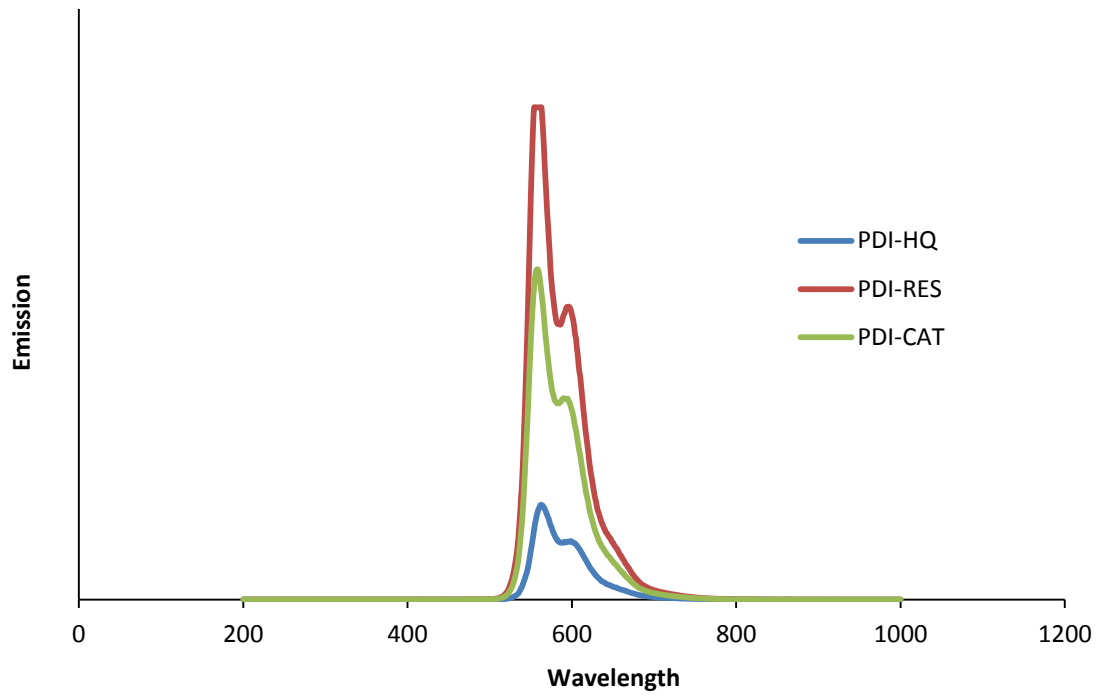


Figure 5.7 Emission Spectra of Dihydroxybenzene Appended PDIs.

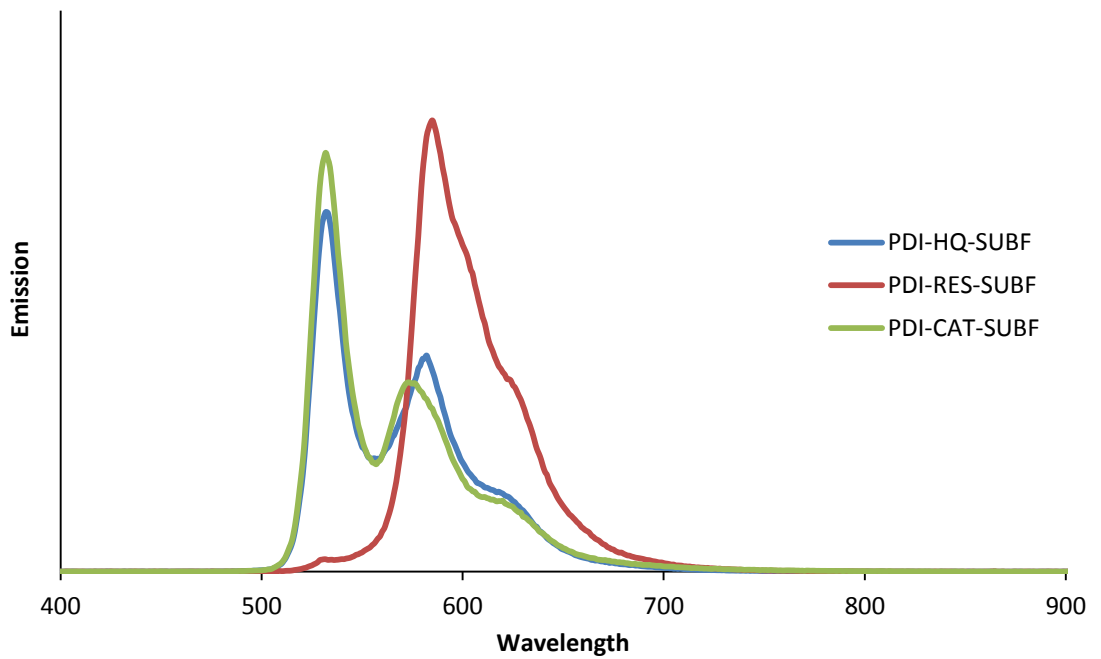


Figure 5.8 Emission Spectra of PDI-SubF Conjugates.

5.3.3 Electrochemical Studies

The redox behavior of the SubPc-PDI was investigated by cyclic voltammetry experiments. The results were compared with those of the reference compounds SubPc-F₁₂, PDI-HQ, PDI-RES, and PDI-CAT (Figure 4.3). All experiments were performed at room temperature in deaerated CH₂Cl₂ solution by bubbling nitrogen gas containing *tetra-n*-butylammonium hexafluorophosphate (TBAPF₆, 0.1 M) as the supporting electrolyte, with a glassy carbon as the working electrode, platinum as the counter electrode, and Ag/AgNO₃ as the reference electrode.

The representative cyclic voltammograms (CVs) of the dihydroxybenzene appended PDIs and PDI-SUBF conjugates are shown in Figures 5.9 and 5.10, respectively. Investigation of the redox features of these compounds reveals that both the oxidative and reductive voltgrams of PDI-SUBF conjugates are not exactly the sum of those of the parent SubPc-F₁₂ and dihydroxybenzene appended PDIs.

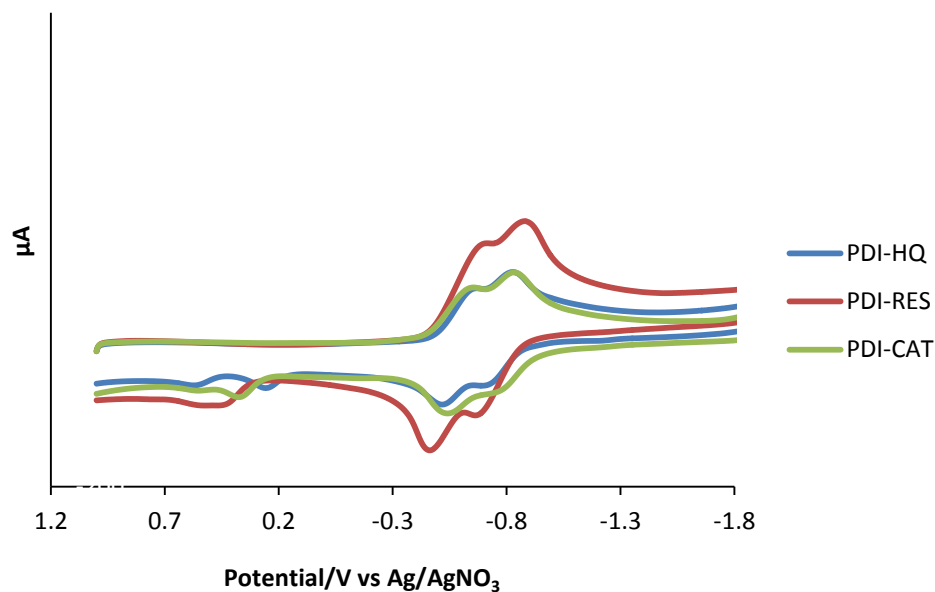


Figure 5.9 Cyclic Voltammogram of Dihydroxybenzene Appended PDIs.

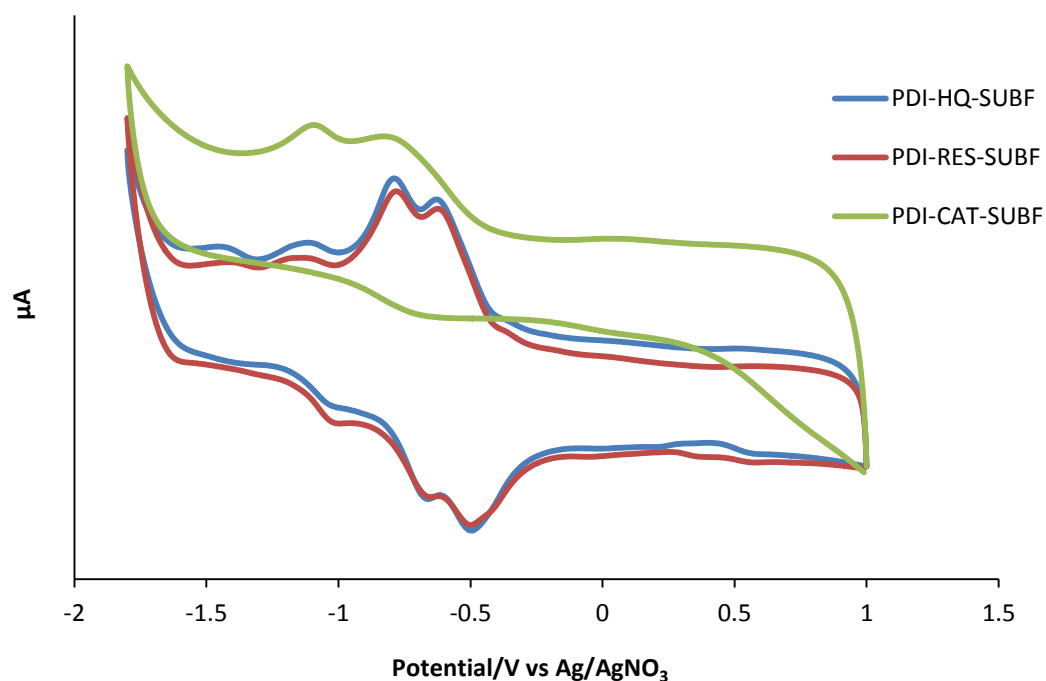


Figure 5.10 Cyclic Voltammogram of PDI-SUBF conjugates.

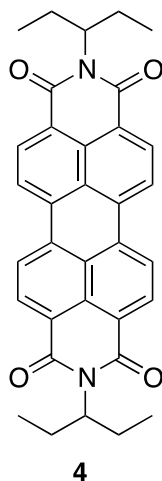
Table 5.1 Electrochemical Data of the Compounds.

Compound	E ¹ (red)	E ² (red)	E ³ (red)	E ¹ (ox)	E ² (ox)	E ³ (ox)	E ⁴ (ox)
PDI-HQ	-0.634	-0.834	-	-0.720	-0.516	0.259	0.560
PDI-RES	-0.709	-0.918	-	-0.655	-0.454	0.448	-
PDI-CAT	-0.654	-0.845	-	-0.781	-0.545	0.378	-
PDI-HQ-SUBF	-0.628	-0.795	-1.445	-1.040	-0.659	-0.485	0.585
PDI-RES-SUBF	-0.624	-0.795	-1.167	-1.002	-0.683	-0.502	0.590
PDI-CAT-SUBF	-0.623	-0.786	-1.101	-1.080	-0.696	-0.513	0.567

5.4 Experimental

Melting points (mp) were determined using a Stuart SMP10 instrument. Both ^1H and ^{13}C NMR spectra were acquired in CDCl_3 or CD_2Cl_2 using a Varian Inova 400 MHz or 600 MHz spectrometer. Chemical shifts (δ) are expressed in ppm relative to residual chloroform (^1H : 7.26 ppm, ^{13}C : 77.0 ppm) or to dichloromethane (^1H : 5.32 ppm, ^{13}C : 54.0 ppm). The sealed tube reaction was conducted in a unit from Chem Glas, Model 1880. Column chromatography was carried out on silica gel (Sorbent Technologies, 230-400 mesh), and thin layer chromatography was performed with polyester sheets precoated with silica gel (Sorbent Technologies). Compounds tetrafluorophthalonitrile (TCI America), catechol (MP Bio medicals), resorcinol, (Alfa Aeser), BCl_3 in *p*-xylene, PTCDA, 3-aminopentane, TCI America (Sigma Aldrich), imidazole (Acros), hydroquinone, bromine (Fischer), TMSA (Acros organics), and $\text{Pd}(\text{PPh}_3)_4$ (Strem, recrystallized with methanol) were purchased from commercial suppliers and used as received or as specified.

5.4.1 Synthesis of *N,N'*-Bis(Ethylpropyl)perylene-3,4,9,10-tetracarboxylic Diimide

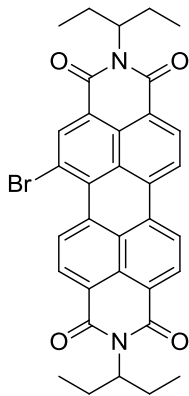


In a 100-mL, single-necked, round-bottomed flask fitted with a condenser and magnetic stir bar was placed perylene tetracarboxylic acid dianhydride, PTCDA (0.5 g, 1.27 mmol) and imidazole (2.46 g, 0.036 mol). The mixture was warmed to 90 °C. The solid imidazole slowly melted and dissolved the PTCDA to give a reddish-orange solution. Then 3-aminopentane (0.22 g, 2.54 mmol) was added to the solution which was heated to 160 °C with continuous stirring. After cooling to room temperature, the solution was treated with water (10 mL), followed by HCl solution (2 N, 70 mL), and was then stirred at room temperature in an open vessel for 12 hr. The dark solid formed was filtered off and washed thoroughly with distilled water until the pH of the filtrate was neutral. The precipitate was dried and column chromatographed over silica gel using CH₂Cl₂:ethyl acetate (20:1).

Yield: 0.65 g (67%). **Mp:** >300 °C (lit,²⁶ **Mp:** >250 °C).

¹H NMR (400 MHz CDCl₃): δ 9.78 (d, 2H), 8.69 (d, 2H), 8.62 (d, 2H), 8.61 (d, 1H), 5.07 (m, 2H), 2.27 (m, 4H), 1.95 (m, 4H), 0.94 (t, 6H), 0.93 (t, 6H).

5.4.2 1-Bromo-*N,N'*-bis(ethylpropyl)perylene-3,4:9,10-tetracarboxylic Diimide



5

A mixture of compound **4** (1.0 g, 1.8 mmol) and bromine (2.91 mL, 0.056 mol) in 50 mL of dichloromethane was stirred at room temperature in a 200-mL, closed round-bottomed flask fitted with a gas inlet and a magnetic stir bar for 32 hr. Excess of bromine was removed by bubbling air through the solution, and the solvent from the reaction mixture was removed under vacuum to give a dark red solid. Column chromatography of the crude solid product was performed over silica gel using MeOH:CH₂Cl₂ (1:20) as the eluent. Three distinct bands were eluted in the order of dibromoperylene diimide (regioisomers of 1,7- and 1,6- dibromo compound), monobromoperylene diimide and unreacted perylene diimide.

Yield: 0.71 g (62%). **Mp:** >300 °C (lit,²⁶ **Mp:** >250 °C).

¹H NMR (400 MHz CDCl₃): δ 9.78 (d, J = 8.4 Hz, 1H), 8.92 (s, 1H), 8.92 (s, 1H), 8.69 (m, 3H), 8.62 (d, 1H), 8.61 (d, 1H), 5.07 (m, 2H), 2.27 (m, 4H), 1.95 (m, 4H), 0.94 (t, 6H), 0.93 (t, 6H).

¹³C NMR (100 MHz CDCl₃): δ 11.06, 11.08, 24.99, 25.04, 57.9, 58.1, 120.8, 122.8, 123.2, 123.5, 123.9, 124.0, 127.1, 128.0, 128.2, 128.8, 129, 130.4, 130.9, 133.6, 133.9, 139.0, 162.9, 163.7, 163.8, 164.1.

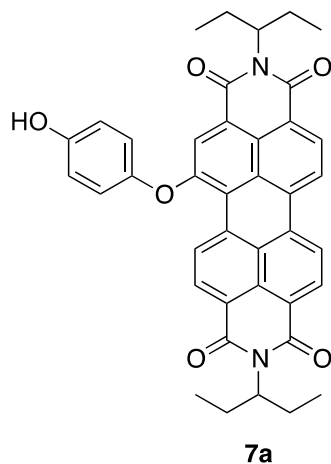
5.4.3 General procedure A for the Synthesis of *o*-, *m*-, and *p*-Dihydroxybenzene Appended Perylene Diimides

A mixture of compound **5** (1.0 equiv), benzene diol (5.0 equiv) and K₂CO₃ (5.0 equiv) was taken in a pre-dried, 50-mL, two-necked, round-bottomed flask fitted with a condenser, a magnetic stir bar and an argon inlet. A solution of dry toluene and dry DMF (4:1) was added to the mixture, and the resulting red-colored solution was stirred under Ar atmosphere for 15 min, followed by heating at 120 °C for 3 h. The solution turned from bright red to a reddish pink color. Dilution of the reaction mixture with CH₂Cl₂, followed by a brine wash and drying (Na₂SO₄), afforded the crude dihydroxybenzene derivatives of perylene diimide with a free hydroxyl group at one end. Further purification was effected by column chromatography over silica gel using ethyl acetate:hexane (1:5).

5.4.4 General procedure B for the synthesis of SubPc appended PDI

A mixture of compound **7** (1.0 equiv) and SubPc-F₁₂ **2** (1.0 equiv) was taken in a dried, 25-mL sealed tube. Dry toluene (2 mL) was added to the reaction mixture which was heated to 180 °C for 3 days. The SubPc-PDI complex was identified as a middle spot that existed between the relatively non-polar SubPc (top) and the polar dihydroxybenzene appended PDI (bottom) on TLC. Column chromatography using ethyl acetate:hexane over silica gel afforded the SubPc-F₁₂ appended perylene diimides.

5.4.5 Synthesis of (4-Hydroxyphenoxy)-N,N'-bis(ethylpropyl)perylene-3,4,9,10-tetracarboxylicacid Bisimide



Compound **5** (0.1 g, 0.16 mmol), *para*-hydroquinone (0.09 g, 0.8 mmol) and K_2CO_3 (0.11 g, 0.8 mmol) were reacted in dry toluene:DMF (4:1 ratio, 10 mL) mixture according to the general procedure A.

Yield: 0.05 g (54%). **Mp:** >300 °C.

1H NMR (400 MHz, $CDCl_3$): δ 9.62 (d, $J = 8.4$ Hz, 1H), 8.62-8.73 (m, 5H), 8.26 (s, 1H), 7.10 (d, $J = 8.8$ Hz, 2H), 6.95 (d, $J = 9.2$ Hz, 2H), 5.2 (bs, -OH, 1H), 5.01-5.11 (m, 2H), 2.33-2.18 (m, 4H), 1.87-1.99 (m, 4H), 0.87-0.94 (m, 12H).

^{13}C NMR (100 MHz $CDCl_3$): δ 157.4, 153.7, 147.9, 134.7, 134.5, 129.5, 128.8, 127.2, 125.7, 123.8, 122.5, 121.8, 117.4, 58.0, 25.2, 11.5.

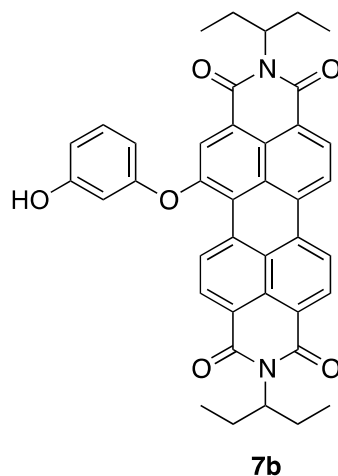
MS (MALDI-TOF) m/z for $C_{40}H_{34}N_2O_6$: Calcd: 638.2417, Found: 638.3216.

ELEMENTAL ANAL.: $C_{40}H_{34}N_2O_6 \cdot 0.4 H_2O$:

Calcd: C, 74.38; H, 5.43; N, 4.34.

Found: C, 74.39; H, 5.57; N, 4.31.

5.4.6 Synthesis of (3-Hydroxyphenoxy)-N,N'-bis(ethylpropyl)perylene-3,4,9,10-tetracarboxylicacid Bisimide



Compound **5** (0.1 g, 0.16 mmol), resorcinol (0.09 g, 0.8 mmol) and K_2CO_3 (0.11 g, 0.8 mmol) were reacted in a dry toluene:DMF (4:1 ratio, 10 mL) mixture according to the general procedure A.

Yield: 0.05 g (54%). **Mp:** >300 °C

1H NMR (400 MHz, $CDCl_3$): δ 9.42 (d, $J=11.2$ Hz, 1H), 8.52-8.64 (m, 5H), 8.23 (s, 1H), 7.26 (t, 1H), 6.78 (d, $J=2.4$, 1H), 6.68-6.70(m, 3H), 5.01-5.04 (m, 2H), 2.18-2.28 (m, 4H), 1.86-1.97 (m, 4H), 0.87-0.93 (m, 12H).

^{13}C NMR (100 MHz $CDCl_3$): δ 158.0, 155.9, 134.2, 133.6, 131.4, 129.2, 128.5, 128.4, 126.8, 125.8, 122.3, 112.7, 111.6, 107.2, 58.0, 25.1, 11.4.

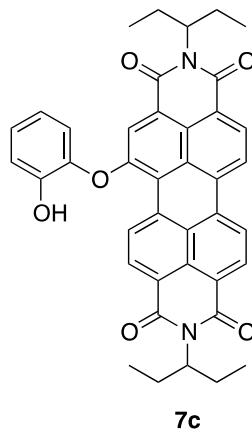
MS (MALDI-TOF) m/z for $C_{40}H_{34}N_2O_6$: Calcd: 638.2417, Found: 638.2613

ELEMENTAL ANALYSIS: $C_{40}H_{34}N_2O_6 \cdot 0.5 H_2O$:

Calcd: C, 74.17; H, 5.45; N, 4.32.

Found: C, 74.42; H, 5.79; N, 4.02.

5.4.7 Synthesis of (2-Hydroxyphenoxy)-N,N'-bis(ethylpropyl)perylene 3,4,9,10-tetracarboxylicacid Bisimide



Compound **5** (0.1 g, 0.16 mmol), catechol (0.09 g, 0.8 mmol), and K_2CO_3 (0.11 g, 0.8 mmol) were reacted in dry toluene:DMF (4:1 ratio, 10 mL) solution according to the general procedure A.

Yield: 0.05 g (48%). **Mp:** > 300 °C.

1H NMR (400 MHz, $CDCl_3$): δ 9.50 (d, $J = 8.4$ Hz, 1H), 8.59-8.6 (m, 4H), 8.50 (d, $J = 8$ Hz, 1H), 8.23 (s, 1H), 7.18-7.23 (m, 3H), 6.96-7.03 (m, 2H), 5.92 (bs, -OH, 1H), 5.01-5.04 (m, 2H), 2.18-2.28 (m, 4H), 1.86-1.97 (m, 4H), 0.87-0.93 (m, 12H).

^{13}C NMR (100 MHz $CDCl_3$): δ 156.1, 147.8, 141.4, 134.2, 133.5, 129.1, 128.4, 126.9, 126.8, 125.8, 123.6, 123.0, 122.3, 121.7, 120.5, 117.7, 57.7, 24.9, 11.3.

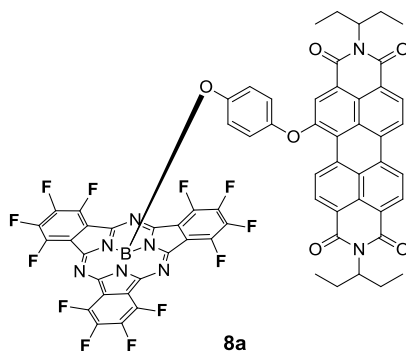
MS (MALDI-TOF) m/z for $C_{40}H_{34}N_2O_6$: Calcd: 638.2417, Found: 638.2765

ELEMENTAL ANAL.: $C_{40}H_{34}N_2O_6 \cdot 0.6 H_2O$:

Calcd: C, 73.97; H, 5.46; N, 4.31.

Found: C, 73.97; H, 5.50; N, 4.34.

5.4.8 Synthesis of *p*-SubPc Appended PDI



A mixture of compound **7a** (0.05 g, 0.078 mmol) and SubPc **2** (0.050 g, 0.078 mmol) was reacted in dry toluene according to the general procedure B in a sealed tube.

Yield: 0.023g (24%). **Mp:** >300 °C.

¹H NMR (400 MHz, CDCl₃): δ 9.39 (d, J = 8.4 Hz, 1H), 8.59-8.68(m, 5H), 7.89 (s, 1H), 6.65 (d, J = 8.8 Hz, 2H), 5.44 (d, J = 8 Hz, 2H), 4.94-5.10 (m, 2H), 2.22-2.27 (m, 4H), 1.89-1.95 (m, 4H), 0.86-0.92 (m, 12H).

¹³C NMR (100 MHz, CDCl₃): δ 156.3, 148.9, 148.5, 143.7, 143.3, 141.8, 141.6, 134.5, 134.3, 133.6, 129.2, 128.4, 126.9, 125.5, 123.5, 122.7, 122.3, 121.1, 120.0, 117.1, 114.9, 57.7, 57.5, 29.6, 29.5, 24.9, 11.3, 11.2.

MS (MALDI-TOF) *m/z* for C₆₄H₃₃BF₁₂N₈O₆: Calcd: 1248.2424, Found: 1248.5341.

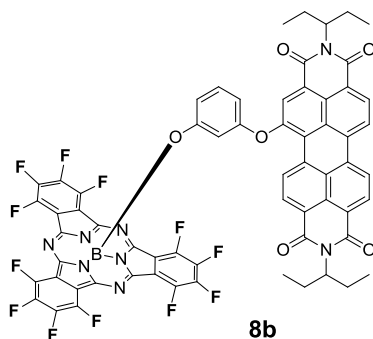
ELEMENTAL ANAL.: C₆₄H₃₃BF₁₂N₈O₆·0.2 H₂O:

Calcd: C, 61.38; H, 2.69; N, 8.95.

Found: C, 56.11; H, 2.57; N, 7.50.

Repeated, long term vacuum drying or extensive washings of the solid with pentane did not remove water and residual hexane impurities.

5.4.9 Synthesis of *m*- SubPc Appended PDI



A mixture of **7b** (0.05 g, 0.078 mmol) and SubPc **2** (0.050 g, 0.078 mmol) was reacted in dry toluene (2 mL) according to the general procedure B in a sealed tube.

Yield: 0.025g (26%). **Mp:** >300 °C.

¹H NMR (600 MHz, CD₂Cl₂): δ 9.17 (d, J = 11.2 Hz, 1H), 8.52-8.64 (m, 4H), 8.49 (d, J = 5.6 Hz, 1H), 7.83 (s, 1H), 6.89 (t, J = 5.2 Hz, 1H), 6.50 (d, J = 8.4 Hz, 1H), 6.68-6.70(s, 1H), 5.30 (s, 1H), 5.21 (d, J = 8.4 Hz, 1H), 4.90-5.06 (m, 2H), 2.18-2.28 (m, 4H), 1.86-1.97 (m, 4H), 0.87-0.93 (m, 12H).

¹³C NMR (100 MHz, CD₂Cl₂): δ 161.9, 156.1, 155.0, 153.6, 148.8, 143.9, 143.5, 142.2, 141.8, 134.5, 133.5, 131.1, 129.5, 128.7, 128.4, 127.1, 126.4, 124.2, 123.9, 122.8, 115.2, 113.2, 110.2, 57.8, 25.2, 11.4.

MS (MALDI-TOF) *m/z* for C₆₄H₃₃BF₁₂N₈O₆: Calcd: 1248.2424, Found: 1248.7211.

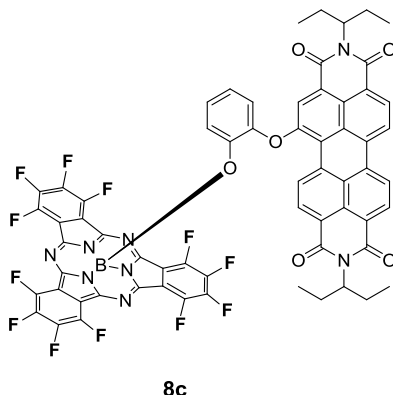
ELEMENTAL ANAL.: C₆₄H₃₃BF₁₂N₈O₆·0.2 H₂O:

Calcd: C, 61.38; H, 2.69; N, 8.95.

Found: C, 57.61; H, 2.63; N, 7.94.

Repeated, long term vacuum drying or extensive washings of the solid with pentane did not remove water and residual hexane impurities.

5.4.10 Synthesis of *o*- SubPc Appended PDI



A mixture of **7c** (0.05 g, 0.078 mmol) and SubPc **2** (0.050 g, 0.078 mmol) was reacted in dry toluene (2 mL) according to the general procedure B in a sealed tube.

Yield: 0.017 g (18%). **Mp:** >300 °C.

¹H NMR (400 MHz, CDCl₃): δ 8.71 (m, 5H), 8.64 (s, 1H), 8.41 (d, J = 5.2 Hz, 1H) 7.4 (s, 1H), 6.99 (m, 1H), 6.86-6.88 (m, 2H), 5.31-5.32 (m, 1H), 5.13-5.16 (m, 2H), 2.17-2.27 (m, 4H), 1.84-1.96 (m, 4H), 0.87-0.95 (m, 12H).

¹³C NMR (100 MHz CDCl₃): δ 164.0, 163.6, 163.2, 162.6, 139.0, 133.5, 133.3, 133.1, 130.9, 130.3, 129.0, 128.8, 128.1, 128.0, 127.0, 124.1, 123.8, 123.5, 123.1, 122.8, 120.8, 58.1, 57.9, 25.0, 24.9, 11.7, 11.6.

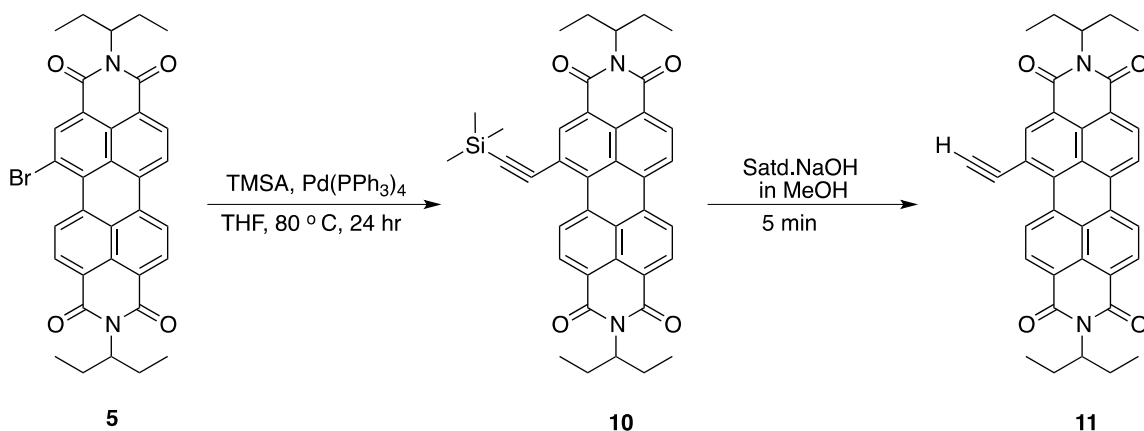
MS (MALDI-TOF) *m/z* for C₆₄H₃₃BF₁₂N₈O₆: Calcd: 1248.2424, Found: 1248.3432.

ELEMENTAL ANALYSIS: C₆₄H₃₃BF₁₂N₈O₆·2H₂O:

Calcd: C, 59.83; H, 2.90; N, 8.72.

Found: C, 57.94; H, 2.84; N, 7.82.

Repeated, long term vacuum drying or extensive washings of the solid with pentane did not remove water and residual hexane impurities.



Scheme 5.2 Synthesis of Terminal Alkyne Substituted PDI.

5.4.11 Synthesis of 1-Trimethylsilylacetylene-*N,N'*-bis(ethylpropyl)perylene-3,4,9,10-tetracarboxylic Diimide (**10**)

In a well dried, 100-mL, three-necked, round-bottomed flask fitted with a condenser, a gas inlet and a magnetic stir bar was placed compound **5** (0.3 g, 0.49 mmol). A solution of dry TEA:THF (20 mL, 1:3) was added, and the resulting red solution was purged with Ar for 15 min. Then Pd(PPh₃)₄ (0.010 g, 0.0049 mmol), CuI (0.0035 g, 0.0049 mmol) and TMSA (3.1 mL, 1.5 mmol) were added to the reaction mixture which was stirred at reflux condition for 12 h. The solvent was removed under vacuum, and the resulting mixture was subjected to silica gel chromatography under gravity using CH₂Cl₂ as the eluent to give **10**. (Scheme 5.2).

Yield: 0.45 g (93%). **Mp:** >300 °C.

¹H NMR (400 MHz, CDCl₃): δ 10.42 (2d 2H), 8.82 (s, 1H), 8.80 (s, 1H), 8.40 (m, 10H), 4.78 (m, 4H), 2.77 (m, 8H), 1.14 (d, 24H), 0.96 (d, 24H), 0.42 (s, 9H).

¹³C NMR (100 MHz, CDCl₃): δ 165.3, 165.1, 164.6, 164.2, 164.00, 163.97, 163.5, 139.4, 138.7, 134.7, 134.6, 134.54, 134.52, 134.33, 134.32, 134.30, 134.28, 134.0, 123.41, 123.21, 123.18, 123.1, 123.03, 123.01, 122.99, 122.88, 122.85, 122.6, 122.5, 121.98, 121.96, 120.0, 119.93, 119.90, 107.21, 107.15, 107.1, 105.9, 65.27, 65.25, 65.19, 65.18, 29.12, 29.10, 29.05, 29.0, 21.80, 21.76, 21.7, 20.58, 20.56, 20.51, 20.49, 0.40.

5.4.12 Synthesis of 1-Ethynyl-*N,N'*-bis(ethylpropyl)perylene-3,4:9,10-tetracarboxylic Diimide (11)

To a solution of 1-trimethylsilylacetylene-*N,N'*-bis(ethylpropyl)perylene-3,4:9,10-tetracarboxylic diimide **10**, (135 mg, 0.22 mmol) in CHCl₃ (20 mL) was added 1 mL of a saturated solution of NaOH in MeOH. The mixture was stirred for 5 min. Water (30 mL) was added, and the mixture was extracted with CHCl₃. The organic extracts were washed with water and dried (Na₂SO₄). The solvent was removed by rotary evaporation. The residue was purified by chromatography on silica gel, eluting with CHCl₃ to give 104 mg (87%) of 1-ethynyl-*N,N'*-bis(ethylpropyl)perylene-3,4:9,10-tetracarboxylic diimide (**11**) as a red solid.

Yield: 0.065 g (69%). **Mp:** >300 °C.

¹H NMR (400 MHz, CDCl₃): δ 10.17 (d, 1H), 8.76 (s, 1H), 8.67- 8.56 (m, 5H), 5.12-4.99 (m, 2H), 3.94 (s, 1H), 2.29-2.22 (m, 4H), 2.00-1.92 (m, 4H), 0.94 (t, 12H).

¹³C NMR(100 MHz, CDCl₃): δ 164.4, 163.1, 139.4, 135.2, 134.5, 133.9, 133.7, 131.5, 131.1, 130.8, 129.0, 128.8, 127.2, 127.1, 126.6, 123.4, 123.1, 118.7, 87.9, 84.7, 57.9, 57.8, 25.1, 25.0, 11.4.

5.5 References

1. Petty, M. C.; Bryce, M. R.; Bloor, D. *An Introduction to Molecular Electronics*. 1995, Oxford University Press, New York.
2. Prasad, P. N.; Williams, D. J. *Introduction to Nonlinear Optical Effects in Molecules and Polymers*. 1990, Wiley, Brisbane.
3. Roest, M. R.; Verhoeven, J. W.; Schuddeboom, W.; Warman, J. M.; Lawson, J. M.; Paddon-Row, M. N. *J. Am. Chem. Soc.* **1996**, 118, 1762-1768.
4. Gust, D.; Moore, T. A.; Moore, A. L. *Acc. Chem. Res.* **1993**, 26, 198-205.
5. Paddon-Row, M. N. *Acc. Chem. Res.* **1994**, 27, 18-25.
6. Kardos, M. D.R.P. 276956 Oct 10 1913. *Friedlanders Fortschr Teerfarbenfabr.* **1917**, 12, 492.
7. Gonzalez-Rodriguez, D.; Torres, T.; Guldi, D. M.; Rivera, J.; Herranz, M. A.; Echegoyen, L. *J. Am. Chem. Soc.* **2004**, 126, 6301-6313.
8. Gonzalez-Rodriguez, D.; Torres, T.; Herranz, M. A.; Echegoyen, L.; Carbonell, E.; Guldi, D. M. *Chem. Eur. J.* **2008**, 14, 7670-7679.
9. Gonzalez-Rodriguez, D.; Torres, T.; Olmstead, M. M.; Rivera, J.; Angeles, H. M.; Echegoyen, L.; Atienza, C. C.; Guldi, D. M. *J. Am. Chem. Soc.* **2006**, 128, 10680-10681.
10. Ebeid, E. Z. M.; El-Daly, S. A.; Langhals, H. *J. Phys. Chem.* **1988**, 92, 4565-4568.
11. Ford, W. E.; Kamat, P. V. *J. Phys. Chem.* **1987**, 91, 6373-6380.
12. Ambroise, A.; Kirmaier, C.; Wagner, R. W.; Loewe, R. S.; Bocian, D. F.; Holten, D.; Lindsey, J. S. *J. Org. Chem.* **2002**, 67, 3811-3826.

13. Gregg, B. A.; Cormier, R. A. *J. Am. Chem. Soc.* **2001**, *123*, 7959-7960.
14. Prathapan, S.; Yang, S. I.; Seth, J.; Miller, M. A.; Bocian, D. F.; Holten, D.; Lindsey, J. S. *J. Phys. Chem. B.* **2001**, *105*, 8237-8248.
15. Tomizaki, K.; Loewe, R. S.; Kirmaier, C.; Schwartz, J. K.; Retsek, J. L.; Bocian, D. F.; Holten, D.; Lindsey, J. S. *J. Org. Chem.* **2002**, *67*, 6519-6534.
16. van, d. B. T.; Hayes, R. T.; Zhao, Y.; Bushard, P. J.; Weiss, E. A.; Wasielewski, M. R. *J. Am. Chem. Soc.* **2002**, *124*, 9582-9590.
17. Xiao, S.; El-Khouly, M. E.; Li, Y.; Gan, Z.; Liu, H.; Jiang, L.; Araki, Y.; Ito, O.; Zhu, D. *J. Phys. Chem. B.* **2005**, *109*, 3658-3667.
18. Romero-Nieto, C.; Guilleme, J.; Fernandez-Ariza, J.; Rodriguez-Morgade, M. S.; Gonzalez-Rodriguez, D.; Torres, T.; Guldi, D. M. *Org. Lett.* **2012**, *14*, 5656-5659.
19. Herbst, W. *Industrial Organic Pigments: Production, Properties, Applications.* 2003, John Wiley & Sons, Weinheim.
20. Struijk, C. W.; Sieval, A. B.; Dakhorst, J. E. J.; van, D. M.; Kimkes, P.; Koehorst, R. B. M.; Donker, H.; Schaafsma, T. J.; Picken, S. J.; van, d. C. A. M.; Warman, J. M.; Zuilhof, H.; Sudholter, E. J. R. *J. Am. Chem. Soc.* **2000**, *122*, 11057-11066.
21. Law, K. Y. *Chem. Rev.* **1993**, *93*, 449-486.
22. Cespedes-Guirao, F. J.; Roperro, A. B.; Font-Sanchis, E.; Nadal, A.; Fernandez-Lazaro, F.; Sastre-Santos, A. *Chem. Commun.* **2011**, *47*, 8307-8309.
23. Chen, Z.; Zheng, Y.; Yan, H.; Facchetti, A. *J. Am. Chem. Soc.* **2009**, *131*, 8-9.
24. Geissler, G.; Remy, H. *Ger. Pat. Appl.* DE 1130099, **1959**; Chem. Abstr., **1962**, 57, P11346f).

25. Wescott, L. D.; Mattern, D. L. *J. Org. Chem.* **2003**, 68, 10058-10066.
26. Huang, C.; Barlow, S.; Marder, S. R. *J. Org. Chem.* **2011**, 76, 2386-2407.
27. Langhals, H.; Demmig, S.; Huber, H. *Spectrochim. Acta, Part A* **1988**, 44A, 1189-1193.
28. Ahrens, M. J.; Fuller, M. J.; Wasielewski, M. R. *Chem. Mater.* **2003**, 15, 2684-2686.
29. (a.) Chen, Z.; Debije, M. G.; Debaerdemaeker, T.; Osswald, P.; Wurthner, F. *Chem. Phys. Chem.* **2004**, 5, 137-140.
30. Zugenmaier, P.; Duff, J.; Bluhm, T.L. *Cryst. Res. Technol.* **2000**, 35, 1095-1115.

5.6 Appendices

Figure 5.11 ^1H NMR Spectrum of **7a**

Figure 5.12 ^{13}C NMR Spectrum of **7a**

Figure 5.13 ^1H NMR Spectrum of **7b**

Figure 5.14 ^{13}C NMR Spectrum of **7b**

Figure 5.15 ^1H NMR Spectrum of **7c**

Figure 5.16 ^{13}C NMR Spectrum of **7c**

Figure 5.17 ^1H NMR Spectrum of **8a**

Figure 5.18 ^{13}C NMR Spectrum of **8a**

Figure 5.19 ^1H NMR Spectrum of **8b**

Figure 5.20 ^{13}C NMR Spectrum of **8b**

Figure 5.21 ^1H NMR Spectrum of **8c**

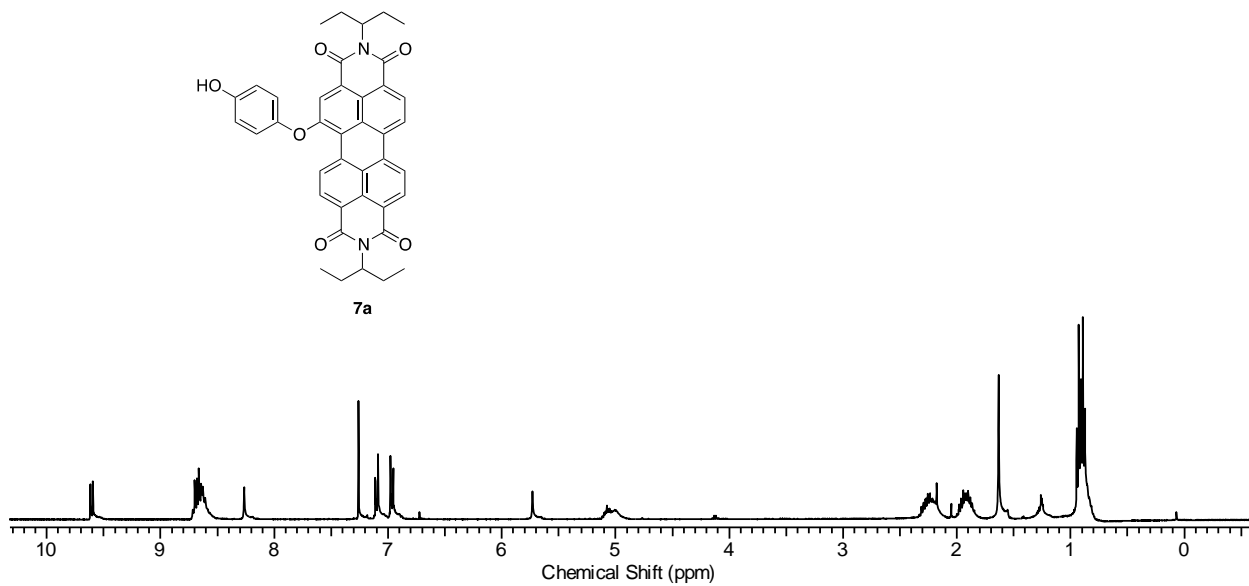


Figure 5.11 ^1H NMR Spectrum of **7a**

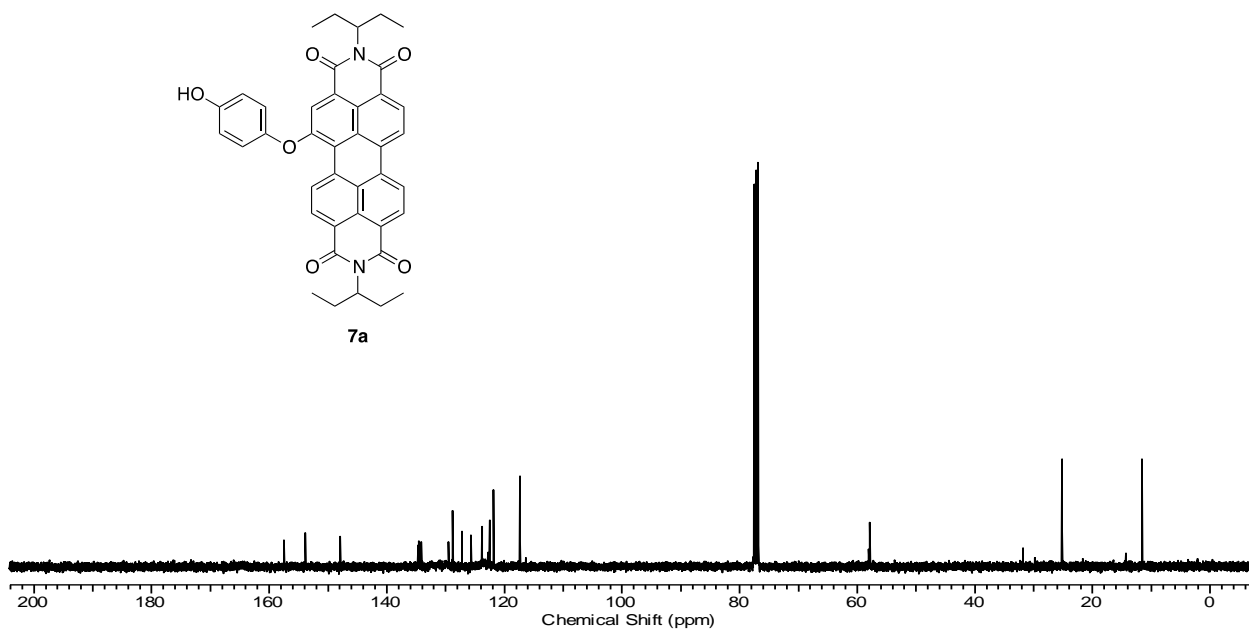


Figure 5.12 ^{13}C NMR Spectrum of **7a**

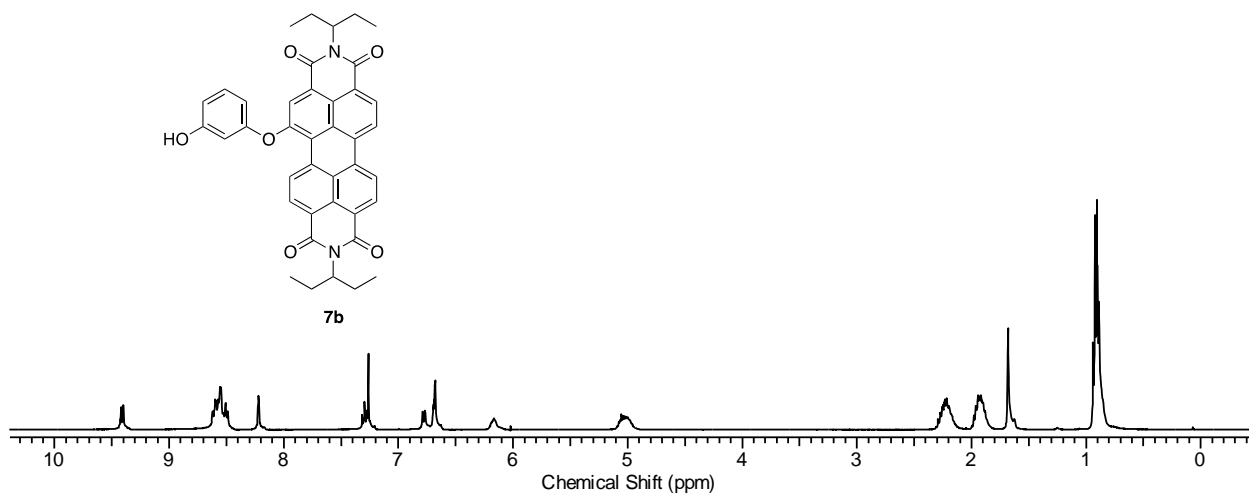


Figure 5.13 ¹H NMR Spectrum of **7b**

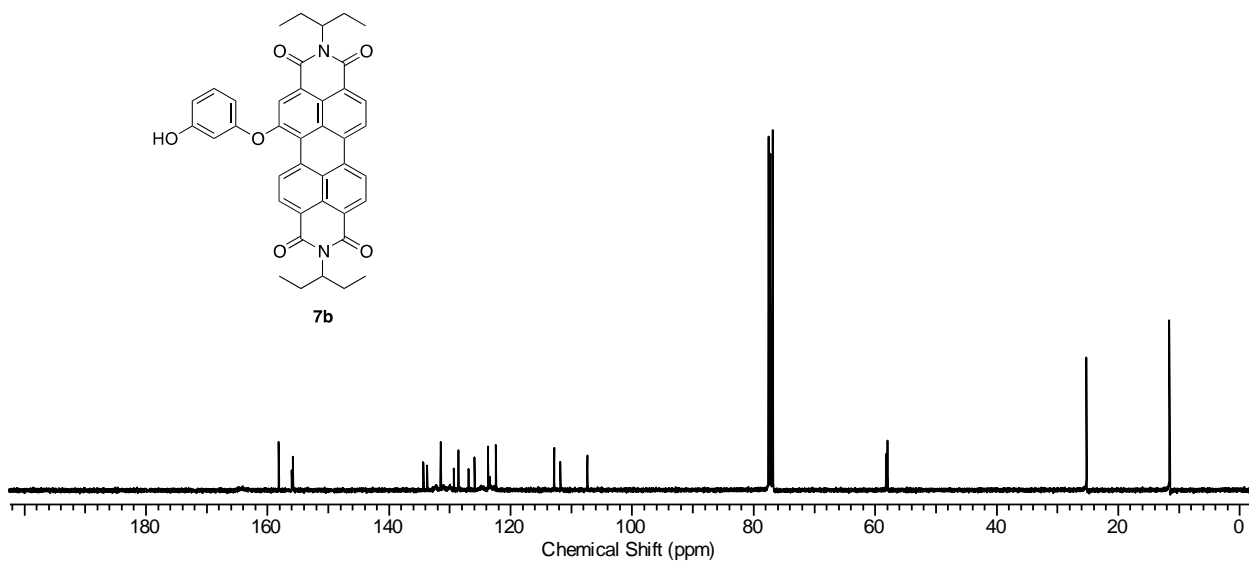


Figure 5.14 ¹³C NMR Spectrum of **7b**

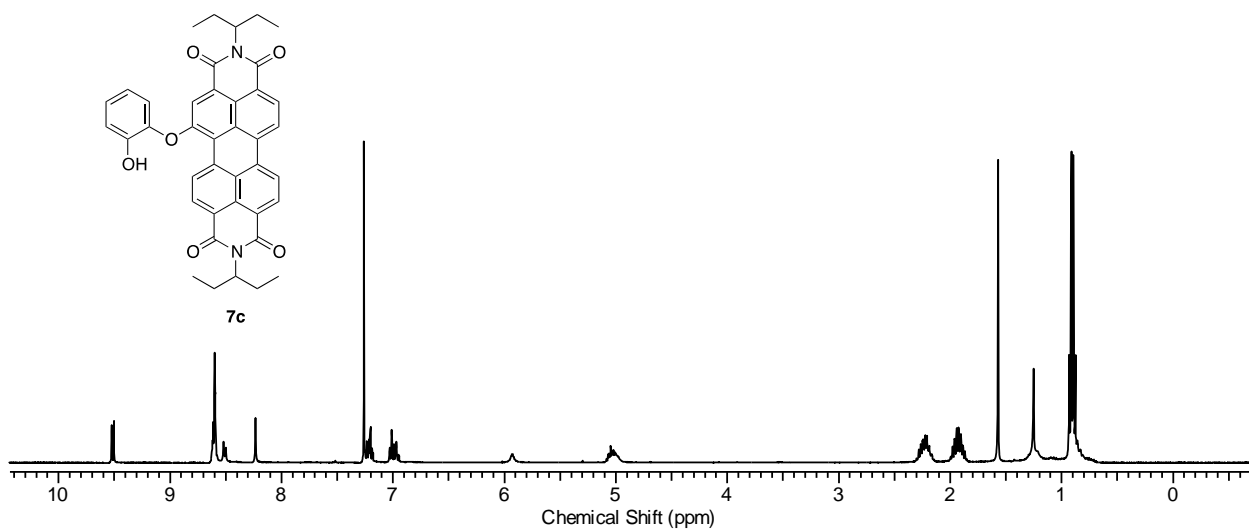


Figure 5.15 ^1H NMR Spectrum of **7c**

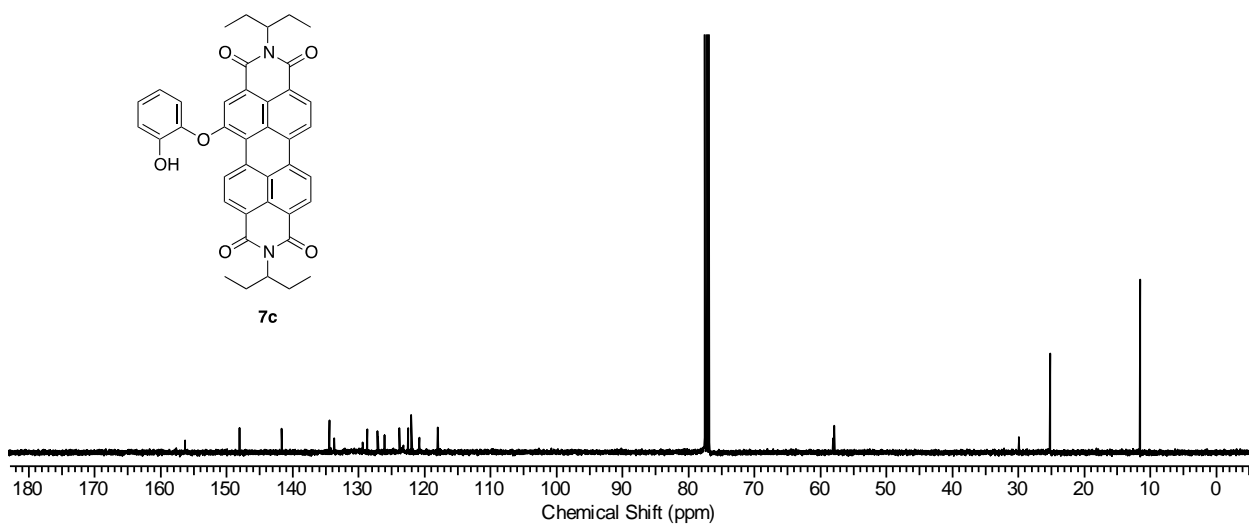


Figure 5.16 ^{13}C NMR Spectrum of **7c**

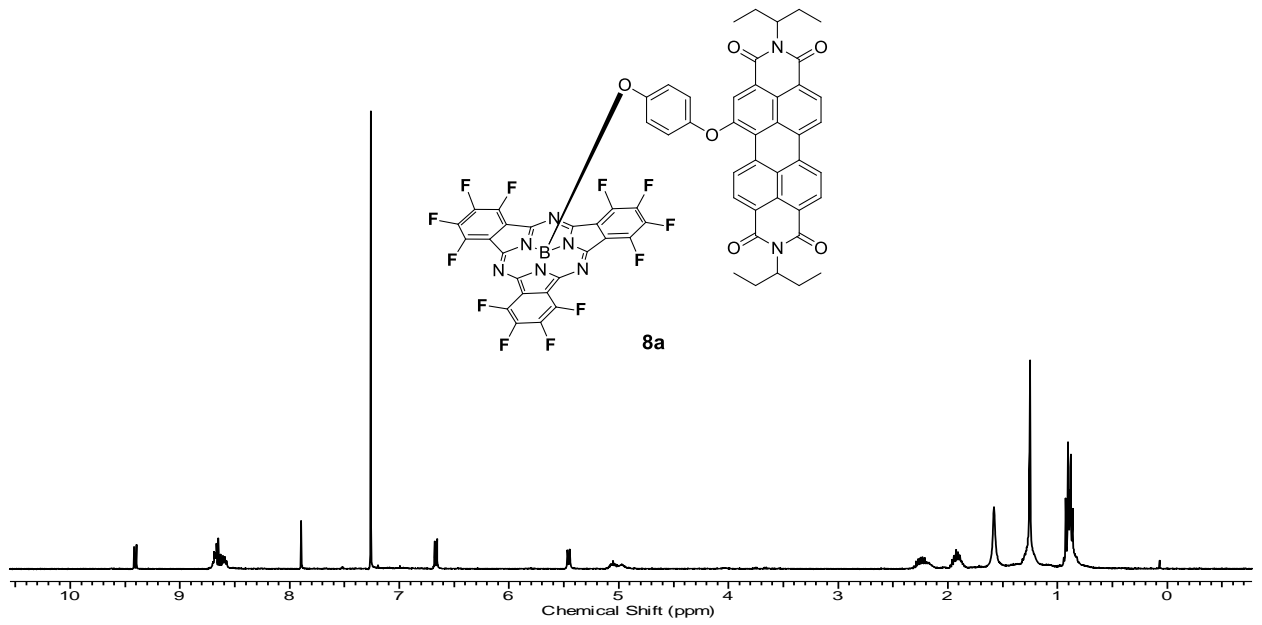


Figure 5.17 ^1H NMR Spectrum of **8a**

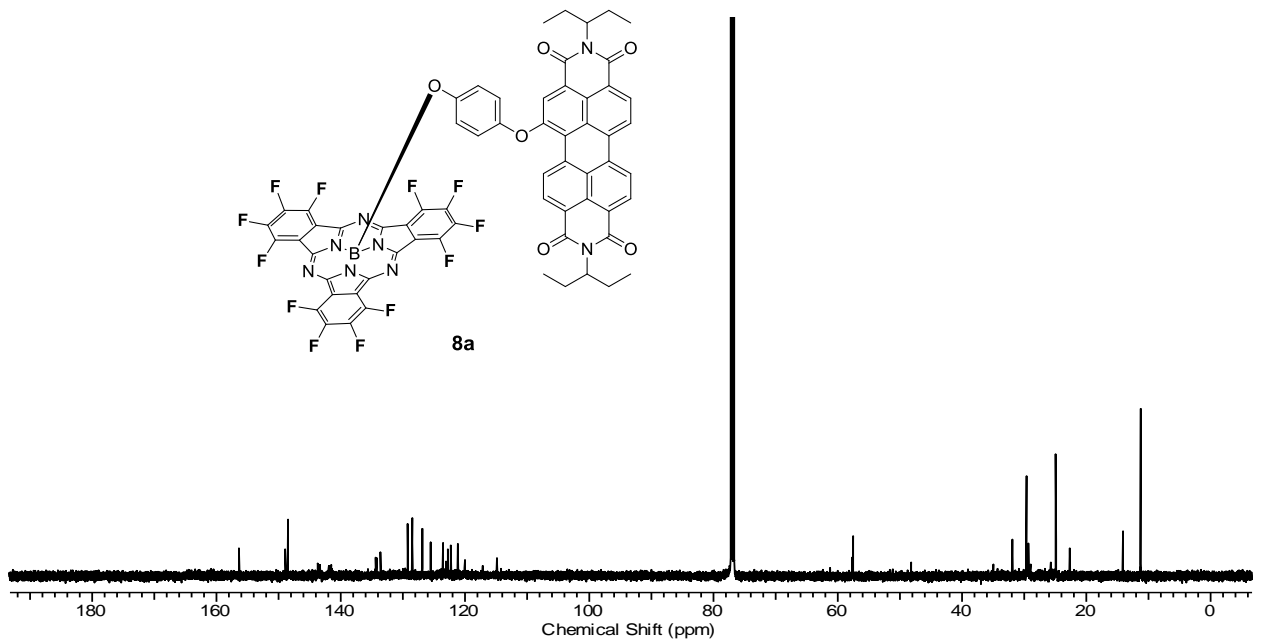


Figure 5.18 ^{13}C NMR Spectrum of **8a**

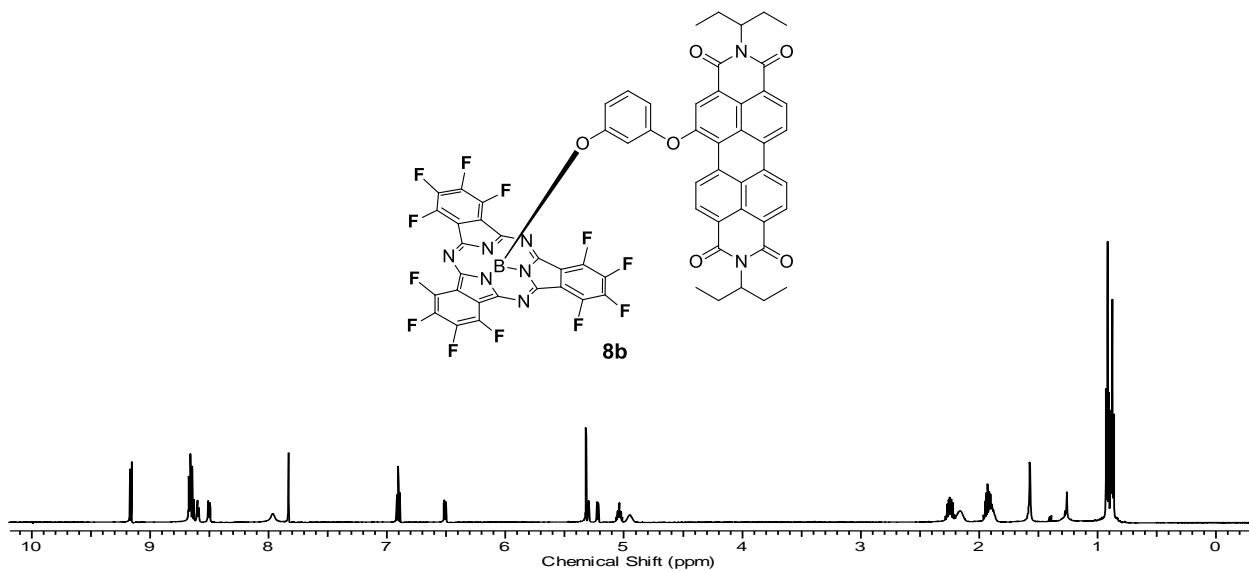


Figure 5.19 ^1H NMR Spectrum of **8b**

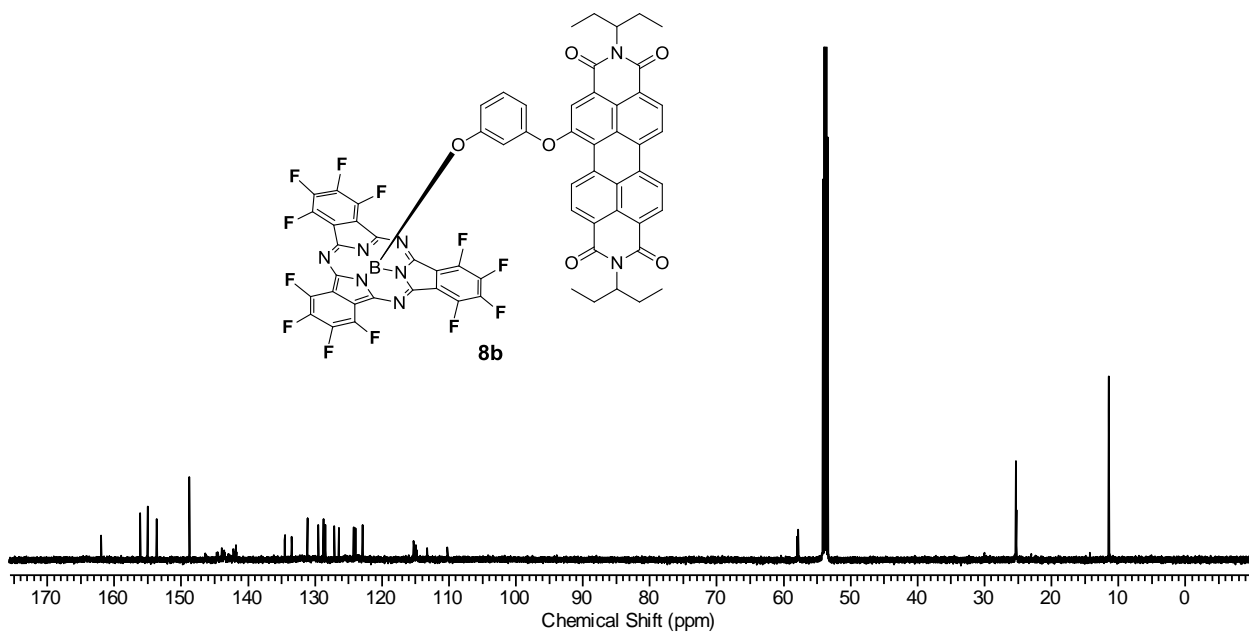


Figure 5.20 ^{13}C NMR Spectrum of **8b**

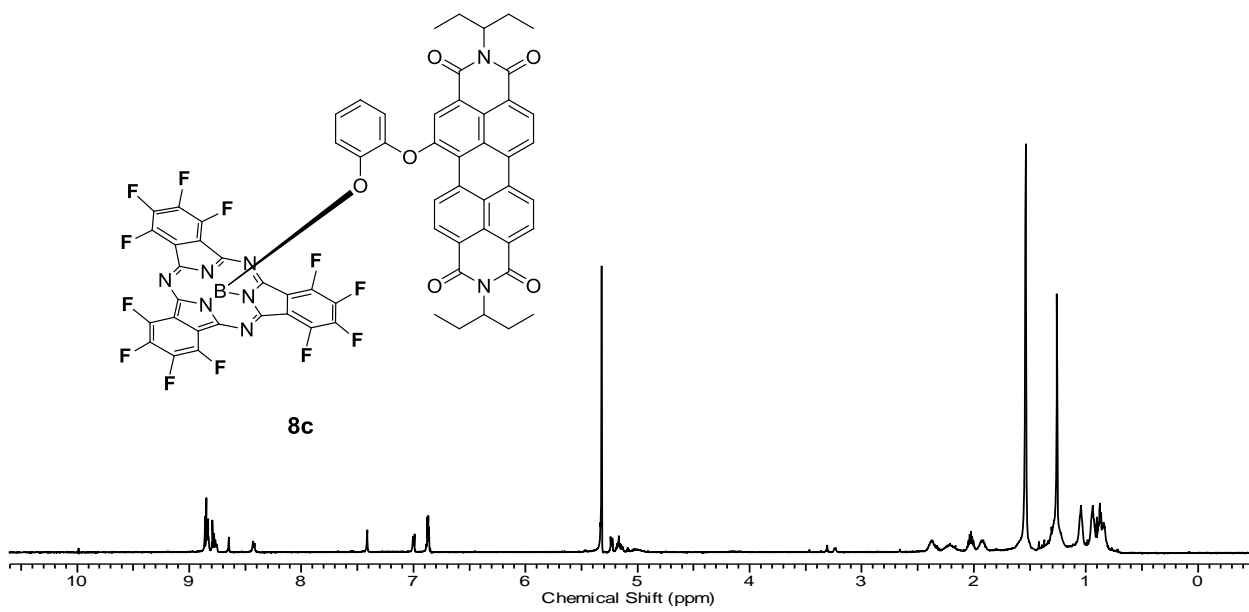


Figure 5.21 ^1H NMR Spectrum of **8c**

CHAPTER VI

RESULTS AND DISCUSSION

SYNTHESIS OF SUBPHTHALOCYANINE FUSED DIMERS

6.1 Introduction

In 1991 Kobayashi exemplified the extension of the π -conjugation of the SubPc aromatic core in the synthesis of a subphthalocyanine (SubPc) fused dimer (Figure 6.1).¹ Condensation of an excess of 4-*tert*-butylphthalonitrile and 1,2,4,5-tetracyanobenzene with diphenylboron bromide afforded the subphthalocyanine dimer after purification.

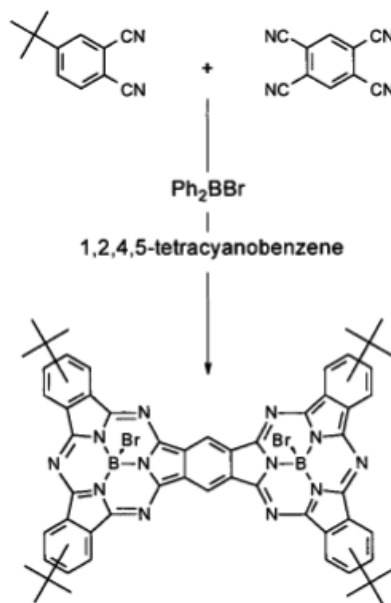


Figure 6.1 Synthesis of a SubPc Fused Dimer.

However, this novel dimer was revisited by Torres et al, who characterized a fluoro substituted SubPc dimer.² As a consequence of the concave nature of the SubPc macrocycle, the fused dimer exists as syn and anti topoisomers² which are represented in Figure 6.2.

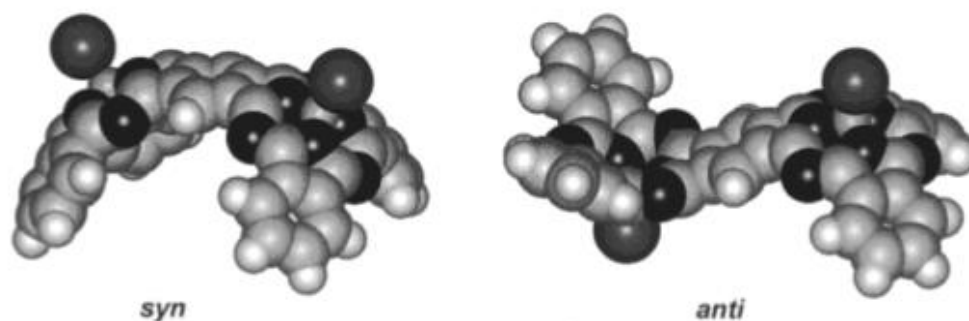


Figure 6.2 Syn and Anti Topoisomers of a SubPc Fused Dimer.

The topoisomers are separable by column chromatography. As a matter of fact, these fused systems possess the added interest in that they are among the very few known examples of curved pi-surfaces.³ Unlike the fused phthalocyanine and porphyrine⁴ systems which display very similar UV-Vis absorption features as the corresponding mononuclear macrocycles, the SubPc dimers show a large bathochromic shift of their Q-band (120 nm),⁵ compared to the monomeric SubPc, and present a distinctive blue color in solution. Moreover, the Q bands of the dimers have characteristic multiband, fine structure consisting of four major absorptions,⁵ a fact which has received no explanation thus far. One important aspect of the SubPc dimer is that it can impart higher solubility than the corresponding monomer because of the concave geometry of the macrocycle for which no reason has been mentioned in the literature so far.

6.2 Crown ethers

Crown ethers are prominent class of macrocyclic host compound because of their ability to bind inorganic as well as organic cations. Crown ethers also bind some neutral substrates strongly and selectively.⁶ They also serve as platforms for the design of new macrocyclic host molecules such as cryptands,⁷ rotaxanes and catenanes.⁸ Modifications of the crown ethers can be made by introduction of the substituents which in turn allows variation of their complexing properties and enables them to be incorporated into polymeric backbones. Crown ethers also facilitate the preparation of new macrocyclic receptors, such as lariat ethers⁹ (crown ethers with side chains), and polymers with exceptional properties.¹⁰ Benzocrown ethers have some special advantages over their aliphatic analogs as there is possible facile introduction of the substituents in the benzene ring. Benzocrown ethers containing dicyano groups are of particular interest since they can act as phthalonitrile precursors for the synthesis of the corresponding phthalocyanines and subphthalocyanines under specific conditions.¹¹

6.3 Synthesis of Crown ethers

Although methodologies concerning the construction of crown ethers (Figure 6.3) generate considerable interest in synthetic chemistry, their synthesis is often inefficient,¹² since cyclization is usually accompanied by a side process of polycondensation. This means that macrocyclization reactions have to be carried out at low concentrations. However, the effect of both oligo- and polycondensations can be suppressed when the ring closure is performed by any one of the following three strategies, namely (i) high dilution principle,¹³ (ii) template method¹², and (iii) cesium effect.¹⁴ A good alternative to

the traditional methods is the synthesis of macrocyclic compounds is under phase transfer catalysis (PTC) conditions.¹⁵

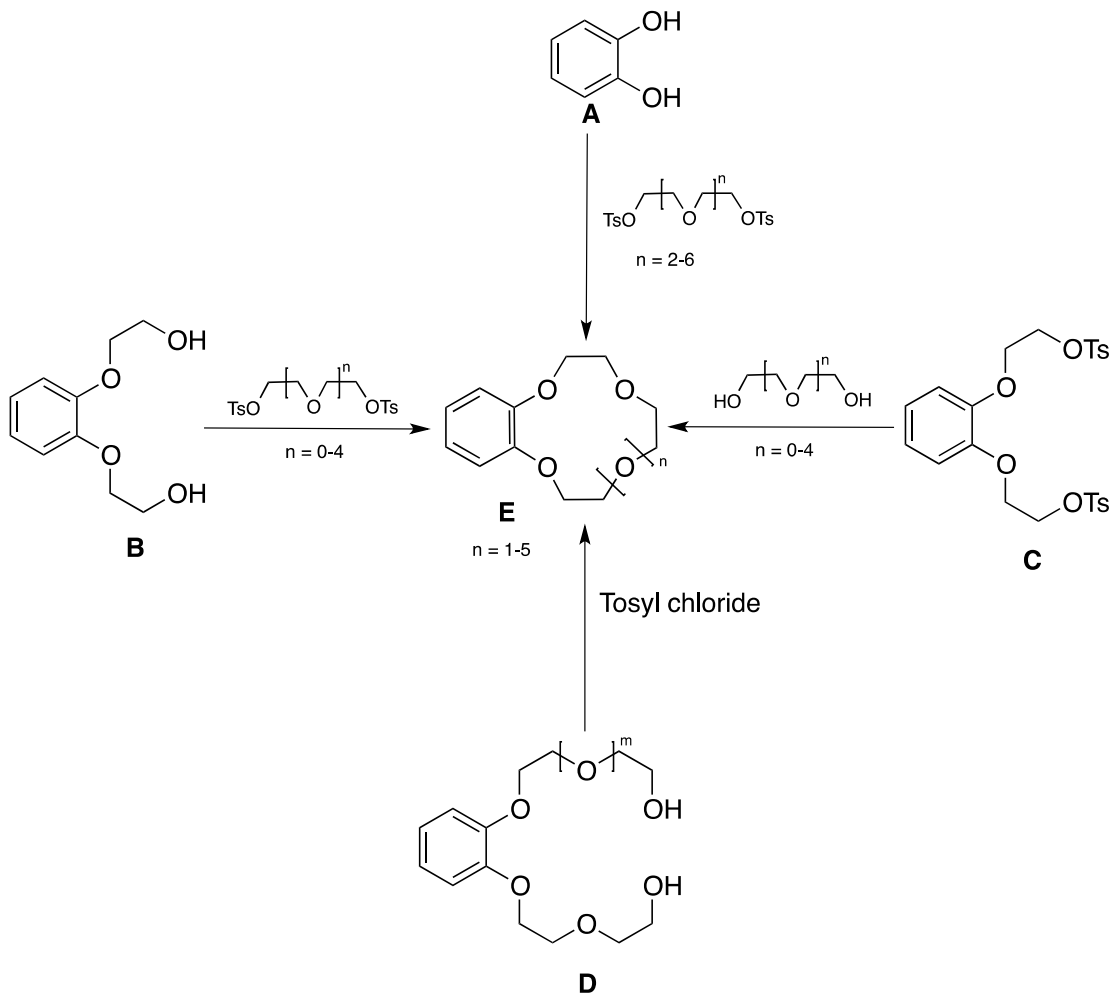


Figure 6.3 Synthesis of Benzocrown Ethers

The hypothesis of PTC is based primarily on two different criteria:¹⁵

- (i) The formation of new carbon-oxygen bonds by reactions of anions generated by deprotonation of alcohols and phenols represent a widely exploited part of PTC applications.

- (ii) The rates of nucleophilic reactions under PTC conditions increase which, in turn, should also result in an increase in the yields of macrocyclic compounds.

6.3.1 Methods of synthesis of benzocrown ethers

In general, the synthesis of benzocrown ethers (Figure 6.3) is effected by any one of the four procedures:

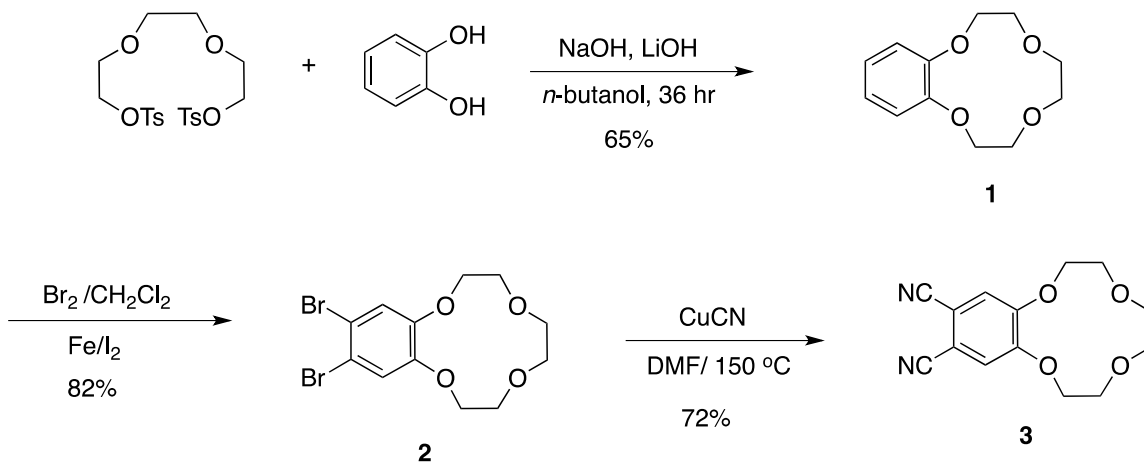
- (i) reaction of catechol **A** with oligo(ethylene glycol) ditosylates,
- (ii) alkylation of bis(*o*-phenylene)glycol **B** with the corresponding oligo(ethylene glycol) ditosylates,
- (iii) reaction of bis(*o*-phenylene)glycol ditosylate **C** with oligo(ethylene glycols),
- (iv) intramolecular ring closure of bis(*o*-phenylene)glycols **D** generated *in situ*.

Procedure (i) is most attractive due to the inexpensive starting materials, namely catechol and oligo(ethylene glycol) ditosylates. In contrast, procedures (ii)–(iv) require the preparation of the starting bis(*o*-phenylene)glycols **B** and **D**.

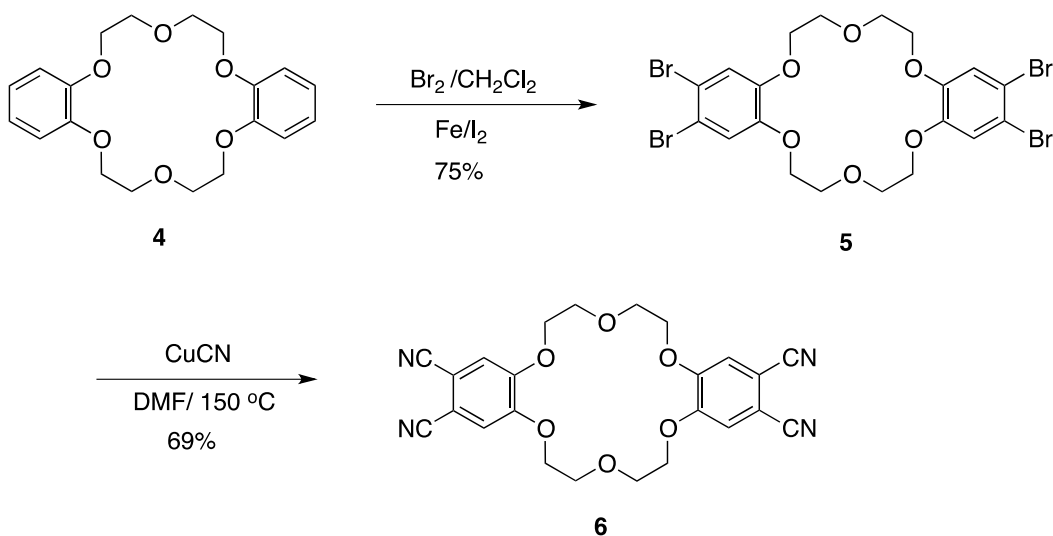
6.4 Experimental

Melting points (mp) were determined using a Stuart SMP10 instrument. Both ^1H and ^{13}C NMR spectra were acquired in CDCl_3 using a Varian Inova 400 MHz or a Gemini 300 MHz spectrometer. Chemical shifts (δ) are expressed in ppm relative to residual chloroform (^1H : 7.26 ppm, ^{13}C : 77.0 ppm) or to TMS. Column chromatography was carried out on silica gel (Sorbent Technologies, 230-400 mesh), and TLC was done with polyester sheets precoated with silica gel (Sorbent Technologies). (Ethane-1,2-diylbis(oxy))bis(ethane-2,1-diyl)bis(4-methylbenzenesulfonate) (Sigma Aldrich),

catechol (Alfa Aesar), CuCN (Alfa Aesar), dibenzo 18-crown-6 (Sigma-Aldrich), *n*-BuCl (Sigma-Aldrich), and BCl₃ in *p*-xylene (Sigma-Aldrich) were purchased from commercial suppliers and used as received unless otherwise indicated. The synthesis of 12-crown-4 (**3**) is illustrated in Scheme 6.1 and that of a 18-crown-6 (**6**) in Scheme 6.2.

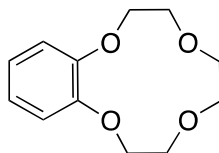


Scheme 6.1 Synthesis of a 12-crown 4.



Scheme 6.2 Synthesis of a 18-crown 6.

6.4.1 Synthesis of a Benzo-12-crown-4



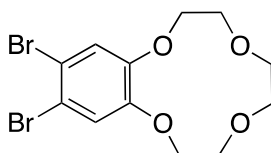
1

In a 250-mL, three-necked, round-bottomed flask fitted with a condenser and magnetic stir bar was placed a mixture of sodium hydroxide (1.2 g, 0.03 mol) and lithium hydroxide (1.2 g, 0.05 mol) dissolved in water (5 mL) and EtOH (74 mL). The reaction mixture was heated to reflux for 1 hr. A mixture of catechol (3.0 g, 0.027 mol) and (ethane-1,2-diylbis(oxy))bis(ethane-2,1-diyl) bis(4-methylbenzenesulfonate) (12.3 g, 0.027 mol) was dissolved in EtOH (25 mL) and slowly added to the reaction mixture through a syringe pump over a period of 25 h (discharging 1 mL per h). After completion of the addition, the reaction mixture was stirred at reflux temperature for 11 h. After cooling to room temperature, 1 mL of 2 N HCl was added, and the mixture was stirred for 4 hr. The precipitated solid was filtered, and was redissolved in ethyl acetate (100 mL). The organic layer was washed with water (30 mL), followed by a brine wash (30 mL) and drying (Na₂SO₄). The solvent was evaporated under vacuum to give a crude solid which was column chromatographed with ethyl acetate:hexane (1:5) to give **1** as a white solid.

Yield: 3.9 g (65%). **Mp:** 43-44 °C (lit¹¹, 44 °C)

¹H NMR (400 MHz, CDCl₃): δ 3.79 (s, 4H), 3.84-3.86 (m, 4H), 4.16-4.19 (m, 4H), 6.92-7.0 (m, 4H).

6.4.2 Synthesis of a 4,5-Dibromobenzo-12-crown-4



2

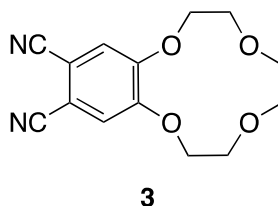
A solution of **1** (0.45 g, 2 mmol) in CH_2Cl_2 (5 mL), was placed in a 50-mL, two-necked, round-bottomed flask fitted with an 10-mL addition funnel and a magnetic stirrer. A catalytic amount of Fe and iodine were also added to the reaction mixture. A solution of bromine (0.21 mL, 4 mmol) in CH_2Cl_2 (5 mL) was added dropwise over a period of 4 h, maintaining the temperature between 0-5 °C. The reaction mixture was then slowly allowed to attain room temperature, and was stirred for an additional 30 min. After completion of the reaction, as judged by TLC, the reaction mixture was diluted with CH_2Cl_2 (50 mL) and washed with saturated aqueous NaHSO_3 solution (20 mL), followed by a water wash (10 mL) and drying (Na_2SO_4). The solvent was evaporated under reduced pressure to give the crude material which was further purified by column chromatography over silica gel using ethyl acetate:hexane (1:99) to give pure **2** as a white solid.

Yield: 0.62 g (82%).

Mp: 78-80 °C (lit¹¹, 79 °C).

¹H NMR (400 MHz, CDCl_3): δ 3.75 (s, 4H), 3.84-3.86 (m, 4H), 4.15-4.19 (m, 4H), 7.21 (s, 2H).

6.4.3 Synthesis of a 4,5-Dicyanobenzo-12-crown-4



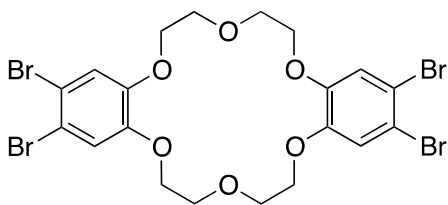
A solution of **2** (0.1 g, 0.2 mmol) in dry DMF (10 mL) was taken in a 50-mL three-necked, round-bottomed flask fitted with a condenser, a stir bar and a gas inlet. The system was degassed by bubbling with Ar for 15 min, and CuCN (0.11 g, 1.3 mmol) was added to the reaction mixture under argon atmosphere. The mixture was heated to 150 °C for 9 h with continuous stirring. After completion of the reaction, as judged by TLC, the reaction mixture was allowed to cool to room temperature, and TMEDA (2 mL) was added for complexation with Cu. Then conc. NH₄OH (28-30% NH₃ basis, 100 mL) was added to precipitate the product which was collected by vacuum filtration. The precipitate was redissolved in CH₂Cl₂ (25 mL), and the solution was dried (Na₂SO₄) and the solvent was evaporated to afford a pale yellow residue which was chromatographed over silica gel by eluting with ethyl acetate:hexane (1:5) to afford **3** as a white solid.

Yield: 0.051 g (72%).

Mp: 45-46 °C (lit,¹¹ Mp: 46 °C).

¹H NMR (400 MHz, CDCl₃): δ 3.75 (s, 4H), 3.84-3.86 (m, 4H), 4.17-4.25 (m, 4H), 7.28 (s, 2H).

6.4.4 Synthesis of a Dibromodibenzo-18-crown-6



5

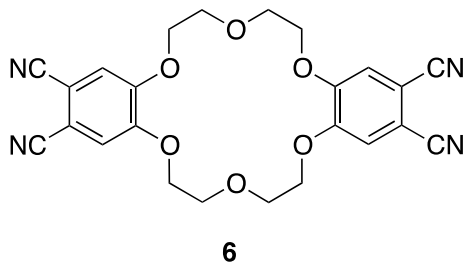
A solution of **4** (1 g, 2.7 mmol) in CH_2Cl_2 (30 mL) was taken in a 100-mL, two-necked, round-bottomed flask fitted with a 10-mL addition funnel and a stir bar. A catalytic amount of Fe and iodine were also added to the reaction mixture. A solution of bromine (0.62 mL, 12 mmol) in CH_2Cl_2 (20 mL) was added dropwise over a period of 4 h maintaining the temperature between 0-5 °C. The reaction mixture was then slowly allowed to attain room temperature. The mixture was stirred for an additional 30 min. After completion of the reaction, as judged by TLC, the reaction mixture was diluted with CH_2Cl_2 (100 mL) and washed with saturated aqueous NaHSO_3 solution (20 mL), followed by water (10 mL) and drying (Na_2SO_4). The solvent was evaporated under reduced pressure to give the crude material which was further purified by column chromatography over silica gel using ethyl acetate:hexane (1:30) to give pure **5** as a white solid.

Yield: 1.4 g (75%).

Mp: 132-135 °C (lit,¹ Mp: 133 °C).

¹H NMR (400 MHz, CDCl_3): δ 3.75 (s, 4H), 3.84-3.86 (m, 4H), 4.15-4.19 (m, 4H), 7.21 (s, 2H).

6.4.5 Synthesis of a Dicyanodibenzo-18-crown-6



A solution of **5** (0.2 g, 0.3 mmol) in dry DMF (10 mL) was taken in a 50-mL, three-necked round-bottomed flask fitted with a condenser, a stir bar and a gas inlet. The system was degassed for 15 min by bubbling with Ar. This was followed by the addition of CuCN (0.26 g, 2.9 mmol) to the reaction mixture under argon atmosphere and heating at 150 °C for 9 h with continuous stirring. After completion of the reaction, as judged by TLC, the reaction mixture was allowed to cool to room temperature, and TMEDA (5 mL) was added for complexation with Cu. Concentrated NH₄OH (28-30% NH₃ basis, 5 mL) was then added to precipitate the product which was collected by vacuum filtration. The precipitate was redissolved in CH₂Cl₂ (10 mL), and the solution was dried (Na₂SO₄) and the solvent was evaporated to afford a pale yellow residue which was chromatographed over silica gel by eluting with ethyl acetate:hexane (1:5) to afford **3** as a white solid.

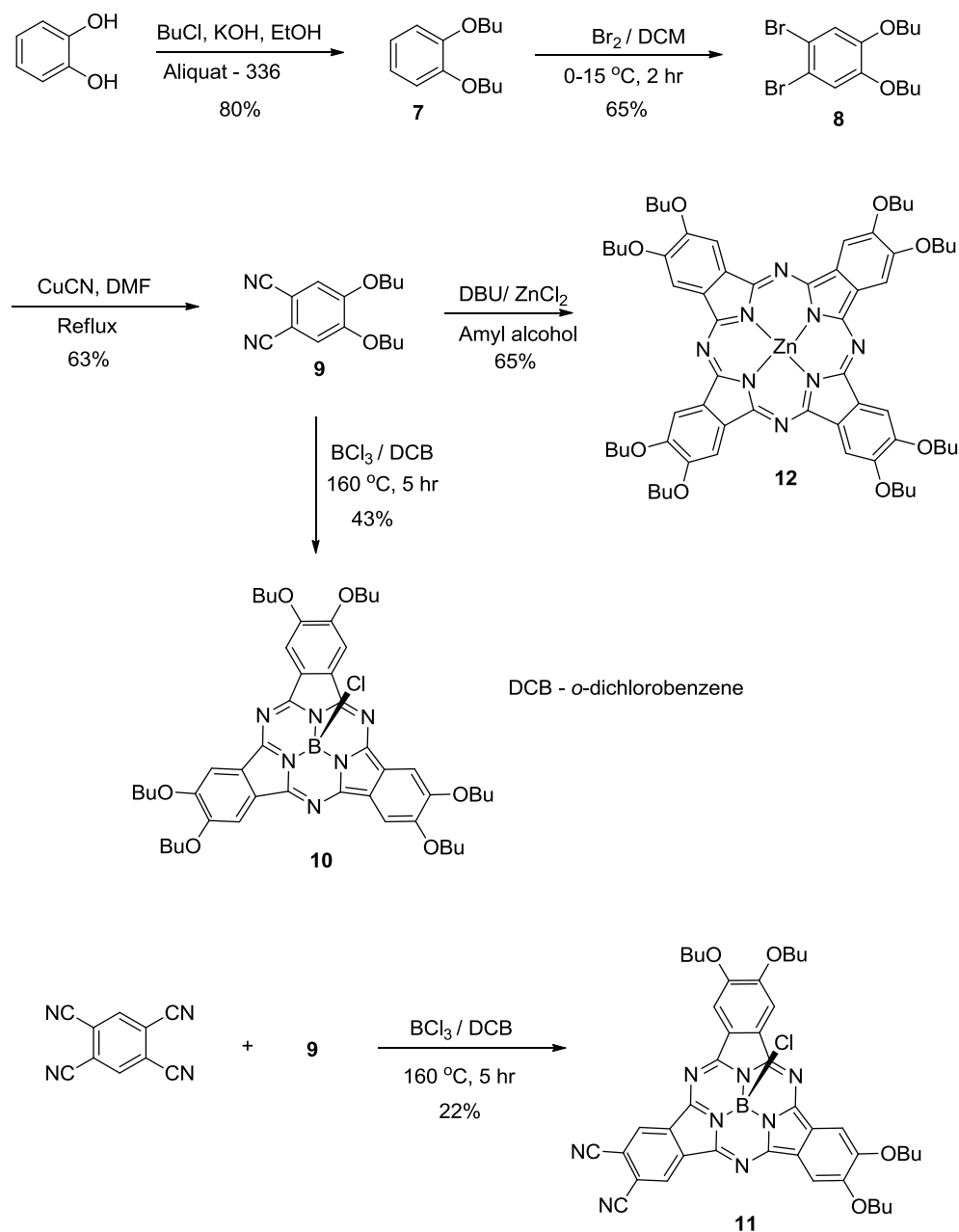
Yield: 0.093 g (69%).

Mp: 125-127 °C (lit,¹⁵ Mp: 127 °C).

¹H NMR (400 MHz, CDCl₃): δ 3.75 (s, 4H), 3.84-3.86 (m, 4H), 4.17-4.25 (m, 4H), 7.28 (s, 2H).

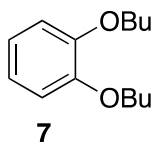
6.5 Synthesis of Phthalocyanine and Subphthalocyanine from Catechol

The general method of synthesis is illustrated in Scheme 6.3.



Scheme 6.3 Synthesis of SubPc and Pc.

6.5.1 Synthesis of 1,2-Dibutoxybenzene

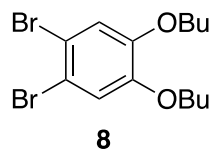


In a 100-mL, single-necked, round-bottomed flask fitted with a condenser and a stir bar was placed a mixture of catechol (0.5 g, 0.0045 mol), *n*-butyl chloride (2.49 g, 0.027 mol), KOH (1.38 g, 0.0247 mol), ethanol (5 mL) and an aliquat of trioctylmethylammonium chloride, (aliquat-336) (0.1 mL). The mixture was stirred for 5 min. The resulting pale yellow mixture was degassed with Ar for 15 min. The reaction mixture was then refluxed at 85 °C for 72 hr. Total consumption of the starting material was observed *via* TLC after 72 hr. The viscous dark-colored solution obtained was then cooled to RT, and the solid material was filtered out through a pad of celite. The filtrate was diluted with CH₂Cl₂ (2 x 50 mL) and washed with brine (2 x 25 mL), dried (Na₂SO₄), filtered and concentrated to get the crude material. Flash chromatography of the crude material using ethyl acetate:hexane (1:20) afforded **7** as a clear pale yellow liquid.

Yield: 0.8 g (80%) (lit,¹¹ 84%).

¹H NMR (400 MHz, CDCl₃): δ 6.88 (s, 4H), 4.02-3.98 (t, J = 4.4 Hz, 4H), 1.86-1.78 (m, 4H), 1.58-1.45 (m, 4H), 1.02-0.98 (t, J = 4.8 Hz, 6H).

6.5.2 Synthesis of 1,2-dibromo-4,5-dibutoxybenzene



In a 100-mL, two-necked, round-bottomed flask equipped with an addition funnel, and a magnetic stirrer was placed a solution of 1,2 dibutoxybenzene (0.2 g, 0.89 mmol) in CH_2Cl_2 (5 mL). The resulting pale yellow solution was cooled to 0 °C in an ice bath. A solution of bromine (0.102 mL, 0.0019 mol) in CH_2Cl_2 (5 mL) was added dropwise with continuous stirring, maintaining the temperature at 0-5 °C. The orange-colored solution was stirred at 0 °C for 2 h. After the complete consumption of the starting material, the reaction mixture was poured into a beaker containing a saturated, aqueous solution of NaHSO_3 (10 mL) to destroy the excess bromine. The organic layer was separated, washed with saturated, aqueous bicarbonate solution (10 mL), washed with brine (10 mL), dried (Na_2SO_4), filtered and evaporated under reduced pressure to give the crude material. Purification was effected by column chromatography using ethyl acetate:hexane (1:10). Pure dibromo compound **8** was obtained as a pale yellow oil which gradually turned into a white solid.

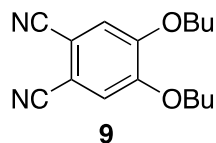
Yield: 0.21 g (65%).

Mp: 28-29 °C (lit,¹¹ **Mp:** 28 °C).

^1H NMR (400 MHz, CDCl_3): δ 7.05 (s, 2H), 3.98-3.92 (t, $J = 4.4$ Hz, 4H), 1.84-1.76 (m, 4H), 1.56-1.42 (m, 4H) 1.01-0.96 (t, $J = 5.2$ Hz, 6H).

^{13}C NMR (100 MHz, CDCl_3): δ 148.3, 146.0, 144.1, 141.4, 119.3, 114.8.

6.5.3 Synthesis of 4,5-Dibutoxyphthalonitrile



A solution of **8** (7.06 g, 18.57 mmol) in DMF (200 mL) was degassed in a 100-mL, two-necked, round-bottomed flask equipped with a condenser and a magnetic stir bar. Then Copper (I) cyanide (8.3 g, 92.86 mmol) was added to the solution, and the mixture was further degassed by purging Ar. The reaction mixture was heated to reflux for 12 h, and progress of the reaction was monitored by TLC. After cooling to RT, TMEDA (20 mL) was added for complexation with Cu. Then conc. NH_4OH (100 mL) was added to precipitate the product which was collected by vacuum filtration. The precipitate was redissolved in CH_2Cl_2 (200 mL), dried (Na_2SO_4) and evaporated to dryness to afford a pale yellow residue which was chromatographed by eluting with ethyl acetate:hexane (1:5) to afford **9** as a white solid.

Yield: 3.16 g (63%).

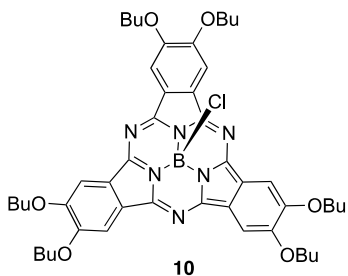
Mp: 138-139 °C (lit,¹¹ Mp: 137 °C).

IR (CH_2Cl_2): 3058, 2930, 1780, 1743, 1486, 1265, 116, 967, 779, 739, 698.

^1H NMR (400 MHz, CDCl_3): δ 7.13 (s, 2H), 4.07 (t, $J = 4.4$ Hz, 4H), 1.85 (m, 4H), 1.50 (m, 4H) 0.98 (t, $J = 5.2$ Hz, 6H).

^{13}C NMR (100 MHz, CDCl_3): δ 148.3, 146.0, 144.1, 141.4, 119.3, 114.8;

6.5.4 Synthesis of SubPc-OBu



A solution of **9** (0.819 g, 3.0 mmol) in *o*-dichlorobenzene (20 mL) was degassed for 15 min with Ar in a 100-mL, two-necked, round-bottomed flask fitted with a condenser, a gas inlet and a stir bar. Boron trichloride (1 mL, 1 M solution in *p*-xylene) was then added dropwise, maintaining the temperature between 25-30 °C. The reaction mixture was heated to reflux at 160 °C for 5 h. The solution slowly turned from a pale yellow to a deep red colored solution upon refluxing. After cooling to room temperature, the mixture was passed through a plug of silica gel, followed by washing the plug with CH₂Cl₂ to remove impurities and then with THF to extract the product. The organic layer was dried, (Na₂SO₄) and evaporated to dryness. Column purification of the crude product using ethyl acetate:hexane (1:1) afforded **10** as a pink solid.

Yield: 1.7 g (43%). **Mp:** > 300 °C.

¹H NMR (400 MHz, CDCl₃): δ 8.20 (s, 4H), 4.29-4.40 (m, 10H), 1.96-2.01 (q, J = 7.4 Hz, 8H), 1.51-1.62 (q, J = 7.6 Hz, 8H), 1.06-1.08 (q, J = 7.6 Hz, 20H).

¹³C NMR (100 MHz, CDCl₃): δ 148.2, 146.0, 145.6, 145.4, 144.1, 141.4, 119.3, 114.8.

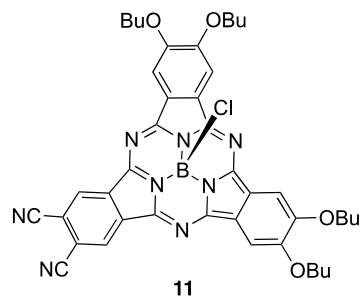
MS (MALDI-TOF) *m/z* for C₄₈H₆₀BClN₆O₄: Calcd: 862.4356; Found: 862.4903.

ELEMENTAL ANAL.: C₄₈H₆₀BClN₆O₄·0.5 H₂O·0.2 C₆H₁₄:

Calcd: C, 66.43; H, 7.23; N, 9.45.

Found: C, 65.62; H, 7.39; N, 7.85.

6.5.5 Synthesis of SubPc-(OBu)₄ (CN)₂



Dry compound **9** (1.22 g, 4 mmol) and tetracyanobenzene (0.1 g, 0.05 mmol) were placed in a 100-mL, two-necked, round-bottomed flask fitted with a condenser gas inlet and a stir bar. The system was flushed with argon for ~10 min to remove air and moisture. Boron trichloride (2 mL, 1 M solution in *p*-xylene) was then added dropwise maintaining the temperature between 25-30 °C. The mixture was stirred at 140 °C for 7 hr. A change of color was observed from pale yellow, to pink to a final thick, reddish-blue solution. After cooling, the solvent was evaporated to give a dark blue solid which was chromatographed by eluting with ethyl acetate:hexane (1:10) to afford **11** as reddish blue solid.

Yield: 1.13 g (22%). **Mp:** > 250 °C.

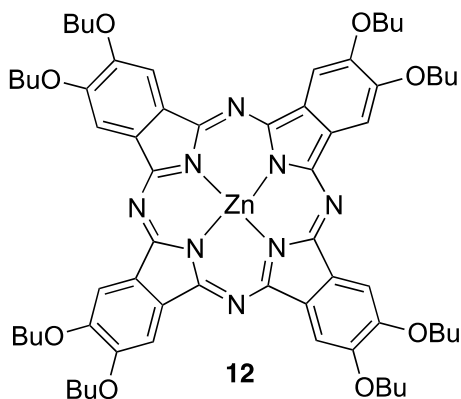
¹H NMR (400 MHz, CDCl₃): δ 9.25 (s, 2H), 8.20 (s, 4H), 4.29-4.40 (m, 10H), 1.96-2.01 (m, 8H), 1.51-1.62 (m, 8H), 1.06-1.08 (m, 20H).

¹³C NMR (100 MHz, CDCl₃): δ 155.2, 153.4, 152.7, 151.1, 143.8, 129.1, 128.7, 126.5, 124.6, 116.1, 112.3, 105.0, 104.6, 69.4, 31.0, 31.0, 19.2, 13.9.

MS (MALDI-TOF) *m/z* for C₆₈H₂₇BF₁₂N₁₀O₂Zn: Calcd: 768.3111; Found: 768.4312.

Compound is unstable. MALDI-TOF was performed. Hexanes and water could not be removed *via* vacuum pressure for 16 h or by repeated washing with pentane.

6.5.6 Synthesis of Pc-(OBu)₈



The starting material **9** (0.1 g, 0.3 mmol), DBU (0.1 g, 0.7 mmol), ZnCl₂ (0.002 g, 0.018 mmol) and amyl alcohol (5 mL) were all placed in a 50-mL, two-necked, round-bottomed flask fitted with a condenser and a magnetic stir bar. The reaction mixture was heated to reflux for 138 °C for 6 h. Complete consumption of the starting material was observed *via* TLC, and the reaction mixture was allowed to cool to room temperature. Water (5 mL) was added to the reaction mixture, and the product was extracted with ethyl acetate (50 mL), dried (Na₂SO₄) and evaporated to dryness to give **12** as a green solid.

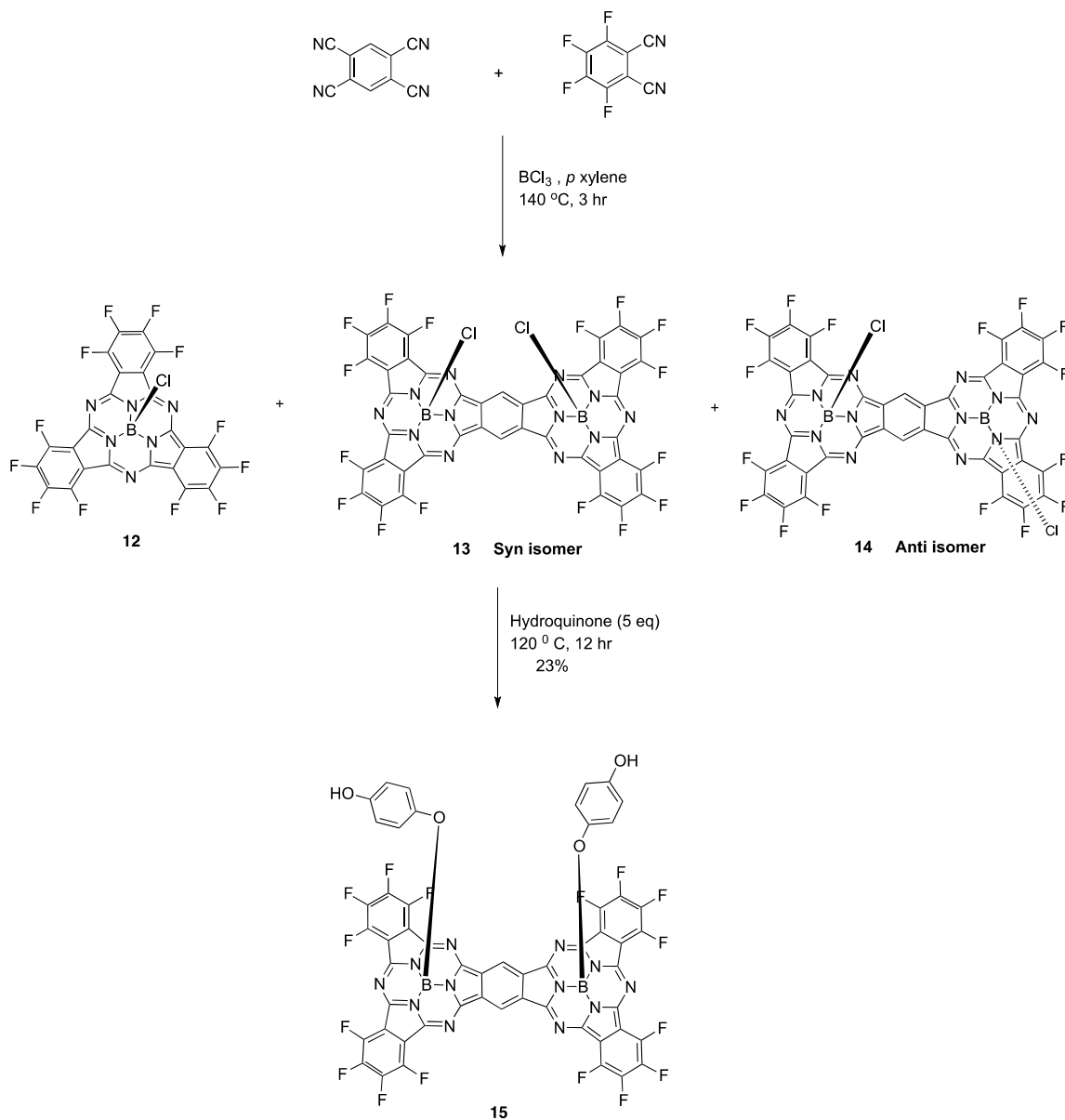
Yield: 75 mg (65%).

Mp: > 300 °C (lit,¹¹ **Mp:** >250 °C)

¹H NMR (400 MHz, CDCl₃): δ 9.25 (s, 2H), 8.20 (s, 4H), 4.29-4.40 (m, 10H), 1.96-2.01 (q, 8H), 1.51-1.62 (q, 8H), 1.06-1.08 (q, 20H).

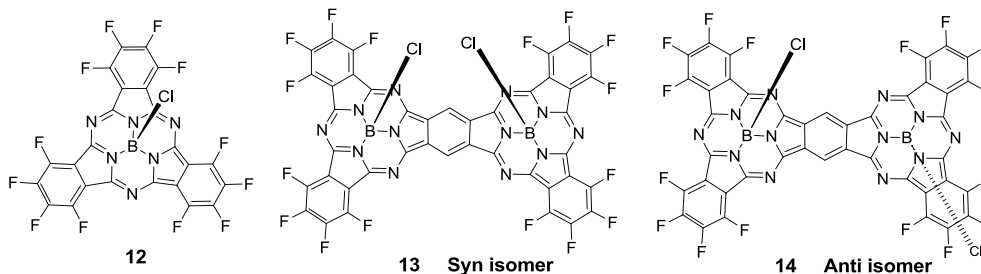
6.6 Synthesis of Subphthalocyanine fused dimers

The synthesis of a subphthalocyanine fused dimer is depicted in Scheme 6.4



Scheme 6.4 Synthesis of SubPc Fused Dimers.

6.6.1 Synthesis of SubPc fused dimers **12**, **13**, and **14**



In a pre-dried, 100-mL, three-necked, round-bottomed flask fitted with a condenser, was placed dry samples of tetracyanobenzene (0.05 g, 0.28 mmol) and tetrafluorophthalonitrile (0.561 g, 2.81 mmol). After flushing the system with Ar for 10 min, BCl₃ (5.0 mL, 1 M solution p-xylene) was added dropwise. The reaction mixture was refluxed for 3 h, and, after allowing it to cool to room temperature, the system was flushed with argon. The resulting dark purple slurry was evaporated to dryness under vacuum and subjected to column chromatography on silica gel using ethyl acetate:hexane (1:20). Three different products **12**, **13**, and **14** formed which were observed distinctly on the column as purple, blue and blue bands, respectively.

SubPc (F)₁₂ (12)

Yield: 0.26 g (43%). **Mp:** >300 °C (lit,² **Mp:** >250 °C).

SubPc Fused dimer - Syn (13)

Yield: 0.027 g (9%). **Mp:** >300 °C (lit,² **Mp:** >250 °C).

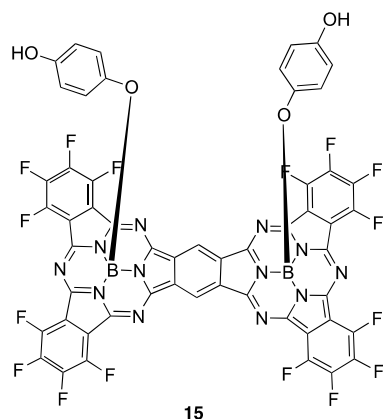
¹H NMR (400 MHz, CDCl₃): δ 10.48, (s, 2H)

SubPc Fused dimer -anti (14)

Yield: 0.033 g (13%). **Mp:** >300 °C (lit,² **Mp:** >250 °C).

¹H NMR (400 MHz, CDCl₃): δ 10.46 (s, 2H).

6.6.2 Synthesis of SubPc dimer – Hydroquinone (15)



A mixture of **13** (0.05 g, 0.01 mmol) and *p*-hydroquinone (0.045 g, 0.05 mmol) was refluxed in dry toluene (2 mL) in a 50-mL, single-necked, round-bottomed flask fitted with a condenser and magnetic stirrer for 12 hr. The reaction mixture was allowed to cool to room temperature, the solvent was evaporated and the crude material was purified by column chromatography over silica gel using ethyl acetate: hexane (1:5).

Yield: 15 mg (23%).

Mp: >300 °C.

¹H NMR (400 MHz, CDCl₃): δ 6.6 (d, J = 4H), 5.2 (d, J = 4H).

6.7 References

1. Kobayashi, N. *Chem. Commun.* **1991**, 1203-1205.
2. Claessens, C. G.; Torres, T. *Angew. Chem.* **2002**, 41, 2561-1564.
3. (a) Yamaguchi, Y. J. *Chem. Phys.* **2004**, 120, 7963-7970. (b) Kawase, T.; Tanaka, K.; Shinono, N.; Y.; Oda, M. *Angew. Chem.* **2004**, 43, 1722-1724.
4. Luo, Q.; Cheng, S.; Tian, H. *Tetrahedron Lett.* **2004**, 45, 7737-7740.
5. Iglesias, R.S.; Claessens, C. G.; Torres, T.; Herranz, M. A.; Ferro, V. R. *J. Org. Chem.* **2007**, 72, 2967-2977.
6. Pederson, C. J. *Angew. Chem.* **1988**, 27, 1021-1024
7. Viout, P.; Lehn, J. -M. *Macrocyclic Chemistry*, 1993, VCH, New York.
8. Fyfe, M. C. T.; Stoddart, J. F. *Adv. Supramol. Chem.* **1999**, 5, 1-6
9. Gokel, G. W. *Chem. Soc. Rev.* **1992**, 21, 39-45
10. Gibson, H. W. *Macromol. Chem. Phys.* **2000**, 201, 815.
11. Gao, Y.; Ma, P.; Chen, Y.; Zhang, Y.; Bian, Y.; Li, X.; Jiang, J.; Ma, C. *Inorg. Chem.* **2009**, 48, 45-54.
12. Laidler, D. A.; Stoddart, J. F. *In the Chemistry of Ethers, Crown Ethers*, Wiley, 1980, 1-58, Chichester.
13. Knops, P.; Sendhoff, N.; Mekelburger, H.-B.; Vogtle, F. *Top. Curr. Chem.* **1992**, 161, 3-7
14. Ostrowicki, A.; Koeppe, E.; Vogtle, F. *Top. Curr. Chem.* **1992**, 161, 39-43
15. Bogaschenko, T.; Basok, S.; Kulygina, C.; Lyapunov, A.; Lukyanenko, N. *Synthesis.* **2002**, 2266-2270.

6.8 Appendices

Figure 6.4 ^1H NMR Spectrum of **10**

Figure 6.5 ^{13}C NMR Spectrum of **10**

Figure 6.6 Mass Spectrum of **10**

Figure 6.7 ^1H NMR Spectrum of **11**

Figure 6.5 ^{13}C NMR Spectrum of **10**

Figure 6.8 Mass Spectrum of **11**

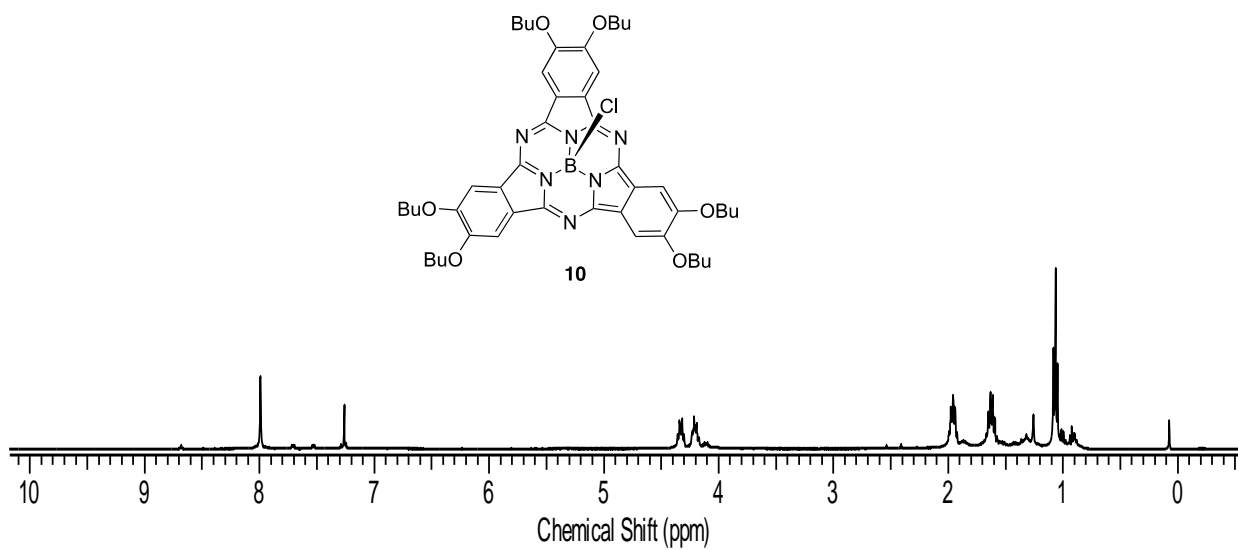


Figure 6.4 ^1H NMR Spectrum of **10**.

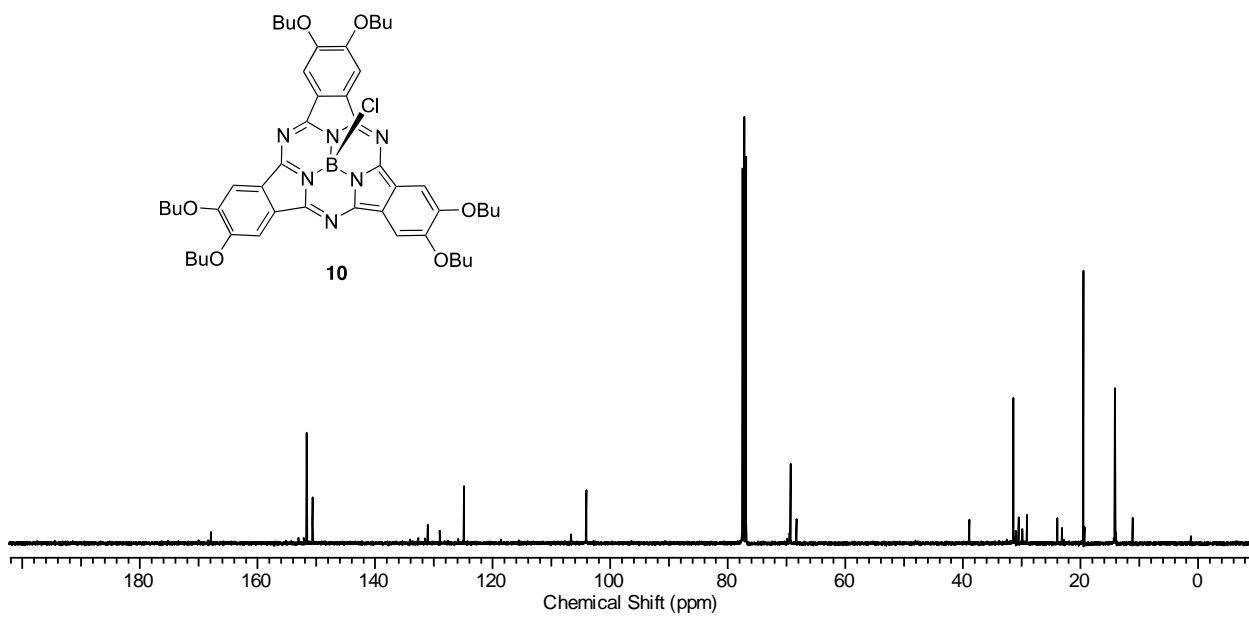


Figure 6.5 ^{13}C NMR Spectrum of **10**.

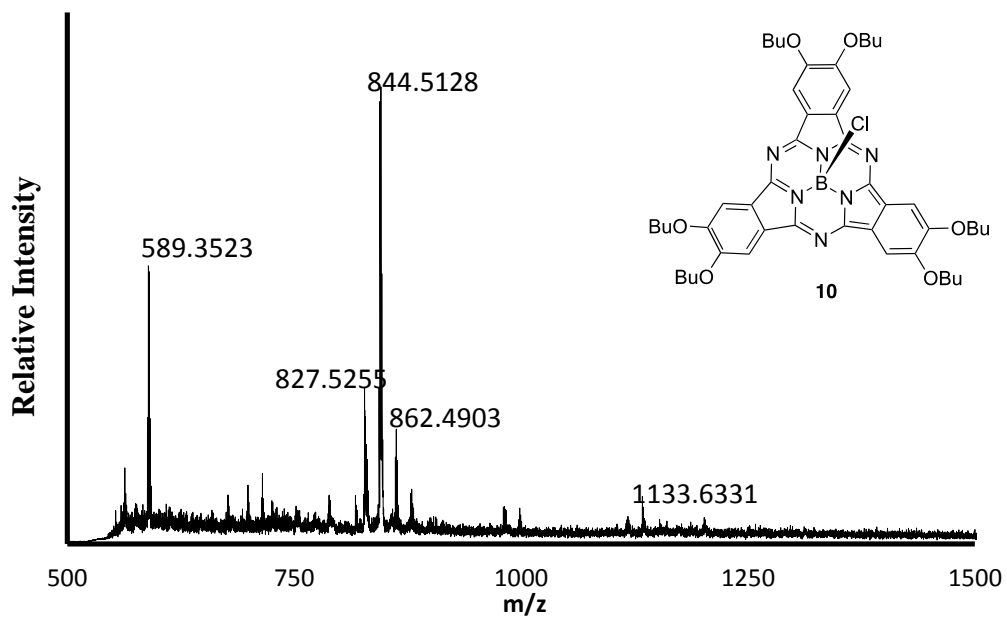


Figure 6.6 Mass Spectrum of **10**.

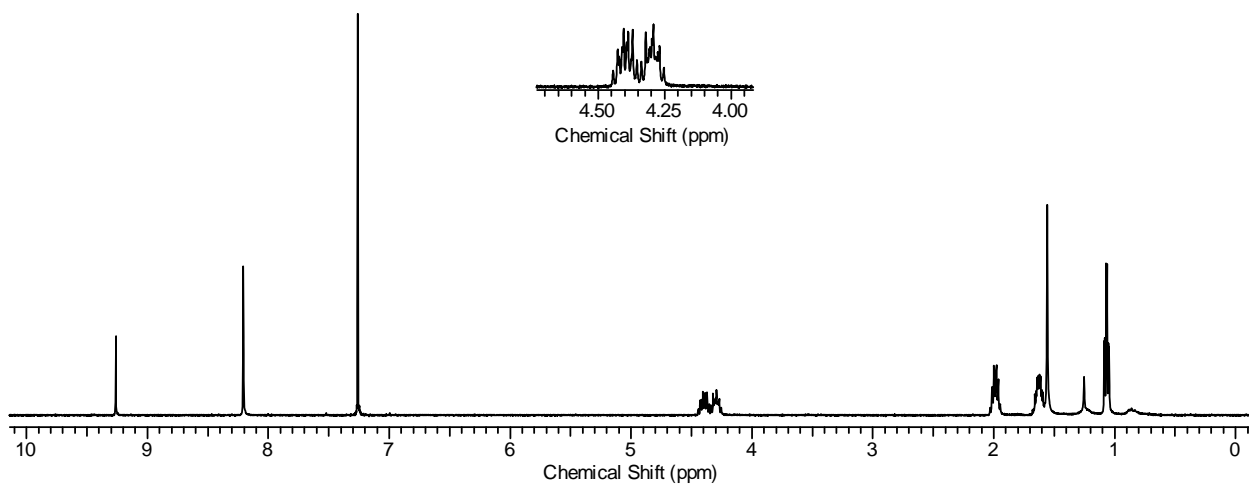


Figure 6.7 ^1H NMR Spectrum of **11**.

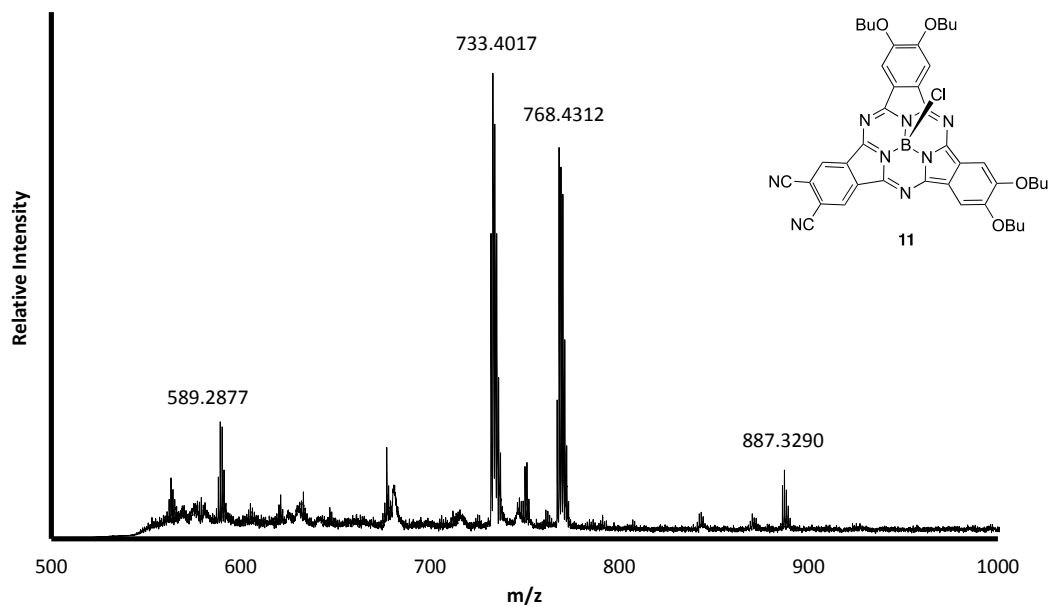


Figure 6.8 Mass Spectrum of **11**.

CHAPTER VII

RESULTS AND DISCUSSION

SYNTHESIS OF STRAINED PORPHYRINOPHANES AS NOVEL SYSTEMS FOR REACTIVITY

7.1 Introduction

Porphyrins have a rich and extensive history in chemistry due to their impressive array of properties.¹ A distinctly unique aspect of the aromatic porphyrin system is the high degree of conformational flexibility that results in six symmetrical modes of deformation.² This intrinsic property is speculated as the mechanism in which the same porphyrin cofactors are able to do chemically diverse reactions in biological systems. Non-planar distortion in porphyrins induces a significant effect on the properties as it alters the oxidation potentials, the basicity of the nitrogen atoms, the axial ligand binding affinity, and the net dipole.³ The synthesis and properties of flexible, covalently linked ‘face-to-face’ stacked porphyrins have been explored as systems for bimetallic cooperativity in reduction catalysis. However, with flexible spacers, true co-facial arrangement was not realized.⁴ In order to achieve optimum π - π overlap, stacked porphyrins undergo a lateral shift of about 5 Å. As a means to offset this phenomena, ‘pacman’ porphyrins⁵ were extensively studied. Although their unique geometry allow them to bind small molecules, and subsequently perform proton coupled electron transfer

(PCET) in acidic media, the porphyrins in these systems still undergo cofacial slipping due to π - π stacking.⁶

7.2 Specific aims and Significance of the Research

The present research employs non-self-complementary H-bonding as a means to assemble and impart structural stabilization to novel, highly deformed porphyrinophanes (cofacial porphyrins; Figure 7.1). The particular aims of the research were to develop a library of non-slipped cofacially stacked porphyrins with varied linker lengths and types that could lead to distinct modes of deformation. The distortion caused by H-bonding was also expected to affect the localized environment inside the diporphyrinophanes. The size of the cavity available for binding small molecules is determined by the length of the covalent linker.⁴ A modest arrangement could be envisioned between a pyridyl group and a corresponding carboxylic acid porphyrin (Figure 7.1).⁷ Functionalized dipyrromethane condensed with 3-pyridine carbaldehyde and methyl 3-formylbenzoate to afford the corresponding H-bond acceptor and H-bond donor moieties, respectively.

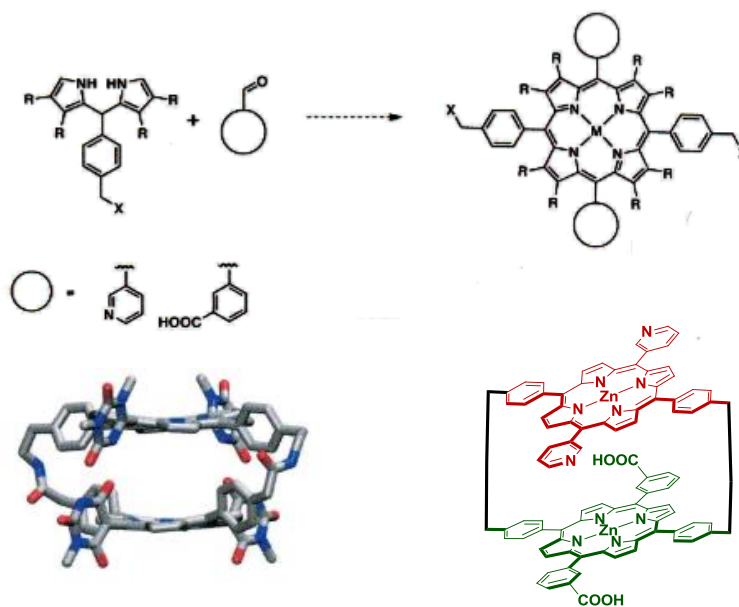


Figure 7.1 Representation of the Synthesis of the Deformed Porphyrinophanes.

Covalent linkage of the H-bond donor and acceptor moieties to form the expected co-facial diporphyrinophanes can be constructed by ring closing metathesis (RCM) due to its ease of application and versatile synthesis.^{8,9} As stated previously, many of the non-H-bonded diporphyrinophanes have a metal-metal slipping distance of 5 Å, as demonstrated by X-ray crystallography.⁴ The stabilization energy gained by π - π co-facial stacking depends on the number of incorporated H-bonding moieties. As suggested by the molecular modeling (Figure 7.2), the extent of deformation is dependent upon both the H-bonding moiety employed and the type/length of the linker. For the larger cavities, it was of interest to investigate Diels-Alder reactions within the enclosed space. Diporphyrinophanes with smaller cavities can be explored as systems for binding small molecules e.g., dinitrogen, dioxygen, dihydrogen, and carbon monoxide.

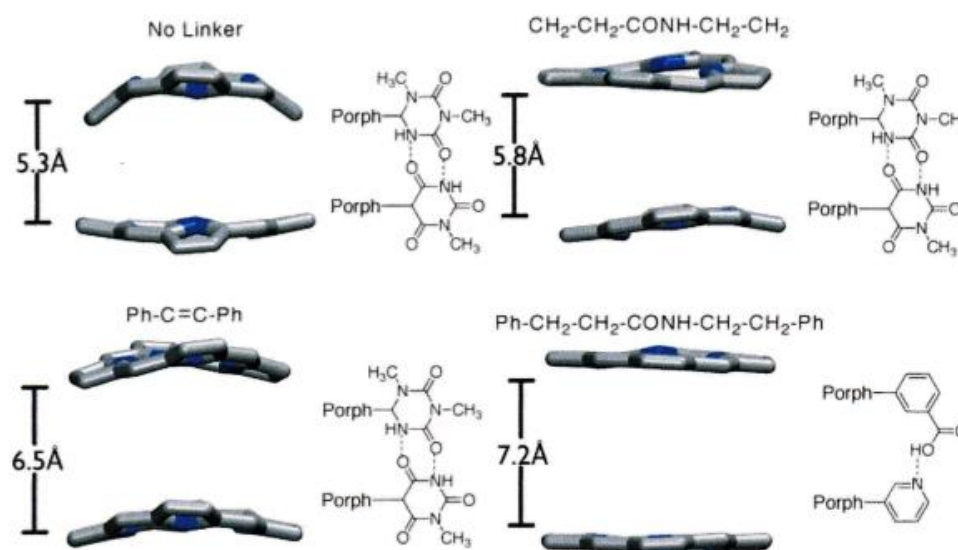


Figure 7.2 A Representative Sample of Deformation of the Free-Base Porphyrin

7.3 Applications

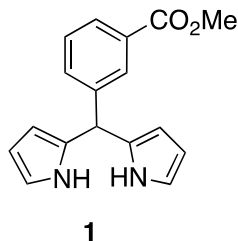
Exploitation of this novel methodology allows one to control the global deformation of the porphyrin and its subsequent properties giving rise to novel media for understanding metal-porphyrin small molecule interactions. The special diporphyrinophanes described in this study have a number of applications. Our focus is primarily on the exploitation of such systems as mimics for biologically relevant processes.^{10,11} Particularly, as a method to understand how the extent of controlled deformation affects the ability to bind small molecules for subsequent reactivity studies, such as proton coupled electron transfer (PCET).^{12,13}

7.4 Experimental

Melting points (mp) were determined using a Stuart SMP10 instrument. Both ¹H and ¹³C NMR spectra were acquired in CDCl₃ using a Varian Inova 400 MHz/300 MHz spectrometers. Chemical shifts (δ) are expressed in ppm relative to residual chloroform (¹H: 7.26 ppm, ¹³C: 77.0 ppm) or to TMS. Column chromatography was carried out on silica gel (Sorbent Technologies, 230-400 mesh), and TLC was performed with polyester sheets precoated with silica gel (Sorbent Technologies). Compounds, methyl 3-formylbenzoate, benzaldehyde, (Sigma-Aldrich), *p*-aminobenzyl alcohol (Aldrich), trifluoroacetic acid (Alfa Aesar), *p*-hydroxybenzaldehyde (Alfa Aesar), 3-chloro-3-methyl-1-butyne (Sigma-Aldrich), 4-bromobenzaldehyde (Alfa Aesar) trimethylsilyl acetylene (Fisher) were purchased from commercial suppliers and used as received unless otherwise indicated.

7.5 Synthesis of Model Porphyrins

7.5.1 Synthesis of 5-(3-Methoxycarbonylphenyl)dipyrromethane (**1**)

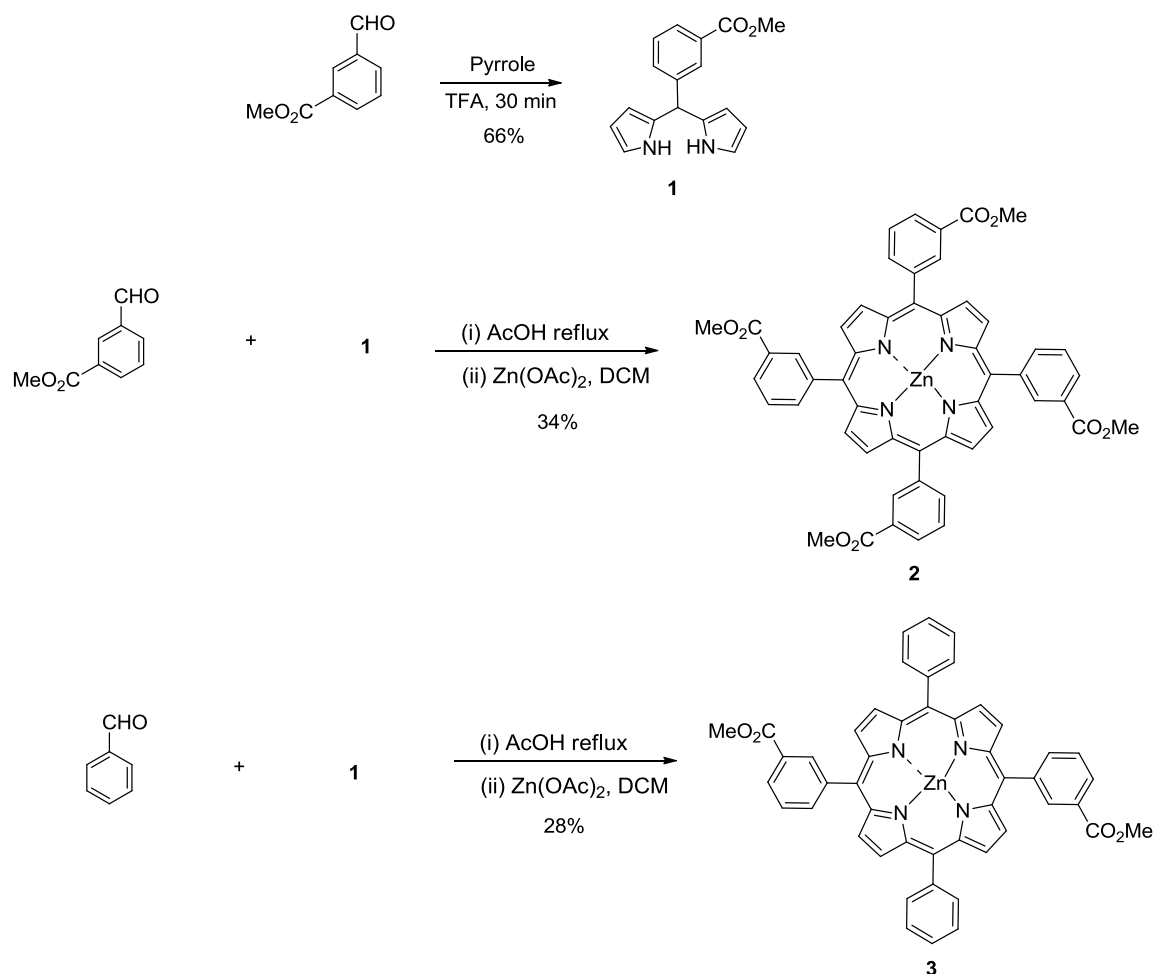


A solution of methyl 3-formylbenzoate (0.5 g, 0.003 mol) and freshly distilled pyrrole (8.4 mL, 0.12 mol) was placed in a 250-mL, two-necked, round-bottomed flask fitted with a magnetic stirrer and a gas inlet. The solution was degassed by bubbling argon through the solution for 15 min at room temperature. Then TFA (23 μ L, 0.0003 mol) was added, and the resulting mixture was stirred for 20 min at which point no starting material was seen on TLC analysis. The crude material was diluted with CH_2Cl_2 (30 mL) and washed with 0.1 M NaOH (25 mL), followed by a brine wash and drying (Na_2SO_4). The solvent and the unreacted pyrrole were removed under vacuum. The crude material was flash chromatographed using ethyl acetate:hexane (1:5) over silica gel to give the pure dipyrromethane **1b**.

Yield: 0.56 g (66%).

Mp: 125-127 $^\circ\text{C}$ (lit²⁰ 124-127 $^\circ\text{C}$).

^1H NMR (300 MHz, $\text{DMSO}-d_6$): δ 3.81 (s, 3H); 5.53 (s, 1H); 5.67 (s, 2H); 5.91 (m, 2H); 6.64 (s, 2H); 7.42 (m, 2H); 7.80 (m, 2H), 10.61 (br s, 2H).



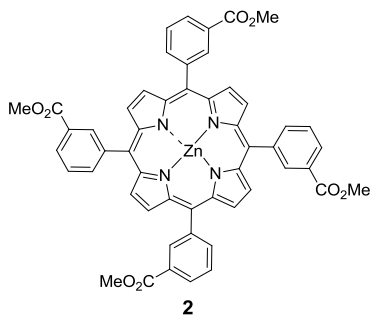
Scheme 7.1 Synthesis of Model Porphyrins.

7.5.2 General Procedure for the Synthesis of Porphyrins

In a single-necked, round-bottomed flask fitted with a condenser and magnetic stirrer was placed dipyrromethane **1** (1.0 equiv) and the corresponding aldehyde (1.0 equiv). Then acetic acid (20 volumes) was added to the reaction mixture which was refluxed with continuous stirring at 120 °C for 4 h. The reaction mixture became a thick black suspension which was allowed to cool to room temperature. The solvent was evaporated, and the residue was dissolved in ethyl acetate (20 mL). The ethyl acetate solution was treated with 1 M NaOH, followed by a brine wash. The organic layer was

separated, dried (Na_2SO_4) and evaporated to dryness to yield a black solid. The product was redissolved in CH_2Cl_2 (20 mL), the solution was passed through a pad of silica to remove most of the impurities. Evaporation of the solvent under vacuum afforded the base porphyrin which was used directly in the metallation by zinc. Metallation of the porphyrin by zinc occurred with greater ease when a solution of the product in CH_2Cl_2 :MeOH mixture (1:1) was stirred with $\text{Zn}(\text{OAc})_2 \cdot 2\text{H}_2\text{O}$ for 12 h. The solvent was evaporated, and the residue was extracted with ethyl acetate (2 x 20 mL). The resulting solution was washed with brine, dried (Na_2SO_4), and concentrated to provide a dark purple solid which was then flash chromatographed using ethyl acetate:hexane (1:8) to afford a pure compound.

7.5.3 Synthesis of tetra-*meso*-(3-Methoxycarbonylphenyl)porphyrinato-zinc (2)



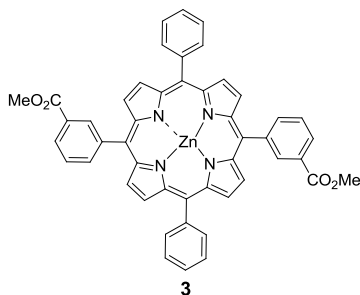
Compound **1** (0.1 g, 0.35 mmol) and methyl 3-formylbenzoate (0.057 g, 0.35 mol) were treated with acetic acid (20 mL) according to the general procedure. Metallation of the crude porphyrin with $\text{Zn}(\text{OAc})_2 \cdot 2\text{H}_2\text{O}$ (0.1 g, 0.45 mmol) in CH_2Cl_2 :MeOH (1:1 mixture, 4 mL) afforded the zinc porphyrin **2**.¹⁵

Yield: 0.11g (34%).

Mp: >300 °C.

^1H NMR (400 MHz CDCl_3): δ 3.96 (s, 12H), 7.84 (t, J = 10.8 Hz, 4H), 8.40 (d, J = 9.6 Hz, 4H), 8.46 (d, J = 10.8 Hz, 2H), 8.89 (br s, 12H).

7.5.4 5,15-Bis(3-Methoxycarbonylphenyl)-10,20-bis(4-phenyl)porphinatozinc(II)



Compound **1** (0.1 g, 0.00035 mol) and benzaldehyde (0.037 g, 0.00035 mol) were treated with acetic acid (20 mL) according to the general procedure A. Metallation of the crude porphyrin with $\text{Zn}(\text{OAc})_2 \cdot 2\text{H}_2\text{O}$ (0.1 g, 0.45 mol) in CH_2Cl_2 :MeOH (1:1 mixture, 4 mL) afforded the zinc porphyrin **3**.

Yield: 79 mg (28%).

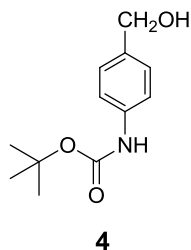
Mp: >300 °C.

^1H NMR (400 MHz CDCl_3): δ 3.96 (s, 12H), 7.84 (t, $J = 10.4$ Hz, 2H), 7.75 (m, 6H), 8.21 (d, $J = 7.6$ Hz, 4H), 8.42 (d, $J = 10$ Hz, $J = 10$ Hz, 2H), 8.49 (d, 2H), 8.86 (d, 4H), 8.89 (s, 2H), 8.96 (d, 4H).

7.6 Amine substituted porphyrins

The synthesis of the amine substituted porphyrins is depicted in Scheme 7.2.

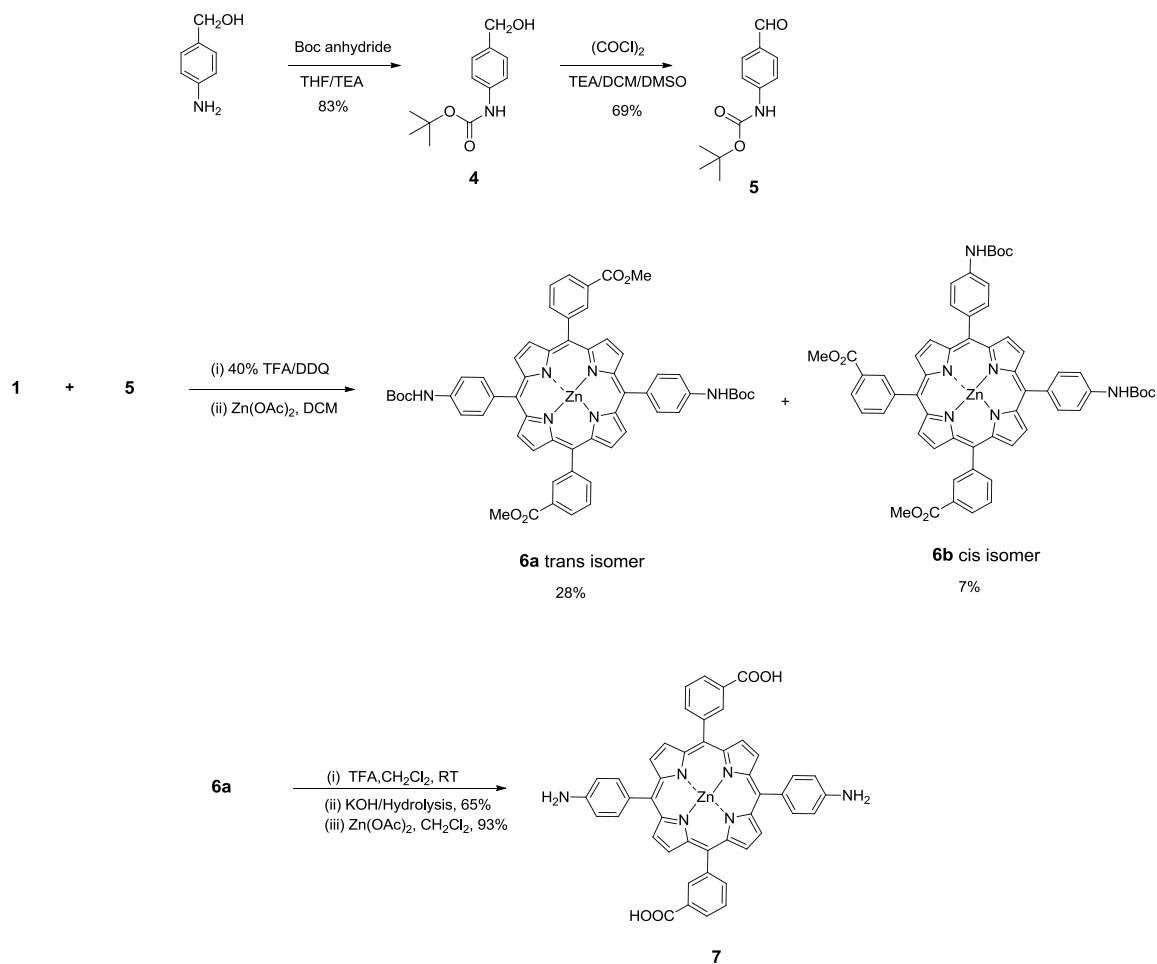
7.6.1 Synthesis of 4-[N-(tert-Butyloxycarbonyl)amino]benzyl alcohol (**4**)



To a solution of *p*-aminobenzyl alcohol (3 g, 0.24 mol) in THF (50 mL) in a two-necked, 100-mL, round-bottomed flask fitted with a magnetic stirrer, was added triethylamine (6.7 mL, 0.0487 mol) and Boc anhydride (7.97 g, 0.0365 mol). The solution was stirred at room temperature for 24 h, and the reaction was monitored by TLC. Then water (35 mL) was added to the reaction mixture, and the product was extracted with ethyl acetate (2 x 30 mL), followed by a brine wash. The organic layer was separated, dried (Na₂SO₄), filtered and evaporated to give **4** as a pale yellow liquid.

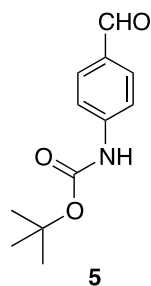
Yield: 4.5 g (83%).

¹H NMR (400 MHz, CDCl₃): δ 1.88 (s, 6H), 2.76 (s, 1H), 7.21 (d, 2H), 7.77 (d, 2H), 9.84 (s, 1H).



Scheme 7.2 Synthesis of Amine Substituted Porphyrins.

7.6.2 Synthesis of 4-[N-(tert-Butyloxycarbonyl)amino]benzaldehyde (5)



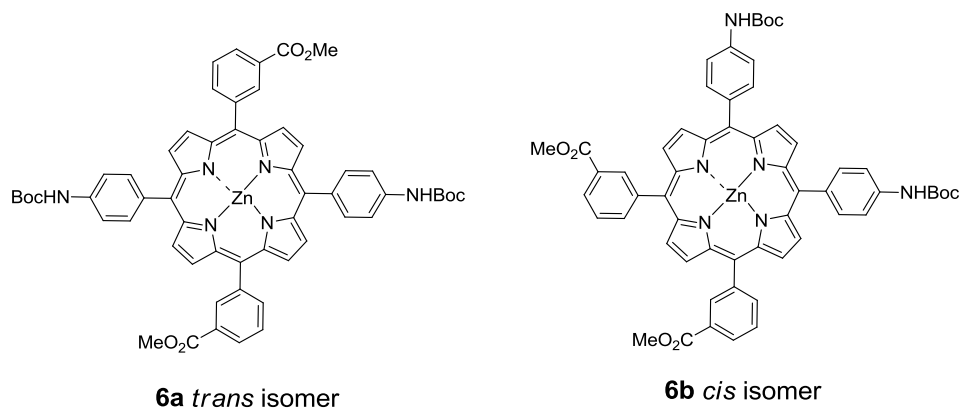
In a 100-mL, two-necked, round-bottomed flask fitted with a rubber septum and an addition funnel was placed a mixture of CH_2Cl_2 (1.15 mL) and DMSO (0.54 mL, 7.73 mmol). The solution was cooled to $-78\text{ }^\circ\text{C}$ using a dry ice-acetone bath. Oxalyl chloride

(0.71 mL, 8.2 mmol) was added dropwise, and the solution was stirred for 30 min maintaining the temperature at -78 °C. Compound **4** (1.15 g, 5.1 mmol) was dissolved in CH₂Cl₂ (3 mL) added dropwise to the reaction mixture which was stirred at -78 °C for 30 min. TEA (3.59 mL, 25.7 mmol) was then added, and the pale yellow solution obtained was stirred for 15 min. The product was extracted in ethyl acetate (2 x 10 mL), and the organic layer was separated, washed with brine, dried (Na₂SO₄), filtered and evaporated under reduced pressure to give **5** as a white solid.

Yield: 0.98 g (69%). **Mp:** 136-138 °C (lit,¹⁶ **Mp:** 138 °C).

¹H NMR (400 MHz, CDCl₃): δ 1.88 (s, 6H), 2.76 (s, 1H), 7.21 (d, 2H), 7.77 (d, 2H), 9.84 (s, 1H).

7.6.3 Synthesis of *cis*- and *trans*- 5,15-Bis[(4-*tert*-Butoxycarbonylamino)phenyl]-10,20-bis(3-methoxycarbonylphenyl)porphinatozinc(II) (**6a**, **6b**)



A sample of **1** (0.5 g, 1.7 mmol) and aldehyde **5** (0.39 g, 1.78 mmol) were dissolved in CH₂Cl₂ (190 mL) in a 100-mL, single-necked, round-bottomed flask fitted with a magnetic stirrer. Then TFA (0.236 mL, 3.18 mmol) was added, and the reaction mixture was stirred at room temperature for 30 min. This was followed by the addition

of dichlorodicyanobenzoquinone (DDQ, 0.606 g, 0.00267 mol), and the reaction mixture was stirred at room temperature for 2 h. After completion of the reaction, as judged by TLC, the reaction mixture was neutralized with TEA (3 mL). The crude mixture obtained was filtered through a pad of silica, followed by washing with CH₂Cl₂. The filtrate was evaporated to dryness to give a dark purple solid. A mixture of methanol and CH₂Cl₂ (10 mL, 1:1) and Zn(OAc)₂·2H₂O (0.5 g, 0.0022 mol) was added to the purple solid, and the resulting solution was stirred overnight at room temperature. The solvent was evaporated from the reaction mixture, and the crude material obtained was extracted in CH₂Cl₂ (30 mL), washed with brine, dried (Na₂SO₄), filtered and evaporated under reduced pressure. Column chromatography of the metallated porphyrin mixture using ethyl acetate:hexane (1:8) afforded a purple solid mixture of *cis*- and *trans*-substituted porphyrins. The isomers were further separated by column chromatography using toluene:methanol (20:1). The *cis*- isomer eluted from the column first.

trans- 6a

Yield: 0.5 g (28%). **Mp:** >300 °C.

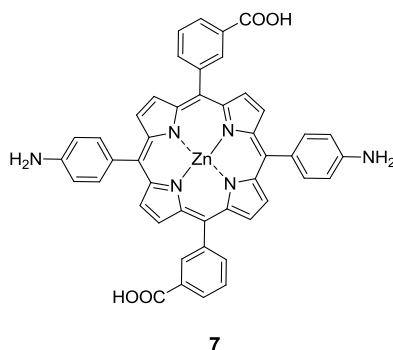
¹H NMR (400 MHz, CDCl₃): δ 1.63 (s, 18H), 3.92 (s, 6H), 7.72 (d, J = 7.6 Hz 4H), 7.82 (t, J = 7.6 Hz, 2H), 8.12 (d, J = 8.4 Hz, 4H), 8.42 (d, J = 7.6 Hz, 2H), 8.45 (d, J = 8.4 Hz, 2H), 8.85 (d, J = 4.4, 4H) 8.99 (d, J = 4.4, 4H).

cis- 6b

Yield: 0.12 g (7%). **Mp:** >300°C.

¹H NMR (400 MHz, CDCl₃): δ 1.63 (s, 18H), 3.96 (s, 6H), 7.72-7.77 (q, J = 7.6 Hz, 4H), 7.84 (t, J = 7.6 Hz, 2H), 8.12 (d, J = 8.4 Hz, 4H), 8.42 (d, J = 7.6 Hz, 2H), 8.48 (d, J = 8.4 Hz, 2H), 8.85 (d, 3H; s, 2H), 8.86 (s, 4H), 8.95 (d, 2H).

7.6.4 Synthesis of 5,15-Bis[(4-Amino)phenyl]-10,20-bis(3-methoxycarbonyl phenyl)porphine (7)



A solution of **6a** (0.1 g, 0.097 mmol) in CH_2Cl_2 (10 mL) was cooled to 0 °C in a 100-mL, single-necked, round-bottomed flask fitted with a magnetic stirrer. Then TFA (0.021 mL, 0.2 mmol) was added slowly dropwise. The solution changed from purple to a green color. The reaction mixture was stirred at room temperature for 2 h. The Boc deprotection was monitored by a polar spot in the TLC analysis corresponding to the amine. The reaction mixture was neutralized with 0.1 M NaOH (3 mL) and extracted with ethyl acetate (2 x 10 mL). The organic layer was separated, dried (Na_2SO_4), filtered and evaporated to dryness to afford the aminoporphyrin **7** as a purple solid.

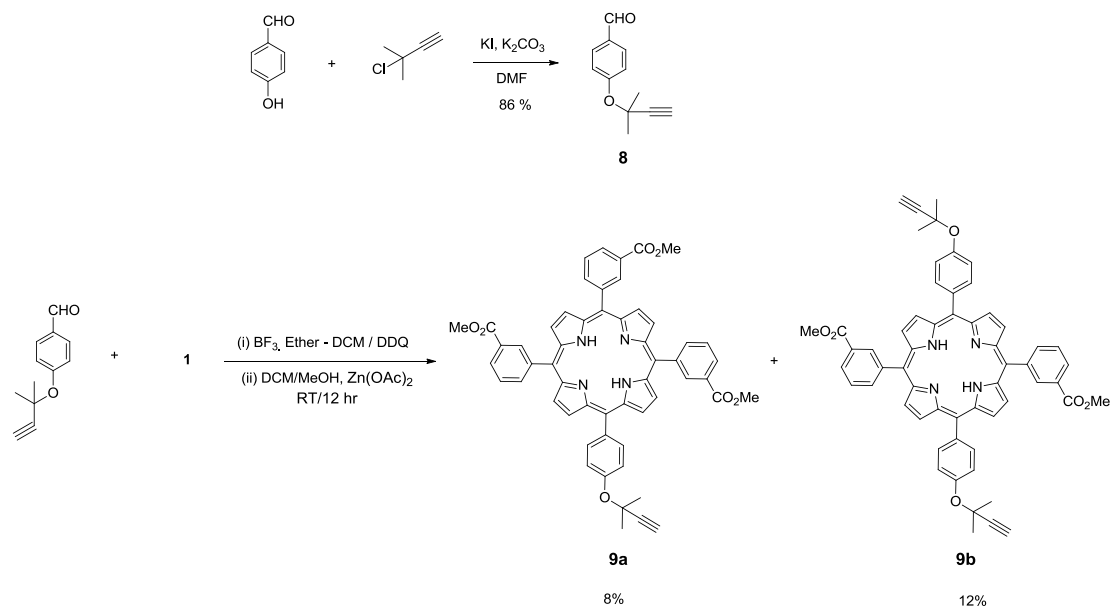
Yield: 0.05 g (72%).

Mp: >300 °C.

$^1\text{H NMR}$ (400 MHz, CDCl_3): δ 1.83 (s, 18H), 3.92 (s, 6H), 4.04 (bs, 4H), 7.06 (d, $J=7.6$ Hz, 4H), 7.82 (t, $J=7.6$ Hz, 2H), 7.97 (d, $J=7.6$ Hz, 4H), 8.38 (d, $J=8$ Hz, 2H), 8.46 (d, $J=8.4$ Hz, 2H), 8.73 (d, $J=4.8$ Hz, 4H), 8.89 (s, 2H) 8.94 (d, $J=4.4$ Hz, 4H).

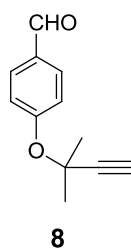
7.7 Synthesis of Porphyrins with Terminal Alkyne Group (A)

The synthetic route for the terminal alkyne substituted porphyrins is shown in Scheme 7.3.



Scheme 7.3 Synthesis of Terminal Alkyne Substituted Porphyrin.

7.7.1 Synthesis of 4-[(2-Methylbut-3-yn-2-yl)oxy]benzaldehyde (**8**)



A mixture of *p*-hydroxybenzaldehyde (1.0 g, 0.0081 mol) and 3-chloro-3-methyl-1-butyne (13.43 g, 0.1210 mol) was placed in a 100-mL, two-necked, round-bottomed flask fitted with a condenser and a magnetic stirrer. Dry DMF (40 mL) was added to the flask, and the system was purged with Ar for 15 min. Anhydrous K₂CO₃ (2.0 g, 0.002

mol) and KI (2.28 g, 0.0137 mol) were added, and the reaction mixture was stirred at 65 °C for 24 h under an Ar atmosphere. The heterogenous mixture was allowed to cool to RT and was then filtered. The filtrate was extracted with ethyl acetate (2 x 20 mL), washed with brine, dried (Na₂SO₄), filtered and evaporated under vacuum to give the crude material. Further purification was achieved by flash chromatography using ethyl acetate:hexane (2:8) to give **8** as a yellow oil.¹⁷

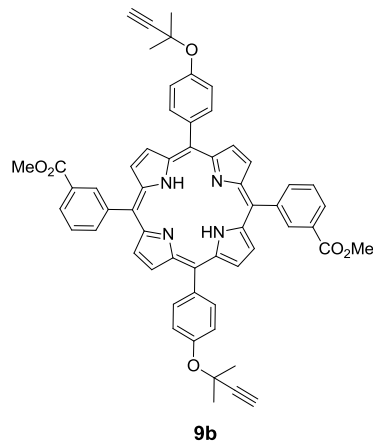
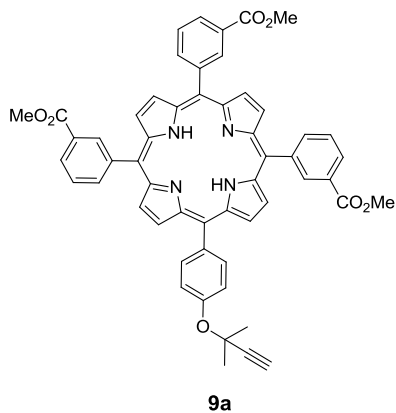
Yield: 1.31 g (86%).

¹H NMR (400 MHz, CDCl₃): δ 9.84 (s, 1H), 7.77 (d, J = 4.4 Hz, 2H), 7.21 (d, J = 4 Hz, 2H), 2.76 (s, 1H), 1.88 (s, 6H).

7.7.2 Synthesis of **9a** and **9b**

In a 100-mL, single-necked, round-bottomed flask fitted with a nitrogen bubbler and a magnetic stirrer was added a solution of **8** (0.067 g, 0.0003 mol) and dipyrromethane **1** (0.1 g, 0.0003 mol) dissolved in dry CH₂Cl₂ (50 mL). The system was degassed for about 15 min with Ar. Then BF₃ etherate (0.09 mL, 0.7 mmol) was added slowly to the reaction mixture which was stirred at RT. A change in color was observed from pale yellow to a dark brown solution. The round-bottomed flask was covered with aluminium foil, and the system was stirred at RT for 1 h during which time a color change occurred from a dark brown to a purple solution. Then DDQ (0.12 g, 0.534 mmol) was added to the reaction, and the solution was purged with argon with continuous stirring for 1.3 h. The solvent was evaporated, and the crude material was filtered through a pad of silica–celite, followed by washing with CH₂Cl₂ :ethyl acetate (3:1, 450 mL). The filtrate was then evaporated to dryness, and the product was further purified by column chromatography using ethyl acetate:hexane (1:5) to give a mixture of

two fractions which yielded porphyrins **9a** and **9b** as a purple solid. The compound **9a** eluted first from the column.



9a

Yield: 0.036 g (8%). **Mp:** >300 °C.

¹H NMR (400 MHz, CDCl₃): δ 1.88 (s, 6H), 2.76 (s, 1H), 3.99 (s, 9H), 7.60 (d, J = 8.1 Hz, 2H), 7.83 (t, J = 7.8 Hz, 3H), 8.10 (d, J = 8.4 Hz, 2H), 8.39 (d, J = 7.5 Hz, 2H), 8.48 (d, J = 8.1, 2H), 8.79 (s, 6H), 8.90 (s, 2H) 8.92 (d, J = 4.8 Hz, 2H)

9b

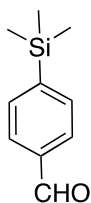
Yield: 0.057 g (12%). **Mp:** >300 °C.

¹H NMR (400 MHz, CDCl₃): δ 1.88 (s, 12H), 2.76 (s, 2H), 3.99 (s, 6H), 7.60 (d, J=7.8 Hz, 4H), 7.83 (t, J=8.1 Hz, 2H), 8.10 (d, J=8.7 Hz, 4H), 8.39 (d, J=7.5 Hz, 2H), 8.47 (d, J=8.1 Hz, 2H), 8.77 (d, J = 4 Hz, 4H), 8.90 (d, J = 4 Hz, 4H).

7.8 Synthesis of Porphyrins Containing Terminal Alkyne Group (B)

The synthetic route is shown in Scheme 7.4.

7.8.1 Synthesis of 1-Bromo-4-(trimethylsilyl)benzene, (10)



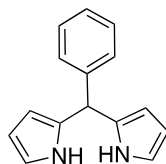
10

To a clean, dry, three-necked, round bottomed flask equipped with a condenser and a stir bar was added 4-bromobenzaldehyde (0.5 g, 0.27 mmol) dissolved in dry triethylamine (0.02 M). The system was purged with Ar for 15 min which was followed by the addition of Pd(PPh₃)₄ (5.0 mol%), CuI (2.5 mol%) and TMSA (1.15 mL, 0.81 mmol). The reaction mixture was stirred at 100 °C for 15 hr. After completion of the reaction as examined by TLC, the thick solution obtained was diluted with CH₂Cl₂ and washed with brine. The organic layer was separated, dried (Na₂SO₄), concentrated under vacuum to give the crude material, which was then column chromatographed over silica gel using ethyl acetate:hexane (1: 20) to afford **10** as a colorless oil.

Yield: 0.40 g (85%). (lit,¹⁸ 83%)

¹H NMR (400 MHz, CDCl₃): δ 0.25 (s, 9H); 7.36 (d, 2H), 7.46 (d, 2H).

7.8.2 Synthesis of 5-Phenyldipyrromethane (11)



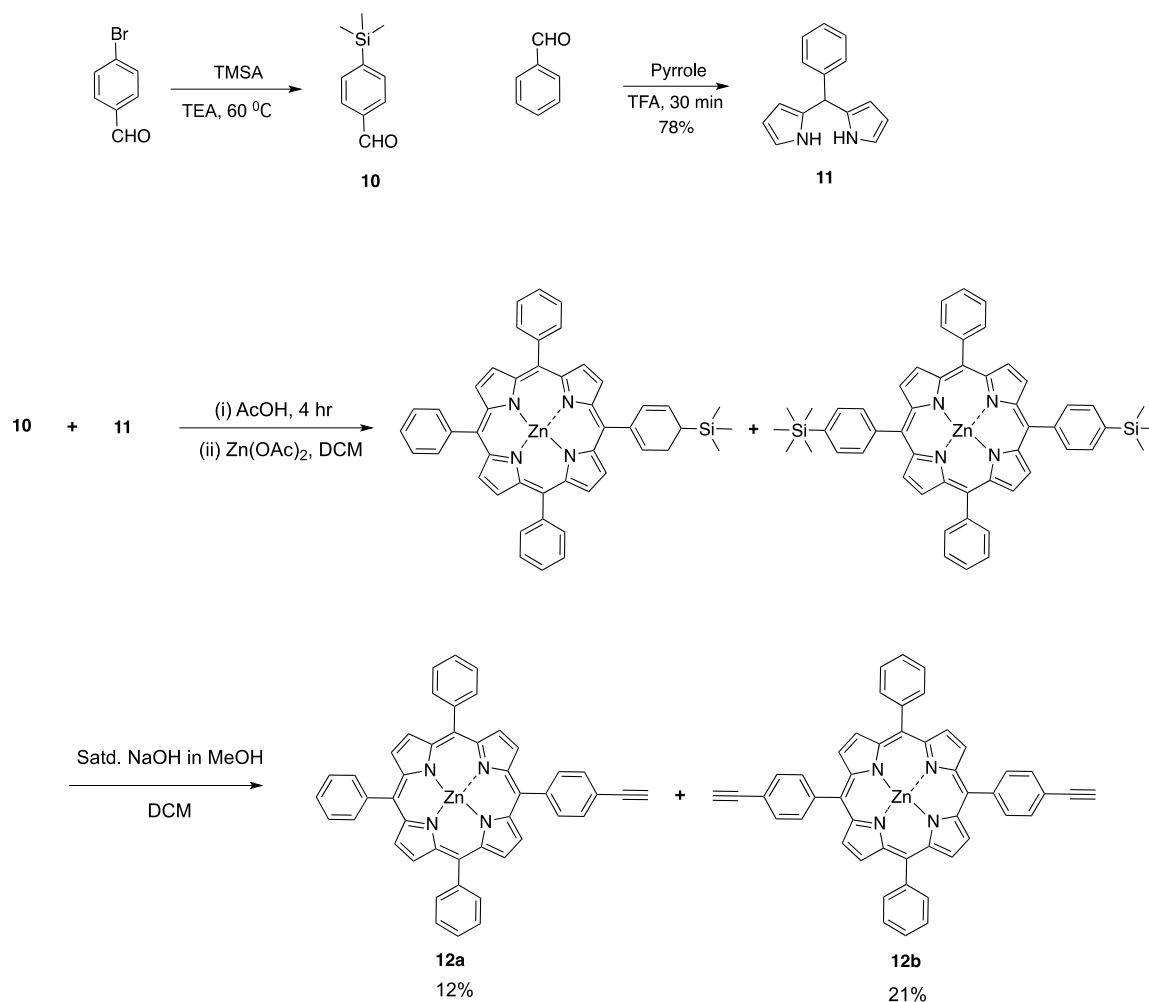
11

A solution of benzaldehyde (0.5 g, 0.0047 mol) and freshly distilled pyrrole (13 mL, 0.188 mol) was placed in a 250-mL, two-necked, round-bottomed flask fitted with a magnetic stirrer and a gas inlet. The solution was degassed by bubbling argon through the solution for 15 min at room temperature. Then TFA (35 μ L, 0.47 mmol) was added, and the resulting mixture was stirred for 20 min at which point no starting material was seen *via* TLC analysis. The crude material was diluted with CH_2Cl_2 (30 mL) and washed with 0.1 M NaOH (25 mL), followed by a brine wash and drying (Na_2SO_4). The solvent and the unreacted pyrrole were removed under vacuum. The crude material was flash chromatographed using ethyl acetate:hexane (1:9) over silica gel to give the pure dipyrromethane **1a**.

Yield: 0.81 g (77.8 %).

Mp: 100-102 $^\circ\text{C}$ (lit,¹⁹ **Mp:** 101 $^\circ\text{C}$).

^1H NMR (400 MHz, CDCl_3): δ 5.47 (s, 1H); 5.91 (s, 2H); 6.15-6.18 (m, 2H); 7.21-7.32 (m, 5H); 7.91 (br s, 2H).

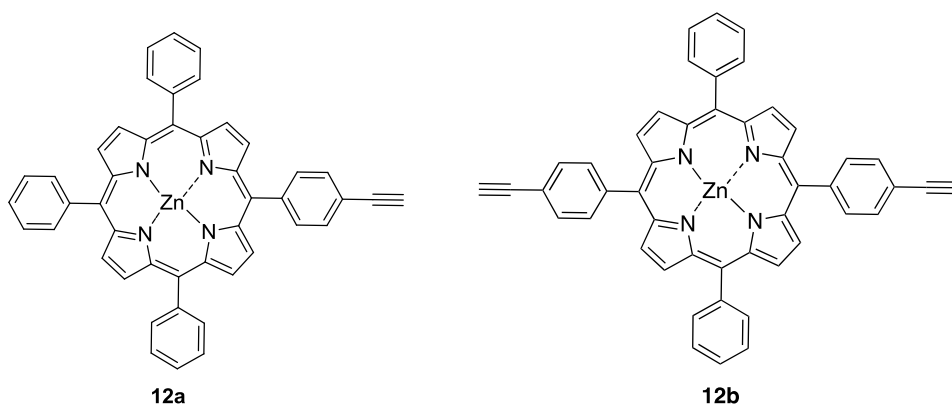


Scheme 7.4 Synthesis of Terminal Alkyne Substituted Porphyrins from 4-Bromo Benzaldehyde.

7.8.3 Synthesis of porphyrins **12a**, **12b**

The synthesis of **12a** and **12b** was effected by reacting compound **10** (0.09 g, 0.45 mmol) and **11** (0.1 g, 0.45 mmol) in acetic acid (20 mL) according to the general procedure. Metallation of the crude porphyrin with $\text{Zn(OAc)}_2 \cdot 2\text{H}_2\text{O}$ (0.1 g, 0.45 mmol) in CH_2Cl_2 :MeOH (1:1 mixture, 4 mL) afforded the zinc porphyrin. The blackish purple crude material was column chromatographed over silica gel using ethyl acetate:hexane

(1:3). The mixture containing the substituted silyl porphyrins were reacted with saturated NaOH in MeOH solution for 5 min. The reaction was monitored by TLC. After complete consumption of the starting material, water (10 mL) was added to the reaction mixture, and the product was extracted with CH₂Cl₂ (20 mL), dried (Na₂SO₄), and filtered. The solvent was evaporated, and the crude mixture of porphyrins was subjected to column chromatography using ethyl acetate:hexane (1:9) over silica gel to give **12a** and **12b**. The fraction **12a** eluted first from the column.



12a 5-(3-Ethynylphenyl)-10,15,20-triphenylporphinatozinc(II)

Yield: 0.037 g (12 %). **Mp:** >300 °C.

¹H NMR (400 MHz, CDCl₃): δ 9.0 (d, J = 8 Hz, 2H), 8.9 (s, 6H), 8.2 (d, J = 8 Hz, 2 H), 8.28 (d, J = 8 Hz, 2H), 7.8 (d, J = 6.4 Hz, 2H), 7.76 (m, 9H), 3.1 (s, 1H)

12b 5,10-Bis(3-Ethynylphenyl)-15,20-triphenylporphinatozinc(II)

Yield: 0.06 g (21%). **Mp:** >300 °C.

¹H NMR (400 MHz, CDCl₃): δ 8.93 (d, J = 10.4 Hz, 8H), 8.18 (d, J = 8 Hz, 4H), 7.88 (d, J = 6.8 Hz, 4H), 7.75 (d, J = 6.4 Hz, 4H), 7.76 (m, 6H), 3.1 (s, 2H).

7.9 Covalent linkage of the porphyrins

The poor solubility of the porphyrins prevented the synthesis of the diporphyrinophanes. Although all the porphyrins with the ester and phenyl groups were soluble in solvents, such as chloroform, CH₂Cl₂, ethyl acetate, etc., the corresponding carboxylic acid porphyrins were soluble only in highly polar solvents such as DMF and DMSO. Moreover, the pyridyl porphyrins formed cofacial aggregates which restricted their solubility to polar solvents. The formation of the cofacial aggregates was attributed to the N(py)-Zn coordination.²⁰

7.10 References

1. Kadish, K. M.; Smith, K. M.; Guillard, R. *The Porphyrin Handbook*, 2000, Vol.1, Academic Press, San Diego.
2. Senge, M. O. *Chem. Commun.* **2006**, 243-256.
3. Shelnutt, J. A.; Song, X. -Z.; Ma, J. -G. *Chem. Soc. Rev.* **1998**, 27, 31-42.
4. Collman, J. P.; Wagenknecht, P. S.; Hutchinson, J. E. *Angew. Chem.* **1994**, 106, 1620-39.
5. Chang, C. J.; Loh, Z. -H.; Shi, C.; Anson, F. C.; Nocera, D. G. *J. Am. Chem. Soc.* **2004**, 126, 10013-10020.
6. Rosenthal, J.; Nocera, D. G. *Acc. Chem. Res.* **2007**, 40, 543-553.
7. Nakazawa, J.; Mizuki, M.; Shimazaki, Y.; Tani, F.; Naruta, Y. *Org. Lett.* **2006**, 8, 4275-4278.
8. Grubbs, R. H.; Miller, S. J.; Fu, G. C. *Acc. Chem. Res.* **1995**, 28, 446-452.

9. Nakagawa, H.; Ogawa, K.; Satake, A.; Kobuke, Y. *Chem. Commun.* **2006**, 1560-1562.
10. Aitken, J. B.; Shearer, E. L.; Giles, N. M.; Lai, B.; Vogt, S.; Reboucas, J. S.; Batinic-Haberle, I.; Lay, P. A.; Giles, G. I. *Inorg. Chem.* **2013**, 52, 4121-4123.
11. Xu, J.; Wu, J.; Zong, C.; Ju, H.; Yan, F. *Anal. Chem.* **2013**, 85, 3374-3379.
12. Zitova, A.; Hynes, J.; Kollar, J.; Borisov, S. M.; Klimant, I.; Papkovsky, D. B. *Anal. Biochem.* **2010**, 397, 144-151.
13. Maitani, M. M.; Zhan, C.; Huang, C.-C.; Mochizuki, D.; Suzuki, E.; Wada, Y. *Bull. Chem. Soc. Jpn.* **2012**, 85, 1268-1276.
14. Matsuo, T.; Tohi, Y.; Hayashi, T. *J. Org. Chem.* **2012**, 77, 8946-8955.
15. Bruckner, C.; Zhang, Y.; Rettig, S. J.; Dolphin, D. *Inorg. Chim. Acta.* **1997**, 263, 279-286.
16. Rochford, J.; Chu, D.; Hagfeldt, A.; Galoppini, E. *J. Am. Chem. Soc.* **2007**, 129, 4655-4665.
17. Rai, R.; Katzenellenbogen, J. A. *J. Med. Chem.* **1992**, 35, 4150-4159.
18. Kyogoku, K.; Hatayama, K.; Yokomori, S.; Seki, T.; Tanaka, I. *Agric. Biol. Chem.* **1975**, 39, 667-672.
19. Ye, B. -H.; Naruta, Y. *Tetrahedron.* **2003**, 59, 3593-3601.
20. Singh, K.; Behal, S.; Hundal, M. S. *Tetrahedron.* **2005**, 61, 6614-6622.

7.11 Appendices

Figure 7.3 ^1H NMR Spectrum of **6a**

Figure 7.4 ^1H NMR Spectrum of **7**

Figure 7.5 ^1H NMR Spectrum of **9a**

Figure 7.6 ^1H NMR Spectrum of **9b**

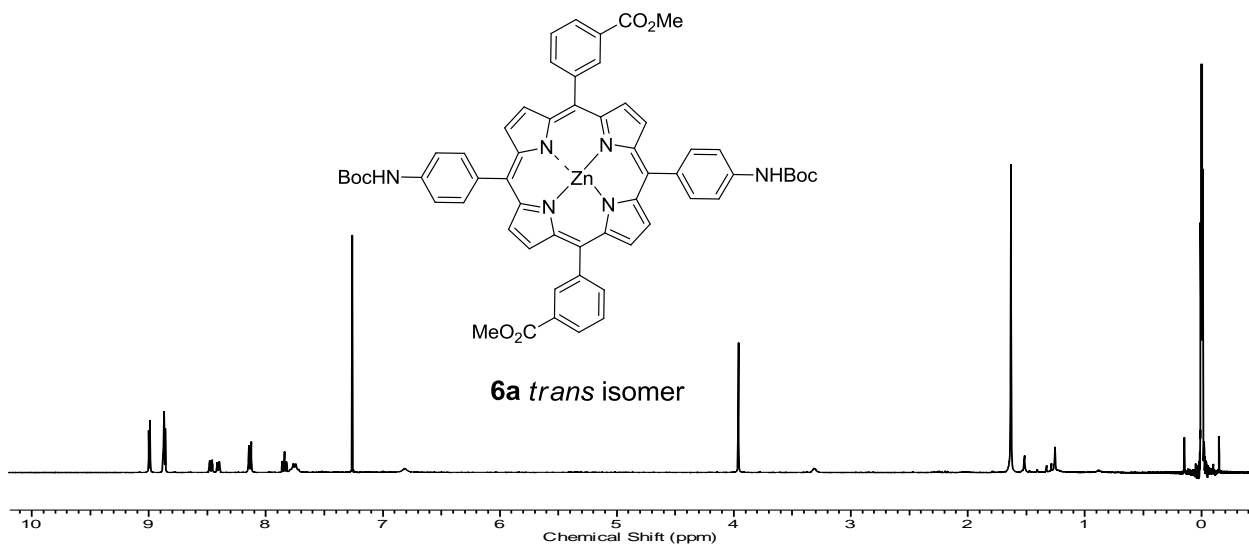


Figure 7.3 ^1H NMR Spectrum of **6a**

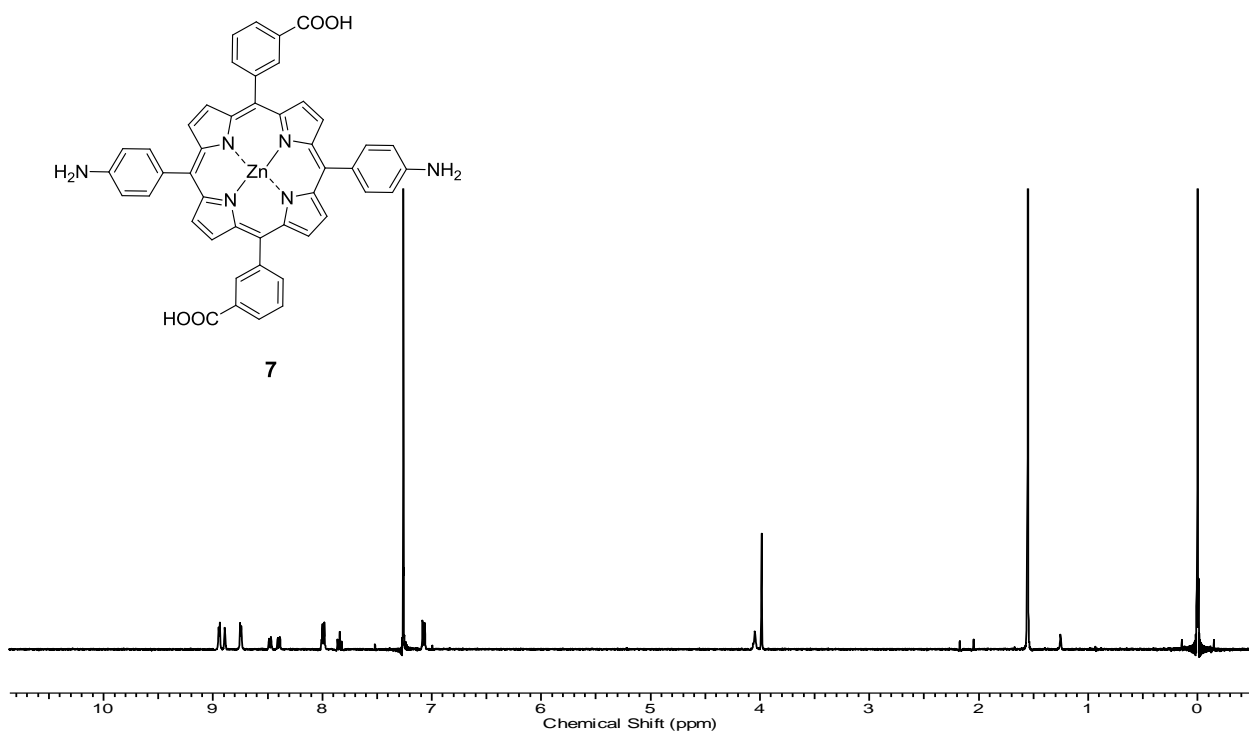


Figure 7.4 ^1H NMR Spectrum of **7**

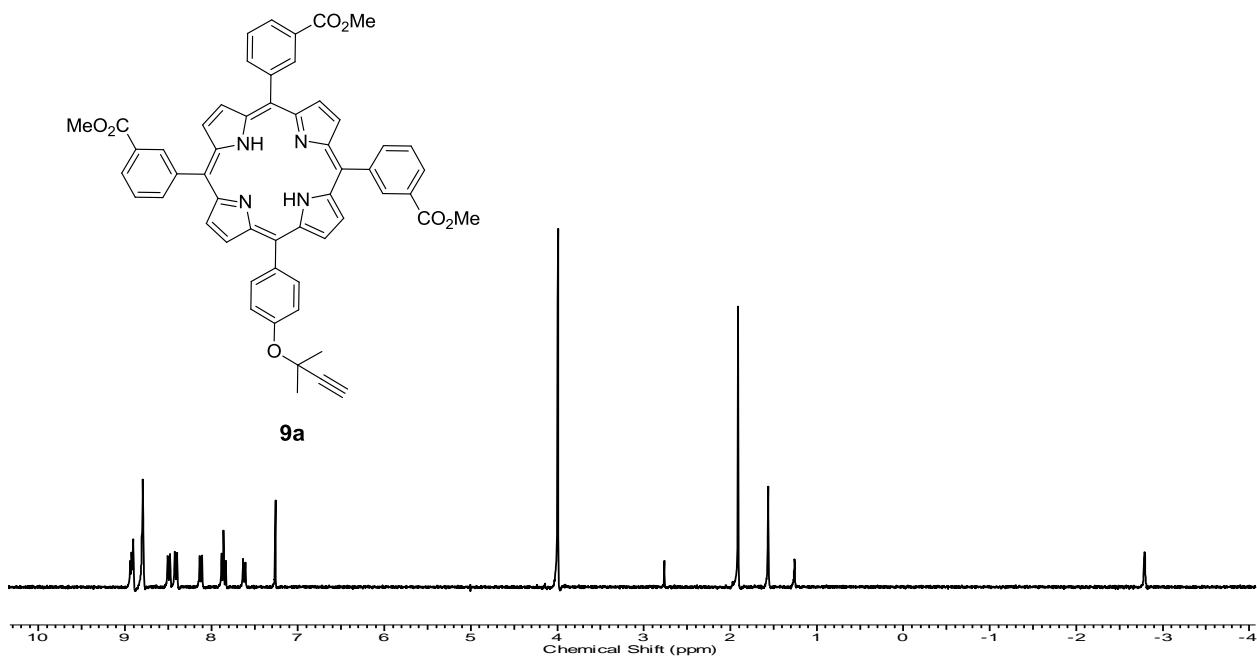


Figure 7.5 ^1H NMR Spectrum of **9a**

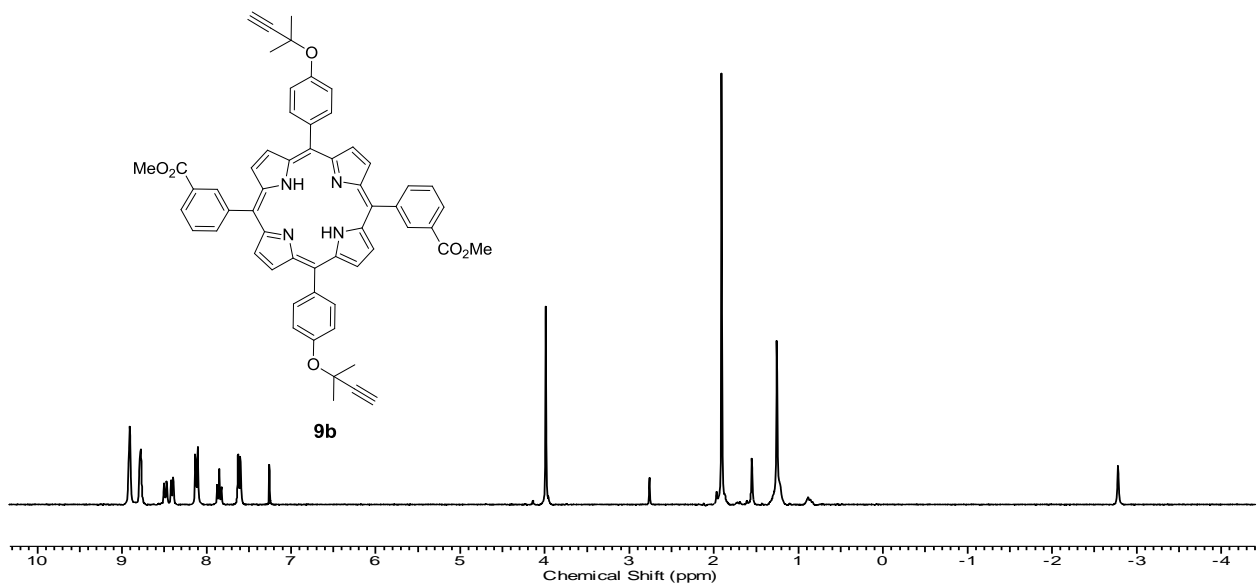


Figure 7.6 ^1H NMR Spectrum of **9b**

CONCLUSIONS

Three symmetrical and unsymmetrical subphthalocyanine dimers have been synthesized, and their structures were characterized by ^1H NMR, ^{13}C NMR and Mass spectroscopy. The photophysical studies were investigated by UV-Vis and fluorescence spectroscopy.

A series of donor acceptor conjugates of porphyrins and subphthalocyanines were synthesized. Characterization of the synthesized conjugates was performed by ^1H NMR, ^{13}C NMR, ^{19}F NMR and MALDI-TOF spectroscopy. The redox behavior of the conjugates was analyzed by cyclic voltammetry experiments.

The axial reactivity of fluorosubstituted subphthalocyanine was examined on *o*-, *m*- and *p*-dihydroxybenzene appended perylene diimides. Structural characterization of the perylene-SubPc conjugates was done by ^1H NMR, ^{13}C NMR and MALDI-TOF spectroscopy.

Various *meso*-substituted porphyrins were synthesized using different reaction conditions. Their structures were characterized by ^1H NMR and ^{13}C NMR spectroscopy.

VITA

LAKSHMI CHOCKALINGAM KASI VISWANATH

Candidate for the Degree of

Doctor of Philosophy

Thesis: SYNTHESIS AND CHARACTERIZATION OF ELECTRON
DONOR/ACCEPTOR SUBPHTHALOCYANINE DERIVATIVES AND
PORPHYRIN METAL COMPLEXES

Major Field: CHEMISTRY

Biographical:

Personal Data:

Born (1983) in Tuticorin, India to C. Kasi Viswanath and C. K. V. Revathi
Citizenship: Indian

Education:

Completed the requirements for the Bachelor of Science in Chemistry at Madras University, Chennai, Tamilnadu, India, in 2004.

Completed the requirements for the Master of Science in Applied Chemistry at Anna University, Chennai, Tamilnadu, India, in 2006.

Experience: Senior Research Officer at Sanmar Speciality Chemicals Ltd., 2006-2009.

Completed the requirements for the Master of Philosophy in Chemistry at Madurai Kamaraj University, Chennai, Tamilnadu, India, in 2009.

Completed the requirements for the Doctor of Philosophy/Education Chemistry at Oklahoma State University, Stillwater, Oklahoma, in July, 2013.